

Evaluation of earth pressure and performance of shoring
systems for Québec sensitive clay: Experimental and
numerical study

by

Miah ALAM

MANUSCRIPT-BASED THESIS PRESENTED TO ÉCOLE DE
TECHNOLOGIE SUPÉRIEURE IN PARTIAL FULFILLMENT FOR THE
DEGREE OF DOCTOR OF PHILOSOPHY
Ph.D.

MONTREAL, DECEMBER 03, 2021

ÉCOLE DE TECHNOLOGIE SUPÉRIEURE
UNIVERSITÉ DU QUÉBEC

Copyright © All right reserved, Miah Alam, 2021

© Copyright reserved

It is forbidden to reproduce, save or share the content of this document either in whole or in parts. The reader who wishes to print or save this document on any media must first get the permission of the author.

BOARD OF EXAMINERS

THIS THESIS HAS BEEN EVALUATED
BY THE FOLLOWING BOARD OF EXAMINERS

Mr. Omar Chaallal, Thesis Supervisor
Department of Construction Engineering, École de technologie supérieure

Mr. Amar Khaled, Member of the jury
Department of Construction Engineering, École de technologie supérieure

Mr. Hakim Bouzid, President of the Board of Examiners
Department of Mechanical Engineering, École de technologie supérieure

Mr. Nouredine Ghlamallah, External Evaluator
Vice-president, Geosciences, Englobe, Quebec

THIS THESIS WAS PRESENTED AND DEFENDED
IN THE PRESENCE OF A BOARD OF EXAMINERS AND PUBLIC
ON NOVEMBER 09, 2021
AT ÉCOLE DE TECHNOLOGIE SUPÉRIEURE

ACKNOWLEDGEMENTS

Firstly, I would like to express my admiration to my supervisor Professor Omar Chaallal for his continuous support during my Ph.D. study, for his patience, motivation, and immense knowledge. His guidance helped me during my research period as well as writing of this thesis and papers. I am also grateful to him that he has given me a chance to work in this research project and added a new field to my career path.

I would like to thank l'Institut de recherche Robert-Sauvé en santé et en sécurité du travail (IRSST) for their great contribution to this research project as a donor and initiator. Again, I am gratefully thanking to Mr. André Lan and Mr. Bertrand Galy of IRSST for their enormous support and valuable time. I am also grateful to Professor Denis LeBoeuf and his team members Jose Fidelis Zanavelo, Sébastien Dourlet and Christian Juneau from Université Laval (UL) for their continuous support in the experiments and information.

Finally, I would like to give thank and mention the names of our team (ETS) members Mr. Richard Prowt, Mr. John Lescelleur and Mr. Jonathan Auger for their constant support and contributions to the experiments and instrumentation, and all other technicians who helped us at Louisville site during the experiment.

Last but not the least, my sincere thanks also go to my family, especially my beloved parents, my wife and three kids for their endless love and support in all stages of my life.

Évaluation de la pression des terres et de la performance des systèmes d'étançonnement pour l'argile sensible du Québec : étude expérimentale et numérique

Miah ALAM

RÉSUMÉ

Les effondrements sont très fréquents dans l'industrie de la construction et présentent un risque très grave pour les travailleurs qui opèrent à l'intérieur de tranchées ou d'excavations. Des études montrent que les excavations ou les tranchées dans les sols argileux sensibles du Québec sont extrêmement dangereuses en raison d'une possible perte grave et soudaine de la résistance au cisaillement du sol sur les structures. Des structures de support flexibles et semi-flexibles sont utilisées comme supports temporaires pour les côtés verticaux des excavations. La répartition de la pression du sol dépend du type de sol, de l'étalement et de la méthode de mise en œuvre. Généralement, aucune solution théorique consensuelle satisfaisante n'est disponible pour estimer la pression du sol pour ce type de structure porteuse avec des cloisons soumises à des pressions de sol en argile sensible. De nombreux chercheurs ont proposé des solutions théoriques pour estimer la pression de sol sur un support temporaire flexible. Une lacune de recherche a été observée pour l'étalement de caissons de tranchées à de faibles profondeurs inférieures à 6 m et pour les interactions sol-structure (ISS). Par conséquent, l'interaction entre la masse du sol et le support, la flexibilité dans le développement des charges latérales et le mouvement des éléments structuraux doivent être étudiés pour un étalement en caisson de tranchée. La présente étude de recherche s'est concentrée sur l'évaluation de la pression de la terre sur les systèmes structuraux de soutènement. Une étude expérimentale, numérique et paramétrique a été menée pour étudier la pression du sol sur un étalement temporaire de caissons de tranchée flexible en argile sensible en tenant compte de l'ISS.

Dans l'étude expérimentale in-situ, deux caissons de tranchées « empilé l'un sur l'autre » conformément à la réglementation américaine OSHA et placés à l'intérieur de la tranchée pour couvrir une profondeur d'excavation totale de 6 m. La pression de sol a été suivie par des cellules de pression totale (TPC). Les résultats des essais sur le terrain ont été présentés en termes de distribution de la pression du sol en fonction de la profondeur d'excavation avec et sans une surcharge de surface de 45 kPa à proximité du bord d'un côté de la tranchée.

L'étude numérique par éléments finis (EF) utilisant PLAXIS-3D (logiciel ISS) a été réalisée pour reproduire et valider le test expérimental in-situ à grande échelle et a étudié la pression de la terre sur les parois d'étalement de tranchée temporaire flexible pratiquée dans un sol argileux sensible. Le modèle de tranchée d'excavation a été considéré comme une l'argile non linéaire et anisotrope. Les modèles de sols constitutifs de Mohr-Coulomb (MC) et de sol durcissant (HS) ont été considérés pour l'analyse par EF. Différentes valeurs du facteur de réduction du module du sol (MRF) et du coefficient de pression du sol au repos (K_0) ont été considérées pour valider le modèle.

VIII

Par ailleurs, deux études paramétriques par éléments finis ont été réalisées en utilisant le même logiciel PLAXIS-3D pour atteindre les deux objectifs suivants : (i) évaluer la pression effective du sol sur le bouclier de la tranchée en acier pour le till, le sable sec, humide de compacité lâche ainsi que pour le sol argileux sensible ; (ii) évaluer les effets de la géométrie et du matériau du caisson de tranchée (acier et aluminium) sur la pression du sol.

En outre, une autre étude de cas expérimentale sur le terrain a été réalisée pour étudier la pression du sol sur une tranchée par étalement hydraulique vertical en aluminium avec des feuilles de contreplaqué dans une tranchée d'argile molle et sensible. Les procédures d'installation, d'instrumentation et d'essai sur le terrain sont présentées pour ce type d'étalement hydraulique vertical en aluminium avec feuille de contreplaqué (Speed Shore) conformément aux directives de l'OSHA des États-Unis et placées à l'intérieur de la tranchée pour couvrir la profondeur totale de 2,4 m (8 pi) des fouilles. La pression de sol a été saisie par des cellules de pression totale (TPC). Les résultats des essais sur le terrain sont présentés en termes de répartition de la pression du sol le long de la profondeur de l'excavation avec et sans une surcharge de surface de 30 kPa à proximité du bord d'un côté de la tranchée.

Les résultats obtenus révèlent le potentiel d'utilisation d'un système d'excavation et d'étalement de tranchée existant pour différents types de sol et valident ses performances avec des résultats théoriques et expérimentaux reportés dans la littérature. Les résultats de la présente étude ont également servi à développer un guide permettant de choisir un système d'étalement en fonction de la classe de sol du Québec. Ce guide constitue un outil très utile pour l'ingénieur praticien œuvrant dans le domaine.

Mots-clés : Étayage de tranchées et d'excavation ; Codes et directives d'excavation ; Pression du sol sur la structure flexible ; Cellule de pression totale ; PLAXIS-3D ; Méthode des éléments finis ; Argile molle et sensible ; Modélisation des sols et des structures ; Caissons de tranchées en acier et aluminium.

Evaluation of earth pressure and performance of shoring systems for Quebec sensitive clay: experimental and numerical study

Miah ALAM

ABSTRACT

Cave-ins are very frequent in the construction industry and present a very serious risk for workers who operate inside trenches or excavations. Studies show that excavations or trenches in Quebec sensitive clay soils are extremely hazardous due to possible severe and sudden loss of soil shear strength. Flexible and semi-flexible supporting structures are used as temporary supports for the vertical sides of excavations. The earth pressure distribution depends on the type of soil, the shoring, and the method of implementation. Generally, no satisfactory consensual theoretical solutions are available to estimate soil pressure for this type of supporting structure with partitions facing land pressures in sensitive clay. Many researchers have suggested theoretical solutions to estimate the earth pressure on a flexible temporary support. A research gap has been observed for trench box shoring at shallow depths of less than 6 m and for soil-structure interactions (SSI). Therefore, the interaction between the soil mass and the support, flexibility in the development of lateral loads, and the movement of structural elements need to be studied for a trench box shoring. This research study focused on the evaluation of earth pressure on retaining structural systems. An Experimental, numerical, and parametric study was carried out to investigate the soil pressure on a temporary flexible trench box shoring in sensitive clay taking into account SSI.

In the experimental field test procedures, two trench boxes ‘stacked upon each other’ in conformity with United-States OSHA regulations and placed inside the trench to cover a total depth of excavation of 6 m. Earth pressure was mentioned using total pressure cells (TPC). The field test results were presented in terms of soil pressure distribution along with the depth of excavation with and without a 45 kPa surface surcharge load applied next to the edge of one side of the trench.

The Finite-Element (FE) numerical study using PLAXIS-3D (SSI- software) was carried out to reproduce and validate the full-scale experimental in-situ test and investigated the earth pressure on a flexible temporary trench box shield in soft and sensitive clay soil. The excavation trench model was considered as nonlinear and anisotropic clay. Both Mohr-Coulomb (MC) and hardening soil (HS) constitutive soil models were considered for FE-analysis. Different values of the soil-modulus reduction factor (MRF) and of the coefficient of earth pressure at rest (K_0) were considered to validate the model.

Also, two parametric finite element studies have been carried out using the same computer software to meet the two following specific objectives: (i) to evaluate the effective soil pressure on the steel trench box shield for Till, Dry, Wet and Loose sand and sensitive clay soil; (ii) to assess the effects of the trench box material type (Steel and Aluminum) and geometry on the earth pressure.

Furthermore, an additional field experimental case study was carried out to investigate the soil pressure on a trench by vertical aluminum hydraulic shoring with plywood sheeting in soft and sensitive clay trench. The installation, instrumentation, and field test procedures are presented for this type of vertical aluminum hydraulic shoring with plywood sheeting (so-called Speed shore) in conformity with United-States OSHA guidelines and placed inside the trench to cover the total 2.4 m (8 ft.) depth of excavation. Earth pressure was monitored using total pressure cells (TPC). The field test results are presented in terms of soil pressure distribution along the depth of excavation with and without a 30 kPa surface surcharge load next to the edge of one side of the trench.

The results obtained reveal the potential use of an existing trench excavation and shoring system for different types of soil and validate its performance with theoretical and experimental results reported in the literature. They also allowed to develop a decision making-guideline that will allow the selection of a shoring system given the Quebec soil classes. This guideline is a very useful tool for practicing engineers in the field.

Keywords: Trench and excavation shoring; Excavation codes and guidelines; Soil pressure on flexible structure; Total pressure cell; Finite element method; Soft and sensitive clay; PLAXIS-3D; Soil and structural modelling; Steel and Aluminum trench boxes.

TABLE OF CONTENTS

| | Page |
|--|------|
| INTRODUCTION..... | 1 |
| 0.1 General | 1 |
| 0.2 Problem statement | 2 |
| 0.3 Objectives of the research | 3 |
| 0.4 Methodology | 4 |
| 0.5 Research impact on engineering applications and originality | 4 |
| 0.6 Organization of dissertation | 5 |
| CHAPTER 1 LITERATURE REVIEW | 7 |
| 1.1 Introduction | 7 |
| 1.2 Earth pressure on retaining structure | 7 |
| 1.3 Available techniques, codes, and methods used to calculate earth pressure on shoring walls..... | 9 |
| 1.4 Excavation base stability | 13 |
| 1.5 Movement and ground deformation of the support system..... | 15 |
| 1.6 Excavation stage..... | 17 |
| 1.7 System stiffness | 17 |
| 1.8 Review of field and laboratory experimental research..... | 19 |
| 1.9 Review of Finite element analysis research | 21 |
| CHAPTER 2 PROTECTION PRACTICES FOR TRENCH AND EXCAVATION IN QUEBEC SENSITIVE CLAY SOILS: REVIEW OF CODES, GUIDELINES, AND RESEARCH NEEDS | 25 |
| 2.1 Abstract | 25 |
| 2.2 Introduction | 25 |
| 2.3 Statistics for Accidents Related to Excavation and Trench Work | 26 |
| 2.4 Comparison of Excavation Protection Practices, Codes and Guidelines in Different Jurisdictions..... | 28 |
| 2.5 Recent Research on Excavations or Trenches with Shoring and Research Needs | 34 |
| 2.6 Conclusions | 43 |
| CHAPTER 3 FIELD TEST OF TEMPORARY EXCAVATION WALL SUPPORT IN SENSITIVE CLAY | 45 |
| 3.1 Abstract | 45 |
| 3.2 Introduction | 45 |
| 3.3 Full-Scale Field Experimental Program | 49 |
| 3.3.1 Soil Characteristics of the Field Experimental Site..... | 49 |
| 3.3.2 Excavation and Shoring Geometry..... | 51 |
| 3.3.3 Instrumentation..... | 54 |
| 3.3.4 Laboratory Verification and Field Installation of Test Equipment | 55 |
| 3.3.5 Excavation and Installation of Protection Systems | 58 |

| | | |
|-----------|---|-----|
| 3.3.6 | Concrete Block (Surcharge Load) Installation | 61 |
| 3.3.7 | Data Recording Unit and Data Collection | 62 |
| 3.3.8 | Data Preparation..... | 63 |
| 3.4 | Field Test Results and Discussion | 64 |
| 3.4.1 | Temperature Effect | 64 |
| 3.4.2 | Soil Pressure over the Time Period (May 14–August 10, 2018) | 65 |
| 3.4.3 | Surcharge Load Effect on Soil Pressure | 68 |
| 3.4.4 | Total Pressure Curve..... | 69 |
| 3.4.5 | Theoretical Calculations | 72 |
| 3.5 | Conclusions..... | 75 |
| | | |
| CHAPTER 4 | FLEXIBLE TEMPORARY SHIELD IN SOFT AND SENSITIVE CLAY: 3D FE MODELING OF EXPERIMENTAL FIELD TEST | 77 |
| 4.1 | Abstract..... | 77 |
| 4.2 | Introduction..... | 77 |
| 4.3 | Finite-element analyses..... | 79 |
| 4.4 | Parameters for FE | 79 |
| 4.4.1 | Soil Modelling | 80 |
| 4.4.2 | Structural modelling..... | 80 |
| 4.4.3 | Generating the Mohr-Coulomb (MC) model..... | 84 |
| 4.4.4 | Interface model | 87 |
| 4.4.5 | Water head variations | 89 |
| 4.4.6 | Mesh generation..... | 90 |
| 4.5 | Construction steps and phases in PLAXIS-3D simulation | 90 |
| 4.5.1 | Construction step 0: Initial Phase | 91 |
| 4.5.2 | Construction step 1: Phase 1 | 92 |
| 4.5.3 | Construction step 2: Phase 2 | 92 |
| 4.5.4 | Construction step 3: Phase 3 | 92 |
| 4.5.5 | Construction step 4: Phase 4..... | 92 |
| 4.6 | Analysis using Mohr-Coulomb (MC) models and Results..... | 94 |
| 4.6.1 | MC model with modulus reduction factor (MRF)..... | 95 |
| 4.6.2 | Mohr-Coulomb reduction factor with shear strain..... | 96 |
| 4.6.3 | Validation of the MC model | 97 |
| 4.7 | Simulation analysis using the hardening soil (HS) material model..... | 99 |
| 4.8 | Overall Results and Comparisons..... | 101 |
| 4.9 | Conclusions..... | 105 |
| | | |
| CHAPTER 5 | SOIL-STRUCTURE INTERACTION OF FLEXIBLE TEMPORARY TRENCH BOX: PARAMETRIC STUDIES USING 3D FE MODELLING | 107 |
| 5.1 | Abstract..... | 107 |
| 5.2 | Introduction..... | 107 |
| 5.3 | Finite-element analyses..... | 110 |
| 5.3.1 | Parameters for FE | 110 |
| 5.3.2 | Soil Modelling | 110 |

| | | |
|-----------|--|-----|
| 5.3.3 | Structural modelling | 111 |
| 5.4 | Generating the Mohr-Coulomb (MC) model | 116 |
| 5.4.1 | Interface model..... | 118 |
| 5.4.2 | Mesh generation | 119 |
| 5.5 | Construction steps and phases in PLAXIS-3D simulation for sensitive blue clay .. | 120 |
| 5.6 | Calculations with different K_0 | 120 |
| 5.7 | Construction steps and phases in PLAXIS-3D simulation for till, dry sand and wet sand | 121 |
| 5.8 | Parametric studies for steel and aluminum trench box for plate and strut geometry | 123 |
| 5.9 | Overall Results and Comparisons | 124 |
| 5.10 | Conclusions | 132 |
| CHAPTER 6 | FIELD TEST PERFORMANCE OF HYDRAULIC SHORING WITH PLYWOOD SHEETING IN A SOFT AND SENSITIVE CLAY | 133 |
| 6.1 | Abstract | 133 |
| 6.2 | Introduction | 133 |
| 6.3 | Full-scale field experimental program | 136 |
| 6.3.1 | Soil Characteristics of the Field Experimental Site..... | 136 |
| 6.3.2 | Excavation and Shoring Geometry..... | 138 |
| 6.3.3 | Instrumentation..... | 140 |
| 6.3.4 | Laboratory Verification and Field Installation of Test Equipment | 142 |
| 6.3.5 | Excavation and installation of protection systems | 144 |
| 6.3.6 | Concrete Block (Surcharge load) Installation | 146 |
| 6.3.7 | Data Recording Unit and Data Collection..... | 147 |
| 6.3.8 | Data Preparation | 148 |
| 6.4 | Field test results and discussion | 149 |
| 6.4.1 | Temperature effect | 150 |
| 6.4.2 | Soil pressure over the time period (May 15–August 10, 2018) | 151 |
| 6.4.3 | Surcharge load effect on soil pressure..... | 153 |
| 6.4.4 | Total pressure curve | 155 |
| 6.4.5 | Theoretical calculations..... | 155 |
| 6.5 | Conclusion..... | 158 |
| | CONCLUSIONS AND RECOMMENDATIONS | 161 |
| | APPENDIX I DECISION SUPPORT SYSTEM..... | 167 |
| | APPENDIX II METHODOLOGY | 171 |
| | BIBLIOGRAPHY | 175 |

LIST OF TABLES

| | Page |
|-----------|---|
| Table 1.1 | Field performance data inside an excavation or trench20 |
| Table 1.2 | Published finite-element research related to excavation shoring in soft clay24 |
| Table 2.1 | Occupational accidents statistics regarding soil cave-ins in trenches or excavations.....27 |
| Table 2.2 | Selection of excavation safety methods for excavation shoring systems assuming the soil classification adopted by the Canadian provinces and the United States29 |
| Table 2.3 | Existing clauses related to excavation or trenching protections and soil classification in various codes and regulations (CSAO, 2009) (OSHA, 1989) (British Standards Institution, 2009) (BCOSHA, 2009) ...30 |
| Table 2.4 | Comparison among different codes in terms of soil classification32 |
| Table 2.5 | Comparison of existing guidelines.....33 |
| Table 2.6 | Field performance data inside an excavation or trench39 |
| Table 2.7 | Published finite-element research related to excavation shoring in soft clay42 |
| Table 3.1 | Undrained shear strength from the soil based on DSS testing51 |
| Table 3.2 | Effective stress parameters from DSS testing51 |
| Table 3.3 | Geometric and structural properties of the shield52 |
| Table 3.4 | Pressure cell identification and capacities55 |
| Table 3.5 | Experimental vs. theoretical and field performance soil pressures at different trench depths in soft clay soil.....74 |
| Table 4.1 | Geometric and mechanical properties of box shield protection used for FE simulation in Plaxis-3D82 |
| Table 4.2 | Calculation of E for different layers of plastic brown and sensitive blue clay86 |

| | | |
|------------|---|-----|
| Table 4.3 | Properties for Louiseville soil and Mohr-Coulomb material model parameters used for FE modeling | 88 |
| Table 4.4 | Seasonal water head variations readings | 89 |
| Table 4.5 | Construction sequence of FE modeling in Plaxis-3D | 91 |
| Table 4.6 | Soil pressure for different depths of excavation by Plaxis-3D MC model without MRF [option B] compared with experimental..... | 94 |
| Table 4.7 | Calculation of modulus reduction factor and corresponding Elastic modulus (E) and Shear modulus (G)..... | 95 |
| Table 4.8 | Calculation of modulus reduction factor and corresponding Elastic modulus (E) and Shear modulus (G) from shear strain | 97 |
| Table 4.9 | Soil pressure at different depths of the excavation by Plaxis-3D MC model with different K_0 | 98 |
| Table 4.10 | Properties of Louiseville soil and Hardening soil (HS) material model parameters used for FE modeling | 100 |
| Table 4.11 | Comparison of soil pressures on flexible temporary shield in soft and sensitive clay excavated trench | 101 |
| Table 5.1 | Plate properties (steel and aluminum) of trench box shield protection used for FE simulation in PLAXIS-3D..... | 113 |
| Table 5.2 | Strut properties (steel and aluminum) of trench box shield protection used for FE modelling in PLAXIS-3D | 113 |
| Table 5.3 | Soil properties for sensitive blue clay, till, dry and wet sand model parameters used for FE modelling in PLAXIS-3D..... | 117 |
| Table 5.4 | Parameters for different layers of sensitive blue clay | 118 |
| Table 5.5 | Construction sequence of FE modelling for sensitive blue clay in PLAXIS-3D. | 119 |
| Table 5.7 | Soil pressure on steel and aluminum protection shield boxes with different strut diameters and plate thicknesses | 131 |
| Table 6.1 | Experimental versus Leroueil et al. (2003) undrained soil shear strength values at Louiseville experimental site | 137 |
| Table 6.2 | Undrained shear strength from the soil based on DSS testing..... | 138 |

| | | |
|--------------|--|-----|
| Table 6.3 | Effective stress parameters from DSS testing..... | 138 |
| Table 6.4 | Geometric properties of the shield..... | 139 |
| Table 6.5 | Pressure cell identification and capacities | 140 |
| Table 6.6 | Experimental vs. theoretical and field performance soil pressures at different trench depths in soft clay soil..... | 156 |
| Table-A II-1 | Detailed methodology as related to the phases of the research program..... | 173 |

LIST OF FIGURES

| | Page |
|--|------|
| Figure 1.1 Apparent earth pressure diagram for sand and stiff and soft to medium clay | 9 |
| Figure 1.2 Comparison of apparent lateral earth pressure coefficients with basal stability index | 14 |
| Figure 1.3 Mechanism of base failure | 15 |
| Figure 1.4 Typical profiles of movement for braced and tied back walls | 15 |
| Figure 1.5 Dimensionless settlement profiles recommended for estimating the distribution of settlement adjacent to excavation in different soil types | 16 |
| Figure 1.6 Staged development of earth pressure in a braced excavation | 17 |
| Figure 1.7 Chart for estimating lateral movement (and settlements) for support systems in clays..... | 18 |
| Figure 1.8 Bearing capacity values | 19 |
| Figure 2.1 Apparent earth pressure diagram for sand and stiff and soft to medium clay | 36 |
| Figure 3.1 Apparent earth pressure diagram for soft to medium clay | 47 |
| Figure 3.2 Geotechnical properties of Louiseville clay deposit data | 50 |
| Figure 3.3 First and second steel trench box protection system at the experimental site..... | 52 |
| Figure 3.4 Field test setup details for trench boxes..... | 53 |
| Figure 3.5 Strut locations in the two elevation sides along the trench..... | 54 |
| Figure 3.6 Preparation and verification of pressure cells in the ETS lab before being transported to the site installation | 56 |
| Figure 3.7 Steps to install the pressure cells on the steel wall plate of the trench box..... | 57 |

| | | |
|-------------|---|----|
| Figure 3.8 | Pressure cells are fixed on the side of the first and second trench boxes | 58 |
| Figure 3.9 | Excavation/construction sequence | 59 |
| Figure 3.10 | Installation of the first (lower) trench box into the trench | 59 |
| Figure 3.11 | Excavation continued to make room to accommodate the second (upper) trench box in the trench..... | 60 |
| Figure 3.12 | Second (upper) trench box is being placed on top of the first (lower) box in the trench..... | 60 |
| Figure 3.13 | Sand was used to fill the space between the shoring exterior wall and the surrounding soil..... | 61 |
| Figure 3.14 | Concrete blocks (surcharge load) installed on one side of the trench..... | 62 |
| Figure 3.15 | Components of the data recording unit at the experimental site..... | 63 |
| Figure 3.16 | First week's hourly temperature at different trench depths as recorded by pressure cells, 2018 | 65 |
| Figure 3.17 | First week's hourly pressure after temperature correction on the trench box protection, 2018 | 66 |
| Figure 3.18 | Maximum daily soil pressure after temperature correction on the trench box protection (May 14–August 10, 2018)..... | 68 |
| Figure 3.19 | Blown-up view of the last week of soil pressure to observe the effects of surcharge loading (concrete blocks) at the trench | 69 |
| Figure 3.20 | Experimental soil pressure on trench box wall vs. depth..... | 70 |
| Figure 3.21 | Surrounding soil washed away by heavy rainfall affecting pressure cell at 0.9 m..... | 71 |
| Figure 3.22 | Recorded accumulated precipitation quantities (in mm) for each month from May to August 2018 at the Louiseville field test site | 71 |
| Figure 3.23 | Likely “fixed end condition” developed at the lower end of the first trench box due to 300 mm insertion into the soil..... | 72 |
| Figure 3.24 | Theoretical calculation of soil pressure on the trench box wall using the TPM equation | 73 |

| | | |
|-------------|---|-----|
| Figure 3.25 | Experimental vs. theoretical soil pressure curves with respect to trench depth..... | 75 |
| Figure 4.1 | Geometric profile and excavation contour in Plaxis-3D simulation of trench: (a): Experimental values of soil shear strength at Louiseville site; (b): Plaxis-3D model profile for Louiseville soil (Number of soil elements: 23221; MC soil model) | 81 |
| Figure 4.2 | Elevation views of trench and shield | 81 |
| Figure 4.3 | Strut spacing and locations in the two assembled box shields (stacked upon each other) | 83 |
| Figure 4.4 | Structural simulation of the two assembled box shields (stacked upon each other) protection in Plaxis-3D (Number of structural elements: 1050; MC soil model) | 84 |
| Figure 4.5 | Experimental hinge joint between two plate walls of assembled box shields (stacked upon each other) | 85 |
| Figure 4.6 | Experimental hinge joint between plate and strut of box shield..... | 85 |
| Figure 4.7 | Interfaces in Plaxis-3D model..... | 89 |
| Figure 4.8 | Mesh generation of the soil and structural elements in Plaxis-3D..... | 90 |
| Figure 4.9 | Plaxis-3D simulation for the construction steps | 93 |
| Figure 4.10 | Plaxis-3D simulation for the construction step 4 (Phase 4) with overloading as per experimental site..... | 94 |
| Figure 4.11 | Soil pressure at different depth of trench with different K_0 values..... | 99 |
| Figure 4.12 | Maximum soil pressure vs. trench depth for different options of analysis..... | 104 |
| Figure 5.1 | Geometric profile and excavation contour in PLAXIS-3D simulation of trench: (a): Experimental values of undrained shear strength of sensitive blue clay (Louiseville clay) (b): PLAXIS-3D model profile for sensitive blue clay (number of soil elements: 23221; MC soil model) (c): PLAXIS-3D model profile for till, dry and wet sand (number of soil elements: 23221; MC soil model) | 111 |
| Figure 5.2 | Elevation views and strut locations in the two assembled box shields (stacked upon each other) along the trench..... | 114 |

| | | |
|-------------|---|-----|
| Figure 5.3 | Structural simulation view of the two assembled box shields (stacked upon each other) with protection in PLAXIS-3D (number of structural elements: 1050; MC soil model)..... | 115 |
| Figure 5.8 | Comparisons of soil pressure for different types of soil by numerical analysis with theoretical values in the trench | 126 |
| Figure 5.9 | Soil pressure (Louiseville clay) on steel versus aluminum trench box shields with the same geometry | 127 |
| Figure 5.10 | Soil pressure (Louiseville clay) on steel and aluminum trench box shields with different plate thicknesses | 128 |
| Figure 5.11 | Soil pressure (Louiseville clay) on steel trench box shields with different plate thicknesses and strut diameters | 129 |
| Figure 5.12 | Soil pressure (Louiseville clay) on aluminum trench box shields with different plate thicknesses and strut diameters | 130 |
| Figure 6.1 | Hydraulic shoring protection system | 139 |
| Figure 6.2 | (a) Pressure cells are attached to the plywood frame; (b) Pressure are placed on the cell; (c) cells are tested by the SENSLOG in the ETS lab before site installations | 141 |
| Figure 6.3 | Pressures cells installation on the Plywood shield at the site before installations in the trench | 141 |
| Figure 6.4 | Test setup details for Hydraulic shoring (with plywood sheeting) in trench excavation | 142 |
| Figure 6.5 | Excavation / Construction sequences for Hydraulic shoring with Ply wood sheeting in a trench | 144 |
| Figure 6.6 | Detail installation process of Hydraulic shoring with Plywood in a shallow trench of soft and sensitive clay | 146 |
| Figure 6.7 | Concrete blocks (surcharge load) placing in a trench of soft and sensitive clay | 147 |
| Figure 6.8 | Data recording unit in the experimental site | 148 |
| Figure 6.9 | First week hourly temperature at different depths of trench | 150 |
| Figure 6.10 | Hourly temperature (15th May-10th August) at different depths of trench | 151 |

| | | |
|--------------|---|-----|
| Figure 6.11 | First week hourly pressure after temperature correction for trench | 152 |
| Figure 6.12 | Maximum daily soil pressure after temperature correction for trench (15th May – 10th August, 2018)..... | 153 |
| Figure 6.13 | Blow up of last week soil pressure to see the effects of surcharge (concrete block) loading at trench | 154 |
| Figure 6.14 | Experimental vs. theoretical soil pressure curves with respect to trench depth | 156 |
| Figure 6.15 | Recorded accumulated precipitation quantities (in mm) for each month from May to August 2018 at the Louiseville field test site | 157 |
| Figure 6.16 | Some of irregularities found during and after the installation process of Hydraulic shoring (with Plywood sheeting) in this type of soft and sensitive clay | 158 |
| Figure A I-1 | Preliminary decisions | 169 |
| Figure A I-2 | Sloping options | 170 |
| Figure A I-3 | Shoring and shielding options | 171 |

LIST OF ABBREVIATIONS

| | |
|---------|--|
| ASP | Association Sectorielle Paritaire |
| CFEM | Canadian Foundation Engineering Manual |
| CSST | The Commission de la santé et de la sécurité du travail |
| CSAO | Construction Safety Association of Ontario |
| CIRIA | Construction Industry Research and Information Association |
| DSS | Direct Simple Shear |
| ETS | École de technologie supérieure |
| ESS | Excavation Support System |
| FHWA | Federal Highway Administration |
| FEA | Finite-Element Analysis |
| FTP | File transfer protocol |
| HS | Hardening soil |
| IRSST | Institut de recherche Robert-Sauvé en santé et en sécurité du travail |
| LU | Linear units |
| MC | Mohr-Coulomb |
| MDDELCC | Ministère du Développement durable, de l'Environnement et de la Lutte contre les changements climatiques |
| MRF | Modulus reduction factor |
| NIOSH | National Institute for Occupational Safety and Health |
| NBS | National Bureau of Standards |
| NBCC | National Building Code of Canada |
| OSHA | Occupational Safety and Health Administration |

| | |
|--------|--|
| OPPBTP | Organisme Professionnel de Prévention du Bâtiment et des Travaux Publics |
| OHSR | Occupational Health & Safety Regulation |
| OCR | Over consolidation ratio |
| PLAXIS | Plane strain and axial symmetry |
| PI | Plasticity Index |
| SSI | Soil-Structure Interaction |
| SCCI | Safety Code for the construction industry |
| TPM | Terzaghi and Peck method |
| TPC | Total pressure cell |
| UL | Université Laval |

LIST OF SYMBOLS

| | |
|------------|--|
| B | Width of the excavation |
| C_f | Pressure cell calibration factor |
| C_T | Calibration factor for temperature |
| C_u | Soil shear strength |
| d | Depth of soft layer below the bottom of excavation |
| E | Soil elastic moduli |
| E_{max} | Maximum elastic moduli |
| G | Shear modulus |
| G_{max} | Maximum shear modulus |
| H | Height of the supported bank |
| K_A | Coefficient of earth pressure |
| K_0 | Jaky's coefficient |
| K_{2max} | Empirical factor that varies according to void ratio |
| L | Current reading in linear units |
| L_0 | Initial reading in linear units |
| m | Empirical factor |
| N | Dimensionless number |
| N_c | Bearing capacity of the soil |
| N_s | Stability number |
| P | Earth pressure in kilopascals |
| P_C | Corrected pressure |

| | |
|---------------|--|
| R_{inter} | Strength reduction factor |
| S_u | Average undrained shear strength value over the height of the wall H |
| S_{ub} | Average undrained shear strength value below the excavation depth H |
| S | Current barometric pressure reading |
| S_0 | Initial barometric pressure reading |
| T | Current temperature reading |
| T_0 | Initial temperature reading |
| W_e | Lateral weight effect |
| γ | Unit weight of soil |
| p_A | Apparent earth pressure |
| ΔK | Factor related to bottom heave stability |
| τ_{rel} | Relative shear stress |
| τ_{mob} | Mobilized shear stress |
| τ_{max} | Maximum shear stress |
| ν | Poisson's ratio |
| σ'_m | Effective mean stress |
| σ'_v | Vertical effective stress |
| σ'_h | Horizontal effective stress |
| δ_v | Vertical settlement of soil |
| δ_{vM} | Maximum vertical settlement of soil |

INTRODUCTION

0.1 General

The work of trenching or excavation exposes the construction workers to many risks. During earth excavation work, landslides are very frequent and present the most serious risk. This is very often underestimated by the construction industry. Study reports show that 1 to 2 deaths per year occur due to landslides. This represents around 1% of deaths due to accidents in Quebec (Lan, 2013). These fatal accidents are attributed to the lack of shoring and safe working methods. The industry is more sensitive with this risk and health and safety training (HST) policy and focus now significantly on the excavations and trenching excavations. Since 2016 to 2017, health and safety policies have undergone major changes in Canada. HST has now become a value and a skill. The assessment of the qualifications of firms is now also based on good results in terms of HST. HST culture has changed considerably lately.

In Quebec, more than 7460 excavations are carried out annually, and 75% of them are deeper than 4 feet. This indicates the importance of selecting the shoring system during earth excavation work for safety. In total, 26 shoring systems have been identified. They are classified into four distinct categories: caissons, hydraulic cylinders, pipes and trench boxes. These are common shoring systems available in the market and used in Québec. However, there is a need for tools and guidelines to help selecting the shoring and shielding system best suited to the soil class (Lan, *et al.*, 2008).

Safe earth excavation or trenching in soft clay soil are of two types: unsupported (sloped) and supported (braced) shoring. Sloped excavations are used when they are shallow or when the site dimensions allow digging embankments with gentle slopes to ensure their safety. For other conditions, excavations without retaining wall can cause human and material losses. The design (sloping, benching, etc.) and execution of work must be performed strictly in accordance with local regulatory requirements. For clay, excavations may present many

challenges and must be carried out with great caution. It was seen that when excavating in sensitive clays, landslides were very common within days or weeks after the excavation was completed. A major finding is that the stability of excavations evolves over time depending on the dissipation of pore water pressures. The planning of excavations in clay and carrying out the work must be performed with great care by experienced professional engineers (CFEM, 2006).

Supported excavations are most common in the construction field. The flexible and semi-flexible supporting structures are used as temporary supports for the vertical sides of excavations. Generally, no satisfactory theoretical solutions are available to estimate soil pressure for the supporting structures with partitions facing land pressures.

In addition, these shored excavations give rise to various complex phenomena such as base stability, horizontal movement and ground deformations, hydrostatic uplift and excavation-induced deformations. Researchers have shown a vast and growing interest in this field to resolve those problems with their extensive endeavor. The current study aims at addressing these issues that arise during the earth excavation and to develop a decision-making guideline for the selection of shoring system suitable for Quebec soil classes.

0.2 Problem statement

According to the Ministère de Développement Durable, Environnement et Lutte Contre les Changements Climatiques, Quebec soils are overall soft and sensitive of glacial and with post marine deposit (MDDELCC, 2020). Quebec territorial analysis shows that 51 serious and fatal accidents were reported to the Commission de la santé et de la sécurité du travail (CSST) between May 1974 to January 2013 at the excavation work sites. Landslide is the most serious risk and most frequent during earth excavation work, which is very often underestimated. The main causes of accidents are the lack of proper shoring and safe working methods. Article 3.15.3 of the Quebec Code de sécurité pour les travaux de construction (CSTC) stated that, it is mandatory to shore up any trench in accordance with engineering plan ((SCCI, 2020). But

there are not enough details in the guidelines. Numerical and experimental results are not very clear for this type of sensitive soil with specific depth and width in this region. International regulations in this area of study, such as OSHA and Cal/OSHA, have revealed the importance of the two following aspects: (i) classification of soils, which helps the entrepreneur in choosing the right method of excavation and shoring and (ii) selection method for shoring systems adapted to the soil classification.

To overcome this deficiency, the Institut de recherche Robert-Sauvé en santé et en sécurité du travail (IRSST) has taken an initiative to undertake a research study aiming at classifying the Quebec soils and selection of shoring systems for trench excavation in collaboration with Université Laval (UL) and École de Technologie Supérieure (ÉTS). The objectives of the IRSST initiative are as follows: (1) to classify soils in urban areas of Quebec; (2) to develop a simple method for determining the in-situ class of soil of a site for performing excavation and shoring; (3) to validate the strength and behavior of shoring systems for different classes of soil and loading conditions; and (4) to develop a decision support system for selecting a shoring system integrating geological, geotechnical and structural factors.

0.3 Objectives of the research

The main objective of the research program is to develop a decision making-guideline (An example of this decision making flow chart is shown in Appendix I) that will allow the selection of a shoring system given the Quebec soil classes.

Specific objectives are as follows:

- 1) Evaluate earth pressure;
- 2) Validate performance of existing shoring systems experimentally by suitable field test setup;
- 3) Develop a numerical FE model to generalize the behavior;
- 4) Develop a guideline to select a shoring system.

0.4 Methodology

The methodology involves analytical, numerical, as well as experimental in-situ investigations of shoring systems.

The analytical and numerical studies will include:

- 1) The literature review of theoretical aspects including earth pressure of different types of classified soils (Quebec soils) and the load transfer mechanism to the shoring system;
- 2) These pressure envelopes will then be used for structural analysis by FEM for the shoring systems following an approach taking into account the soil-structure interaction (SSI).

The in-situ experimental investigation will include the following activities:

- 1) Testing of a vertical open trench without support shoring system but following the sloping and trenching guidelines; (accomplished by UL);
- 2) Testing of a vertical trench support box-type steel or aluminum; (accomplished by ETS);
- 3) Testing of a vertical trench with screen-type support shoring or shielding. (accomplished by ETS).

The numerical investigation will include simulations by 3D software. In particular, the following systems will be analysed using FEM:

- 1) Simulation of a vertical open trench without support shoring system; (accomplished by UL);
- 2) Simulation of a vertical trench support box-type steel or aluminum; (accomplished by ETS);
- 3) Simulation of a vertical trench with screen-type support shoring or shielding; (accomplished by ETS).

Detailed methodology as related to the phases of the research program is described in Appendix II.

0.5 Research impact on engineering applications and originality

Sensitive soft clay of Quebec soils is unique. The safety of the construction workers is very fragile in excavated trench of this type of soil. IRSST recognized it and provide funding to address it.

The results of this study will be used to develop a decision-making system, which is a very useful tool for practicing engineers in the field. Therefore, it will provide a strategy for preventing risks of landslides at the source. It will also establish practical criteria for a safe workplace and selection strategy of shoring system given the Quebec soil class.

0.6 Organization of dissertation

In addition to Introduction chapter, this research thesis is organised into six chapters (Chapters 1-6) as follows:

Chapter 1 presents a review of literature of previous studies on Earth pressure on retaining structures.

Chapter 2 presents the first published article from this Ph.D. program. The article is titled “Protection practices for trench and excavation in Quebec sensitive clay soils: Review of codes, guidelines, and research needs”.

Chapter 3 presents details and results related to the experimental study on full-scale field test performance of a flexible temporary shield in soft and sensitive clay soil; The published article is entitled: "Field Test of Temporary Excavation Wall Support in Sensitive Clay".

Chapter 4 titled, “Flexible Temporary Shield in Soft and Sensitive Clay: 3D-FE Modelling of Experimental Field Test”, presents the published paper on the 3D-FE modelling of experimental field test and comparison with field test data.

Chapter 5 presents the parametric studies by 3D-FE modelling of flexible temporary trench box in different types of soil. This numerical study was reported in an article bearing the title: of “Soil-Structure Interaction of Flexible Temporary Trench Box: Parametric studies using 3D FE Modelling ”.

Chapter 6 presents the published paper related to the experimental study on hydraulic shoring (with Plywood sheeting) in a soft and sensitive clay. This paper is titled "Field Test Performance of Hydraulic Shoring with Plywood Sheeting in a Soft and Sensitive Clay "

Finally, a summary and conclusions drawn from this research are presented along with recommendations for future works.

CHAPTER 1

LITERATURE REVIEW

1.1 Introduction

The present research study related to “the evaluation of earth pressure and performance of shoring systems for Quebec sensitive clay” is a complex as it depends on many inter-related mechanisms. The understanding of the basis of such mechanisms and phenomena as well as setting the context to better apprehend the subject is of paramount importance. This context setting is covered by the following subsections: (i) earth pressure on retaining structure; (ii) available techniques, codes, and methods used to calculate earth pressure on shoring walls; (iii) excavation base stability; (iv) movement and ground deformation of the support system; (v) excavation stage; (vi) system stiffness; (vii) review of field and laboratory experimental research; and (viii) review of finite element analysis research.

1.2 Earth pressure on retaining structure

Earth pressure behind a flexible screen is different from a rigid retaining wall. The pressure distribution depends on the type of soil, shoring, and method of implementation. Supported excavations are most common in the construction field. The flexible and semi-flexible supporting structures are temporary support for the vertical sides of excavations. Generally, no theoretical satisfactory solutions are available to estimate soil pressure for the supporting structures with partitions facing land pressures. According to the Canadian Foundation Engineering Manual (CFEM 2006), in excavations in sensitive clays, slope failures are very common within days or weeks after the excavation is completed. A significant finding is that the stability of excavations depends on the overall time required to dissipate pore water pressures (CFEM, 2006).

The technical report by Lan *et al.* (2008) pointed out that in Quebec, more than 7460 excavations are carried out annually and that 75% of them are deeper than 1.22 m (4 ft). This indicates the importance of tools that can be used to choose the appropriate shoring system for safety during earth excavation work. The same study report identified a total of 26 common shoring systems that are available in the market and used in Quebec. These systems can be classified into four distinct categories: caissons, hydraulic cylinders, pipes, and trench boxes. Clearly, there is a need for guidelines for selecting the shoring and shielding system that is best suited to the soil class (Lan *et al.*, 2008).

Shored excavations give rise to various complex behavioural phenomena such as base instability, horizontal movement, ground deformation, hydrostatic uplift, and excavation-induced deformations (CFEM, 2006). Researchers have shown a large and growing interest in this field to resolve these problems with their extensive endeavours. OSHA (2015) identifies various modes of geotechnical breakage inside trenches or excavations without shoring, such as tension, sliding, toppling, bulging, heaving, squeezing, and boiling. Five main factors were found to affect the stability of excavation walls, particularly for soft and sensitive clays: soil shear strength, excavation duration, excavation geometry, water table, and working methods (Lafleur *et al.*, 1987).

The earth pressure distribution depends on the type of soil, the shoring, and the method of implementation. Generally, no satisfactory theoretical solutions are available to estimate soil pressure for supporting structures with partitions facing land pressures in sensitive clay (NBCC, 2015). Many researchers have suggested theoretical solutions to estimate the earth pressure on a flexible temporary support. For rigid retaining structures such as weight-standing walls, soil and water pressures can be calculated in many cases from theory (CFEM, 2006). For a rigid wall such as a retaining wall, the passive earth pressure created behind the wall is different from that generated on a flexible screen; the elements do not repeat the same stresses and deform differently. The pressure distribution depends on the type of shield and the method of implementation. Consequently, for an excavation shield, the Canadian Foundation

Engineering Manual (CFEM, 2006) recommends the use of pressure envelopes from empirical data.

1.3 Available techniques, codes, and methods used to calculate earth pressure on shoring walls

According to Rankine (1857), the total active thrust over the excavation depth on a smooth wall for clays can be expressed as:

$$P_{\text{Rankine}} = 0.5(\gamma H^2 - 4s_u H) \quad (1.1)$$

This method typically uses Rankine active and passive earth pressure coefficients. However, excavation support systems designed to limit movement do not develop Rankine earth pressure conditions. Nevertheless, the method presents advantages related to simplicity and ease of calculation. To determine the apparent earth pressure for sand and soft to medium clay, Terzaghi and Peck (1967) proposed a soil pressure diagram for a temporary retaining structure, as illustrated in Figure 1.1.

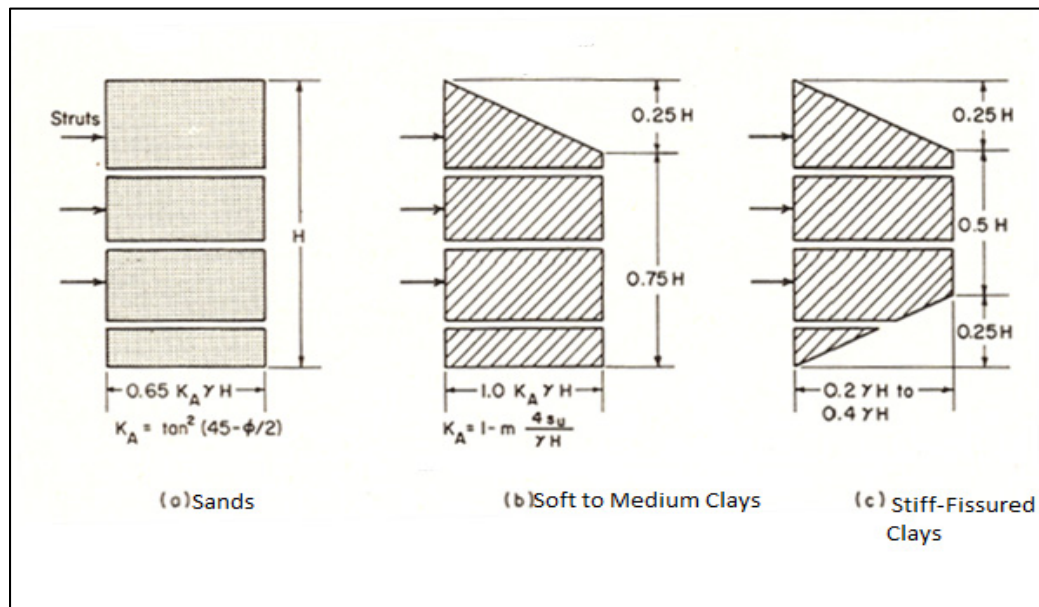


Figure 1.1 Apparent earth pressure diagram for sand and stiff and soft to medium clay

Taken from Terzaghi & Peck (1967)

The soil pressure can be calculated as follows:

$$p_A = K_A \gamma H, \quad (1.2)$$

where $K_A = 1 - m \frac{4s_u}{\gamma H}$. The total pressure P_A is given by:

$$P_A = 0.775H \quad p_A = 0.775 (\gamma H^2 - m 4s_u H) \quad (1.3)$$

where m is an empirical factor accounting for potential base instability effects in deep excavations in soft clays. When the excavation is underlain by deep soft clay and dimensionless number ($N = \gamma H/s_u$) exceeds 4, then m is set to 0.4; otherwise, m is set to 1 (Flaate, 1966). These formulas are clearly understood and easy to estimate. However, the method does not account for the development of soil failure below the bottom of the excavation. Indeed in this method assumes that the distance from the lowest strut to the excavation bottom corresponds to 20% of the excavation depth and that the load on the lowest strut is computed by multiplying the pressure (p_A) by half the distance to the strut above plus half the distance below the bottom of the excavation.

Henkel (1971) proposed to modify the equation of the Terzaghi and Peck method (TPM) used to calculate soil pressure in medium to soft clays by assuming a failure mechanism compatible with a deeper location of the fracture plane. Back-calculated values by Henkel indicated that TPM underestimates the coefficient of active earth pressure. Assuming the basal stability phenomenon, Henkel (1971) proposed that apparent earth pressure for soft to medium clay be rather calculated as follows:

$$p_A = \left(1 - \frac{4s_u}{\gamma H} + \Delta K\right) \gamma H \quad (1.4)$$

where ΔK is a factor related to bottom heave stability, given by:

$$\Delta K = \frac{2B}{H \left(1 - \frac{5.14 S_{ub}}{\gamma H} \right)} \quad (1.5)$$

where B is the width of the excavation and S_{ub} is the average undrained shear strength value below the excavation depth H . The Henkel method is limited to cases where the clay soils on the retained side of the excavation and below the excavation have a constant value for the undrained shear strength of soil.

The Federal Highway Administration (FHWA, 1999) recommends an apparent earth pressure with different levels of ground anchors for stiff to hard clays. In this way, apparent earth pressure diagrams are used to estimate the pressure of stiff to hard clay excavations on the anchor supports. The forces at different levels of ground anchors are easy to determine. This method results in the lower braces carrying smaller loads. That observation has misled engineers to extrapolate the apparent lateral earth pressure to zero at subgrade. That assumption is not backed by any scientific evidence (Konstantakos, 2015). The work of FHWA resulted in alternative formulations for deposits of sand and stiff clay. Stress distribution is particularly influenced by the position of the struts or anchors, and improved formulations are now recommended. From the proposed modification of apparent lateral earth pressure diagrams, the subgrade reaction at the bottom of excavation is easy to calculate. If tighter deformation control is required or when fully undrained conditions are to be expected, then the virtual reaction at the subgrade level must take into account increased lateral earth pressures that can reach close to 50% of the total vertical stress at the subgrade level. Excavations with clays on both wall sides, if fully dewatered, will not satisfy this method (Konstantakos, 2015).

The National Building Code of Canada (NBCC, 2015) proposes a method to determine the earth pressure envelope for the design of temporary supports for soft to firm clays. For cantilever support, the design total pressure is equal to $1.0 P_A$, where:

$$P_A = \rho g H - 2C_u \quad (1.6)$$

where ρ = total (bulk) density of soil (submerged if below ground water), kg/m^3 , C_u = undrained shear strength, H = depth of cut (m), and g = acceleration due to gravity (m/s^2). The total pressure P_A should be not less than $0.15 \rho g H^2$ and may be computed using short-term strength if the excavation is open for a limited period. Regardless of whether pressures are negative or zero, the minimum positive pressure indicated should be used. In this method, the pressure distribution envelope for cantilever support is triangular. This cantilever support can restrict the movement of adjacent soil. This type of support is generally very poor and should be avoided in soft sensitive clays. For braced or tied-back support, the design total pressure lies between $0.4 \rho g H^2$ and $0.8 \rho g H^2$. The higher range should be used where the clay is of soft consistency and the lower range where the clay is of firm consistency. This value may be conservative for non-homogeneous, non-sensitive sandy-silt cohesive soil of firm consistency. If the stability number $(N) = (\rho g H + \text{overload})/C_u$ approaches 5 to 6, use of the higher range is recommended. At this depth, base heave may also take place, and suitable precautions should be taken. For braced or tied-back supports, the pressure distribution envelope is rectangular. The main drawback of this method stems from its dependency on clay shear strength and stability. Design of a suitable shoring and bracing system in soft to firm clay conditions is not a routine task. Therefore, advice from a professional is required to determine earth pressures, to check overall stability and base heave, and to predict soil movements adjacent to a proposed excavation (NBCC, 2015).

From the above discussion, it appears that calculating earth pressure on a flexible retaining structure is not straightforward. The literature review encompassing previous research has identified some limitations in using Terzaghi and Peck's 1967 apparent earth pressure diagrams to determine earth pressure behind externally loaded braced shoring. It also found that the maximum strut loads are significantly higher than those given by Terzaghi and Peck's apparent earth pressure diagrams. Various soil parameters need to be evaluated and should be considered when designing or validating a shoring system in a soft clay excavation or trench (Yokel *et al.*, 1980). Eventually, published research in this field will guide the professional in charge of the project.

1.4 Excavation base stability

The Terzaghi and Peck Method (TPM) does not consider the development of soil failure below the bottom of the excavation. This is known as base stability. Practical observations and finite element studies have demonstrated that soil failure below the bottom of the excavation can lead to very large movements for temporary flexible walls in soft clays. To measure these phenomena, the researchers use a factor called stability number for the excavation base. For clays, the stability number (N_s) is defined as:

$$N_s = \frac{\gamma_{total} H}{S_u} \quad (1.7)$$

where, S_u = average shear strength of the soil above the bottom of the excavation,
 H = depth of excavation, and γ = unit weight of soil.

Henkel (1971) developed an equation considering the stability number to directly obtain apparent soil pressures coefficient (K_A) for the maximum pressure ordinate for soft to medium clays:

$$K_A = 1 - m \frac{4S_u}{\gamma H} + 2\sqrt{2} \frac{d}{H} \left(1 - \frac{5.14S_{ub}}{\gamma H} \right) \quad (1.8)$$

where $m=1$ according to Henkel (1971) and d = depth of soft layer below the bottom of excavation. The total load was then taken as:

$$P = 0.5K_A\gamma H^2 \quad (1.9)$$

Figure 1.2 shows the values of K_A calculated using Henkel (1971) method for various d/H ratios and considering $S_u = S_{ub}$. This indicates that for $4 < N_s < 6$, Terzaghi & Peck (1967) envelope with $m = 0.4$ is much conservative compared to Henkel (1971) method. Even, for N_s

< 5.14 the Henkel (1971) equation is not valid and apparent earth pressures calculated using $m = 1.0$ in the TPM envelope are unrealistically low. For the range $4 < N_s < 5.14$, a constant value of $K_A = 0.22$ should be used to evaluate the maximum pressure ordinate for the soft to medium clay apparent earth pressure envelope (Henkel, 1971).

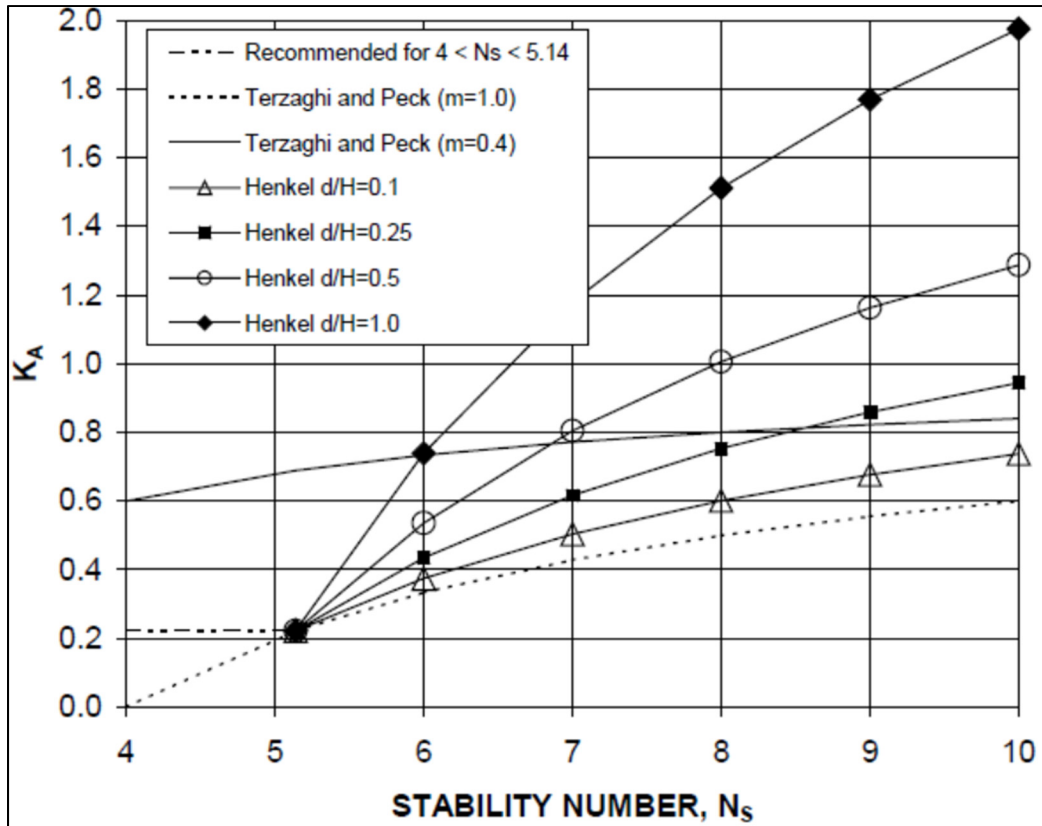


Figure 1.2 Comparison of apparent lateral earth pressure coefficients with basal stability index
Taken from Henkel (1971)

Henkel (1971) method is limited to cases where the clay soils on the retained side of the excavation and below the excavation have a constant value for undrained shear strength. For $N_s > 6$, relatively large areas of retained soil near the excavation base are expected to yield (formation of slip surface) significantly. When large movements below the excavation occurs as the excavation progresses, increased loads on the exposed portion of the wall leads to potential instability of the excavation base as shown in Figure 1.3.

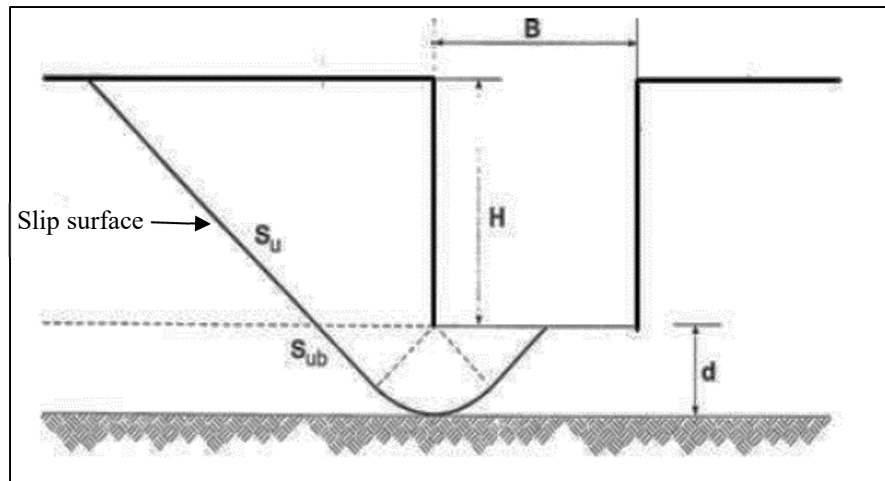


Figure 1.3 Mechanism of base failure
Taken from Henkel (1971)

1.5 Movement and ground deformation of the support system

In flexible and semi-flexible supporting structures, excavations face other major difficulties of movement, e.g. horizontal displacement and vertical settlement, due to the earth pressure and different soil types. Clough & O'Rourke (1990) showed the general pattern of the ground movement and adjacent ground deformation as illustrated in Figure 1.4.

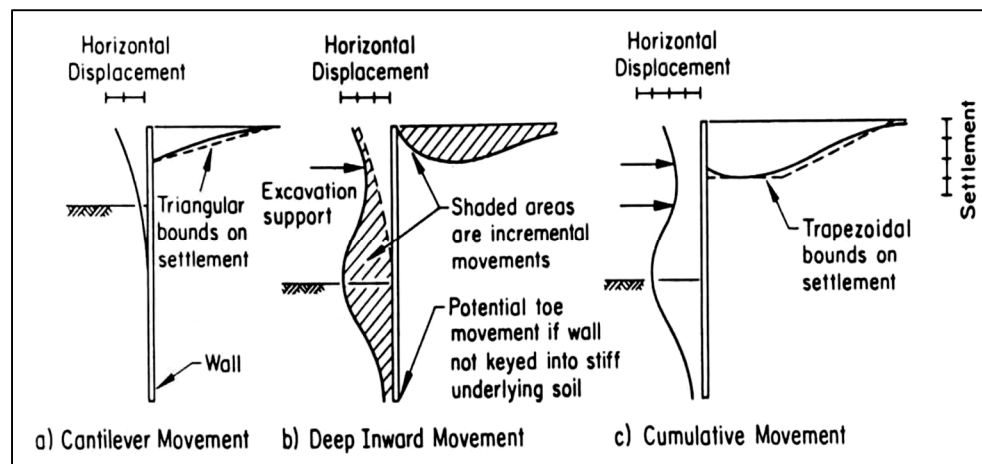


Figure 1.4 Typical profiles of movement for braced and tied back walls
Taken from Clough & O'Rourke (1990)

To estimate the pattern of vertical movement due to the settlement of surface adjacent to the excavation in different soil classes, a dimensionless profile, shown in Figure 1.5, is recommended by Clough & O'Rourke (1990). With the knowledge of maximum settlement, these dimensionless diagrams can be used to obtain an estimate of the actual surface settlement. In using these diagrams, it should be recognized that they are related to settlements caused during the excavation and bracing stages of construction. Excavations in stiff to very hard clays show variable behaviours like 'heave' for some cases. The dimensionless diagram in Figure 1.5 should be used as a conservative estimate, assuming that the wall is stable and not affected by poor construction practices.

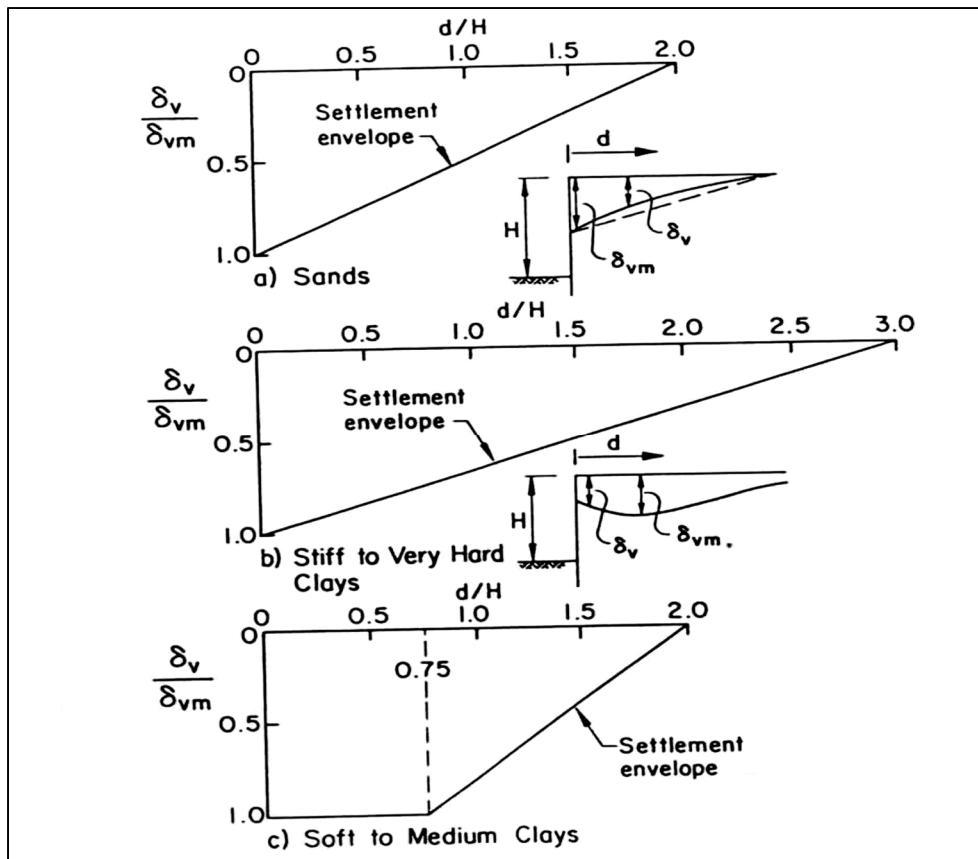


Figure 1.5 Dimensionless settlement profiles recommended for estimating the distribution of settlement adjacent to excavation in different soil types
Taken from Clough & O'Rourke (1990)

1.6 Excavation stage

Bowles (1996) summarized Terzaghi and Peck's design method using apparent earth pressure and produced a diagram of staged earth pressure developed during excavation and strut installation as shown in Figure 1.6.

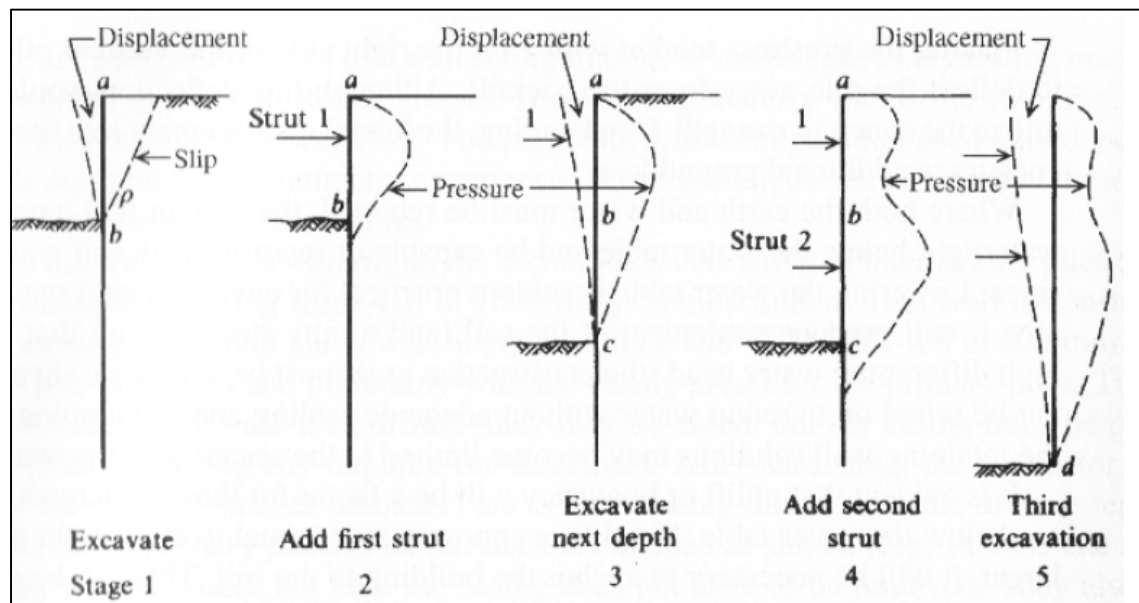


Figure 1.6 Staged development of earth pressure in a braced excavation
Taken from Bowles (1996)

Bowles (1996) found that the strut load produces larger pressure than the active earth pressure and consequently causes increased wall pressure. It follows that, if one measures the pressure in back of this wall, this pressure will be directly related to the strut forces and have little relation to the actual soil pressures involved in moving the wall into the excavation.

1.7 System stiffness

System stiffness is the stiffness of the supporting or the shielding elements used for earth excavation protection. System stiffness is the key element for minimizing the movement that occurs in the excavation. A numerical relationship between normalized maximum wall deformations (δ_n/H), the system stiffness and the factor of safety against basal heave (FOS_{BH})

is shown in Figure 1.7 (Clough & O'Rourke, 1990). The system stiffness is defined as $S = (EI) / (\gamma w h^4)$, where E is the Young's modulus of the wall, I is the moment of inertia per unit length of the wall; h is the average strut spacing, w is the unit weight of the water and γ is the unit weight of the soil. In soft to medium clays, maximum movements are a function of the value of FOS_{BH} which is related to the excavation height to width (H/B) ratio, depth of clay layer (D) under the excavation base and the bearing capacity of the soil (N_c). To calculate N_c factor properly, Skempton (1951) developed a chart, shown in Figure 1.8, that represents the relation between N_c and H/B ratio and shape of the excavation. It is observed that when the FOS_{BH} value is below 1.5, the system stiffness shows a significant influence on movements.

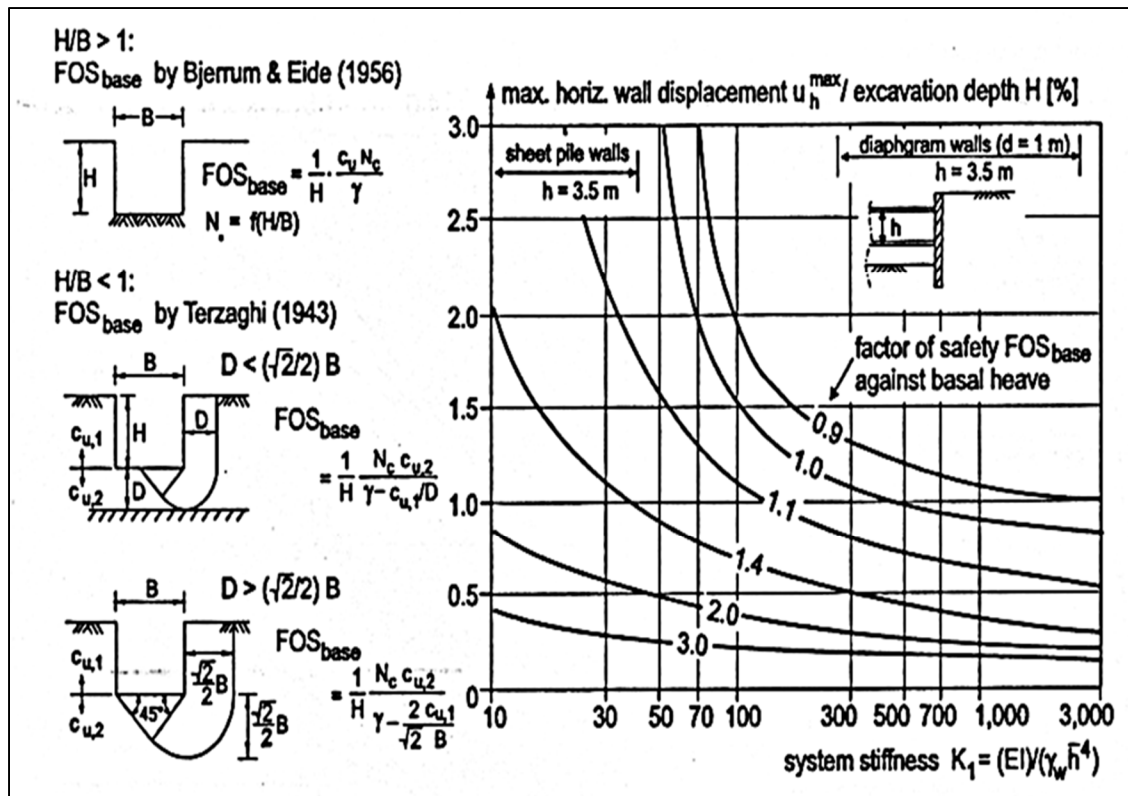


Figure 1.7 Chart for estimating lateral movement (and settlements) for support systems in clays
 Taken from Clough & O'Rourke (1990)

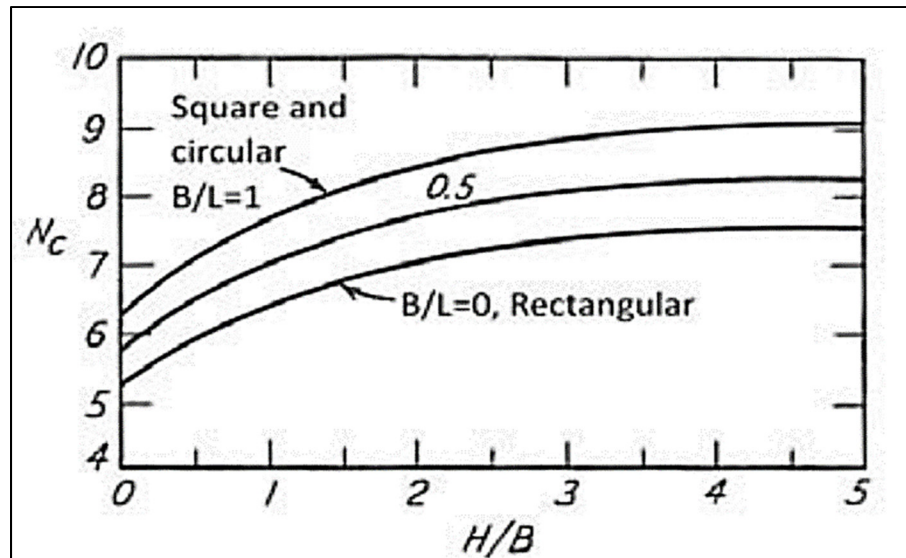


Figure 1.8 Bearing capacity values
Taken from Skempton (1951)

1.8 Review of field and laboratory experimental research

Bose and Som (1998) analyzed an instrumented section of braced cut in 13.6 m deep soft clay. Their study showed that wall length and width of excavation influence the soil-wall deformation as well as the lateral force. According to Wang (2001), the strut loads are variable with construction sequence, shoring stiffness, ground and water conditions, temperature changes, and perhaps more importantly the workmanship of the contractor. Therefore, there exist no method yet that can accurately predict the real structural forces.

Very few published field or laboratory experimental research studies encompass the scope of validation of a flexible temporary shoring used in a trench or an excavation in soft and sensitive clay soil. In addition, there are very few experimental statistics for soil pressure in this type of sensitive clay. Table 1.1 presents the field performance for different types of soil with depths less than 9 m, based on available research.

Table 1.1 Field performance data inside an excavation or trench

| Reference | Depth of Excavation Range (m) | Soil Type | Support Type | Protection Type | Major Findings | Does the method discuss soil pressure in sensitive clay? |
|-------------------------------|-------------------------------|--------------------|---|----------------------------|---|--|
| Casagrande (1973) | 8.5 | Sand | | Concrete wall | Soil pressure | No |
| Goldberg <i>et al.</i> (1976) | 5.9 to 7.9 | Soft to stiff clay | Tied-back anchor, bracing, prestressed, bracing | Diaphragm wall, sheet pile | Maximum horizontal and vertical deflections | No |
| Lan <i>et al.</i> (1999) | 3.7 | Sand, Silty sand | HSS frame | Aluminum panel | Soil pressure | No |
| LaBaw (2009) | 3.048 | Sand and clay | Pneumatic shore strut | Strongback and panel | Field tests measured horizontal and vertical strains | No |
| Bose and Som (1998) | 13.6 | soft clay | braced cut | - | length and width of excavation influence the soil-wall deformation as well as the lateral force | No |

Table 1.1 shows the need for experimental in-situ tests for this type of sensitive clay. In addition, the performance of existing temporary flexible shoring systems for trenches or excavations must be validated. There are two reasons behind studying measured field performance data for excavations or trenches. First, the performance observed in an excavation or trench gives insight and experience that are useful during design and construction of real excavations and trenches. Second, many factors observed from field performance studies cannot be modelled analytically; support wall construction and workmanship are examples of such factors.

1.9 Review of Finite element analysis research

Our understanding of the behaviour of excavations and trenches with flexible retaining walls was enhanced significantly in recent years with the help of numerical finite-element and analytical methods. It is now known that calculating support for an excavation requires careful consideration of global and local soil stability, structural capacity of the supporting elements, and control of ground deformation and pore pressure.

Using finite-element analyses, Goldberg *et al.* (1976) have found that, under a given set of soil conditions, a more rigid wall receives much greater apparent earth pressure than a less rigid flexible wall. Ou *et al.* (1996) has used a three-dimensional finite element technique to study the effect of corners on the deflection behavior of a deep excavation in soft to medium clayey subsoil stratum. A study by Hashash and Whittle (2002) on shoring excavations in clay has shown that the evolution of lateral thrust on a retaining structure (or wall) is a complex function of the flexibility of the retaining structure and the magnitude of shear deformations at depth. Their analyses also revealed the development of an arching effect in the ground in contact with the shoring. Karlsrud and Andresen (2005) concluded that the development of earth pressure on supporting structures set up in sensitive clays is a complex function that depends on the flexibility of the support, the anisotropy property, the thickness of the clay layer in the trench bottom, and deformations in the clay layer.

According to Poulos *et al.* (2002), the construction details, the construction sequence, and the soil-structure interactions have a significant impact on the movements and lateral loads acting on the flexible retaining structure. Karlsrud and Anderson (2005) performed a parametric finite element analysis for a strutted sheet pile wall in soft clay. The modeled excavation is 10 m (32.8 ft) deep and 16 m (52.5 ft) wide. The sheet pile wall is braced internally with four struts at depth 1 m (3.3 ft), 3.5 m (11.5 ft), 6 m (19.7 ft), and 8 m (26.2 ft). The excavation was performed sequentially in five steps to a depth of 0.5 m (1.6 ft) below the struts with successive installation of the struts. The variables were the shear strength of the clay and strut loading.

The parametric study determined the earth pressure and bending moments in the sheet pile wall.

Finno and Blackburn (2006) used a three-dimensional finite element analysis of a 10 m (32.8 ft.) deep excavation sequence in an internally supported excavation through medium stiff clay. They compared between the measured strut loads and the results of the three-dimensional finite element solution. They showed that for uniform excavation sequences, the loading on the lower level struts was under-predicted, whereas the force on the upper struts was over-predicted. Again, Blackburn and Finno (2007) built data in an internally braced excavation in soft clay for a particular site. They found that deformations that occurred at the site were within expected values. They also found that the forces in the internal braces were slightly larger than those expected based on Terzaghi and Peck (1967) apparent earth pressure diagram for soft clays. Kung *et al.* (2007) used finite element method on selected hypothetical excavation cases and using stress-strain behavior of soils at small strain levels in a study of braced excavations. Where they developed a simplified semi-empirical model for estimating maximum wall deflection, surface-settlement profile due to excavation in soft to medium clays.

Lam (2010) showed that a database can be used to investigate the relationship between structural response ratio and soil-structure stiffness ratio and to capture the enormous range of wall stiffnesses between sheet piles and thick diaphragm walls. Wall stiffness was found to have a negligible influence on the magnitude of wall bulging displacements for deep excavations supported by fixed-based walls with stiffnesses ranging from sheet pile walls to ordinary reinforced-concrete diaphragm walls. On the other hand, excavations supported by floating walls were found to be influenced by wall stiffness due to the difference in deformation mechanisms. Therefore, the interaction between the soil mass and the support flexibility in the development of lateral loads and the movements of structural elements is significant.

In a finite-element study, Bryson and Zapata-Medina (2012) clearly showed the influence of: (i) horizontal and vertical strut spacing in an excavation support system (ESS) on lateral deformation; (ii) wall stiffness on lateral wall deformation; and (iii) relative stiffness ratio on

lateral wall deformation in three types of clays. In summary, it was found that previous work also identified that linear elastic finite element modeling is a valid method of analyzing deep excavations. However, such analysis has not been used for shallow excavations to date. Other than earth pressure envelopes proposed by Yokel's in 1979, no research examined the earth pressure and strut loading in braced shallow excavations. Previous research does not present any technical analysis of a typical OSHA recommended trench box shoring system.

Table 1.2 summarizes recently published finite-element analysis (FEA) studies of different types of shoring with different depths of excavation. Some of the key words used to construct the table included FEA on excavation with shoring in different types of soil and computer-aided analysis tools using FEA. Only excavations in different types of clays less than 20 m in depth are presented in this table.

From Table 1.2, a research gap can be observed related on the one hand to trench or excavation 'cage'-type protection shoring at shallow depths and on the other hand to validating its performance using FEA. Existing published models may not be able to capture sensitive clays and shallow excavations less than 6 m in depth. Soil-structure interactions (SSI) are not very clear for this type of sensitive soil with this type of supporting structure. FEA software may be a good tool to obtain insight into the effects of SSI in this type of soil and with this type of support. Outcomes of FEA can be validated using the available literature.

Table 1.2 Published finite-element research related to excavation shoring in soft clay

| Authors (Year) | Type of Soil | Strategies and Methodology | Type of Shoring | Excavation Depth | Analysis Tool and Model | Subject of Discussion | Does the paper discuss trench or excavation shoring cage- type protection and its performance? |
|---------------------------------|---|---|---|-----------------------------|--|---|---|
| Hashash and Whittle (1996) | Soft clay | FEM/ parametric study | Diaphragm wall with support | 20 m | ABAQUS With MIT-E3 | Evolution of stresses around a braced excavation in a deep layer of soft clay. | No |
| Karlsrud and Andersen (2005) | Soft clay | FEM/ parametric study | Sheet pile wall with struts | 10 m | PLAXIS | The importance of clay strength and depth of clay layer on earth pressures, strut loads, and bending moments. | No |
| Konstantakos (2008) | Glacio-marine, glacial till, | FEM/ parametric study | Diaphragm wall with support | 20 m | PLAXIS V8.2 and DEEP 2007 | Show displacement results during a benchmark test. | No |
| LaBaw (2009) | Sand and clay | FEM/ parametric study | Strongback and panel with pneumatic strut | 3.048 m | ABAQUS | Soil pressure from strut loads. | No |
| Marr and Hawkes (2012) | Soft clay | FEM/ parametric study | Wall (but not clear about the type) with strut | 16 m | PLAXIS | Displacement-based design method on designing an excavation protection system to keep movements within allowable limit. | No |
| Bryson and Zapata-Medina (2012) | Soft, medium and stiff clay | FEM/ parametric study | Retaining wall with struts and wales | 12.2 m | PLAXIS- 3D | Semi-empirical design method for the selection of an excavation support system stiffness to limit excavation-related ground movement. | No |

CHAPTER 2

PROTECTION PRACTICES FOR TRENCH AND EXCAVATION IN QUEBEC SENSITIVE CLAY SOILS: REVIEW OF CODES, GUIDELINES, AND RESEARCH NEEDS

Miah Alam ^a, Omar Chaallal ^b, Bertrand Galy ^c

^{a, b} Department of Construction Engineering, École de Technologie Supérieure,
1100 Notre-Dame West, Montreal, Quebec, Canada H3C 1K3.

^c Department of Research, Québec Occupational Health and Safety Research Institute
(IRSST), 505 de Maisonneuve Blvd. West, Montreal, H3A 3C2, Canada

Paper published in *Journal of Safety Science, Elsevier*, November, 2020.

2.1 Abstract

Cave-ins are very frequent in the construction industry and present a very serious risk for workers who operate inside trenches or excavations. Studies show that excavations or trenches in Quebec sensitive clay soils are extremely hazardous due to possible severe and sudden loss of soil shear strength. Many North American and European construction safety authorities have already adopted proper methods and excavation protection practices according to their soil classification. This paper reviews existing construction codes and guidelines, as well as published research studies related to worker safety and protection in excavations and trenches in sensitive clay soil. The paper also discusses the needs for research on prevention strategies to eliminate potential cave-in risk sources from occurring in Quebec sensitive clay soil.

2.2 Introduction

Québec soils are made of soft, compressible, and very sensitive marine and glacio-lacustrine deposits (MELCC, 2020). Because of the nature of this soil, trenching and excavation work exposes construction workers to many risks. During earth excavation work, cave-ins are very frequent and present the most serious risk. Among the top three causes for excavation accidents, “cave ins due to lack of sidewall shoring” was identified in second position by Sanni-Annibire *et al.* (2020), and are also recognized as one of the “fatal-four” by OSHA (2011) as

they fall in the “caught-in/between” category (Albert *et al.*, 2020). Malekitabar *et al.* (2016) also considered cave-ins in their top four accident types, after reviewing accidents databases from OSHA and NIOSH. This phenomenon is very often underestimated by the construction industry (Lan & Daigle, 2009). In particular, clay excavations may present many complex phenomena, such as vertical wall and base instability, horizontal movement and ground deformation, and excavation-induced deformation. When excavating in sensitive clays, cave-ins occurring within days or weeks after completion of the excavation are very common (Lafleur, *et al.*, 1987) (Péloquin, 1992). Workers consider deep trenches to be most hazardous in soft clay. However, a survey shows that of the 265 trench fatalities from 1974 to 1986 in North America, about half occurred in trenches 3 m deep or less (Rice, 1992). Among construction workers buried at the bottom of trenches when walls collapsed, a minimum of one or two deaths per year occurred. This represents approximately 1% of deaths resulting from occupational accidents in Quebec, according to an unpublished internal report cited by Lan and Daigle (2009).

The main objectives of the paper are: (i) to provide an overview of excavation and trench work-related accidents, (ii) to present currently available codes and guidelines for trench excavation protection practices for Quebec sensitive clay soil, and (iii) to compare provincial with international codes and guidelines. The paper also discusses some of the main deficiencies that are currently being addressed by researchers in this field, as well as available published research studies related to protection practices in trenches and excavations. Research needs are also considered.

2.3 Statistics for Accidents Related to Excavation and Trench Work

Unexpected accidents are not new for excavation and trench work in construction. Quebec regional analysis reveals that 51 serious and fatal accidents were reported to the Commission de la Santé et de la Sécurité du travail (CSST) at excavation work sites between May 1974 and January 2013 (Lan, 2013). In addition, some statistics on occupational accidents in Ontario, Quebec, the United States (USA), and France regarding soil cave-ins in trenches or excavations

are presented in Table 2.1. Note that some of the data presented in Table 2.1 were published in Lan & Daigle (2009).

Table 2.1 Occupational accidents statistics regarding soil cave-ins in trenches or excavations

| Name of Place | Period of Occurrence | Excavation Depth Range | Number of Serious Injuries | Number of Fatalities | Major Causes | Reporting Authority |
|----------------------|-----------------------------|-------------------------------|-----------------------------------|-----------------------------|---|---|
| Ontario | 1993 | | 350 | 3–4 | | Construction Safety Association of Ontario (CSAO) |
| Quebec | 1974–2008 | 1.7–10 m | 16 | 44 | -no shoring -inappropriate shoring -steep excavation -improper storage close to excavation -struck by machinery -improper work method. | CSST |
| USA | 1985–1989 | | | 239 | -unprotected -vertical -walled excavations greater than 5 ft. in depth. | Occupational Safety and Health Administration (OSHA) |
| USA | 1992–2001 | | | 542 | -cave-ins | Bureau of Labor Statistics |
| USA | 2003 | 1.52–2.74 m | | 53 | -cave-ins -no shoring | OSHA |
| USA | 2008–2012 | | | 85 | -cave-ins | Bureau of Labor Statistics |
| USA | 2013–2017 | | | 97 | -cave-ins | Bureau of Labor Statistics |
| France | 1978–1987 | 0.5–5m or more | 157 | 118 | -cave-ins -handling, falls -stuck | Organisme Professionnel de Prévention du Bâtiment et des Travaux Publics (OPPBTP) |
| France | 1984–1993 | 0.5–5m or more | 98 | 94 | -cave-ins -handling, falls -stuck | OPPBTP |

These statistics demonstrate the vulnerability of workers inside a trench or excavation within the construction industry. They reveal that all the casualties occurred in excavations less than 10 meters in depth and that the main causes of accidents were the lack of proper shoring and safe working practices. This emphasizes the importance for any governmental or local authority to ensure that occupational health and safety regulations are implemented at the work site to protect workers.

2.4 Comparison of Excavation Protection Practices, Codes and Guidelines in Different Jurisdictions

Excavation works in clay soils must be planned with great care by experienced professional engineers (CFEM, 2006). The selection of how to protect excavations or trenches depends on soil geotechnical properties, excavation geometry, and excavation objectives. This imposes a requirement for each country, state, or province to provide occupational safety and health codes or regulations and standards to meet their own local soil and environmental characteristics. These codes and guidelines will be followed by entrepreneurs during excavation and thereby will protect their skilled workers. Table 2.2 shows the Canadian provincial regulations that have adopted a soil classification system. Again, it is important to note from Table 2.2 that OSHA in the United States and most of the Canadian provinces provide a risk prevention strategy through soil classification and an appropriate choice of protection method to eliminate risk sources.

Furthermore, Table 2.2 shows that, in addition to Quebec, the Canadian provinces of Manitoba, New Brunswick, Nova Scotia, Newfoundland and Labrador, and Prince Edward Island do not yet have any soil classification method. A study by the National Bureau of Standards (NBS) shows the need for a soil classification system that can be used by field supervisors to make rapid decisions on sloping or shoring requirements (Yokel *et al.*, 1980). Some of the codes provide an easier soil classification (or type) by adopting the ‘soil strength factor’ indicator. They have clearly shown the importance of soil classification in choosing the type of shoring for trench or excavation work. Table 2.3 shows how various sections of provincial and

international codes describe the necessity of soil classification in terms of excavation or trenching protection.

Table 2.2 Selection of excavation safety methods for excavation shoring systems assuming the soil classification

Adapted from the Canadian provinces and the United States

| Provincial codes of Canada | Does it have excavation safety instructions? | Does it have a soil classification, which helps the entrepreneur in choosing the right protection method for an excavation (sloping or shoring)? |
|-----------------------------------|---|---|
| British Columbia (BC) OSHA | Yes | Yes |
| OHSA, Ontario | Yes | Yes |
| SCCI Quebec | Yes | Not yet |
| OHSC, Alberta | Yes | Yes |
| OHSR, Manitoba | Yes | Not yet |
| OHSR, Saskatchewan | Yes | Yes |
| OHSA, New Brunswick | Yes | Not yet |
| OHSA, Nova Scotia | Yes | Not yet |
| OHSR, Newfoundland and Labrador | Yes | Not yet |
| OHSA, Prince Edward Island | Yes | Not yet |
| OSHA-USA | Yes | Yes |

In contrast, Quebec excavation works are governed by the Quebec Safety Code for the construction industry (SCCI, 2020). In that code, Article 3.15.3 states that “the employer shall ensure that the banks of an excavation or trench are shored solidly with quality materials in accordance with the plans and specifications of an engineer. Shoring is not required in the following cases:

- Where the trench or excavation is dug out of solid rock or where no workers are required to descend into it;
- Where there is no risk for the bank of the trench or excavation to collapse and where the slope is less than 45° from a point located less than 1.2 m from the bottom; and

- Where there is no risk for the banks of the trench or excavation to collapse and where an engineer can attest that shoring the banks is not required given the slope, nature, and stability of the ground. A copy of the engineer's attestation shall be available on the construction site at all times. Solid rock means rock that cannot be excavated otherwise than by blasting."

Table 2.3 Existing clauses related to excavation or trenching protections and soil classification in various codes and regulations (CSAO, 2009) (OSHA, 1989) (British Standards Institution, 2009) (BCOSHA, 2009)

| Name of Places and their Codes/Regulations | Existing clauses or sections relevant to excavation or trenching protection and soil classification in the code or regulation. |
|--|---|
| Ontario, Canada (In Ontario, Canada trench work is governed by Part III: Excavations in Ontario Regulation 213/91 under the Ontario Ministry of Labour.) | <ul style="list-style-type: none"> • Section 222 discusses the engineered, hydraulic, and prefabricated support systems that are usually used in excavation and trench work and the lateral pressure used to design these systems, which must include hydrostatic pressure and pressure due to overloading, according to generally accepted engineering principles. • Section 226 makes soil identification easier. Classifies soil as type 1, 2, 3, or 4. In the description of each type of soil, there is a strength factor that is consistent with geotechnical engineering practices. • Section 234 outlines different kinds of slopes for different soil classes. • Section 237 provides reasons for not allowing prefabricated or hydraulic support systems to be used in type 4 soil. |
| USA (In the United States, excavation and trench works are performed according to the provisions of Part 1926, Subpart P: Authority of OSHA (Occupational Safety and Health Administration) standards under the US Department of Labor) | <p>OSHA recommends maximum slopes based on the type of soil and provides full details for the design of protection systems.</p> <ul style="list-style-type: none"> • Article 1926.652 explains the requirements for protection systems and has six appendices. These appendices provide information on soil classification and the types of shoring to be used. • Appendix A- soil classification; • Appendix B- sloping and benching according to soil class. |
| United-Kingdom (UK) (the main legislation is the Health and Safety at Work, etc. Act 1974) | <ul style="list-style-type: none"> • The Code of Practice for earthworks (BS 6031) of the British Standards Institution (2009) discusses soil classification systems. |
| BC OSHA (Part 20 of the OHS Regulation, 2009) | <ul style="list-style-type: none"> • BC OSHA recommends maximum slopes based on the type of soils and provides full details for designing protection systems |

| | |
|--|---|
| | <ul style="list-style-type: none"> • Section 20.85 of the OHS Regulation describes each soil class and the related type of shoring to be used. |
|--|---|

From the above code statement, it can be concluded that the Quebec protection system is not very clear and that, contrary to the other codes, it does not refer to any related soil classification to choose the right protection method for an excavation. The question is whether a protection system such as sloping, benching, shielding, or shoring is appropriate for the specific soil condition or soil type under consideration. Table 2.4 presents existing codes and regulations regarding excavations and how they relate to soil classification and excavation protection systems in different parts of the world.

In addition to the trench or excavation safety code, the construction safety guidelines also provide the risk prevention strategies and soil classification systems required to protect the trench or excavation. The OPPBTP (1989) guidelines discuss methods based on current regulations in France. The guidelines focus on the risks present in the soils where excavation work is contemplated and the sloping and shoring required (OPPBTP, 1989), but are not clear about the soil classification system. The trenching practices guide of the Construction Industry Research and Information Association (CIRIA) explains the methods specified in current regulations in the United Kingdom. It focuses on the risks involved in excavation work, trench depth, earth movement, soil identification, soil hydraulic conditions, and the various shoring methods available (Irvine & Smith, 1983). It also provides guidelines on soil identification to help select an appropriate protection system. The guide trenching safety provisions in CSAO (2009) provide information related to the safety of workers that are involved in trenching projects or must enter trenches in the course of their work.

These sections relating to excavations are part of the regulations for construction projects under the Occupational Health and Safety Act of Ontario. This manual explains the causes of injury and death related to trenching, as well as the probable reasons for cave-ins. It also provides three methods of protection against cave-ins and discusses other trenching hazards and safeguards as well as emergency procedures. This information assists workers in identifying trenching hazards and in choosing the appropriate protection required (CSAO, 2009). In

comparison, the accident prevention guide for trenches and excavations of the Quebec Association Sectorielle Paritaire (ASP) - Secteur Construction (2018) illustrates preventive tools and expresses a set of recommendations coming from the regulation respecting occupational health and safety for employers and employees involved in excavation and trench works (S-2.1, r.6) in Quebec. Table 2.5 provides a comparison among the guidelines regarding soil classification for trench and excavation protection and accident prevention methods. The table reveals that the Quebec ASP guide fails to consider soil classification for excavation protection.

Table 2.4 Comparison among different codes in terms of soil classification

| Regulations | Does the code discuss preventive tools and methods for excavation or trenching? | Does the code discuss soil classification? | Does the code discuss excavation protection technique? | |
|--|---|---|---|---|
| | | | Sloping | Shoring/shielding |
| Ontario, Canada | Yes | Yes, it has a very clear soil classification system. | Yes, and it is related to the soil classification. | Yes, and it is related to the soil classification. |
| Quebec, Canada | Yes | Not yet | Yes, with the help of a professional engineer not related to the soil classification. | Yes, with the help of a professional engineer not related to the soil classification. |
| OSHA, USA | Yes | Yes, it has a very clear soil classification system. | Yes, it is related to the soil classification. | Yes, it is related to the soil classification. |
| National Bureau of Standards (NBS) / National Institute for Occupational Safety and Health (NIOSH) (USA) | Yes | Yes, OSHA has engaged NBS to review the technical provisions. | Yes, OSHA has engaged NBS to review the technical provisions. | Yes, OSHA has engaged NBS to review the technical provisions. |
| Australia (Safe Work Australia, 2015) | Yes | Not clear | Yes | Yes |
| United Kingdom (UK) (BS 6031:2009) | Yes | Yes, it has a very clear soil classification system. | Yes, it refers to the soil classification. | Yes, it refers to the soil classification. |

| | | | | |
|--|-----|--|--|--|
| France (Title IV, Title XII, R255 and R293) | Yes | Yes, it has a very clear soil classification system. | Yes, it refers to the soil classification. | Yes, it refers to the soil classification. |
|--|-----|--|--|--|

International regulations in this area of expertise, such as those of OSHA and the California Occupational Safety and Health Administration (Cal/OSHA), have revealed the importance of soil classification. This helps the entrepreneur to choose the right shoring or protection method for trench or excavation work and a selection method for shoring systems that is adapted to the soil classification. It follows that there is a research need within the scope of existing available protection systems used by the construction industry in trenching and excavation. This may include in-situ tests for evaluating soil pressure on shoring systems, load transfer mechanisms between the soil and the structure, and validation and design through numerical studies. These research initiatives will help to develop guidelines or an insightful support system that facilitates the choice of the right shoring system given the soil type.

Table 2.5 Comparison of existing guidelines

| Guide | Does it discuss soil classification? | Does it discuss excavation protection techniques? | | Does it discuss preventive tools and methods for excavation or trenching? |
|--|--------------------------------------|---|-------------------|---|
| | | Sloping | Shoring/shielding | |
| OPPBTP Guide, France | Yes | Yes | Yes | Yes |
| CIRIA Guide, United Kingdom (UK) | Yes | Yes | Yes | Yes |
| BS6031, United Kingdom (UK) | Yes | Yes | Yes | Yes |
| CSAO, Ontario, Canada | Yes | Yes | Yes | Yes |
| ASP Construction, Quebec, Canada | No | Yes | Yes | Yes |
| Commission des normes, de l'équité, de la santé, et de la sécurité du travail (CNESST) | No | Yes | Yes | Yes |
| Australia (safe work) | No | Yes | Yes | Yes |

2.5 Recent Research on Excavations or Trenches with Shoring and Research Needs

Protected earth excavation or trenching in soft clay soils falls into two types: unsupported (sloped) and supported (braced) shoring. Sloped excavations are used when excavation is shallow and when the site dimensions allow digging embankments with gentle slopes to ensure site safety. The design of sloping and benching and the execution of work must be performed strictly in accordance with local regulatory and professional engineering requirements. For clay soil, excavation work may present many complex challenges, and therefore professionals and entrepreneurs must exercise great caution. According to CFEM (2006), in excavations in sensitive clays, slope failures are very common within days or weeks after the excavation is completed. A significant finding is that the stability of excavations depends on the overall time required to dissipate pore water pressures (CFEM, 2006).

Supported excavations are most common in the construction field. Flexible and semi-flexible supporting structures are used as temporary supports for the vertical sides of excavations. The technical report by Lan *et al.* (2008) pointed out that in Quebec, more than 7460 excavations are carried out annually and that 75% of them are deeper than 1.22 m (4 ft). This indicates the importance of tools that can be used to choose the appropriate shoring system for safety during earth excavation work. The same study report identified a total of 26 common shoring systems that are available in the market and used in Quebec. These systems can be classified into four distinct categories: caissons, hydraulic cylinders, pipes, and trench boxes. Clearly, there is a need for guidelines for selecting the shoring and shielding system that is best suited to the soil class (Lan *et al.*, 2008).

Shored excavations give rise to various complex behavioural phenomena such as base instability, horizontal movement, ground deformation, hydrostatic uplift, and excavation-induced deformations (CFEM, 2006). Researchers have shown a large and growing interest in this field to resolve these problems with their extensive endeavours. OSHA (2015) identifies various modes of geotechnical breakage inside trenches or excavations without shoring, such as tension, sliding, toppling, bulging, heaving, squeezing, and boiling. Five main factors were

found to affect the stability of excavation walls, particularly for soft and sensitive clays: soil shear strength, excavation duration, excavation geometry, water table, and working methods (Lafleur *et al.*, 1987).

The earth pressure distribution depends on the type of soil, the shoring, and the method of implementation. Generally, no satisfactory theoretical solutions are available to estimate soil pressure for supporting structures with partitions facing land pressures in sensitive clay (NBCC, 2015). Many researchers have suggested theoretical solutions to estimate the earth pressure on a flexible temporary support. For rigid retaining structures such as weight-standing walls, soil and water pressures can be calculated in many cases from theory (CFEM, 2006). For a rigid wall such as a retaining wall, the passive earth pressure created behind the wall is different from that generated on a flexible screen; the elements do not repeat the same stresses and deform differently. The pressure distribution depends on the type of shield and the method of implementation. Consequently, for an excavation shield, the Canadian Foundation Engineering Manual (CFEM) recommends the use of pressure envelopes from empirical data. According to Rankine (1857), the total active thrust over the excavation depth on a smooth wall for clays can be expressed as:

$$P_{\text{Rankine}} = 0.5(\gamma H^2 - 4s_u H). \quad (2.1)$$

This method typically uses Rankine active and passive earth pressure coefficients. However, excavation support systems designed to limit movement do not develop Rankine earth pressure conditions. Nevertheless, the method presents advantages related to simplicity and ease of calculation. To determine the apparent earth pressure for sand and soft to medium clay, Terzaghi and Peck (1967) proposed a soil pressure diagram for a temporary retaining structure, as illustrated in Figure 2.1.

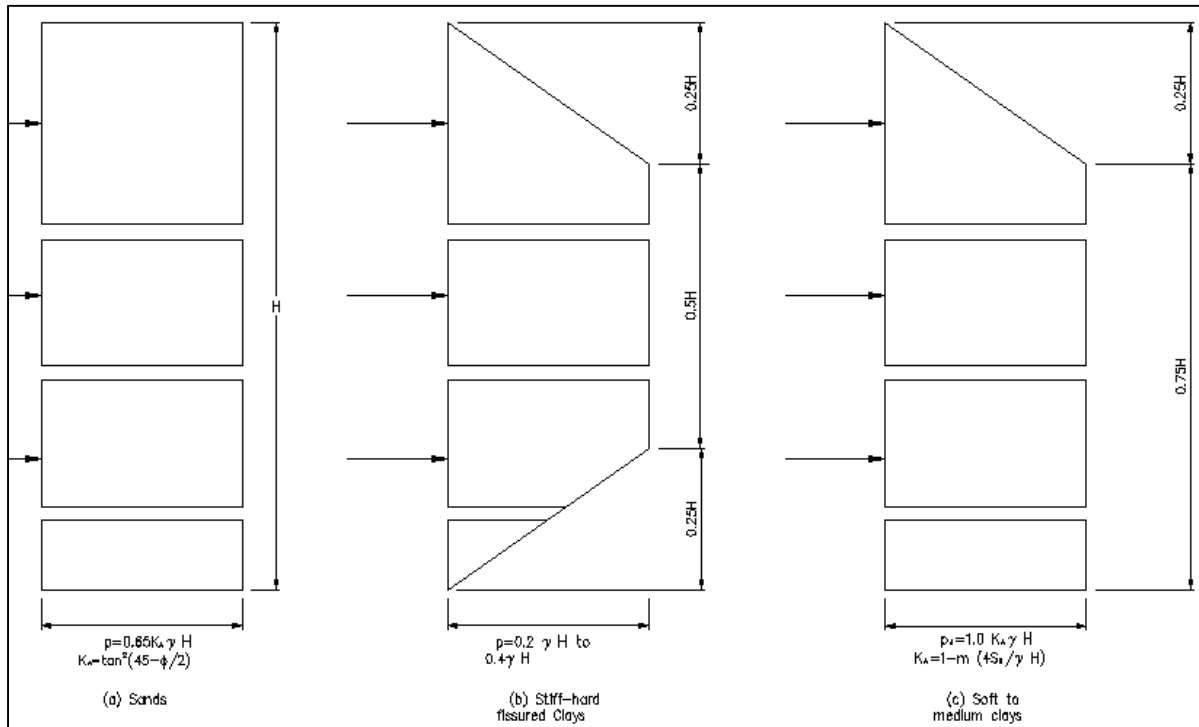


Figure 2.1 Apparent earth pressure diagram for sand and stiff and soft to medium clay
Taken from Terzaghi & Peck (1967)

The soil pressure can be calculated as:

$$p_A = K_A \gamma H, \quad (2.2)$$

where $K_A = 1 - \frac{m 4 s_u}{\gamma H}$

$$P_A = 0.775 H p_A = 0.775 (\gamma H^2 - m 4 s_u H) \quad (2.3)$$

where m is an empirical factor accounting for potential base instability effects in deep excavations in soft clays. When the excavation is underlain by deep soft clay and dimensionless number, $(N = \gamma H / s_u)$ exceeds 4, then m is set to 0.4; otherwise, m is set to 1 (Flaate, 1966). These formulas are clearly understood and easy to estimate, but the method does not account for the development of soil failure below the bottom of the excavation. Again, in this method it was assumed that the distance from the lowest strut to the excavation bottom corresponds to

20% of the excavation depth and that the load on the lowest strut is computed by multiplying the pressure (p_A) by half the distance to the strut above plus half the distance below the bottom of the excavation.

Henkel (1971) proposed to modify the equation of the Terzaghi and Peck method (TPM) used to calculate soil pressure in medium to soft clays by assuming a failure mechanism compatible with a deeper location of the fracture plane. Back-calculated values by Henkel indicated that TPM underestimates the coefficient of active earth pressure. Assuming the basal stability phenomenon, Henkel (1971) proposed that apparent earth pressure for soft to medium clay be calculated as follows:

$$p_A = \left(1 - \frac{4s_u}{\gamma H} + \Delta K\right) \gamma H, \quad (2.4)$$

where ΔK is a factor related to bottom heave stability, given by:

$$\Delta K = \frac{2B}{H \left(1 - \frac{5.14S_{ub}}{\gamma H}\right)}. \quad (2.5)$$

The Henkel method is limited to cases where the clay soils on the retained side of the excavation and below the excavation have a constant value for the undrained shear strength of soil.

The Federal Highway Administration (FHWA, 1999) recommends an apparent earth pressure with different levels of ground anchors for stiff to hard clays. In this way, apparent earth pressure diagrams are used to estimate the pressure of stiff to hard clay excavations on the anchor supports. The forces at different levels of ground anchors are easy to determine. This method results in the lower braces carrying smaller loads. That observation has misled engineers to extrapolate the apparent lateral earth pressure to zero at subgrade. That assumption is not backed by any scientific evidence (Konstantakos, 2015). The work of FHWA resulted

in alternative formulations for deposits of sand and stiff clay. Stress distribution is particularly influenced by the position of the struts or anchors, and improved formulations are now recommended. From the proposed modification of apparent lateral earth pressure diagrams, the subgrade reaction at the bottom of excavation is easy to calculate. If tighter deformation control is required or when fully undrained conditions are to be expected, then the virtual reaction at the subgrade level must take into account increased lateral earth pressures that can reach close to 50% of the total vertical stress at the subgrade level. Excavations with clays on both wall sides, if fully dewatered, will not satisfy this method (Konstantakos, 2015).

The National Building Code of Canada (NBCC, 2015) proposes a method to determine the earth pressure envelope for the design of temporary supports for soft to firm clays. For cantilever support, the design total pressure = $1.0 P_A$, where:

$$P_A = \rho g H - 2C_u, \quad (2.6)$$

where ρ = total (bulk) density of soil (submerged if below ground water), kg/m^3 , C_u = undrained shear strength, H = depth of cut, and g = acceleration due to gravity (m/s^2). P_A should be not less than $0.15 \rho g H^2$ and may be computed using short-term strength if the excavation is open for a limited period. Regardless of whether pressures are negative or zero, the minimum positive pressure indicated should be used. In this method, the pressure distribution envelope for cantilever support is triangular. This cantilever support can restrict the movement of adjacent soil. This type of support is generally very poor and should be avoided in soft sensitive clays. For braced or tied-back support, the design total pressure lies between $0.4 \rho g H^2$ and $0.8 \rho g H^2$. The higher range should be used where the clay is of soft consistency and the lower range where the clay is of firm consistency. This value may be conservative for non-homogeneous, non-sensitive sandy-silt cohesive soil of firm consistency. If the stability number $(N) = (\rho g H + \text{overload})/C_u$ approaches 5 to 6, use of the higher range is recommended. At this depth, base heave may also take place, and suitable precautions should be taken. For braced or tied-back supports, the pressure distribution envelope is rectangular. The main drawback of this method is its dependency on clay shear strength and stability. Design of a

suitable shoring and bracing system in soft to firm clay conditions is not a routine task, and advice from a professional is required to determine earth pressures, to check overall stability and base heave, and to predict soil movements adjacent to a proposed excavation (NBCC, 2015).

From the above discussion, it seems that calculating earth pressure on a flexible retaining structure is not straightforward. Various soil parameters need to be evaluated and should be considered when designing or validating a shoring system in a soft clay excavation or trench (Yokel *et al.*, 1980). Eventually, published research in this field will guide the professional in charge of the project. Published field or laboratory experimental research studies are very few within the scope of validation of a flexible temporary shoring used in a trench or an excavation in soft and sensitive clay soil. In addition, there are very few experimental statistics for soil pressure in this type of sensitive clay. Table 2.6 represents the field performance for different types of soil for depths less than 9 m, based on available research. Table 2.6 shows the need for experimental in-situ tests for this type of sensitive clay. In addition, the performance of existing temporary flexible shoring systems for trenches or excavations must be validated.

There are two reasons behind studying measured field performance data for excavations or trenches. First, the performance observed in an excavation or trench gives insight and experience that are useful during design and construction of real excavations and trenches. Second, many factors observed from field performance studies cannot be modelled analytically; support wall construction and workmanship are examples of such factors.

Table 2.6 Field performance data inside an excavation or trench

| Reference | Depth of Excavation Range (m) | Soil Type | Support Type | Protection Type | Major Findings | Does the method discuss soil pressure in sensitive clay? |
|-------------------------------|-------------------------------|--------------------|---|----------------------------|--|--|
| Casagrande (1973) | 8.5 | Sand | | Concrete wall | Soil pressure | No |
| Goldberg <i>et al.</i> (1976) | 5.9 to 7.9 | Soft to stiff clay | Tied-back anchor, bracing, prestressed, bracing | Diaphragm wall, sheet pile | Maximum horizontal and vertical deflections | No |
| Lan <i>et al.</i> (1999) | 3.7 | Sand, Silty sand | HSS frame | Aluminum panel | Soil pressure | No |
| LaBaw (2009) | 3.048 | Sand and clay | Pneumatic shore strut | Strongback and panel | Field tests measured horizontal and vertical strains | No |

Our understanding of the behaviour of excavations and trenches with flexible retaining walls has developed significantly in recent years with the help of numerical finite-element and analytical methods. It is now known that calculating support for an excavation requires careful consideration of global and local soil stability, the structural capacity of the supporting elements, and control of ground deformation and pore pressure. Using finite-element analyses, Goldberg *et al.* (1976) have found that, under a given set of soil conditions, a more rigid wall receives much greater apparent earth pressure than a less rigid flexible wall. A study by Hashash and Whittle (2002) on shoring excavations in clay has shown that the evolution of lateral thrust on a retaining structure (or wall) is a complex function of the flexibility of the retaining structure and the magnitude of shear deformations at depth. Their analyses also revealed the development of an arching effect in the ground in contact with the shoring. Karlsrud and Andresen (2005) concluded that the development of earth pressure on supporting structures set up in sensitive clays is a complex function that depends on the flexibility of the support, the anisotropy property, the thickness of the clay layer in the trench bottom, and deformations in the clay layer. According to Poulos *et al.* (2002), the construction details, the construction sequence, and the soil-structure interactions have a significant impact on the movements and lateral loads acting on the flexible retaining structure.

Lam (2010) showed that a database can be used to investigate the relationship between structural response ratio and soil-structure stiffness ratio and to capture the enormous range of wall stiffnesses between sheet piles and thick diaphragm walls. Wall stiffness was found to have a negligible influence on the magnitude of wall bulging displacements for deep excavations supported by fixed-based walls with stiffnesses ranging from sheet pile walls to ordinary reinforced-concrete diaphragm walls. On the other hand, excavations supported by floating walls were found to be influenced by wall stiffness due to the difference in deformation mechanisms. Therefore, the interaction between the soil mass and the support flexibility in the development of lateral loads and the movements of structural elements is significant. In a finite-element study, Bryson and Zapata-Medina (2012) clearly showed the influence of horizontal and vertical strut spacing in an excavation support system (ESS) on lateral deformation, of wall stiffness on lateral wall deformation, and of relative stiffness ratio on lateral wall deformation in three types of clays.

Table 2.7 summarizes recently published finite-element analysis (FEA) studies of different types of shoring with different depths of excavation. Some of the key words used to construct the table included FEA on excavation with shoring in different types of soil and computer-aided analysis tools using FEA. Only excavations in different types of clays less than 20 m in depth are presented in this table. From Table 2.7, a research gap can be observed related on the one hand to trench or excavation ‘cage’-type protection shoring at shallow depths and on the other hand to validating its performance using FEA. Existing published models may not be able to capture sensitive clays and shallow excavations less than 6 m in depth. Soil-structure interactions (SSI) are not very clear for this type of sensitive soil with this type of supporting structure. FEA software may be a good tool to obtain insight into the effects of SSI in this type of soil and with this type of support. Outcomes of FEA can be validated using the available literature.

Table 2.7 Published finite-element research related to excavation shoring in soft clay

| Authors (Year) | Type of Soil | Strategies and Methodology | Type of Shoring | Excavation Depth | Analysis Tool and Model | Subject of Discussion | Does the paper discuss trench or excavation shoring cage-type protection and its performance? |
|---------------------------------|--|---------------------------------------|--|-----------------------------|--|--|--|
| Hashash and Whittle (1996) | Soft clay | FEM/ parametric study | Diaphragm wall with support | 20 m | ABAQUS With MIT- E3 | Evolution of stresses around a braced excavation in a deep layer of soft clay. | No |
| Karlsrud and Andersen (2005) | Soft clay | FEM/ parametric study | Sheet pile wall with struts | 10 m | PLAXIS | The importance of clay strength and depth of clay layer on earth pressures, strut loads, and bending moments. | No |
| Konstantakos (2008) | Glacio- marine, glacial till, | FEM/ parametric study | Diaphragm wall with support | 20 m | PLAXIS V8.2 and DEEP 2007 | Show displacement results during a benchmark test. | No |
| LaBaw (2009) | Sand and clay | FEM/ parametric study | Strongback and panel with pneumatic strut | 3.048 m | ABAQUS | Soil pressure from strut loads. | No |
| Marr and Hawkes (2012) | Soft clay | FEM/ parametric study | Wall (but not clear about the type) with strut | 16 m | PLAXIS | Displacement-based design method on designing an excavation protection system to keep movements within allowable limit. | No |
| Bryson and Zapata-Medina (2012) | Soft, medium and stiff clay | FEM/ parametric study | Retaining wall with struts and wales | 12.2 m | PLAXIS-3D | Semi-empirical design method for the selection of an excavation support system stiffness to limit excavation-related ground movement. | No |

2.6 Conclusions

The statement of topics discussed above gives a general idea of the research needs to improve Quebec soil excavation or trench safety. It also provides a better understanding of the generalized behaviour of the shoring system given the Quebec soil class. This study points out the urgency of initiating a study aimed at classifying Quebec soils and selecting appropriate shoring systems for trenches and excavations to overcome the deficiency in the Quebec construction code. Quebec has taken an initiative for soil classification, which will be an asset for the selection of appropriate excavation shoring protection for any construction site in Quebec (Lan & Daigle, 2009). The current study is aimed at addressing these issues raised during earth excavation and developing a decision-making guideline for selecting a shoring system suitable for the Quebec soil class (Lan & Daigle, 2009). The main objectives of the study suggested by the Institut de Recherche Robert-Sauvé en Santé et en Sécurité du Travail (IRSST) are as follows:

- To classify soils in urban areas of the Province of Quebec;
- To develop a simple method for determining the *in-situ* class of soil and to estimate the soil pressure of a site before performing excavation and shoring;
- To validate the strength and behaviour of shoring systems for different classes of soil and loading conditions; and
- To develop a decision-support system for selecting a shoring system considering geological, geotechnical, and structural factors.

CHAPTER 3

FIELD TEST OF TEMPORARY EXCAVATION WALL SUPPORT IN SENSITIVE CLAY

Miah Alam ^a, Omar Chaallal ^b, Bertrand Galy ^c

^{a, b} Department of Construction Engineering, École de Technologie Supérieure,
1100 Notre-Dame West, Montreal, Quebec, Canada H3C 1K3.

^c Department of Research, Québec Occupational Health and Safety Research Institute
(IRSST), 505 de Maisonneuve Blvd. West, Montreal, H3A 3C2, Canada

Paper published in *ISSMGE International Journal of Geoengineering Case Histories*,
May, 2021.

3.1 Abstract

This paper presents the results of a field experimental study carried out to investigate the soil pressure on a temporary flexible trench shoring in sensitive clay. The installation, instrumentation, and field test procedures are presented for two trench boxes “stacked upon each other” in conformity with United States OSHA regulations and placed inside the trench to cover the total 6 m (20 ft) depth of excavation. The field test results are presented in terms of soil pressure distribution along the depth of excavation with and without a 45 kPa surface surcharge next to the edge of one side of the trench. The results reveal the potential use of an existing excavation and trench shoring system in this type of soil and validate its performance with published theoretical results. In terms of soil pressure distribution along the trench, the analytical formulae generally underestimated the experimental values for the type of sensitive clay considered in this study.

3.2 Introduction

Earth excavation and related trench protection safety for workers are growing concerns worldwide. As a protection system, the trench box shield is different from other shoring systems. The reason is that it is intended not only to shore up or otherwise support the trench face, but to also protect workers from cave-ins or similar incidents inside the trench. Multiple

trench boxes can be assembled to create a box system capable of shoring up trenches up to 11 m (35 ft) deep (Macnab, 2002). This system is easy to transport, assemble, and install in narrow trenches. Shields may not be subjected to loads exceeding those that the system can withstand (OSHA, 2015). The earth pressure distribution on a shield depends on the type of soil, the shoring, and the method of implementation. Generally, no satisfactory consensual theoretical solutions are available to estimate soil pressure for this type of supporting structure with partitions facing land pressures in sensitive clay (NBCC, 2015). Many researchers have suggested theoretical solutions to estimate earth pressure on a flexible temporary support. Consequently, for an excavation shield, the Canadian Foundation Engineering Manual (CFEM, 2006) recommends the use of pressure envelopes from empirical data.

Terzaghi and Peck (1967) methods (TPM) for estimating apparent earth pressure are highly popular among practitioners because they are clearly understood and easy to implement. A typical expression is:

$$p_A = K_A \gamma H, \quad (3.1)$$

where K_A is the coefficient of earth pressure, $K_A = 1 - \frac{m^4 s_u}{\gamma H}$, γ is the unit weight of soil, H is the depth of excavation, S_u is the average undrained shear strength value over the height of the wall, and m is an empirical factor accounting for potential base instability effects in deep excavations in soft clays. Figure 3.1 shows a diagram proposed by the authors representing apparent earth pressure on a flexible retaining structure in soft to medium clay.

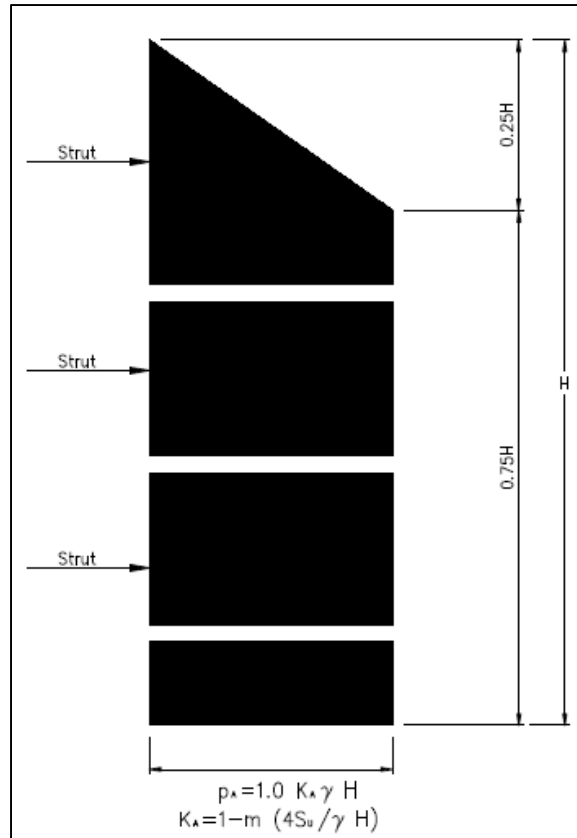


Figure 3.1 Apparent earth pressure diagram
for soft to medium clay
Taken from Terzaghi & Peck (1967)

When the excavation is underlain by deep soft clay and the dimensionless number ($N = \gamma H/s_u$) exceeds 4, then m is set to 0.4; otherwise, m is set to 1.0 (Flaate, 1966). These formulae are clearly understood and easy to estimate; however, the method does not account for the development of soil failure below the bottom of the excavation. Again, in this method, it was assumed that the distance from the lowest strut to the excavation bottom corresponded to 20% of the excavation depth and that the load on the lowest strut was computed by multiplying the pressure (p_A) by half the distance to the strut above plus half the distance below the bottom of the excavation. The total active thrust over the excavation depth on a smooth wall, as suggested by Rankine (1857), is given by:

$$P_{\text{Rankine}} = 0.5(\gamma H^2 - 4s_u H). \quad (3.2)$$

where γ , H , and S_u are as defined above.

On the other hand, to determine the apparent earth pressure for soft to medium clay, Henkel (1971) considered the basal stability phenomena as follows:

$$p_A = \left(1 - \frac{4s_u}{\gamma H} + \Delta K\right) \gamma H, \quad (3.3)$$

where the factor ΔK is related to bottom heave stability as follows:

$$\Delta K = \frac{2B}{H \left(1 - \frac{5.14 S_{ub}}{\gamma H}\right)}. \quad (3.4)$$

where B is the width of the excavation and S_{ub} is the average undrained shear strength value below the excavation depth H . The distributed horizontal earth pressure (lb/ft^2) according to Yokel *et al.* (1980) can be computed using the following equation:

$$p = We (H + 2) \quad (3.5)$$

where We = lateral weight effect (lb/ft^3) and H = height of the supported bank (ft) (2 ft are added to allow for overloading) (Note: $1 \text{ lb/ft}^2 = 48 \text{ Pa}$). The above discussion reveals that calculating earth pressure on a flexible retaining structure is not straightforward and that various soil parameters must be evaluated and considered when designing or validating a shoring system in a soft clay excavation or trench (Yokel *et al.*, 1980).

This study presents a full-scale field test investigation at a unique site made exclusively of soft, sensitive clay soil and located in Louiseville, Quebec, Canada, to evaluate the earth pressure on an excavation with temporary flexible shoring. The trench was 6 m deep, and the shoring consisted of two steel trench boxes stacked upon each other. The field test results are presented in terms of soil pressure with depth of soil. This paper provides a detailed explanation of the

installation phase, including instrumentation, and the test phase. The experimental results are presented and compared with available Rankine (1857), Terzaghi and Peck (1967), and Yokel *et al.* (1980) theoretical apparent earth pressure values and available field performance data reported by LaBaw (2009).

3.3 Full-Scale Field Experimental Program

To meet the objectives related to the evaluation of earth pressure and the performance validation of a temporary shield system, an experimental trench was excavated and an excavation protection system set up at the field test site located in Louiseville, Quebec.

3.3.1 Soil Characteristics of the Field Experimental Site

The field experimental site is located about 100 km north-east of Montreal, on the north shore of the St. Lawrence River. It is along Highway 138, 8 km west of Louiseville village. The elevation of the site is 9.5 m above sea level. The site is known for its so-called sensitive clay soil, and therefore it was selected for the present study. The soil is made up of a 60 m-thick, Champlain Sea high-plasticity clay deposit (Leblond, 1981). According to Leroueil *et al.* (2003), this clay is extremely homogeneous, with 80% clay fraction, 45% average plasticity index, and an average sensitivity (S_t) of 22 (as determined with the Swedish fall cone). Experimental shear tests were performed by Laval University (Quebec City) in the field using a scissometer (Roctest model M-1000). Dourlet (2020) describes the characterization tests conducted on this site. Figure 3.2 shows the shear strength data for undrained soil at the Louiseville experimental site, the soil layers, Atterberg limits, and effective stresses. The preconsolidation stress was obtained from the oedometer consolidation test using Casagrande's (1973) technique. The overconsolidation ratio (OCR) was computed as the effective preconsolidation pressure obtained from the oedometer test divided by the in-situ effective overburden pressure. The average volumetric weight measured was 14.8 kN/m^3 (varying from 14.60 to 14.97 kN/m^3 depending on sample depth). Soil samples were obtained with the large-diameter Laval tube sampler (200 mm diameter, 600 mm height), which has been specifically

developed for sensitive clays (Rochelle *et al.*, 1981). Four soil samples (tubes) were obtained at two different depths: two tubes from 2.13 m to 2.73 m depth, and two tubes from 3.05 m to 3.65 m depth.

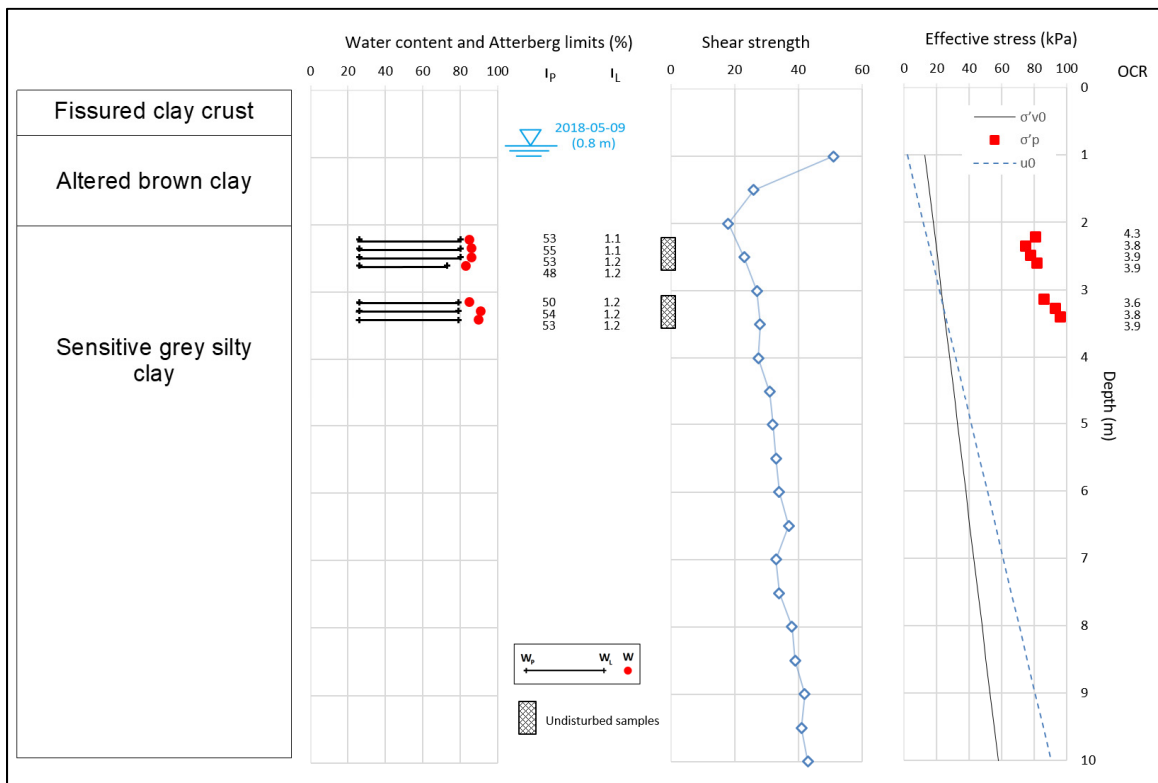


Figure 3.2 Geotechnical properties of Louiseville clay deposit
Taken from Dourlet (2020)

The shear strength profile with depth is very similar to the shear strength profile obtained by Leroueil *et al.* (2003) for Louiseville sensitive clay on the same test site. A comparison of geotechnical parameters for this test site is presented by Dourlet (2020). DSS testing was conducted on soil samples corresponding to 3.05 to 3.65 m depth (two samples retrieved on site). Three DSS tests were conducted on 3.47 m depth samples, under static loading, at a constant volume, but different effective vertical stresses. The details and results of these three tests are summarized in Table 3.1.

Table 3.1 Undrained shear strength from the soil based on DSS testing
Taken from Laval University

| Test | Consolidation | | Initial rupture | | Large deformations | |
|-------------------------|-------------------------|-------|-----------------|--------------|---------------------|--------------|
| | σ'_{vc} (kPa) | ec | S_u (kPa) | g_h (%) | S_{u-gd} (kPa) | g_h (%) |
| DSS _{STAT} -01 | 57 | 2.287 | 28 | 2.3 | 23 | 15 |
| DSS _{STAT} -02 | 25 | 2.290 | 20 | 2 | 22 | 15 |
| DSS _{STAT} -03 | 143 | 1.804 | 40 | 5 | 36 | 15 |

Two of them were undertaken in the overconsolidated domain and one in the normally consolidated domain. In the overconsolidated domain, DSS_{stat}-01 showed a contraction behavior, whereas DSS_{stat}-02 showed a slight dilation behavior. In the normally consolidated domain, DSS_{stat}-03 showed a contraction behavior. Effective stress parameters obtained from DSS tests are presented in Table 3.2. These parameters can be useful for modeling the long-term behavior of the trench. They are comparable to data published by Lefebvre (1981) for Champlain Sea clays, which are a common type of sensitive clay in the Province of Quebec. Extensive characterization and testing of the Louiseville clay (same test site) are presented in Leroueil *et al.* (2003).

Table 3.2 Effective stress parameters from DSS testing
Taken from Laval University

| Domain | DSS tests |
|------------------------------|---|
| Over consolidated domain | $c' = 9 \text{ kPa}$ $f' = 28^\circ$ |
| Normally consolidated domain | $c' = 0 \text{ kPa}$ $f' = 26.5^\circ$ |

3.3.2 Excavation and Shoring Geometry

The trench box system used is illustrated in Figure 3.3, and the geometric and mechanical properties of the trench box are summarized in Table 3.3. This “cage-type shield” or “trench box” is a very common protection system in the construction industry. The excavated area

between the outside of the trench box and the face of the trench should be as small as possible (OSHA, 2015). Considering this recommendation, the contour of the excavation considered in this experiment was 5.59 m (18.33 ft) long and 2.18 m (7.15 ft) wide, accommodating the trench box that was 3.05 m (10 ft) long, 1.75 m (5 ft) wide, and 6 m (20 ft) deep (see Figure 3.4 (a)). Two trench boxes “stacked upon each other” in conformity with the OSHA (2015) procedure were placed into the trench excavation as shown in Figure 3.4 (b) to cover the total depth of excavation, 6 m (20 ft.), and to act as one protection system because they were assembled to each other using “hinge” connections.

Table 3.3 Geometric and structural properties of the shield

| Properties (one-shield geometry) | Steel trench box |
|--|------------------|
| Length, m (ft.) | 3.05 (10) |
| Height, m (ft.) | 3.05 (10) |
| Thickness of the plate, mm (in.) | 100 (4) |
| Strut or spreader tube outer diameter, mm (in.) | 219 (8.61) |
| Strut or spreader tube inner diameter, mm (in.) | 194 (7.63) |
| Cross-sectional area of strut, m ² (in ²) | 8.24E-03 (12.77) |
| Strut or spreader tube moment of inertia, m ⁴ (in ⁴ .) | 4.41E-05 (106) |
| Modulus of elasticity for plate and strut, kN/m ² (ksi) | 2.00E+08 (29007) |
| Shear modulus, kN/m ² (ksi) | 8.00E+07 (11603) |
| Poisson's ratio | 0.30 |

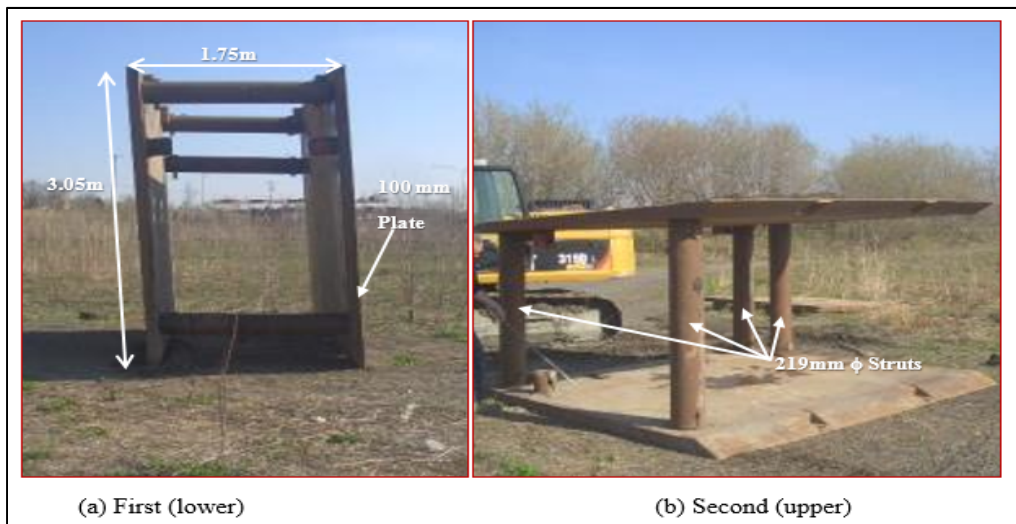


Figure 3.3 First and second steel trench box protection system at the experimental site

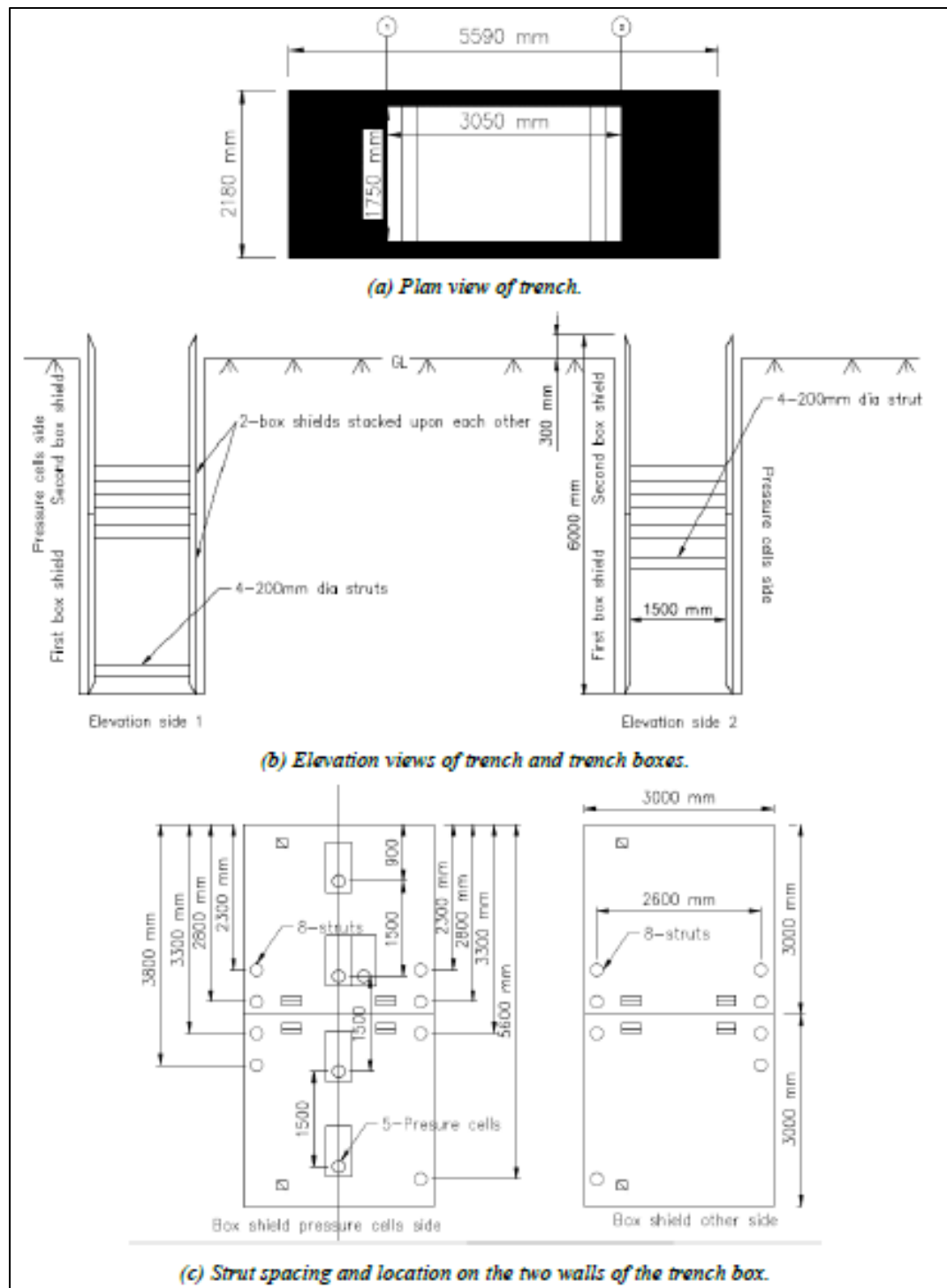


Figure 3.4 Field test setup details for trench boxes

3.3.3 Instrumentation

Table 3.4 shows the identification and capacities of the pressure cells installed on the trench box before its installation. Five vibrating-wire pressure cells (model TPC) were used to capture soil pressure at the following soil depths from the top of the steel trench box: 0.9 m, 2.4 m, 2.4 m, 3.9 m, and 5.4 m. At 2.4 m depth, a pair of cells was used to capture to what extent/scale the pressure varied beyond the centerline of the trench box. The locations of the pressure cells attached to the trench box for the purpose of the test are shown in Figure 3.4(c), and the locations of the struts are shown in Figure 3.5. Pressure cells were installed on only one of the two sides of the trench box. In this experiment, pressure cells were attached on one side, as shown in Figure 3.4(c). The other two sides were open to the soil along the trench, as shown in Figure 3.4(b). Note that the horizontal distance between struts was 2.64 m.

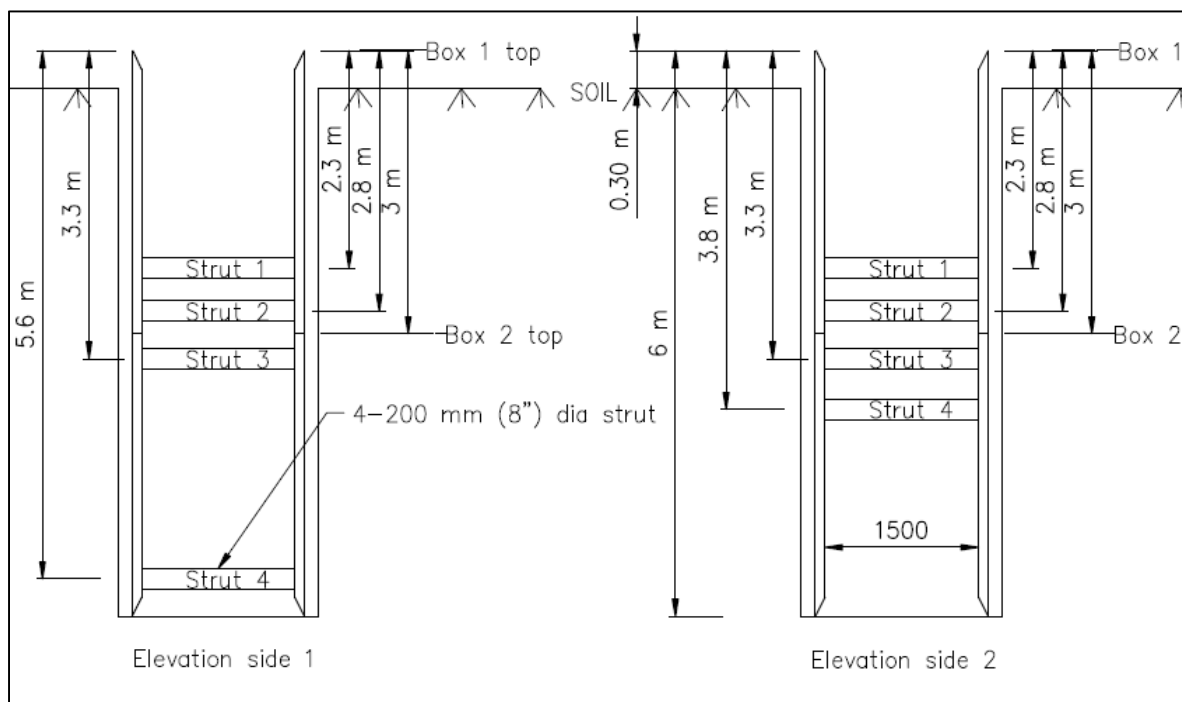


Figure 3.5 Strut locations in the two elevation sides along the trench

3.3.4 Laboratory Verification and Field Installation of Test Equipment

The pressure cells were first individually attached to plywood frames 19 mm thick with epoxy at the ETS laboratory, as illustrated in Figure 3.6(a). Two main reasons justified this initiative: (i) to ensure that the surface receiving the cells was plane (the trench box plate was neither flat nor smooth enough), and (ii) to optimize the time required to attach the pressure cells to the trench box at the experimental site (an open field). After all the pressure cells were bonded to the plywood surface, they were carefully tested in the laboratory to check their functionality under pressure before they were transported to the experimental site (Figure 3.6(b)). For this purpose, the pressure cells were connected individually with the Roctest SENSLOG 1000X datalogger (a turnkey system used for the remote monitoring of virtually any type of instrument), and loads were applied gradually in the structural test laboratory at ETS (Figure 3.6(c)). Note that calibration of the pressure cells was undertaken by the equipment provider and that a calibration document was supplied with the equipment.

Table 3.4 Pressure cell identification and capacities

| Pressure cell identification | Capacity (kPa) |
|------------------------------|----------------|
| B-P1 | 200 |
| B-P2 | 200 |
| B-P3 | 70 |
| B-P4 | 70 |
| B-P5 | 70 |

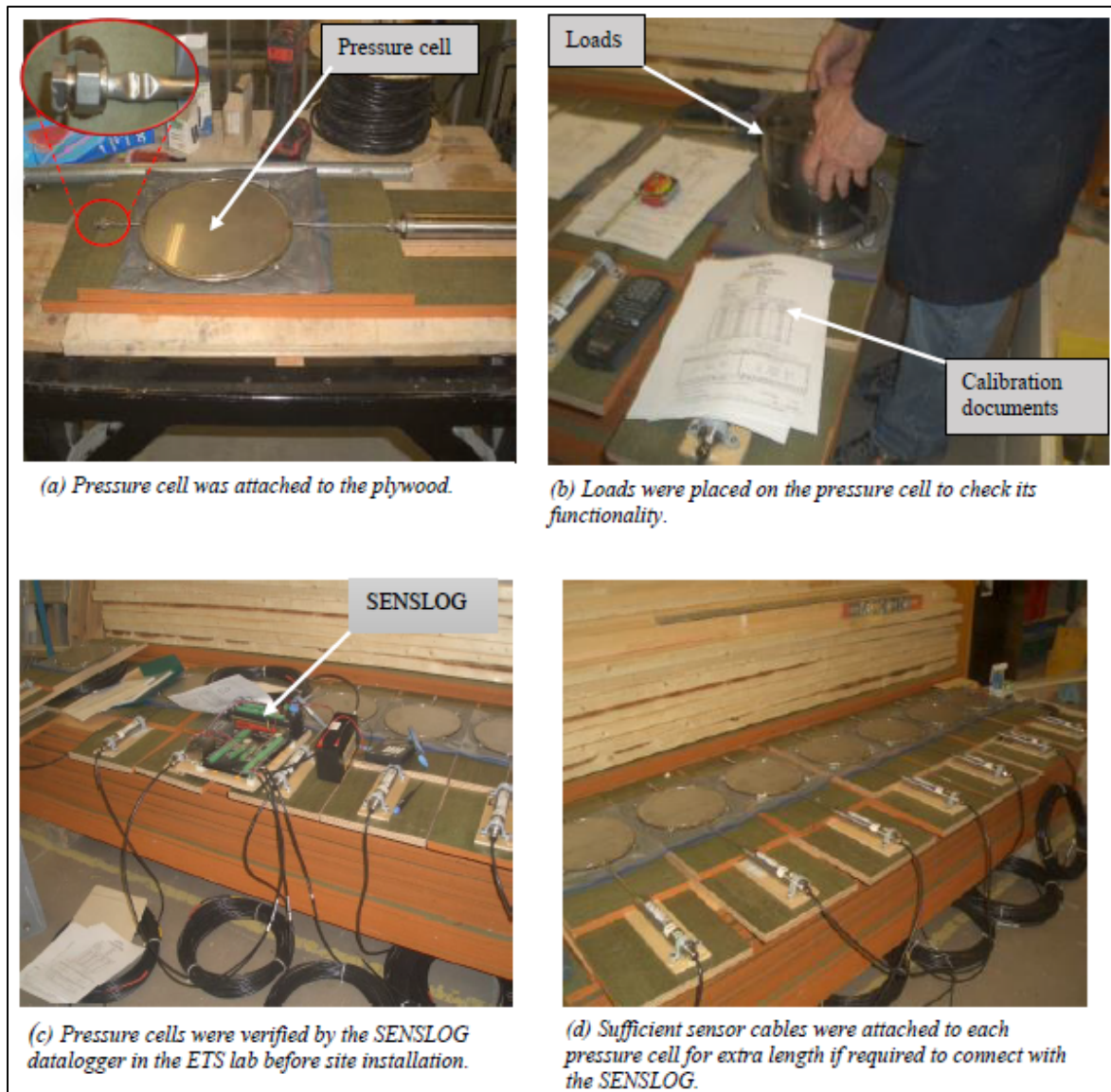


Figure 3.6 Preparation and verification of pressure cells in the ETS lab before being transported to the site installation

For pressure cells B-P1 (at 5.4 m) and B-P2 (at 3.9 m), the 0-200 kPa pressure range was used for calibration, whereas for B-P3 (at 2.4 m), B-P4 (at 2.4 m), and B-P5 (at 0.9 m), the 0-70 kPa range was used. Because the deeper part of the trench experienced more pressure compared to the upper part, two 200-kPa capacity pressure cells were used in the deeper part (approximately twice the expected earth pressure at 5.4 m), and three 70-kPa capacity pressure cells were used in the upper portion (approximately twice the expected earth pressure at 2.4 m). Details of the

pressure cells are provided in Figure 3.4(c) and Table 3.4. Once all the pressure cells had been verified as functional in the laboratory, they were transported to the experimental site. Vibrating wire pressure cells (model TPC) are reliable, faster than all other types, and almost immune to external noise because they rely on the frequency output (Roctest, 2005). A previous experimental study by Lan *et al.* (1999) successfully used this type of pressure cell to measure the apparent earth pressure.

To install the pressure cells on the steel wall plate of the trench box, the following steps were undertaken: (i) the box steel wall plate surface was identified and prepared, and then epoxy was used on both the steel and the plywood surfaces, as illustrated in Figure 3.7; (ii) the plywood holding the pressure cells was attached to the steel wall plate surface; and (iii) to further secure the connections, the plywood was screwed into the steel wall plate as illustrated in Figure 3.8.

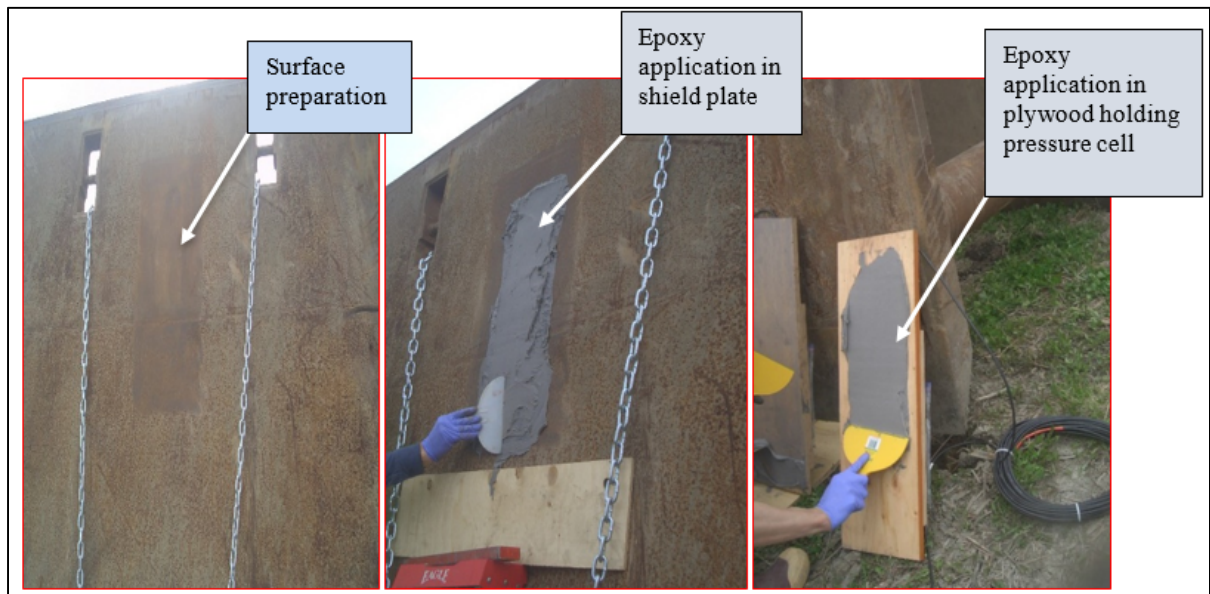


Figure 3.7 Steps to install the pressure cells on the steel wall plate of the trench box



Figure 3.8 Pressure cells are fixed on the side of the first and second trench boxes

3.3.5 Excavation and Installation of Protection Systems

The field tests were performed in 2018 from May 14 to August 8 without surcharge loading and from August 8 to August 10 with a 45 kPa surcharge load consisting of concrete blocks. After all the pressure cells had been bonded to the wall steel plate of the two trench boxes, the top soil (with surface vegetation) was removed from the trench zone. Using an excavator, the trench was excavated to approximately 1.5 m depth from the top, and the first (lower) trench box was installed rapidly to make sure that the surrounding soil would not fall inside the trench, as shown in Figures 3.9 to 3.12 which illustrate the excavation sequence. Thereafter, excavation through the trench box continued gradually until reaching 6 m depth, and the first (lower) box was pushed down to accommodate the second (upper) box, as depicted in Figure 3.11. Finally, the second (upper) trench box was installed on top of the first box as per OSHA guidelines for shields “stacked upon each other”, and the two boxes were assembled using the four “hinge” connections located in the four corners, as shown in Figure 3.12.

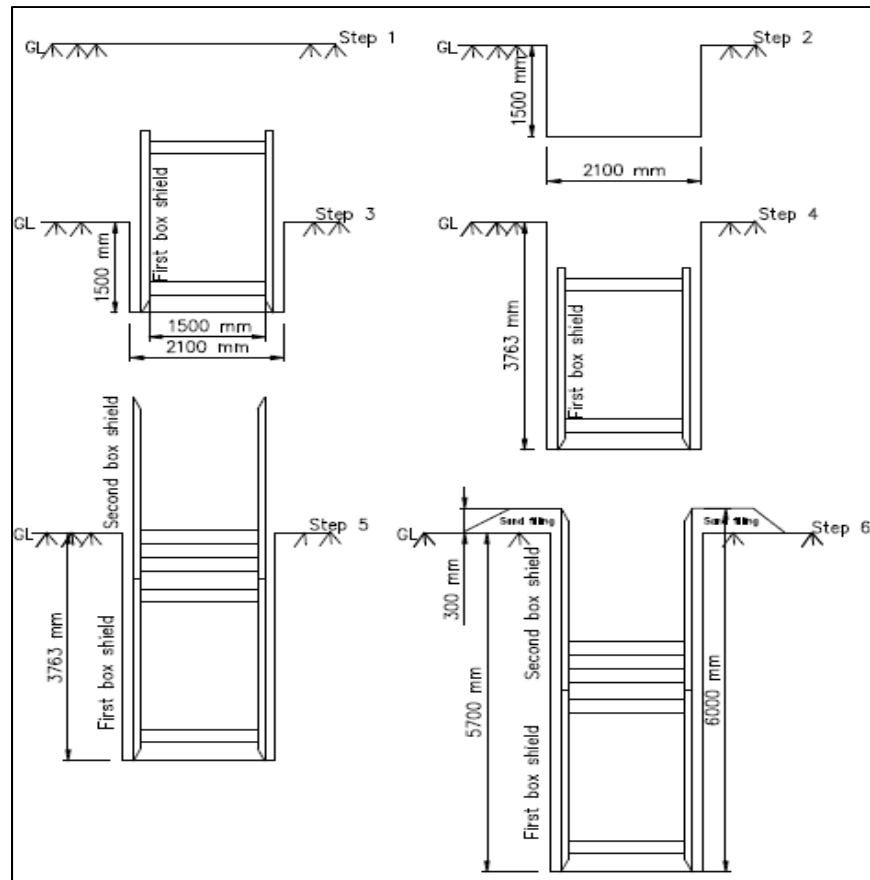


Figure 3.9 Excavation/construction sequence



Figure 3.10 Installation of the first (lower) trench box into the trench



Figure 3.11 Excavation continued to make room to accommodate the second (upper) trench box in the trench



Figure 3.12 Second (upper) trench box is being placed on top of the first (lower) box in the trench

A space between the trench box exterior wall and the surrounding soil ranging from 100 mm to 200 mm was created due to the installation process. OSHA (2015) states that, “the space between the trench boxes and the excavation side is backfilled to prevent lateral movement of the box.” Therefore, after successfully installing the boxes one on top of the other, the empty space between the retaining (shoring) exterior wall and the surrounding soil was backfilled with sand, as shown in Figure 3.13. In addition, the height between the trench box top and the soil surface was kept to 300 mm on both sides (Figure 3.13) in compliance with the SCCI (2020) recommendation that “the shoring shall extend 300 mm above the excavation.” Finally,

the two open ends of the trench were closed by inserting 10 mm-thick sheet piles, thereby preventing loose soil from falling inside the excavation (Figure 3.14).



Figure 3.13 Sand was used to fill the space between the shoring exterior wall and the surrounding soil

3.3.6 Concrete Block (Surcharge Load) Installation

A surcharge load of 45 kPa was applied on one side of the trench using $2.44 \text{ m} \times 0.6 \text{ m} \times 0.6 \text{ m}$ concrete blocks during the period from August 8 to 10, 2018, as illustrated in Figure 3.14. The aim of this loading on the surface of the protection system was to examine the movement of the soil as well as the pressure increase due to the overload. The SCCI standard specifies 1.2 m (4 ft) distance from the excavation (SCCI, 2020). However, OSHA (2015) states that temporary spoil must be placed no closer than 0.61 m (2 ft) from the surface edge of the excavation and that permanent spoil should be placed at some distance from the excavation. In consideration of all these statements, the overload was placed close to the wall to simulate the most unfavorable case.

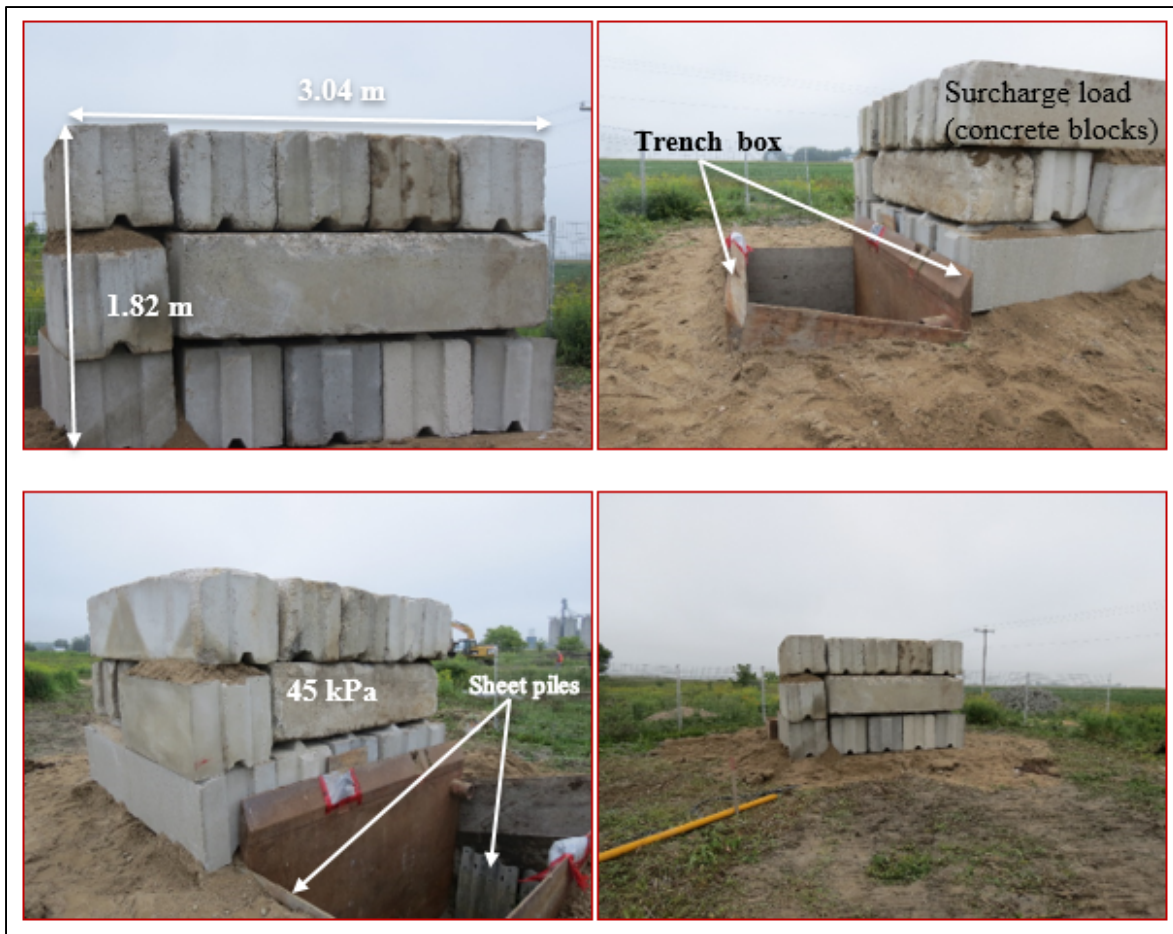


Figure 3.14 Concrete blocks (surcharge load) installed on one side of the trench

3.3.7 Data Recording Unit and Data Collection

All the sensor cables attached to the pressure cells were brought into the small data acquisition trailer and connected to the appropriate box to record the field test data. Figure 3.15 shows the small truck trailer chamber that was used at the experimental site to record the test data in real time during the field experiment. All the pressure cells were connected to the central sensor box by sensor cables. Real-time data were collected using Wi-Fi technology from ETS through a dedicated website of the equipment provider.

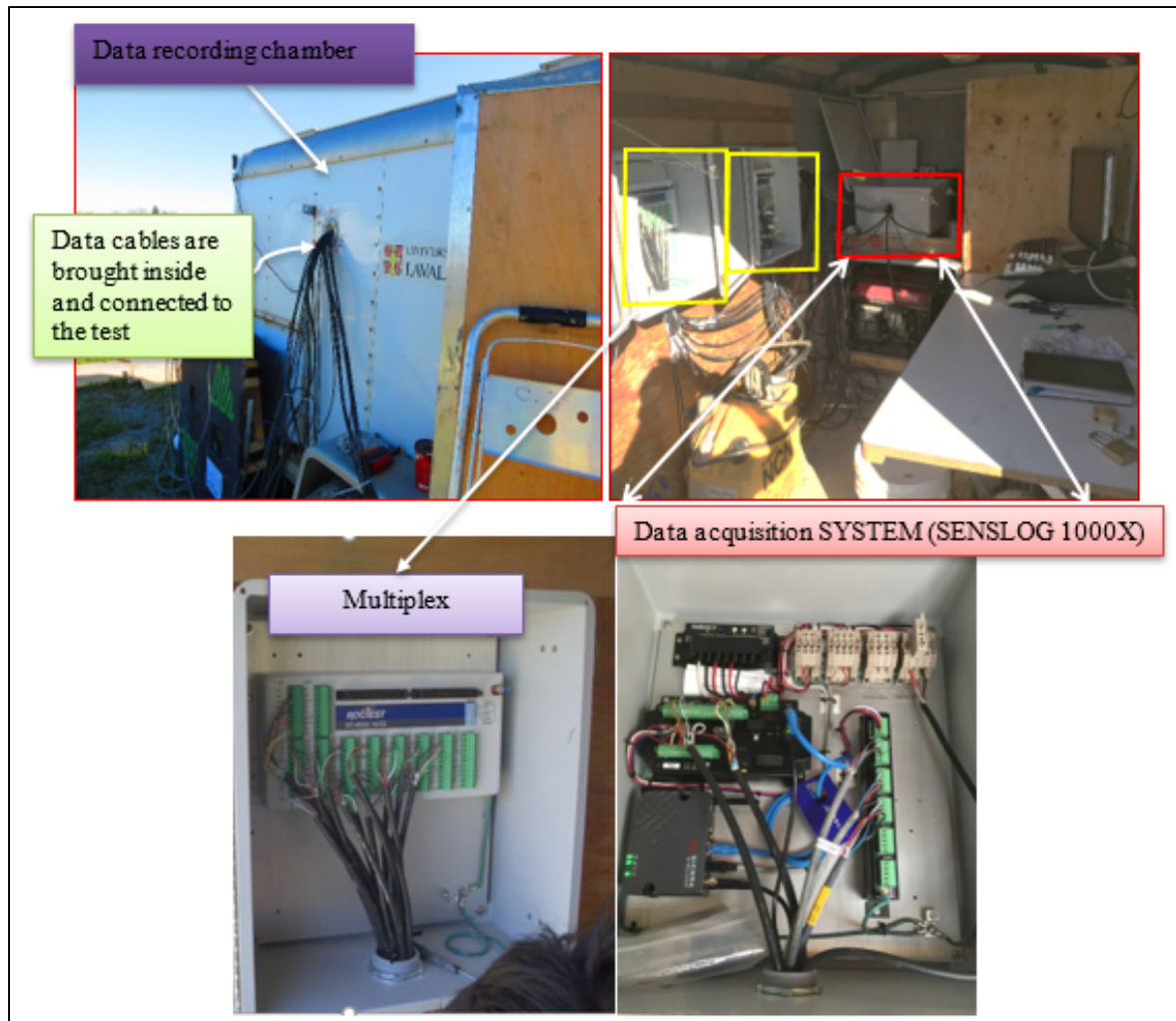


Figure 3.15 Components of the data recording unit at the experimental site

3.3.8 Data Preparation

ETS had access through the file transfer protocol (FTP) to the website at any time (24/7) to check and collect data. To reduce their volume, the data were recorded at intervals of 30 minutes, 24/7. These data were recorded in the form of raw data such as linear units and Hertz, not directly in kilopascals (kPa) for the pressure cells. Therefore, it was necessary to transform the raw data into an appropriate engineering format using the linear equation recommended by the Roctest (2005) instruction manual related to vibrating-wire total pressure cells. This equation was used as follows for each of the pressure cells separately:

$$P = C_f (L - L_0) \quad (3.6)$$

where P = pressure in kilopascals (kPa); C_f = calibration factor (provided on calibration sheets for each pressure cell separately); L = current reading in linear units (LU); and L_0 = initial reading in linear units (LU). Roctest (2005) also provides a more complex polynomial method. However, the linear method is simpler and easier to use, and the maximum error rate was only 0.23% in the present case. Next, a correction was applied to take temperature changes into account using the following equation recommended by Roctest (2005):

$$P_c = P - C_T(T - T_0) - (S - S_0) \quad (3.7)$$

where P_c = corrected pressure in kPa; P = pressure previously calculated in kPa; C_T = calibration factor for temperature (given in the calibration sheet), in kPa/°C; T = current temperature reading in degrees Celsius; T_0 = initial temperature reading in degrees Celsius; S = current barometric pressure reading in kPa; and S_0 = initial barometric pressure reading in kPa. The correction factor for barometric reading expressed in the above equation by the term $(S - S_0)$ was neglected, given its tiny value compared with the pressure measured at depth. All the above equations were used to calculate the earth pressure in the trench using Excel worksheets.

3.4 Field Test Results and Discussion

3.4.1 Temperature Effect

Figure 3.16 shows, the daily temperature at different trench depths as captured by the pressure cells during the first week. The air temperature is also provided for comparison. The figure reveals that the day-versus-night fluctuations of soil temperature were more significant in the upper pressure cells (B-P5, B-P4, B-P3) than in the deeper pressure cells (B-P1, B-P2) in the trench. The uppermost cell (B-P5) experienced minimum and maximum temperatures of 7°C

and 23°C in the first week of the experiment, but the next lower pressure cells (B-P4, B-P3) experienced minimum and maximum temperatures of 9°C and 17°C. Temperature fluctuations were negligible in the deeper pressure cells (B-P1, B-P2).

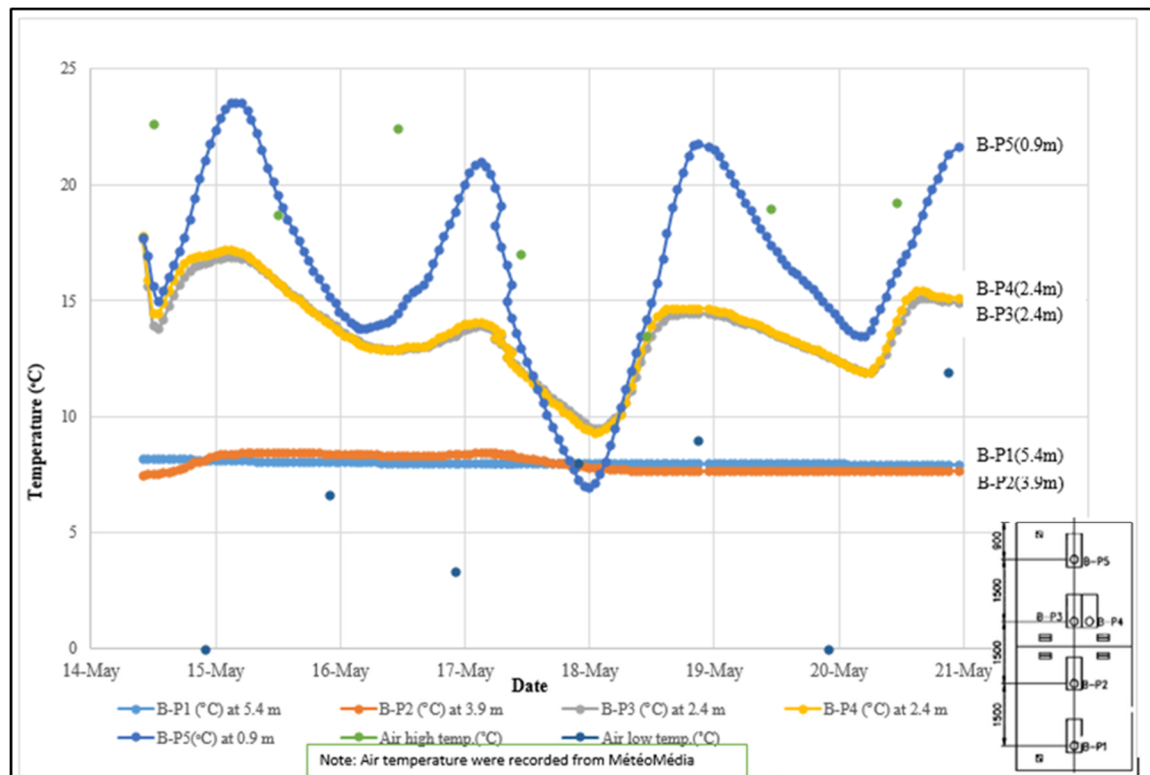


Figure 3.16 First week's hourly temperature at different trench depths as recorded by pressure cells, 2018

3.4.2 Soil Pressure over the Time Period (May 14–August 10, 2018)

From Figures 3.17, 3.18, and 3.23, the following observations can be made:

- The calculations revealed that the temperature correction did not result in major differences in soil pressure. Figure 3.17 presents the recorded hourly soil pressure after temperature correction for the first week (May 14 to 22). It shows how the soil pressure varied with depth during this period. The deeper pressure cells (B-P1, B-P2) experienced higher values in kPa than the upper pressure cells (B-P5, B-P4, B-P3). Note that the pressure cell at 3.9 m (B-P2) depth recorded higher values in kPa than the

cell at 5.4 m (B-P1) depth. However, this can be attributed to the type of trench box used, with fixed end support (Lan *et al.*, 1999).

- Before May 15, the pressure cells experienced higher pressures. However, these higher pressures eased after water that had accumulated in the excavation was pumped out.
- After the trench box was placed in the trench, the negative initial pressure value recorded by pressure cell P5 (0.9 m) was attributed to an artificial effect caused by deflection of the sandwich wall on the outer plane of the shield. One side of the wall was exposed to the sun, resulting in a significant day-to-night temperature variation.

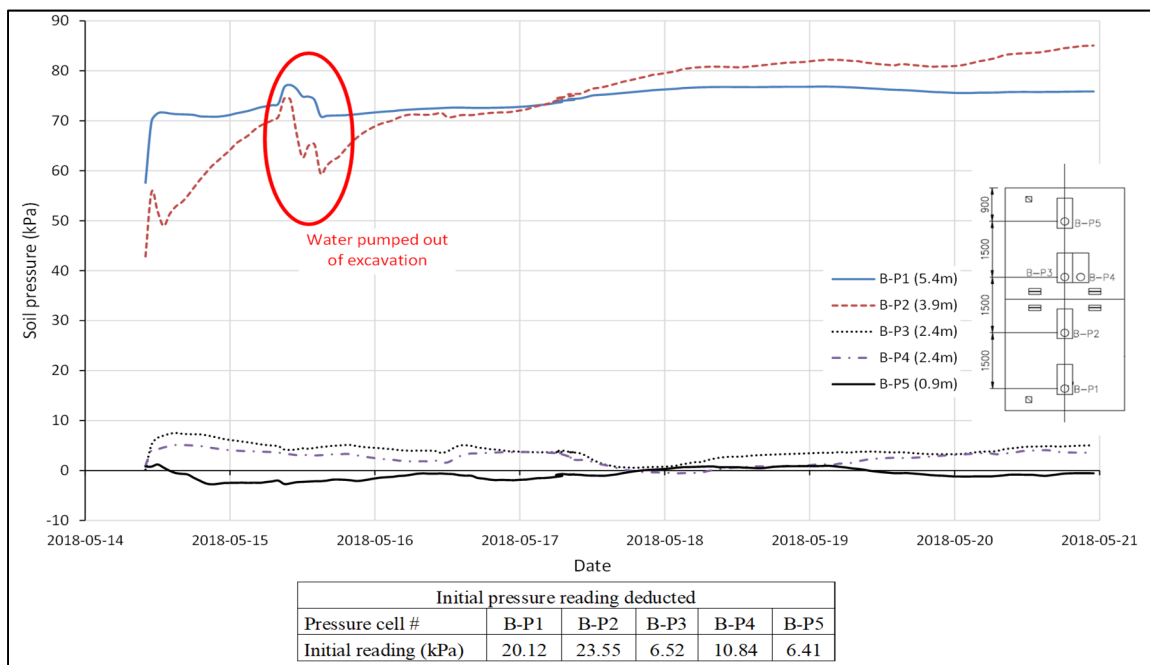


Figure 3.17 First week's hourly pressure after temperature correction on the trench box protection, 2018

Figure 3.18 presents the maximum daily pressure curves after temperature correction at different soil depths from May 14 to August 10, 2018 (i.e., up to the last day of the experiment). Examination of the curves reveals various phenomena that occurred during the period of the experiment:-

- Soil pressures at depths 0.9 m (B-P5) and 2.4 m (B-P4, B-P3) increased gradually.

- The increase in soil pressure at depth 3.9 m (B-P2) was more pronounced than at depth 5.4 m (B-P1). This is attributed to the fact that the bottom end part of the trench box (approximately 300 mm) was embedded into the soil and that the total gravity load of the upper steel trench box was pushing the lower trench box into the ground during the installation process. Thereby the bottom part (approximately 300 mm) of the lower trench box acted more likely as a “fixed end support” (Figure 3. 23).
- Overall soil pressure increased with depth except for the bottom part of the support, which experienced less pressure than the middle part due to the arching effect. With the embedment of the bottom part of the trench box, the soil around the trench box developed an “arching effect,” leading to higher apparent earth pressure just above the bottom of the trench. This phenomenon of nonlinear active earth pressure distribution for flexible retaining structures has been recognized and discussed by numerous authors, including Karlsrud and Andresen (2005), Hashash and Whittle (2002), Mortensen and Andresen (2003), Benmebarek *et al.* (2016), and Bjerrum *et al.* (1972).

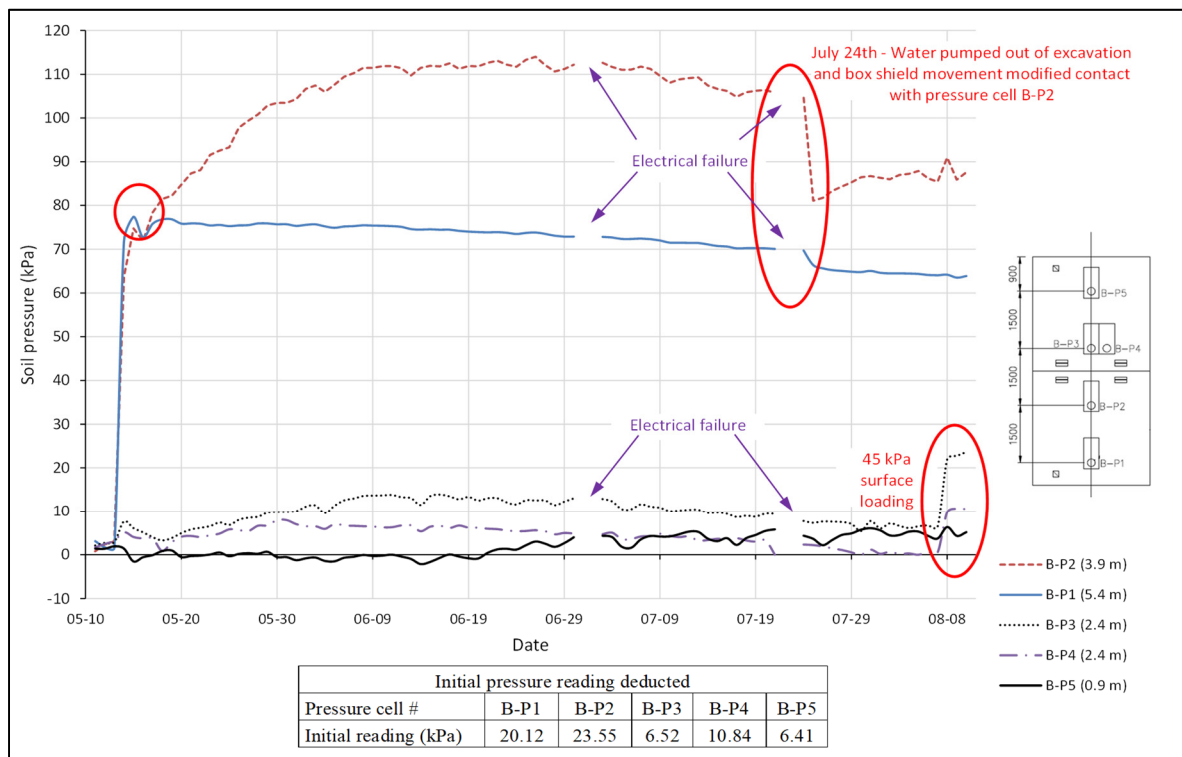


Figure 3.18 Maximum daily soil pressure after temperature correction on the trench box protection (May 14–August 10, 2018)

3.4.3 Surcharge Load Effect on Soil Pressure

Figure 3.19 presents a magnified view of the last week of soil pressure versus depth to evaluate the effects of the overload (concrete blocks) applied near the trench. As expected, soil pressure at depth 2.4 m (B-P4, B-P3) increased rapidly. This contrasts with the minor overload effects observed at depths 3.9 m (B-P2) and 5.4 m (B-P1). Note that the pressure cell at depth 0.9 m (B-P5) recorded almost constant pressure throughout the last week. This can be attributed to the fact that the surrounding soil had been washed away due to heavy rainfall. It can be concluded that the effect of overload was generally more noticeable on the upper part of the trench box than on the lower part. This can also be seen in Figure 3.20, where the effect of the surcharge load was captured by pressure cells B-P2 and B-P3.

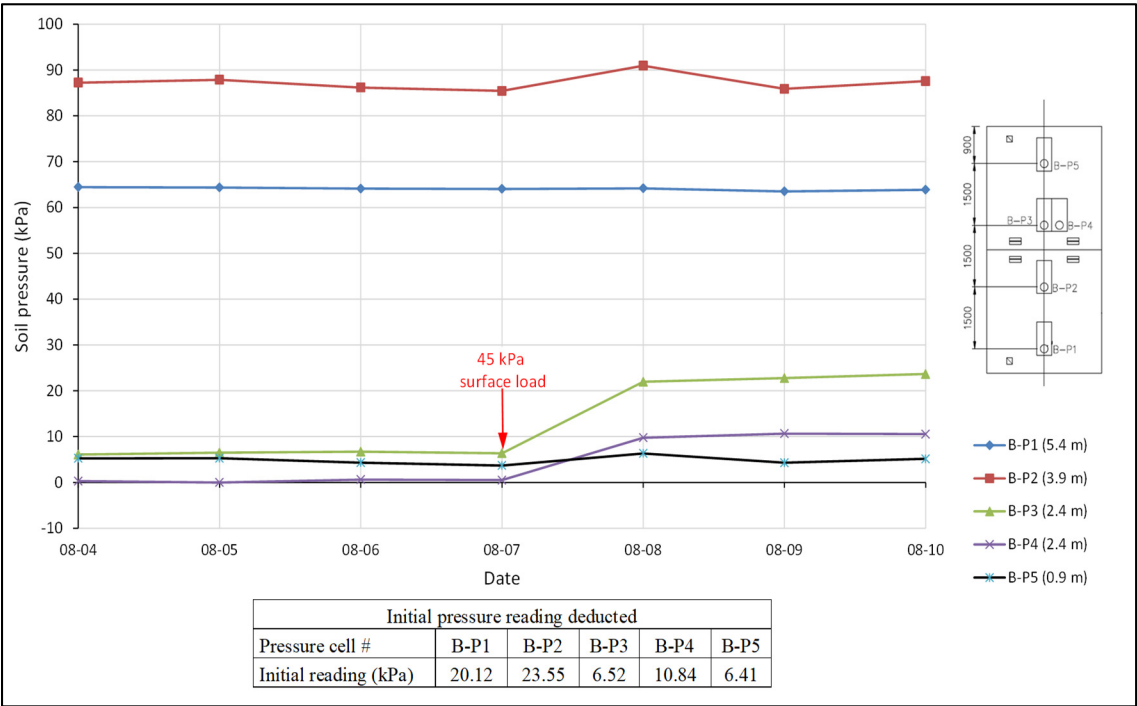


Figure 3.19 Blown-up view of the last week of soil pressure to observe the effects of surcharge loading (concrete blocks) at the trench

3.4.4 Total Pressure Curve

From Figures 3.20, 3.21, and 3.22, the following observations can be made:

- Figure 3.20 presents the absolute maximum soil pressure versus soil depth at the trench excavation with and without surcharge loading. Experimental values were developed based on experimental field test results (from May 14 to August 10, 2018). The soil pressures at depths 0.9 m (B-P5), 2.4 m (B-P4, B-P3), and 3.9 m (B-P2) were observed to increase rapidly.
- In contrast, the soil pressure at 5.4 m (B-P1) did not show a significant increase, probably due to end boundary conditions (more likely “fixed end support”).
- This anomaly can also be explained by other observations. At the beginning of August 2018, it was discovered that the surrounding soil at the pressure cell at 0.9 m depth (B-P5 on the curve) had been totally washed away (Figure 3.21) due to heavy rainfall. Informatively, the precipitation quantities for each month during the test period (May to August 2018) are presented in Figure 3.22.
- Consequently, the pressure cell at 2.4 m depth (B-P3 on the curve) seems to have had less soil above it, resulting in less pressure than expected.
- The pressure cell at 3.9 m depth (B-P2 on the curve) gave the maximum value of soil pressure (114 kPa), which is the expected order of magnitude for this type of experimental excavation trench depth. Using the Plaxis software, Karlsrud and Andresen (2005) computed an apparent earth pressure of 75 to 100 kPa at 4 m depth for a sensitive clay. In an experimental field test performed in silty sand in the urban region of Quebec, Lan *et al.* (1999) recorded an apparent earth pressure of 113 kPa on a trench box at 3.04 m depth, which is of the same order of magnitude as the pressure at 3.9 m depth obtained at the Louiseville field site in the present study.
- At 5.4 m depth, the pressure cell (B-P1) experienced less pressure because the wall of the trench box was inserted approximately 300 mm (12 in.) into the soil, as illustrated

in Figure 3.23, developing thereby a ‘fixed end support’ system, as explained earlier. Therefore, the pressure cell at 5.4 m depth (B-P1) was not able to record the expected pressure without the interference of the so-called ‘fixed end support’.

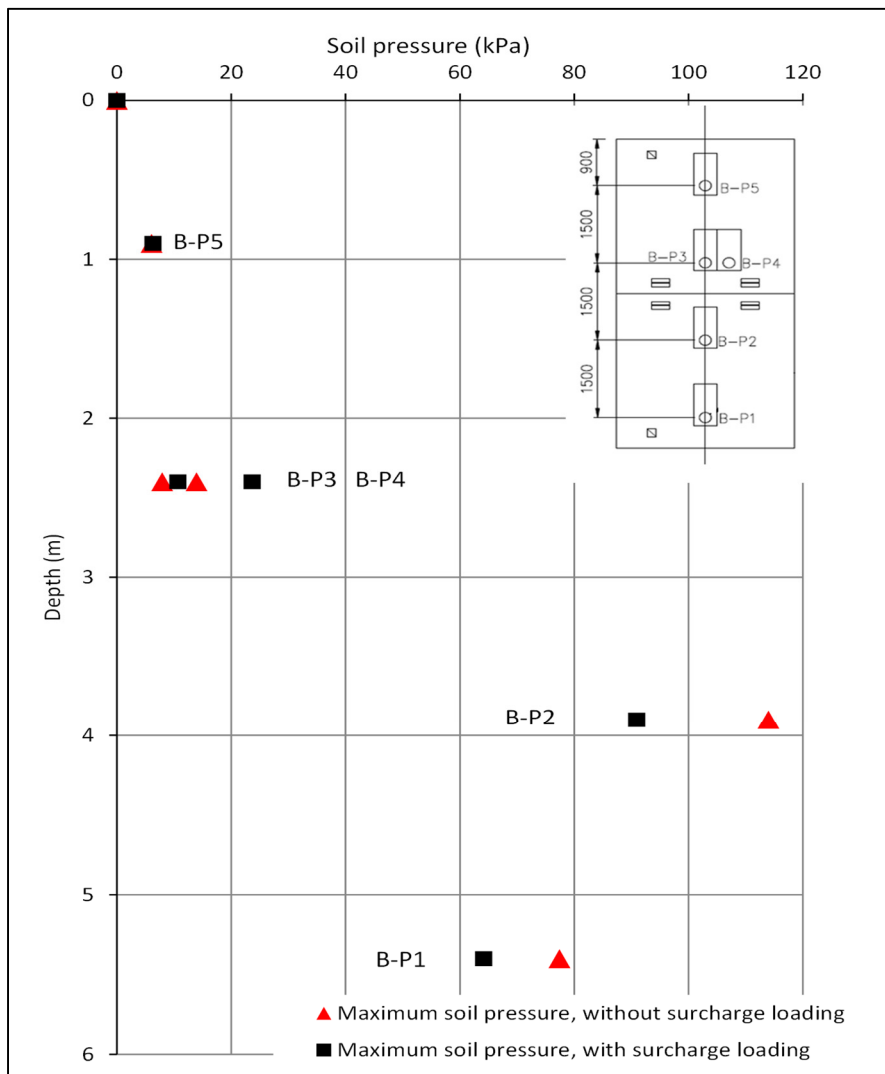


Figure 3.20 Experimental soil pressure on trench box wall vs. depth

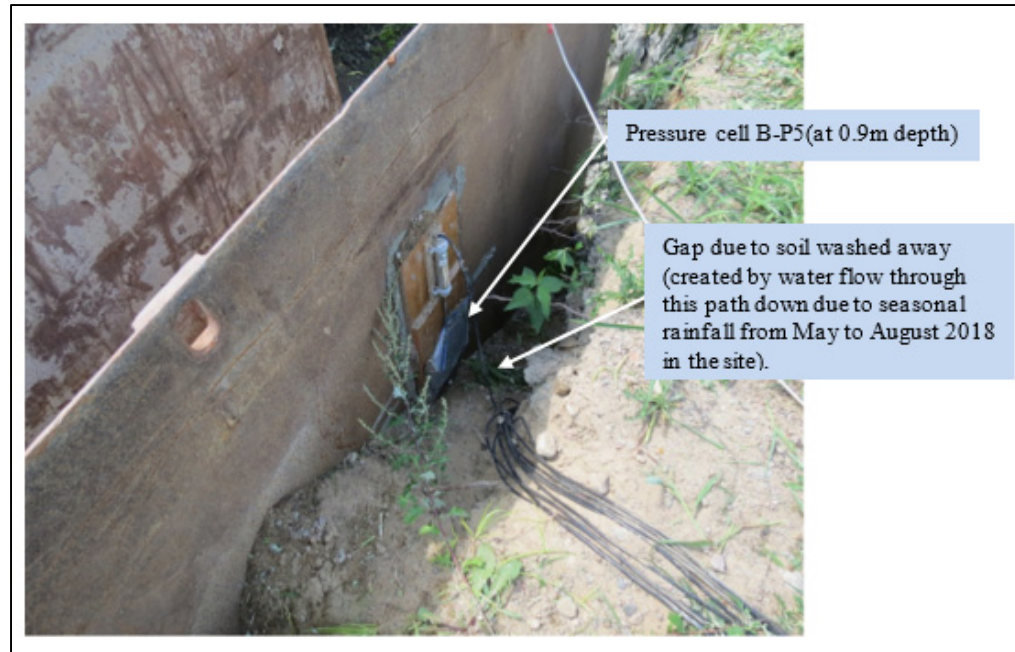


Figure 3.21 Surrounding soil washed away by heavy rainfall affecting pressure cell at 0.9 m

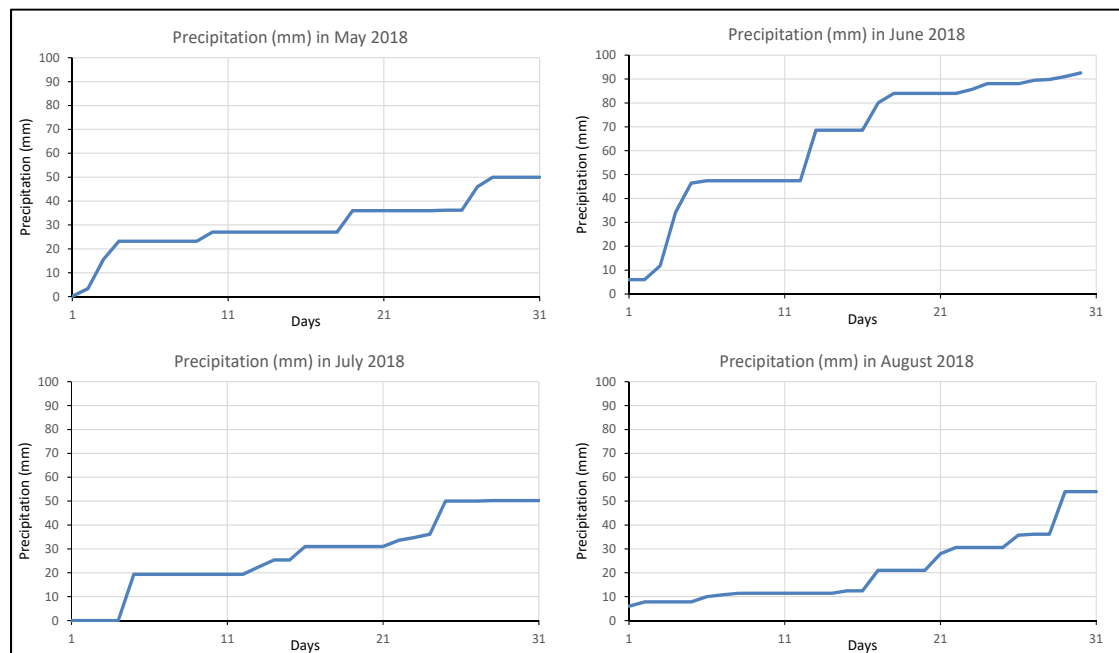


Figure 3.22 Recorded accumulated precipitation quantities (in mm) for each month from May to August 2018 at the Louisville field test site

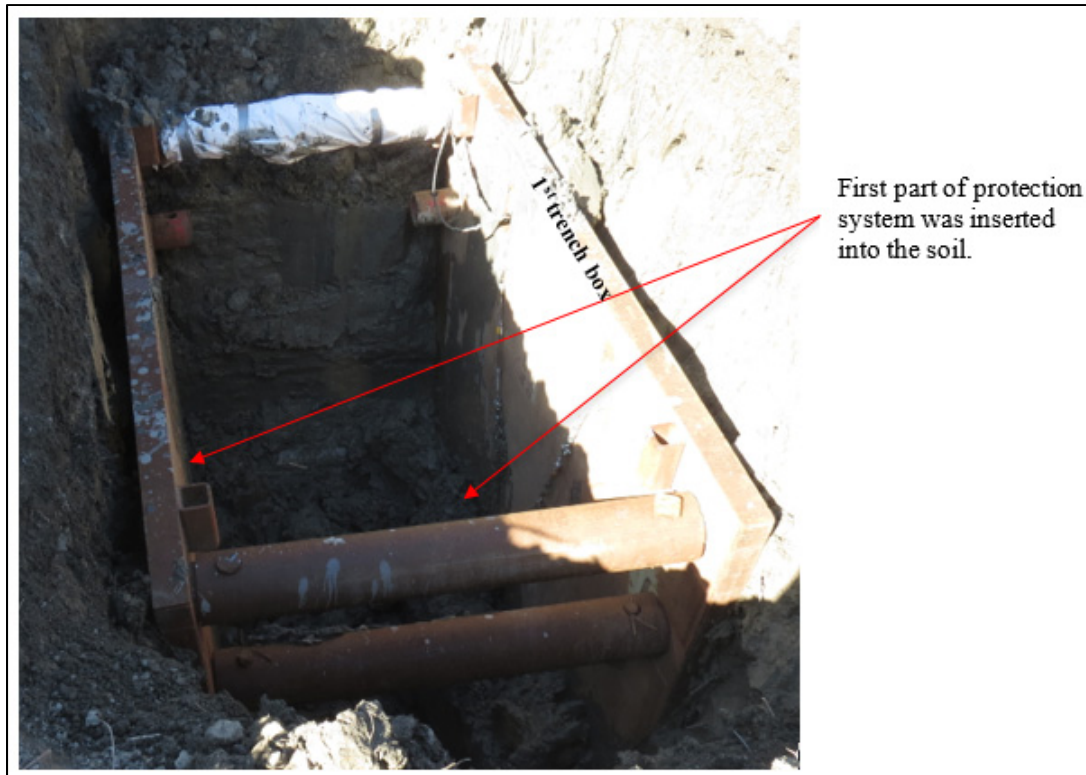


Figure 3.23 Likely “fixed end condition” developed at the lower end of the first trench box due to 300 mm insertion into the soil

3.4.5 Theoretical Calculations

The calculations presented in this section are intended to compare theoretical soil pressure with field test results. Classical theoretical calculations such as the Rankine model and TPM are reasonably accurate to predict apparent earth pressure on flexible retaining structures (such as sheet piles, lagging, etc.), but are not accurate enough for multi-strutted shoring systems such as the trench box used in this study (Macnab, 2002).

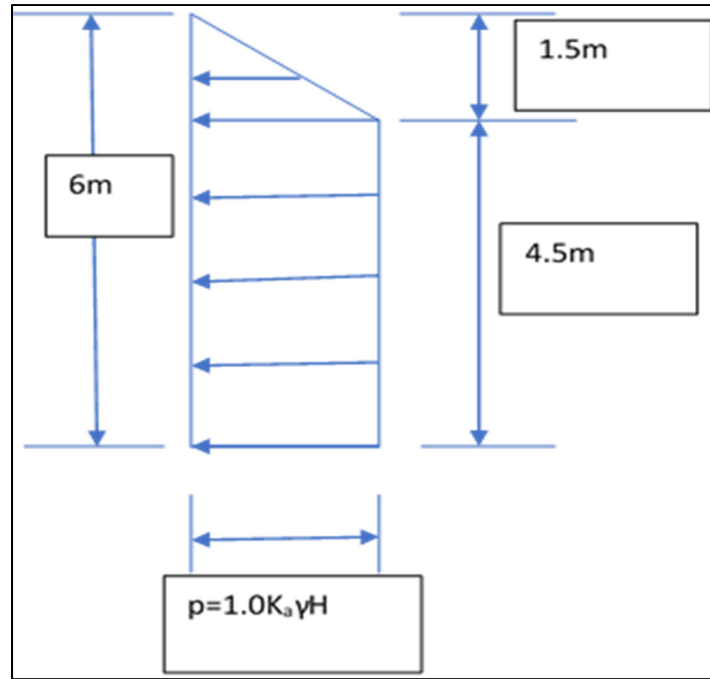


Figure 3.24 Theoretical calculation of soil pressure on the trench box wall using the TPM equation

According to the TPM equation (1) and Figure 3.24, the apparent earth pressure for soft clay in the Louisville soil case is $p_A = 44$ kPa, with $K_A = 1 - m(4S_w/\gamma H) = 0.48$. Active earth pressure formulae developed by Rankine (1857) and Yokel *et al.* (1980) were also used to calculate theoretical soil pressure; the results are summarized in Table 3.5. The maximum experimental strut loads from field performance data recorded in the LaBaw (2009) study (with $\gamma = 18.6$ kN/m³ and $PI = 7.04$ for medium clay) are also provided for comparison in the same table. Calculated theoretical and field performance soil pressures for soft clay soil are compared at different depths of the trench in the present study in Figure 3.25.

Table 3.5 Experimental vs. theoretical and field performance soil pressures at different trench depths in soft clay soil

| Depth from top of the soil (m) | Maximum experimental stress (kPa) | Calculated total active stress from Rankine (1857): $P = 0.5 (\gamma \cdot H^2 - 4S_u H)$ (kPa) | Calculated stress from Terzaghi and Peck (1967): $p_A = 1.0 K_A \cdot \gamma \cdot H$ (kPa) | Calculated stress from Yokel <i>et al.</i> (1980): $p = W_e (H+2)$ (kPa) | Field performance data by LaBaw (2009): Maximum experimental strut load (kPa) |
|--------------------------------|-----------------------------------|--|--|---|--|
| 0 | 0 | 0 | 0 | 75.69 | 0 |
| 0.9 | 6 | 12.69 | 26.4 | 75.69 | 71 |
| 2.4 | 23 | 33.84 | 44 | 75.69 | 67 |
| 3.9 | 114 | 56 | 44 | 75.69 | Not available due to experimental depth |
| 5.4 | 77 | 76.14 | 44 | 75.69 | Not available due to experimental depth |

Note: H= 5.4 m for above calculated stresses.

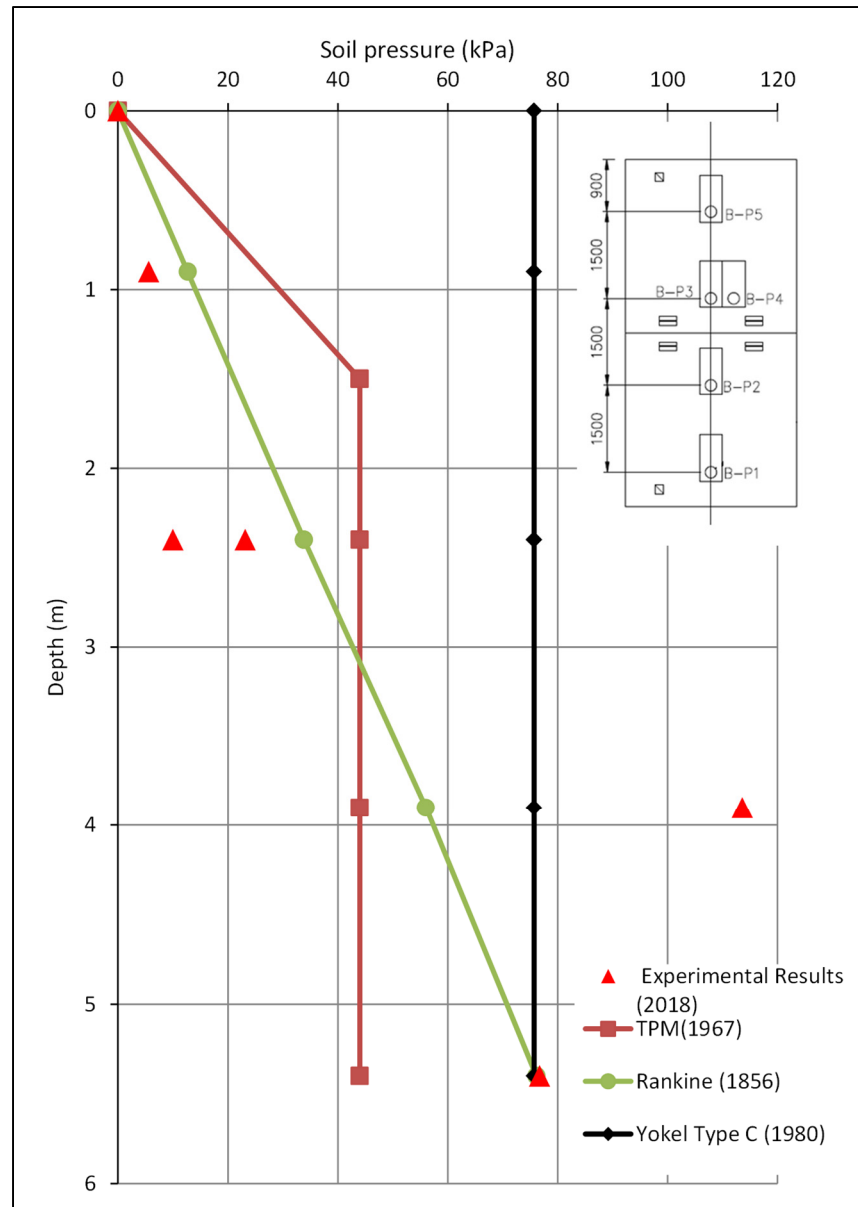


Figure 3.25 Experimental vs. theoretical soil pressure curves with respect to trench depth

3.5 Conclusions

The main objective of the field experimental work was to evaluate the soil pressure on the steel cage (Pro-tech, Pro 4 10 10) trench box at shallow depth in a sensitive clay trench. The study included two steel trench boxes stacked upon each other and assembled using “hinge

connections” to cover the total depth of the 6 m (20 ft) trench in sensitive clay soil. Concrete blocks (representing a 45 kPa surcharge load) were installed very close to the trench to produce an extreme load case on the flexible wall of the trench box. Soil pressures were captured by total pressure cells (TPC) using vibrating-wire transducer technology. Based on the results of this study, the following observations can be made:

- Soil temperature variations were more pronounced in the upper part of the trench than in the deeper part.
- The deeper pressure cells in the trench experienced higher pressures (kPa) than the upper pressure cells. The maximum pressure was 114 kPa (2.38 ksf) at 3.9 m (12.8 ft) from the top.
- The effect of an overload applied close to the trench was more pronounced on the upper part of the trench box than on the deeper part. It followed that the pressure cells at 0.9 m and 2.4 m depths were more influenced by the 45 kPa overload in a short period of time. This reveals the need to maintain the minimum distance of 1.2 m (4 ft) from the excavation when stacking up any materials, in compliance with OSHA and SCCI guidelines.
- Theoretical calculations by Rankine (1857), Terzaghi and Peck (1967), and Yokel *et al.* (1980) for this type of sensitive clay were compared with the pressures obtained from the field test results. Compared to Terzaghi and Peck, analytical values predicted by the Rankine and Yokel formulae were closer to experimental values. In terms of soil pressure along the depth of trench, in general, the analytical formulae underestimated the experimental values for the type of sensitive clay considered in this study.

CHAPTER 4

FLEXIBLE TEMPORARY SHIELD IN SOFT AND SENSITIVE CLAY: 3D FE MODELING OF EXPERIMENTAL FIELD TEST

Miah Alam ^a, Omar Chaallal ^b, Bertrand Galy ^c

^{a, b} Department of Construction Engineering, École de Technologie Supérieure,
1100 Notre-Dame West, Montreal, Quebec, Canada H3C 1K3.

^c Department of Research, Québec Occupational Health and Safety Research Institute
(IRSST), 505 de Maisonneuve Blvd. West, Montreal, H3A 3C2, Canada

Paper published in *Journal of Modelling and Simulation in Engineering*, February, 2021.

4.1 Abstract

A finite-element (FE) numerical study using PLAXIS-3D software was carried out to reproduce and validate a full-scale experimental in-situ test and to investigate the earth pressure on a flexible temporary trench box shield in soft and sensitive clay soil. The excavation trench model was 6 m (20 ft) deep and was considered as nonlinear and anisotropic clay. A 45 kPa (0.94 ksf) surface overload on top of the soil near the trench box was also simulated to produce a maximum load case on the flexible wall of the shield. Both Mohr-Coulomb (MC) and hardening soil (HS) constitutive soil models were considered for FE analysis. Different values of the modulus reduction factor (MRF) and the coefficient of earth pressure at rest (K_0) were considered to validate the model. For a specific shear strength profile, FE analysis with a linear elasto-plastic soil model showed relatively small differences in soil pressure with the field test results along the depth of the trench. Results were also compared with the predictions of well-established analytical formulae.

4.2 Introduction

Over the past decades, various analytical studies have been carried out to improve our understanding of the behavior of braced excavations protection systems (Karlsrud & Andresen, 2005). As a protection system, the trench box shield is different from other braced systems

because, instead of shoring up or otherwise supporting the trench face, it primarily aims to protect workers from cave-ins or similar incidents. Shields shall not be subjected to loads exceeding those that the system can withstand (OSHA, 2015). The earth pressure distribution on a shield depends on the type of soil, the shoring, and the method of installation. Generally, no satisfactory consensual theoretical solutions are available to estimate soil pressure for this type of supporting structure with partitions facing land pressures in sensitive clay (NBCC, 2015). Many researchers have suggested theoretical solutions to estimate earth pressure on a flexible temporary support (Rankine, 1857; Terzaghi and Peck, 1967; Yokel *et al.*, 1980). Consequently, for an excavation shield, the Canadian Foundation Engineering Manual (CFEM, 2006) recommends the use of pressure envelopes from empirical formulae.

Our understanding of the behavior of excavations and trenches with flexible retaining walls has evolved significantly in recent years with the help of numerical FE and analytical methods. Using FE analyses, Goldberg *et al.* (1976) found that under a given set of soil conditions, the higher the wall rigidity, the greater was the apparent earth pressure. A study by Hashash and Whittle (1996) on shoring excavations in clay has shown that the evolution of lateral thrust on a retaining structure (or wall) is a complex function of the flexibility of the retaining structure and the magnitude of shear deformations at depth. Their analyses also revealed the development of an arching effect in the ground in contact with the shoring. Karlsrud and Andresen (2005) concluded that the development of earth pressure on supporting structures set up in sensitive clays is a complex function that depends on the flexibility of the support, the anisotropy property, the thickness of the clay layer in the trench bottom, and deformations in the clay layer. Lam (2010) showed that a mobilized strength design database can be used to investigate the relationship between structural response ratio and soil-structure stiffness ratio and to capture the range of wall stiffnesses between sheet piles and thick diaphragm walls. Bryson and Zapata-Medina (2012) FE work clearly showed the influence of horizontal and vertical strut spacing, wall stiffness, and relative stiffness ratio on lateral wall deformation in an excavation support system (ESS) in three types of clays. However, their work focused on 12 m deep trenches, and a research gap has been observed for trench box shoring at shallower depths of less than 6 m and for soil-structure interaction (SSI) considerations (Alam *et al.*,

2020). It may be worth noting that trenches of less than 6 m are very common in practice and particularly in soft and sensitive clay. Therefore, there is a need to study the interaction between the soft and sensitive soil mass and the support, the flexibility in the development of lateral loads, and the movement of structural elements for shallow trench box shoring.

The objective of this paper is to discuss the details of an FE model and of simulations using the PLAXIS-3D software (Bentley, 2017) to simulate a flexible temporary shield in soft and sensitive clay, with particular emphasis on the Mohr-Coulomb (MC) versus hardening soil (HS) constitutive laws used for the soil layers, the structure and the soil-structure interaction, the sequence of excavation, and the installation of the temporary flexible shield walls. The impact of the shear strength of a specific type of soft and sensitive clay on earth pressures will be studied. The results will also be compared to published theoretical and experimental field test results.

4.3 Finite-element analyses

Numerical analyses of the performance of an excavation support system for most recent deep excavation case histories have required three-dimensional FE analyses (Finno *et al.*, 2007). In addition, Ou *et al.* (2000) have shown that the complex soil-structure interactions of excavation support systems and excavation-induced ground movements are three-dimensional (3D) in nature. To perform this 3D FE analysis (FEA) and obtain a better understanding of these complex soil-structure interactions, the PLAXIS-3D software was used. Analysis output (soil pressure) was compared with field test results obtained for Louiseville, Quebec, Canada (Alam *et al.*, 2020).

4.4 Parameters for FE

To simulate the trench with the excavation protection shield, three types of parameters were used in PLAXIS-3D: (i) soil model parameters for the excavation and surrounding soil,

including all the layers; (ii) structural model parameters for the box shield protection, and (iii) interface parameters.

4.4.1 Soil Modelling

The boundaries of the finite-element models were extended beyond the settlement zone of influence induced by the excavation, as determined in accordance with procedures recommended by Hsieh & Ou (1998). To simulate the trench, a soil model geometry such as soil contour $[(7.5 \text{ m (25 ft.)} \times 12 \text{ m (40 ft.)} \times 15 \text{ m (50 ft.)}]$ was assumed, which was more than twice the excavation contour $[3 \text{ m (10 ft.)} \times 1.5 \text{ m (5 ft.)} \times 6 \text{ m (20 ft.)}]$. The Louiseville soil layers were modelled using three depths and properties: (i) 0 m to 0.6 m (2 ft.) of depth of soil as fissured brown clay; (ii) 0.6 m (2 ft.) to 2 m (6.56 ft.) depth of soil as plastic brown clay; and (iii) 2 m (6.56 ft.) to 15 m (50 ft.) depth of soil as sensitive blue clay in accordance with the stratigraphic profile of the Louiseville soil. Soil properties, especially strength, required careful attention because they are a key factor in the overall performance of the excavation support system (ESS) (Allen Marr & Hawkes, 2010). Supporting this statement, the in-situ value of soil shear strength in Louiseville shown in Figure 4.1(a) was used in this FEA. The soil contour with the trench model is shown in Figure 4.1(b).

4.4.2 Structural modelling

Bryson & Zapata-Medina (2012) indicated that the stiffness of an excavation support system (ESS) is a complex function of the flexural rigidity of the wall element, the structural stiffness of the support elements, the type of connections between the wall and the supports, and the vertical and horizontal spacing of the support system. Therefore, the two trench steel shields ‘stacked upon each other’ to cover the total depth (6 m (20 ft.)) of excavation were simulated according to the geometrical dimensions shown in Figure 4.2 and Table 4.1. The positions and locations of the struts used for simulation are shown in Figure 4.3.

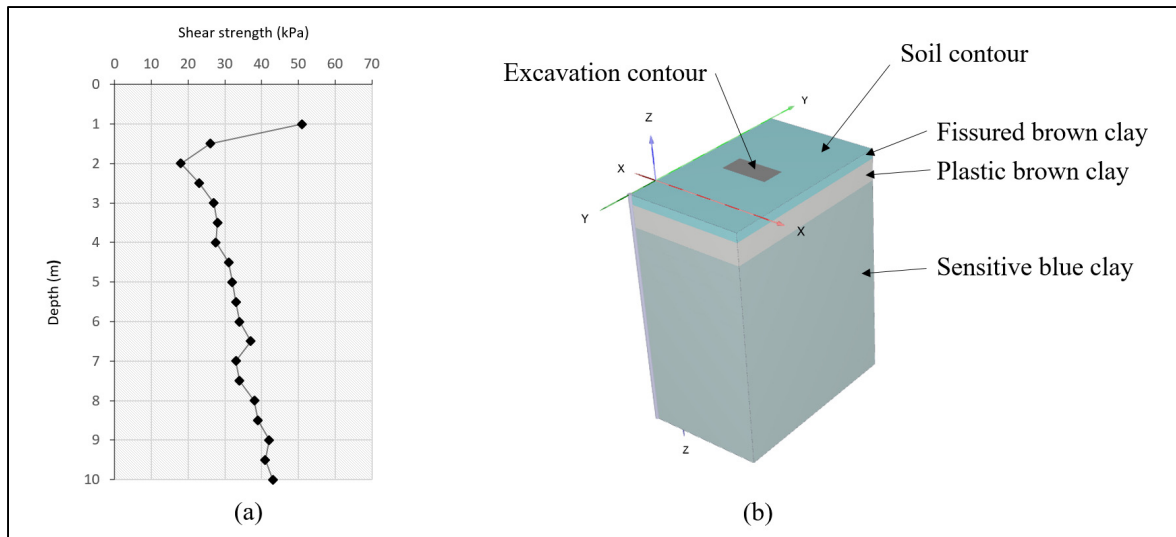


Figure 4.1 Geometric profile and excavation contour in Plaxis-3D simulation of trench: (a): Experimental values of soil shear strength at Louiseville site; (b): Plaxis-3D model profile for Louiseville soil (Number of soil elements: 23221; MC soil model)

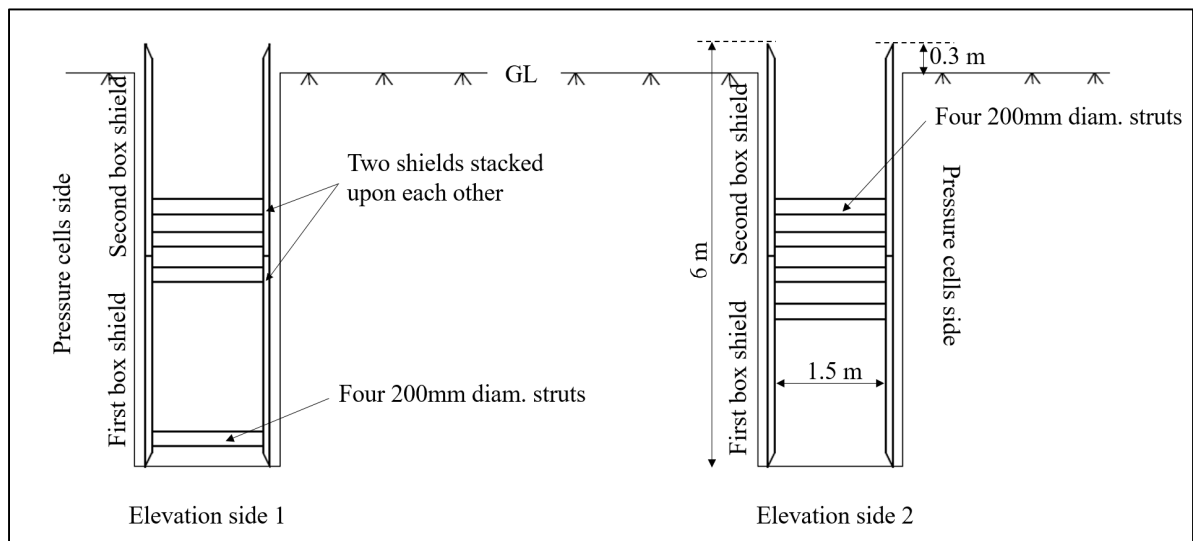


Figure 4.2 Elevation views of trench and shield

Other parameters such as plate and strut mechanical properties are presented in Table 4.1. The Young's modulus (E), shear modulus (G), and Poisson's ratio (ν) of 4.76 mm (3/16 in)-thick A-572 grade 50 steel plate were assumed. Plate unit weight (γ) was calculated from the total weight of the shield, and an equivalent 100 mm (4 in) thick sandwich plate was considered as

per PLAXIS-3D input. For the struts (or spreader tube), Young's modulus (E) and unit weight (γ) were taken from the 200-mm strut SCH80 chart. Cross-sectional area (A) and moment of inertia (I) were calculated from the original strut diameter. The vertical positions of the struts were made different on both sides to allow the excavator to access the soil to be excavated between the two walls of the shield.

Table 4.1 Geometric and mechanical properties of box shield protection used for FE simulation in Plaxis-3D

| Parameter/Properties | Plaxis-3D Nomenclature (Unit) | Strut (Spreader tube) | Plate |
|----------------------------------|--|--------------------------|-----------------------|
| Material Type | Type | Elastic | Elastic, Isotropic |
| Youngs Modulus | E_1 (kN/m ²) | 2×10^8 | 2×10^8 |
| | E_2 (kN/m ²) | | 2×10^8 |
| Unite weight | γ (kN/m ³) | 78.50 | 13.67 |
| Cross section Area | A (m ²) | 0.01 | |
| Moment of Inertia | I_2 xx (m ⁴) | 4.41×10^{-5} | |
| | I_3 yy (m ⁴) | 4.41×10^{-5} | |
| Thickness | d (m) | | 0.10 |
| Poisson's ratio | ν_{12} | | 0.30 |
| Shear Modulus | G_{12} (kN/m ²) | | 8×10^7 |
| | G_{13} (kN/m ²) | | 8×10^7 |
| | G_{23} (kN/m ²) | | 8×10^7 |
| From 200 mm strut SCH80 chart | Outer diameter strut, d_o (mm) | 219 (8.63 in.) | |
| | Inner diameter strut, d_i (mm) | 194 (7.63 in.) | |
| | Area of strut (m ²) | 8.24×10^{-3} | |
| | I_{yy} or I_{xx} for strut (m ⁴) | 4.41×10^{-5} | |
| One shield geometry | Length (m) | 3.0 (10 ft) | |
| | Height (m) | 3.0 (10ft) | |
| | Plate thickness (mm) | 100 (4 in) | |
| | Horizontal distance between struts (m) | 2.6416 (104 in) | |

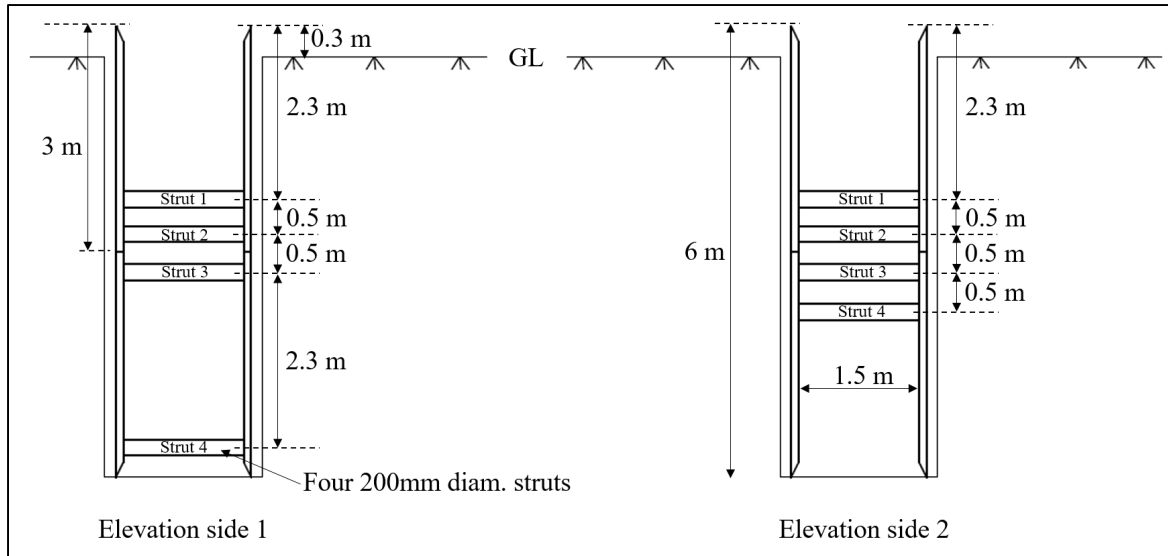


Figure 4.3 Strut spacing and locations in the two assembled box shields (stacked upon each other)

In the PLAXIS-3D simulation, the box shield steel built-in plate walls (sandwich plate as per PLAXIS-3D) are modelled as ‘plate elements’ and the struts as ‘beam elements’. Four-cornered ‘hinge joints’ were used between the two box shields (stacked upon each other) to represent the experimental setup shown in Figures. 4.4 and 4.5. Similarly, the joints between the struts and the plates were simulated as ‘hinge joints’ and were representative of the experimental setup illustrated in Figures. 4.4 and 4.6. Note that the bottom end part of the shield (around 300 mm) was embedded into the soil and that the total gravity load of the upper steel box was pushing the lower box shield into the ground during installation of the experiment. Therefore, the bottom part (around 300 mm) of the lower box acted more likely as a ‘fixed end support’ in the experiment and was represented by a ‘fixed end anchored element’, as illustrated in Figure 4.4.

To analyze the non-linear stress-strain behavior of the soil model in the trench and the soil surrounding the excavation, two constitutive material models, (a) Mohr-Coulomb (MC) and (b) hardening soil (HS), were used in this study.

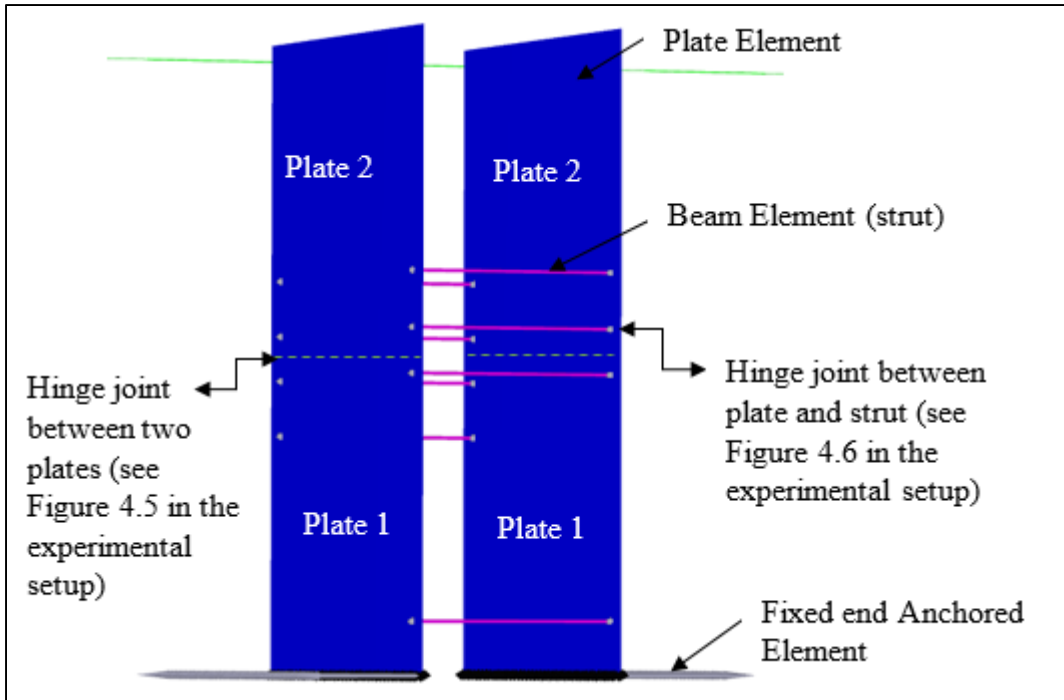


Figure 4.4 Structural simulation of the two assembled box shields (stacked upon each other) protection in Plaxis-3D (Number of structural elements:1050; MC soil model)

4.4.3 Generating the Mohr-Coulomb (MC) model

The MC model is a simple and widely used linear elastic perfectly plastic model. The linear elastic part of the Mohr-Coulomb model is based on Hooke's law of isotropic elasticity, and the perfectly plastic part is based on the MC failure criterion (Bentley, 2017). For a first approximation to see the behavior in general, the MC model was chosen. Table 4.3 shows the soil parameters for the Mohr-Coulomb (MC) model used for finite-element modelling of the Louisville sensitive clay. The soil stiffness moduli (E) at different depths are calculated from the shear strength (C_u) in the Louisville soil test results using the equation proposed by Peck (1975):

$$E = 600 * C_u \quad (4.1)$$

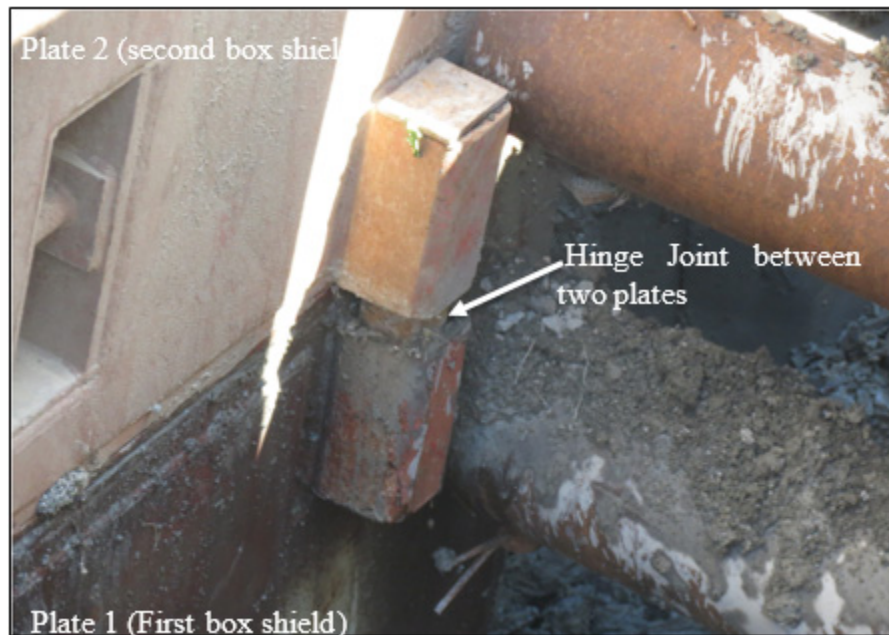


Figure 4.5 Experimental hinge joint between two plate walls of assembled box shields (stacked upon each other)

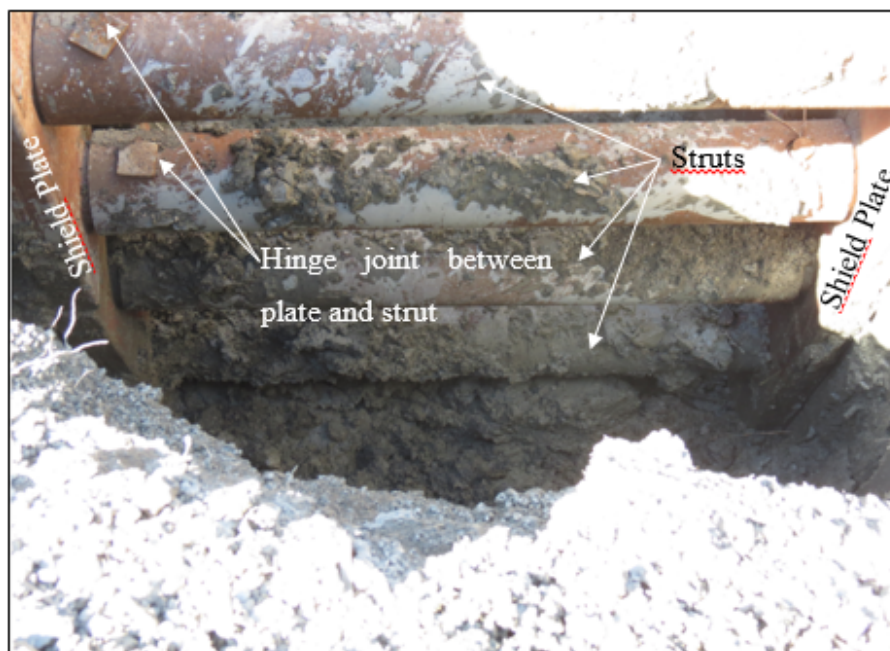


Figure 4.6 Experimental hinge joint between plate and strut of box shield

Table 4.2 Calculation of E for different layers of plastic brown and sensitive blue clay

| Depth (m) | Cu (kPa) | E (kPa) | E _{avg} (kPa) |
|-----------|----------|---------|------------------------|
| 0 | 0 | 0 | 0 |
| 0.6 | 25 | 15000 | 15000 |
| 1 | 51 | 30600 | 20400 |
| 1.5 | 26 | 15600 | |
| 2 | 18 | 10800 | 13600 |
| 2.5 | 23 | 13800 | |
| 3 | 27 | 16200 | 16500 |
| 3.5 | 28 | 16800 | |
| 4 | 27.5 | 16500 | 18100 |
| 4.5 | 31 | 18600 | |
| 5 | 32 | 19200 | 19800 |
| 5.5 | 33 | 19800 | |
| 6 | 34 | 20400 | 20800 |
| 6.5 | 37 | 22200 | |
| 7 | 33 | 19800 | 21000 |
| 7.5 | 34 | 20400 | |
| 8 | 38 | 22800 | 23800 |
| 8.5 | 39 | 23400 | |
| 9 | 42 | 25200 | 25200 |
| 9.5 | 41 | 24600 | |
| 10 | 43 | 25800 | 25800 |
| 11 | 43 | 25800 | 25800 |
| 12 | 45 | 27000 | 27000 |
| 13 | 48 | 28800 | 28800 |
| 14 | 44 | 26400 | 26400 |

Table 4.2 presents the average values of E ($E_{avg.}$) for PLAXIS-3D input. In the soil model, the stress-strain relationship depends on the soil skeleton. The soil response is influenced by pore pressure. This water-skeleton interaction was considered as a plastic calculation using a PLAXIS-3D drainage-type parameter. For the 0.6 m layer of fissured brown clay, ‘drained’ behavior was assumed, and therefore in this layer, no excess pore pressure was generated, and full drainage was assumed due to the low rate of loading. On the other hand, in the saturated soil layer, pore water cannot freely flow through the soil skeleton (due to low permeability) (Bentley, 2017). This phenomenon is described by PLAXIS-3D as an undrained behavior for brown clay and sensitive blue clay. To make sure that the soil skeleton is much more compressible than the pore water, the effective Poisson’s ratio should be less than 0.35 for the undrained (B) condition (Bentley, 2017). For practical reasons, the undrained (B) option was chosen because this method allows the Louiseville shear strengths (S_u) to be used as input parameters in PLAXIS-3D. This does not hold true in the undrained (A) condition, where shear strength (S_u) is rather a consequence of the model, not an input parameter. On the other hand, the undrained (C) condition was not considered because, although the shear strength parameter (S_u) is an input parameter, it cannot provide a prediction of pore pressure. The undrained (C) method is not suitable for consolidation analysis (Bentley, 2017).

4.4.4 Interface model

Interfaces were added as a joint element to the plates for proper modelling of soil-structure interaction. They represent a thin zone of intensely shearing material at the contact between a plate and the surrounding soil. Positive and negative interface were added (local z-direction) on either side of a plate surface (Figure 4.7). The interface properties included material mode, permeability condition, and virtual thickness factor. The interaction between the steel plate wall and the soil was expressed by a suitable strength reduction factor (R_{inter}). This factor relates the interface strength (wall friction and adhesion) to the soil strength (friction angle and cohesion). Recommended values for R_{inter} are as follows: $2/3$ for fissured brown clay and $< 2/3$ for plastic brown and sensitive blue soft clay (Bentley, 2017) (Table 4.3). The interface was assigned an imaginary dimension called the virtual thickness. In the MC and HS models, the

virtual thickness of the interface element varied with mesh type and ranged between 103×10^{-3} m and 154×10^{-3} m. The interface element consisted of pairs of nodes compatible with a six-node triangular side of a soil element or a plate element (Bentley, 2017).

Table 4.3 Properties for Louiseville soil and Mohr-Coulomb material model parameters used for FE modeling

| Parameter /Properties | Plaxis Nomenclature (Unit) | Fissured brown clay | Plastic brown clay | Sensitive blue clay |
|--|--|------------------------|-----------------------|------------------------|
| Depth of layer | m | 0.0 - 0.6 | 0.6 - 2 | 2 - 15 |
| Material model | model | MC | MC | MC |
| Drainage type | type | Drained | Undrained B | Undrained B |
| Unit wt. above phreatic level | γ_{unsat} (kN/m ³) | 16 | 16 | 16 |
| Unit wt. below phreatic level | γ_{sat} (kN/m ³) | 17 | 17 | 17 |
| Young's Modulus | E (kN/m ²) | See Table 4.2 | See Table 4.2 | See Table 4.2 |
| Cohesion | C'_{ref} (kN/m ²) | 5 | 5 | 5 |
| Frictional angle | ϕ [°(degree)] | 28 | 28 | 28 |
| Dilatancy angle | Ψ [°(degree)] | 0 | 0 | 0 |
| Poisson's ratio | ν'_{ur} | 0.3 | 0.3 | 0.3 |
| Interface strength reduction factor | R inter | 0.66 | 0.5 | 0.5 |
| Initial K_0 determination | | 0.53 | 0.53 | 0.53 |
| Soil Type | | | | Very fine |
| <2 m μ | % | 10 | 10 | 74 |
| 2m μ -50m μ | % | 13 | 13 | 11 |

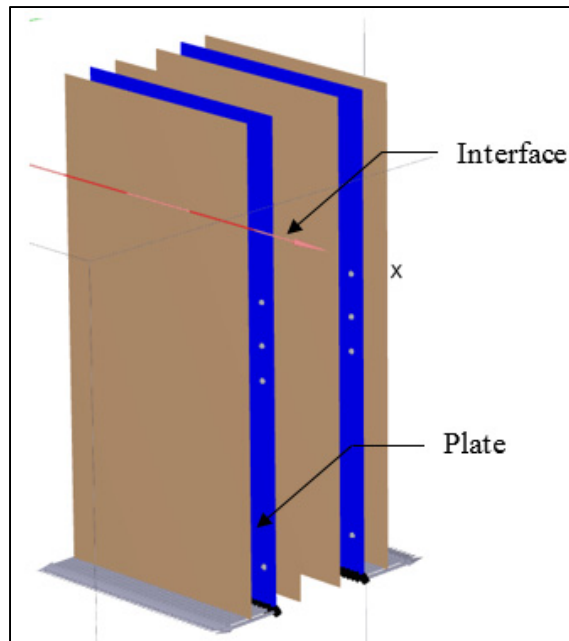


Figure 4.7 Interfaces in Plaxis-3D model

4.4.5 Water head variations

Water pressure has a direct effect on strength of soils, on pressure against the wall, and on uplift of soil in the bottom of the excavation. Many situations are not hydrostatic before the work starts but change during the work. These conditions can be modelled in FEA (Allen Marr & Hawkes, 2010). For the variation in water head, the piezometer readings obtained for different months and presented in Table 4.4 were used separately for the water table height to obtain the maximum soil stress on the protection shield wall.

Table 4.4 Seasonal water head variations readings
Taken from Laval University

| Time Frame | water head form top of soil (m) |
|------------|---------------------------------|
| 14-May-18 | 0.92 |
| 8-Jun-18 | 1.2 |
| 22-Jun-18 | 1.8 |
| 22-Jul-18 | 2 |
| 3-Aug-18 | 2.5 |

4.4.6 Mesh generation

A medium-coarse 10-node element was used for each of the simulation and connectivity plot elements shown in Figure 4.8. This mesh generation process considers the soil, all the structural components, loads, and boundary conditions. As a result of meshing, a total number of elements of 24271, i.e., 23221 soil elements and 1050 structural elements, was reached.

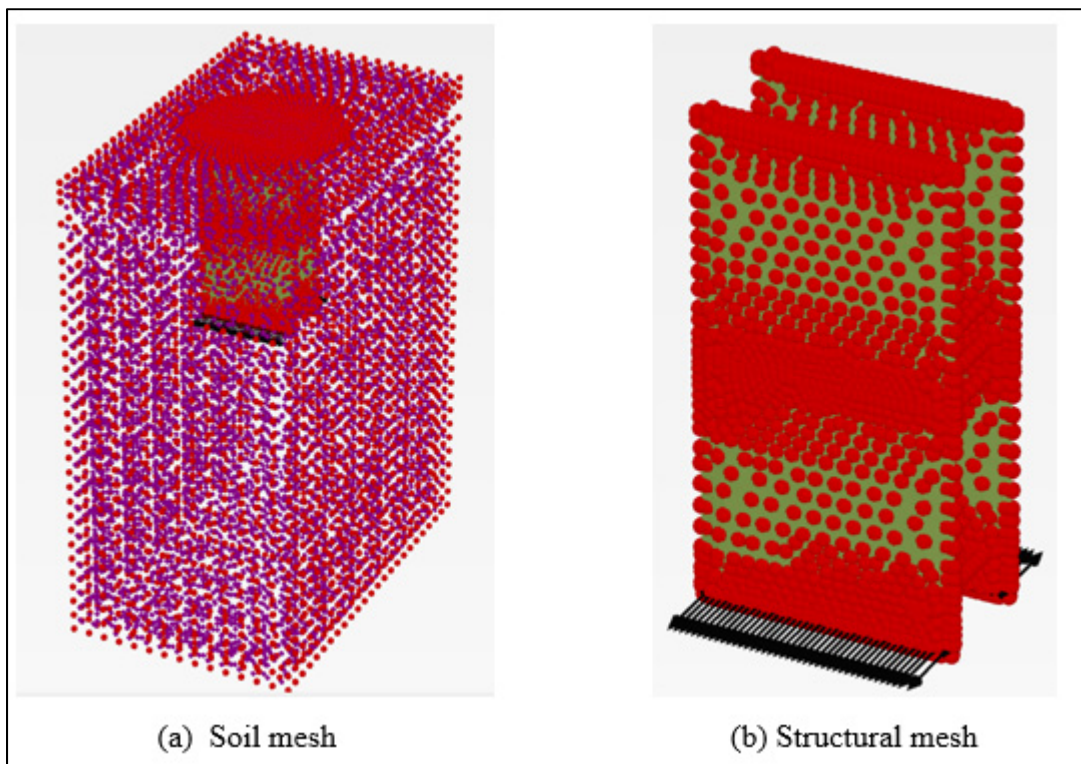


Figure 4.8 Mesh generation of the soil and structural elements in Plaxis-3D

4.5 Construction steps and phases in PLAXIS-3D simulation

Poulos *et al.* (2002) showed that construction details and sequence, as well as soil-structure interaction, have a significant impact on the movements and lateral loads acting on a flexible retaining structure. Therefore, the construction steps constituted a major and critical part of this FE simulation. The model assigned a step-by step excavation sequence including the

structural elements inserted into the excavation. All the phases of the construction sequence are summarized in Table 4.5.

Table 4.5 Construction sequence of FE modeling in Plaxis-3D

| Phase | In the model | Drainage |
|---------|--|-----------------------------------|
| Phase 0 | Only soil elements (no structure) | K_0 - procedure |
| Phase 1 | Excavation (1 st layer, depth: 0.6 m) fissured brown clay | Drained |
| Phase 2 | Excavation (2 nd layer: 0.6 to 2m) Brow clay | Plastic: undrained B (soil model) |
| Phase 3 | Adding structural element | Plastic: undrained B (soil model) |
| Phase 4 | Excavation (3 rd layer: 2m to 6m) sensitive blue clay | Plastic: undrained B (soil model) |

4.5.1 Construction step 0: Initial Phase

In the initial phase, only the natural (undisturbed) soil was considered. No excavation was made in this step, and only K_0 (the parameter to produce initial stress) was considered in the calculations. In general, K_0 values can be specified, $K_0, x = \sigma'_{xx} / \sigma'_{zz}$ in the x-direction and $K_0, y = \sigma'_{yy} / \sigma'_{zz}$ in the y-direction. The default K_0 values are defined by the Jaky (1944) coefficient as follows:

$$K_0 = 1 - \sin \varphi \quad (4.2)$$

where φ = the frictional angle. A staged construction loading type was selected to generate the initial stresses. The initial stresses in a soil body are influenced by the weight of the soil, the water conditions, and the history of its formation. This stress state can be generated using either the K_0 procedure or gravity loading. The K_0 procedure should preferably be used in cases with a horizontal surface and with all soil and phreatic levels parallel to the surface (Bentley, 2017), as in the case under consideration.

4.5.2 Construction step 1: Phase 1

In construction step 1, the first layer (0 m–0.6 m depth) of fissured brown clay was excavated, representing an excavation contour of $[3 \text{ m (10 ft)} \times 1.5 \text{ m (5 ft)} \times 0.6 \text{ m (2 ft)}]$. For this phase, the plastic calculation and the ‘drained’ soil drainage type were selected, as shown in Figure 4.9 (b). Therefore, the soil will behave as in a drained condition, unlike the clay below, which will behave as an undrained medium for short-term analyses.

4.5.3 Construction step 2: Phase 2

In construction step 2, the second layer (0.6 m–2 m depth) of plastic brown clay was excavated, representing an excavation contour of $[3 \text{ m (10 ft)} \times 1.5 \text{ m (5 ft)} \times 2 \text{ m (6.56 ft)}]$, as shown in Figure 4.9 (c). The undrained B soil drainage type and the plastic calculation were assumed for this layer. In this undrained condition, assuming that no water was moving, long- and short-term loading behavior was assessed (Bentley, 2017), including built-up excess pore pressures. In the undrained (B) drainage type, modelling of undrained behavior using effective parameters for stiffness and undrained shear-strength parameters was allowed.

4.5.4 Construction step 3: Phase 3

In this step, a structure consisting of two box-shield excavation protectors ‘stacked upon each other’ $[3 \text{ m (10 ft)} \times 1.5 \text{ m (5 ft)} \times 6 \text{ m (20 ft)}]$ (Figure 4.4) was inserted into the simulated excavation, as shown in Figure 4.9(d). The undrained B soil drainage type and the plastic calculation were assumed for this phase.

4.5.5 Construction step 4: Phase 4

In this construction step, 2 m to 6 m of sensitive blue clay soil was excavated, as shown in Figure 4.9(e). In addition, a 45 kPa (0.94 ksf) surface overload was applied on one side of the

excavation in the PLAXIS-3D model to create an extreme load case, as shown in Figure 4.10. The undrained B soil drainage type and the plastic calculation were also selected for this phase.

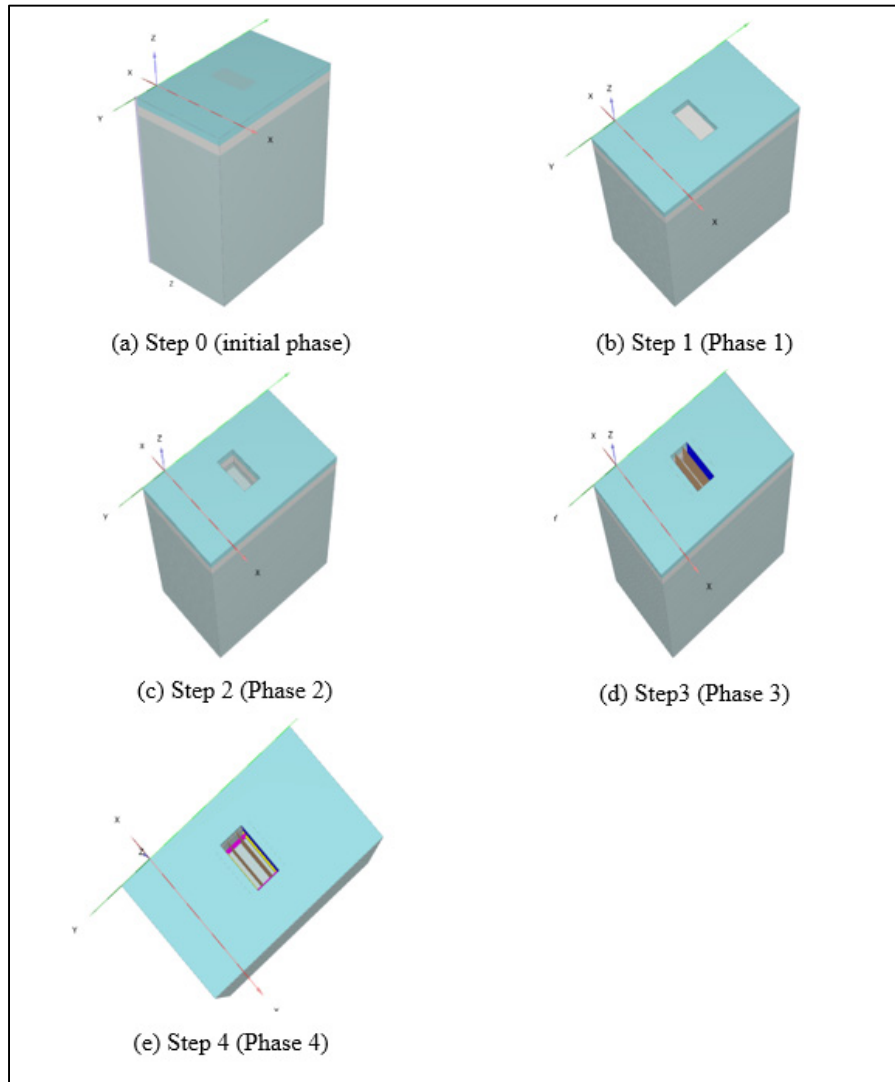


Figure 4.9 Plaxis-3D simulation for the construction steps

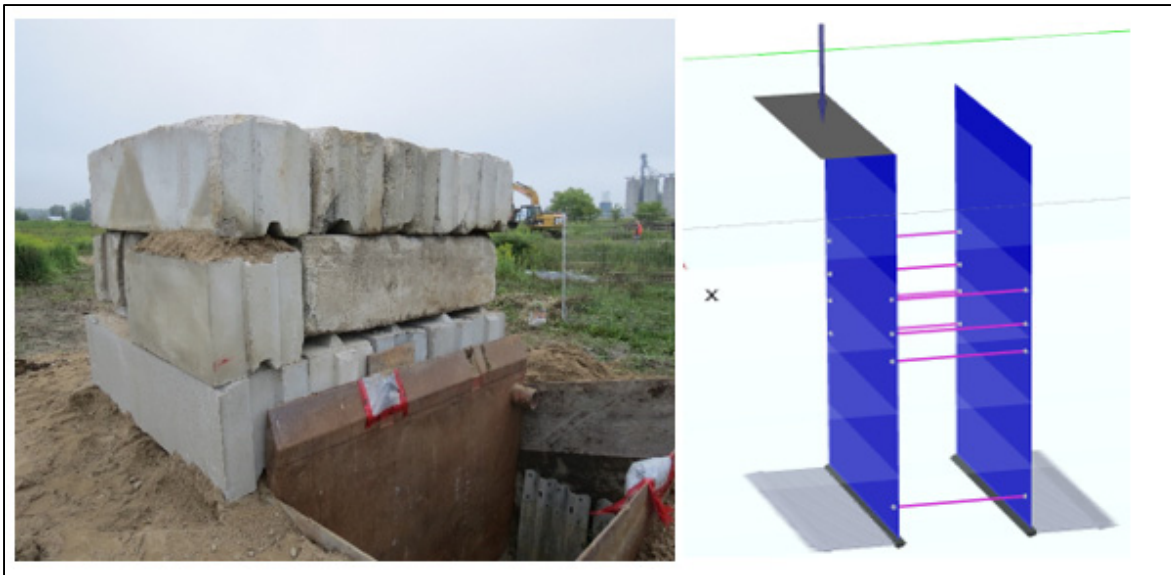


Figure 4.10 Plaxis-3D simulation for the construction step 4 (Phase 4) with overloading as per experimental site

4.6 Analysis using Mohr-Coulomb (MC) models and Results

The MC model represents a ‘first-order’ approximation of soil and rock behavior (Bentley, 2017). For that reason, the MC constitutive model with soil parameters given in Table 4.3 was considered as a first simulation analysis. The obtained soil stresses are presented in Table 4.6 for different depths with and without overloading. These depths are representative of the experimental location of the pressure cells because the objective was to find the soil stress in the PLAXIS-3D simulation at the same locations as in the experimental setup. In Table 4.6, it is very clear that the effect of an overload applied close to the trench was more pronounced on the upper part of the protective shield than on the deeper part (Boussinesq, 1885). It follows that the pressures on the plate at 0.9 m and 2.4 m depths of trench were more influenced by the 45 kPa (0.94 ksf) overload both in the MC simulation and in the experimental results. In contrast, it had negligible effect on the deeper part of the plate.

Table 4.6 Soil pressure for different depths of excavation by Plaxis-3D MC model without MRF [option B] compared with experimental

| Depth from Top (m) | MC model without overloading (kPa) | MC method with overloading (kPa) | Experimental without overloading (kPa) | Experimental with overloading (kPa) |
|--------------------|------------------------------------|----------------------------------|--|-------------------------------------|
| 0 | 0 | 0 | 0 | 0 |
| 0.9 | 3 | 10 | 5 | 6 |
| 2.4 | 39 | 41 | 15 | 23 |
| 3.9 | 51 | 52 | 114 | 114 |
| 5.4 | 79 | 79 | 77 | 77 |

4.6.1 MC model with modulus reduction factor (MRF)

Soft to medium clays may exhibit strength anisotropy, or in other words, their strength varies with the orientation of the failure surface (Allen Marr & Hawkes, 2010). Therefore, the results from the MC model must be verified using another approach. Relative shear stresses were considered, which yield an indication of the stress point to the failure envelope. The relative shear stresses (relative shear stress $\tau_{rel} = [\text{mobilized shear stress } (\tau_{mob}) / \text{maximum shear stress } (\tau_{max})]$) at the end of phases 2 and 4 of the PLAXIS-3D MC model output are shown in Table 4.7. Based on the maximum value of relative shear stress, the mobilized shear strength (τ_{mob}) was then adopted from the modulus reduction vs. mobilized strength curve of undrained Thanet clay soil (Mayne, 2006) to estimate the modulus reduction factor (MRF). The MRF is the ratio of elastic modulus (E/E_{max}) or shear modulus (G/G_{max}). Thanet clay was considered because it is a soft undrained clay, much like the Louiseville clay. New E and G values were computed from the Kramer (1996) equations (4.3) and (4.4) with the corresponding MRF values of the Mayne (2006) curve for each soil layer up to 14 m depth, as shown in Table 4.7:

$$E = Su \text{ (at Louiseville)} * MRF * 1000 \quad (4.3)$$

$$G = G \text{ (at Louiseville)} * MRF * 1000 \quad (4.4)$$

Table 4.7 Calculation of modulus reduction factor and corresponding Elastic modulus (E) and Shear modulus (G)

| Depth | Relative shear stress from Plaxis-3D results | | Value of modulus reduction (E/E_{\max}) or G/G_{\max} factor | E (kPa) | G (kPa) |
|-------|--|---------|--|---------|---------|
| | Phase 2 | Phase 4 | From Mayne (2006) curve (Thanet undrained clay) | | |
| 0 | 0 | 0 | 0 | 0 | 0 |
| 0.6 | 0.4 | 0.4 | 0.205 | 5125 | 3280 |
| 1 | 0.6 | 0.6 | 0.11 | 3740 | 1980 |
| 2 | 0.53 | 0.55 | 0.12 | 2720 | 1800 |
| 3 | 0.754 | 0.885 | 0.1 | 2750 | 1600 |
| 4 | 0.684 | 0.969 | 0.08 | 2413 | 1320 |
| 5 | 0.694 | 0.734 | 0.105 | 3465 | 2205 |
| 6 | 0.635 | 0.968 | 0.65 | 2773 | 1440 |
| 7 | 0.712 | 0.959 | 0.08 | 2800 | 1440 |
| 8 | 0.1 | 0.1 | 0.65 | 25783 | 14950 |
| 9 | 0.04 | 0.053 | 0.75 | 31500 | 19500 |
| 10 | 0.05 | 0.067 | 0.78 | 33540 | 21060 |
| 11 | 0.02 | 0.02 | 0.9 | 34400 | 21600 |
| 12 | 0.011 | 0.011 | 0.9 | 40800 | 24300 |
| 13 | 0.01 | 0.01 | 0.9 | 43200 | 24300 |
| 14 | 0.004 | 0.004 | 0.105 | 39600 | 24300 |

Then these values were used as a PLAXIS-3D input to run the model again and obtain the maximum soil pressures MC with MRF (with E) [option C1] and (with G) [option C2], as shown in Table 4.11.

4.6.2 Mohr-Coulomb reduction factor with shear strain

In this method, the shear strains from the PLAXIS-3D output results of the MC model for each depth shown in Table 4.8 were assumed. The Vucetic (1991) curve [G/G_{\max} vs. cyclic shear strain (γ)] was used to find the corresponding modulus reduction factor (G/G_{\max}). Note that the PI=50 curve was used because the plasticity index (PI) of the Louiseville soil is 42 (Leroueil *et al.*, 2002). With the value of the modulus reduction factor, Equation (4.5) was used to calculate the shear modulus for Louiseville clay:

$$G = MRF * G_{max}. \quad (4.5)$$

Then these values were input to the analysis to obtain the maximum soil pressures MC with MRF (for PI=50) [option C3], as shown in Table 4.11.

Table 4.8 Calculation of modulus reduction factor and corresponding Elastic modulus (E) and Shear modulus (G) from shear strain

| Depth (m) | Shear strain, γ (m/m) (10^{-3}) | Modulus factor (G/G_{max}) value from Vucetic (1991) curve (for PI=50) | G (kPa) | E (kPa) |
|-----------|--|--|---------|---------------------|
| 0 | 0 | 0 | 0 | 0 |
| 0.6 | 0.24 | 0.7 | 11200 | 2.91×10^4 |
| 1 | 0.351 | 0.6 | 10800 | 2.81×10^4 |
| 2 | 0.745 | 0.46 | 6900 | 1.79×10^4 |
| 3 | 0.486 | 0.5 | 8000 | 2.08×10^4 |
| 4 | 1.415 | 0.12 | 1980 | 5.148×10^3 |
| 5 | 0.79 | 0.43 | 9030 | 2.35×10^4 |
| 6 | 1.247 | 0.14 | 2520 | 6.552×10^3 |
| 7 | 0.814 | 0.36 | 6480 | 1.69×10^4 |
| 8 | 0.053 | 0.83 | 19090 | 4.96×10^4 |
| 9 | 0.035 | 0.85 | 22100 | 5.75×10^4 |
| 10 | 0.028 | 0.86 | 23220 | 6.04×10^4 |
| 11 | 0.025 | 0.87 | 23490 | 6.11×10^4 |
| 12 | 0.016 | 0.88 | 23760 | 6.18×10^4 |
| 13 | 0.012 | 0.9 | 24300 | 6.32×10^4 |
| 14 | 0.007 | 0.98 | 26460 | 6.88×10^4 |

4.6.3 Validation of the MC model

To validate the MC model, parameters such as K_0 and the pore pressure must be checked. In practice, K_0 for a normally consolidated soil is often assumed to be related to the friction angle by Jaky's empirical expression (Eq. (2)). In an over-consolidated soil, K_0 would be expected to be larger than the value given by this expression. However, for the Mohr-Coulomb model, the default K_0 value is based on Jaky's formula. Hamouche *et al.* (1995) evaluated the in-situ coefficient of earth pressure at rest for Louiseville sensitive clay. Three values of K_0 (0.55, 1, and 1.5) from the profile were chosen to validate the MC model to take account of fluctuations

in soil pressure with depth: (i) $K_0 = 0.55$ is the value computed from Jaky's formula with $\phi = 27^\circ$, which is a common friction angle for clays or gravity loading; (ii) $K_0 = 1$ represents the case for clay in undrained conditions only (when $\phi = 0$); and (iii) $K_0 = 1.5$ represents the experimental profile at 6 m depth. Table 4.9 and Figure 4.11 show the soil pressures with different K_0 values after analysis using the M-C model.

Table 4.9 Soil pressure at different depths of the excavation by Plaxis-3D MC model with different K_0

| Depth from top (m) | Soil pressure [kPa] | | |
|--------------------|-------------------------------|-----------|-------------|
| | $K_0 = 0.55$ /Gravity loading | $K_0 = 1$ | $K_0 = 1.5$ |
| 0 | 0 | 0 | 0 |
| 0.9 | 1.5 | 10 | 13 |
| 2.4 | 26 | 39 | 55 |
| 3.9 | 44 | 52 | 66 |
| 5.4 | 60 | 79 | 98 |

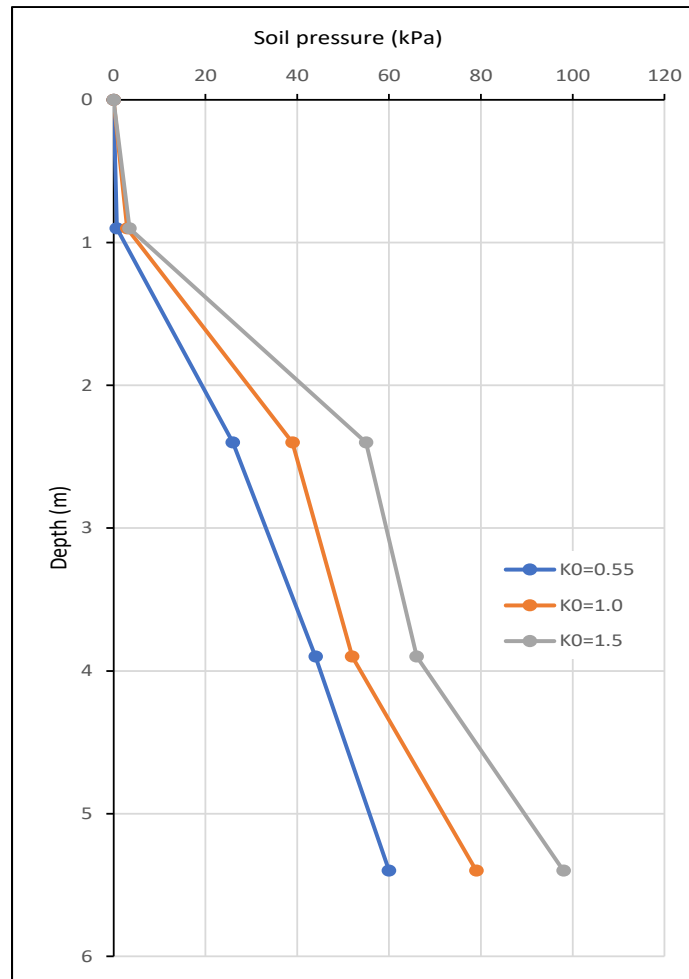


Figure 4.11 Soil pressure at different depth of trench with different K_0 values

4.7 Simulation analysis using the hardening soil (HS) material model

Using the same structural properties and soil layers, the HS model (Schanz *et al.*, 1999) was used to predict the constitutive behavior of the soils. Table 4.10 presents the soil properties used for HS simulation. Allen Marr & Hawkes (2010) stated that for soft clay, the E_{50} modulus varies between 2,500 kPa (52 ksf) and 15,000 kPa (313 ksf). For Chicago soft and undrained clay, E_{50} was reported to be 2,350 kPa (49 ksf) (Bryson & Zapata-Medina, 2012). Considering that Louisville soft and sensitive clay is softer than Chicago clay, its E_{50} modulus was therefore assumed equal to 2000 kPa (42 ksf). For the undrained B in the HS model, the stiffness moduli in the model are no longer stress-dependent, and the model exhibits no

compression hardening. Again, the undrained shear strength (S_u) for the Louiseville soil was an input parameter to the HS model. Soil pressures from the HS model [option A] along the trench depth are presented in Table 4.11.

Table 4.10 Properties of Louiseville soil and Hardening soil (HS) material model parameters used for FE modeling

| Parameter /Properties | Plaxis-3D Nomenclature (Unit) | Fissured brown clay | Plastic brown clay | Sensitive blue clay |
|---|--|------------------------|-----------------------|------------------------|
| Depth of layer | m | 0.0 - 0.6 | 0.6 - 2 | 2 - 15 |
| Material model | model | HS | HS | HS |
| Drainage type | type | Undrained B | Undrained B | Undrained B |
| Unit wt. above phreatic level | γ_{unsat} (kN/m ³) | 16 | 16 | 16 |
| Unit wt. below phreatic level | γ_{sat} (kN/m ³) | 17 | 17 | 17 |
| Secant stiffness for CD triaxial test | $E_{50 \text{ ref}}$ (kN/m ²) | 2×10^3 | 2×10^3 | 2×10^3 |
| Tangent Oedometer stiffness | $E_{\text{oed ref}}$ (kN/m ²) | 2×10^3 | 2×10^3 | 2×10^3 |
| Unloading /reloading stiffness | $E_{\text{ur ref}}$ (kN/m ²) | 1×10^4 | 1×10^4 | 1×10^4 |
| Power for stress level dependency of stiffness | m | 1 | 1 | 1 |
| Shear strength of soil | S_u (kPa) | 29 | 29 | 38 |
| Cohesion | C'_{ref} (kN/m ²) | 5 | 5 | 5 |
| Frictional angle | ϕ [°(degree)] | 28 | 28 | 28 |
| Dilatancy angle | Ψ [°(degree)] | 0 | 0 | 0 |
| Poisson's ratio | ν'_{ur} | 0.3 | 0.3 | 0.3 |
| Interface reduction factor | R_{inter} | 0.65 | 0.5 | 0.5 |
| Initial K_0 determination | K_0 | 0.53 | 0.53 | 0.53 |
| Over-Consolidation ratio | OCR | 1.5 | 1.5 | 3 |
| Pre-overburden pressure | POP (kN/m ²) | 0 | 0 | 0 |
| Soil Type | | | | Very fine |
| < 2 μ | % | 10 | 10 | 74 |
| 2 μ -50 μ | % | 13 | 13 | 11 |

Table 4.11 Comparison of soil pressures on flexible temporary shield in soft and sensitive clay excavated trench

| Depth from top of the soil (m) | In-situ test results | Finite Element Model Analysis Results using Plaxis-3D | | | | | Analytical results | | |
|--------------------------------|----------------------------|---|--------------------------|---------------------------------|---------------------------------|------------------------------------|---|---|--|
| | Experimental -option (kPa) | HS-mode 1 [A] (kPa) | MC without MRF [B] (kPa) | MC with MRF (with E) [C1] (kPa) | MC with MRF (with G) [C2] (kPa) | MC with MRF (for Ip=50) [C3] (kPa) | Calculated stress from Terzaghi and Peck (1967): $p_A = 1.0 K_A \cdot \gamma \cdot H$ (kPa) | Calculated total active stress from Rankine (1857): $P = 0.5 (\gamma \cdot H^2 - 4S_u H)$ (kPa) | Calculated stress from Yokel <i>et al.</i> (1980): $P = W_e (H+0.6)$ (kPa) |
| 0 | 0 | 0 | 0 | 0 | 0 | 0 | 0 | 0 | 75.69 (1.58 ksf) |
| 0.9 (2.95 ft) | 6 (0.125 ksf) | 11 (0.23 ksf) | 10 (0.2 ksf) | 1 (0.02 ksf) | 3 (0.06 ksf) | 4 (0.08 ksf) | 44 (0.92 ksf) | 12.69 (0.265 ksf) | 75.69 (1.58 ksf) |
| 2.4 (7.9 ft) | 23 (0.48 ksf) | 71 (1.48 ksf) | 39 (0.81 ksf) | 43 (0.9 ksf) | 42 (0.88 ksf) | 38 (0.79 ksf) | 44 (0.92 ksf) | 33.84 (0.71 ksf) | 75.69 (1.58 ksf) |
| 3.9 (12.8 ft) | 114 (2.38 ksf) | 105 (2.19 ksf) | 52 (1.08 ksf) | 63 (1.31 ksf) | 62 (1.29 ksf) | 51 (1.06 ksf) | 44 (0.92 ksf) | 56 (1.17 ksf) | 75.69 (1.58 ksf) |
| 5.4 (17.7 ft) | 77 (1.61 ksf) | 143 (3.0 ksf) | 79 (1.65 ksf) | 86 (1.8 ksf) | 84 (1.75 ksf) | 87 (1.81 ksf) | 44 (0.92 ksf) | 76.14 (1.59 ksf) | 75.69 (1.58 ksf) |

4.8 Overall Results and Comparisons

The FEA results were compared to available theoretical predictions and results from the Louisville experimental *in-situ* test. Apparent earth pressure according to the Terzaghi and Peck (1967) methods (TPM) and active earth pressure as developed by Rankine (1857) and Yokel *et al.* (1980) were also used to calculate theoretical soil pressures for Louisville soft and sensitive clay. The results are summarized in Table 4.11 and Figure 4.12. Note that the

experimental values are based on experimental field results for the period from 14 May to 10 August 2018. From Table 4.11 and Figure 4.12, the following comparative observations can be made:

- 1) MC versus HS: Both MC (options B, C1, C2, & C3) and HS (option A) models revealed that the deeper part of the trench experienced higher pressures than the upper part. The maximum pressure at 5.4 m from the top of the trench reached 79 kPa (1.65 ksf) to 87 kPa (1.81 ksf) in the MC models and 143kPa (3.0 ksf) in the HS model. With reference to experimental obtained values, the MC model may be a better option than the HS model when evaluating soil pressure on the box shield in a sensitive clay.
- 2) MC versus theoretical predictions: the MC (options B, C1, C2, & C3) models yielded values closer to the Rankine (1857) and Yokel *et al.* (1980) analytical results, except at 5.4 m (17.7 ft.) in the trench, where TPM was closest to the MC model. This shows that TPM does not predict the same pattern of soil pressure at greater depths in the trench compared to the other analytical methods and the MC model.
- 3) MC versus experimental values: the experimental option showed closer values to the MC (options B, C1, C2, & C3) model results, except at 3.9 m (12.8 ft) from the top of the trench. It follows that the MC method is a good option when in-situ shear-strength values are known to engineers.
- 4) HS versus theoretical predictions: HS (option A) model results were closer to the Yokel *et al.* (1980) analytical value at 2.4 m from the top of the trench. Results also show that the Yokel method overestimated earth pressure in the upper part of the trench, compared to the HS method that overestimated earth pressure in the deeper part of the trench.
- 5) HS versus experimental values: HS (option A) at 3.9 m trench depth yielded a pressure closer to the in-situ experimental test value. The reason for this may be that the elastic

modulus (E_{50}) assumed in the HS model at 3.9 m depth was extremely close to the measured site value of 2000 kPa (42 ksf). This brings out that the HS model may be a good option to compare soil pressure with experimental values in a trench box shield when the in-situ shear strength of the soil must be assumed.

The MC model offers some advantages because fewer input geotechnical parameters are required, yet the model yields acceptable results (compared to experimental values) for the engineer when using common in-situ geotechnical parameters such as shear strength. Clearly, precise modelling of the sensitive clay excavation would require more advanced behavioral laws, such as HS, and the input parameters of those constitutive models should be fine-tuned and adjusted based on experimental laboratory soil testing.

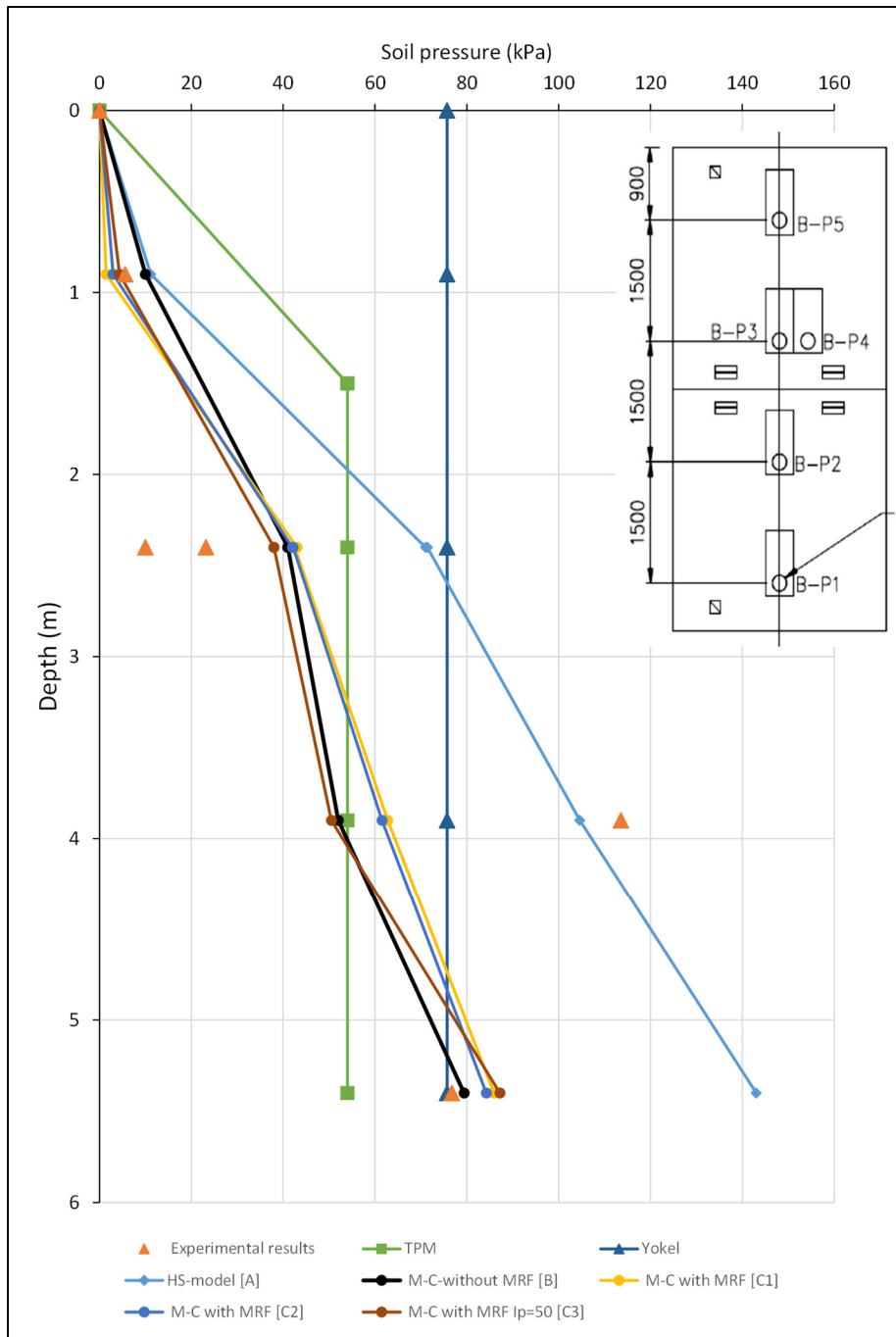


Figure 4.12 Maximum soil pressure vs. trench depth for different options of analysis

4.9 Conclusions

The FE simulations using the PLAXIS-3D software presented in this paper confirm the measurements of earth pressures on the steel cage-type temporary shield protection at shallow depth in a soft and sensitive clay trench. The study included simulation of two steel box shields stacked upon each other, using ‘hinge connections’ to cover the total trench depth of 6 m (20 ft) in sensitive clay soil. Surface loads (representing a 45 kPa overload) located close to one side of the trench were simulated to produce a critical load case on the flexible wall of the shield. Two constitutive material models were used for the simulation analyses: (a) Mohr-Coulomb (MC) and (b) hardening soil (HS). Based on the FEA, the following conclusions can be drawn:

- Both HS and MC models revealed that the deeper part of the trench experienced higher pressures (kPa) than the upper part. The maximum pressure reached 143 kPa (3.0 ksf) and 87 kPa (1.81 ksf) at 5.4 m from the top of the trench for the option [A] and option [C3] models respectively.
- Option [A] of the HS model at 3.9 m trench depth yielded a pressure closer to the in-situ experimental test value than options [B], [C1], [C2], and [C3] of the MC model. This occurred because the elastic modulus ($E_{50} = 2000$ kPa) assumed in the HS model at that depth was extremely close to that on site.
- Options [C1], [C2], and [C3] of the MC model with MRF results were comparable to those of option [B] of the MC model without MRF, showing thereby the key role played by the precise shear strength parameters.
- Comparisons of theoretical predictions by Rankine (1857), Terzaghi and Peck (1967), and Yokel *et al.* (1980) for this type of soft and sensitive clay with FEA results revealed that the pressures obtained using Rankine and Yokel analytical formulae were closer to the simulated and experimental values than those of Terzaghi and Peck. Along the depth of trench, the analytical formulae underestimated soil pressure around 4 m depth for this type of sensitive clay.

CHAPTER 5

SOIL-STRUCTURE INTERACTION OF FLEXIBLE TEMPORARY TRENCH BOX: PARAMETRIC STUDIES USING 3D FE MODELLING

Miah Alam ^a, Omar Chaallal ^b, Bertrand Galy ^c

^{a, b} Department of Construction Engineering, École de Technologie Supérieure,
1100 Notre-Dame West, Montreal, Quebec, Canada H3C 1K3.

^c Department of Research, Québec Occupational Health and Safety Research Institute
(IRSST), 505 de Maisonneuve Blvd. West, Montreal, H3A 3C2, Canada

Paper published in *Journal of Modelling and Simulation in Engineering*, September, 2021.

5.1 Abstract

This paper presents the results of two parametric finite-element studies that were carried out using the PLAXIS-3D finite element (FE) computer code. The following objectives and corresponding parameters were considered: (i) to evaluate the soil pressure on the steel trench box shield; the parameters studied were related to soil type and material, and the study considered till, dry sand, wet sand and sensitive clay soil; (ii) to assess the effect of trench box material and geometry on earth pressure; the parameters studied were related to trench box material (steel versus aluminum) as well as geometry (plate thickness and strut diameter). These studies included simulation of two steel (or aluminum) trench box shields stacked upon each other, using ‘hinge connections’ to cover the total 6 m (20 ft) deep trench. A Mohr-Coulomb (MC) constitutive material model was chosen for FE analysis (FEA). The FEA results were compared to empirical apparent earth pressure diagrams for a sensitive clay. Comparisons showed that the parameters related to the soil and the trench box have a significant influence on earth pressures.

5.2 Introduction

Evaluation of horizontal earth pressure is of major importance when designing any soil retaining structure (Zhang *et al.*, 1998; Potts and Fourie, 1986). In the last few years, various

analytical studies have been carried out to improve our understanding of the behaviour of braced excavation protection systems (Karlsrud and Andresen, 2005). As a protection system, the trench box shield is different from other shoring systems. It is intended not only to shore up or otherwise support the trench face, but also to protect workers from cave-ins or similar incidents inside the trench. Trench boxes can be assembled together to create a box system capable of shoring up trenches up to 11 m (35 ft.) deep (Macnab, 2002). This system is easy to transport, assemble, and install in narrow trenches. Shields may not be subjected to loads exceeding those that the system can withstand (OSHA, 2015). The earth pressure distribution on a shield depends on the type of soil, the shoring, and the method of installation. Many researchers have suggested theoretical solutions to estimate earth pressure on a flexible temporary support (Rankine, 1857; Terzaghi and Peck, 1967; Yokel *et al.*, 1980). Consequently, for an excavation trench shield, the Canadian Foundation Engineering Manual (CFEM, 2006) recommends the use of pressure envelopes from empirical formulae.

Our understanding of the behaviour of excavations and trenches with flexible retaining walls has evolved significantly in recent years with the help of numerical FE and analytical methods. Using FE analyses, Goldberg, *et al.*, (1976) found that under a given set of soil conditions, the higher the wall rigidity, the greater was the apparent earth pressure. A study by Hashash and Whittle (1996) on shoring excavations in clay has shown that the evolution of lateral thrust on a retaining structure (or wall) is a complex function of the flexibility of the retaining structure and the magnitude of shear deformations at depth. Their analyses also revealed the development of an arching effect in the ground in contact with the shoring (Bjerrum *et al.*, 1972; Hashash and Whittle, 2002; Mortensen and Andresen, 2003; Karlsrud and Andresen, 2005; Benmebarek *et al.*, 2016). Karlsrud and Andresen (2005) concluded that the development of earth pressure on supporting structures set up in soft clays is a complex function that depends on the flexibility of the support, the anisotropy property, the thickness of the clay layer in the trench bottom, and deformations in the clay layer.

Lam (2010) showed that a mobilized strength design database can be used to investigate the relationship between structural response ratio and soil-structure stiffness ratio and to capture

the range of wall stiffnesses between sheet piles and thick diaphragm walls. Bryson and Zapata-Medina (2012) clearly showed the influence of horizontal and vertical strut spacing, of wall stiffness, and of relative stiffness ratio on lateral wall deformation in an excavation support system (ESS) in three types of clays. Bryson and Zapata-Medina (2012) defined a relative stiffness ratio that relates the stiffness of the soil to the stiffness of the excavation support system. This relative stiffness ratio depends on Young's modulus of the soil; Young's modulus of the wall; moment of inertia per unit length of the wall; average horizontal support spacing; average vertical support spacing; total height of the wall; excavation depth; average unit weight of the soil; and undrained shear strength of the soil at the bottom of the excavation. Therefore, the interaction between soil mass and support structure is significant in the development of lateral loads. A recently published paper by (Alam *et al.*, 2020) showed that modern 3D FEM studies on clay trench SSI focused mainly on depth greater than 10 m and on retaining wall or diaphragm wall. Not that many studies have been published on FEM of soil-structure interaction (SSI) with trench boxes in shallow depth trenches of clayey soil. LaBaw (2009) evaluated earth pressure for a standard construction shoring (pneumatic shoring with steel panel) system, which provides an adequate and safe emergency rescue for first responders in medium clay of 2.4 m depth of trench excavation by 3D FEA using Abaqus software. Alam *et al.* (2021) compared a full-scale experimental in situ test of 6 m depth with 3D FEM to investigate the earth pressure on a flexible temporary trench box shield in soft and sensitive clay soil using PLAXIS-3D software.

This paper presents the influence of soil parameters and shield material type and geometry on the earth pressures on a flexible temporary trench box shield. An FE model of simulations using the PLAXIS-3D software (Bentley, 2017) shows a comprehensive picture of the influence of soil parameters on earth pressures on a flexible temporary trench box shield in till, dry sand, wet sand and sensitive clay. These FEM analysis results are also compared to published empirical apparent earth pressure diagrams (Terzaghi and Peck, 1967). The influence of shield material type and geometry on the earth pressure in a trench excavation is also presented.

5.3 Finite-element analyses

Numerical analyses of excavation support system performance for most recent deep excavation case histories have required three-dimensional FE analyses (Finno *et al.*, 2007; Arai *et al.*, 2008; Hou *et al.*, 2009). In addition, Ou *et al.* (2000) have shown that the complex soil-structure interactions of excavation support systems and excavation-induced ground movements are three-dimensional (3D) in nature. FEA software may be a useful tool to obtain in-depth information on the effect of SSI on this type of trench box wall support (Alam *et al.*, 2020). To perform this 3D FEA and achieve a better understanding of these complex soil-structure interactions, the PLAXIS-3D software was used.

5.3.1 Parameters for FE

To simulate the trench with the excavation protection shield, three types of parameters were used in PLAXIS-3D: (i) soil model parameters for the excavation and surrounding soil, including all the layers; (ii) structural model parameters for the box shield protection, and (iii) interface parameters.

5.3.2 Soil Modelling

To simulate the trench, a soil model geometry was assumed as soil contour [(7.5 m (25 ft) × 12 m (40 ft.) × 15 m (50 ft.)), which was more than twice the size of the excavation contour [3 m (10 ft) × 1.5 m (5 ft) × 6 m (20 ft)] following recommendations by Hsieh and Ou (1998) and Plaxis manual (Bentley, 2017) for shallow trench excavations. The soil layers for sensitive blue clay were modelled using three depths and three properties: (i) 0 m to 0.6 m (2 ft) of depth of soil as fissured brown clay; (ii) 0.6 m (2 ft) to 2 m (6.56 ft) depth of soil as plastic brown clay; and (iii) 2 m (6.56 ft) to 15 m (50 ft) depth of soil as sensitive blue clay (Louiseville clay), in accordance with the stratigraphic profile of the Louiseville soil (Alam, *et al.*, 2021). Soil properties, especially strength, required careful attention because they are a key factor in overall excavation support system (ESS) performance (Allen Marr and Hawkes, 2010).

Supporting this statement, the *in-situ* value of soil undrained shear strength in Louiseville shown in Figure 5.1(a) was used in this FEA. The soil contour with the trench model is shown in Figure 5.1(b). On the other hand, till, dry sand, wet sand layers were modelled using 0.0 to 15 m depths of the properties of each type of sand, as shown in Figure 5.1(c), with varying stiffness parameters along the depth.

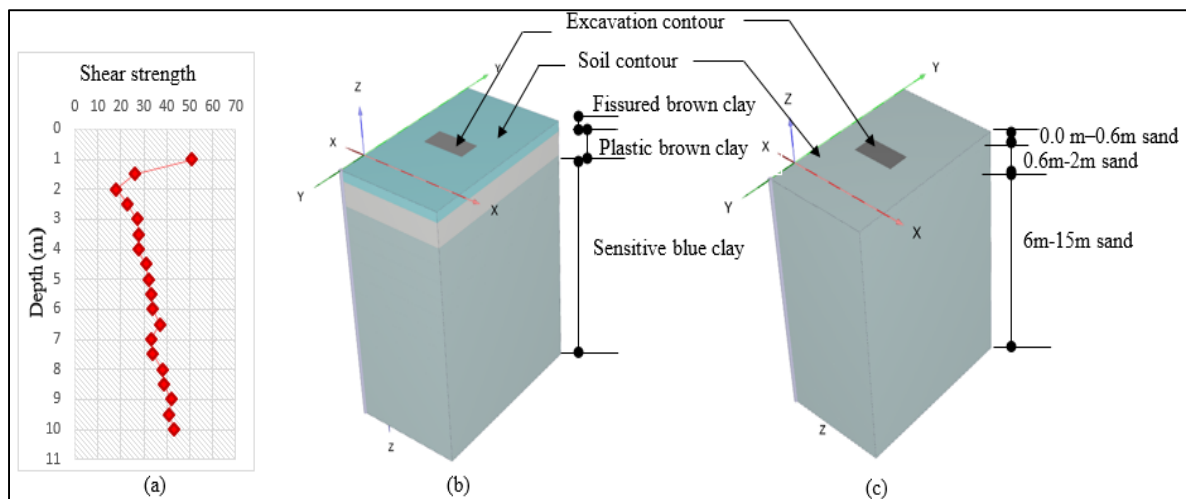


Figure 5.1 Geometric profile and excavation contour in PLAXIS-3D simulation of trench:
 (a): Experimental values of undrained shear strength of sensitive blue clay (Louiseville clay) (b): PLAXIS-3D model profile for sensitive blue clay (number of soil elements: 23221; MC soil model) (c): PLAXIS-3D model profile for till, dry and wet sand (number of soil elements: 23221; MC soil model)

5.3.3 Structural modelling

Bryson and Zapata-Medina (2012) indicated that the stiffness of an excavation support system (ESS) is a complex function of the flexural rigidity of the wall element, the structural stiffness of the support elements, the type of connections between the wall and the supports, and the vertical and horizontal spacing of the support system. Therefore, the two trench steel shields ‘stacked upon each other’ to cover the total depth (6 m (20 ft)) of excavation were simulated according to the geometrical dimensions given in Tables 5.1 and 5.2, and the positions and locations of the struts used for simulation are shown in Figure 5.2. Other parameters such as plate and strut mechanical properties are also presented in Tables 5.1 and 5.2. Young’s

modulus (E), shear modulus (G), and Poisson's ratio (ν) of 4.76 mm (3/16 in.) thick A-572 grade 50 steel plate were considered. Unit weight (γ) of the trench box plates was calculated from the real weight of the trench box used for experimental test, divided by its real volume, to account for the "sandwich type" construction of the trench box plates. The real thickness of sandwich plates was considered as PLAXIS-3D input for the plate geometry. Four different thicknesses were considered in the parametric study: 200 mm (8 in.), 150 mm (6 in.), 100 mm (4 in.), and 75 mm (3 in.). For the struts (or spreader tube), Young's modulus (E) and unit weight (γ) were taken for 200 mm (8 in.), 100 mm (4 in.), and 50 mm (2 in.) strut diameter from the SCH80 chart. Cross-sectional area (A) and moment of inertia (I) were calculated from the original strut diameter.

The vertical positions of the struts were kept different on both sides as per the in situ experimental test at the Louiseville site. Note that 200 mm (8 in.) strut diameter and 100 mm (4 in.) shield plate were used for till, dry sand, wet sand and sensitive clay soil analysis, whereas other dimensions were used for geometric influence FE analysis.

Table 5.1 Plate properties (steel and aluminum) of trench box shield protection used for FE simulation in PLAXIS-3D

| Parameter/Property | PLAXIS Nomenclature | Steel Plate | | | | Aluminum Plate | | | |
|--------------------|--------------------------------------|--------------------|--------------------|--------------------|--------------------|---------------------|---------------------|---------------------|---------------------|
| | | 200 mm (8 in.) | 150 mm (6 in.) | 100 mm (4 in.) | 75 mm (3 in.) | 200 mm (8 in.) | 150 mm (6 in.) | 100 mm (4 in.) | 75 mm (3 in.) |
| Material Type | Type | Elastic, Isotropic | Elastic, Isotropic | Elastic, Isotropic | Elastic, Isotropic | Elastic, Isotropic | Elastic, Isotropic | Elastic, Isotropic | Elastic, Isotropic |
| Young's modulus | E1 (kN/m ²) | 2×10 ⁸ | 2×10 ⁸ | 2×10 ⁸ | 2×10 ⁸ | 7×10 ⁷ | 7×10 ⁷ | 7×10 ⁷ | 7×10 ⁷ |
| Unit weight | γ (kN/m ³) | 11.59 | 11.86 | 13.67 | 15.70 | 2.68 | 3.22 | 4.29 | 4.99 |
| Thickness | d (m) | 0.20 | 0.15 | 0.10 | 0.08 | 0.20 | 0.15 | 0.10 | 0.08 |
| Poisson's ratio | ν ₁₂ | 0.30 | 0.30 | 0.30 | 0.30 | 0.30 | 0.30 | 0.30 | 0.30 |
| Shear modulus | G ₁₂ (kN/m ²) | 8×10 ⁷ | 8×10 ⁷ | 8×10 ⁷ | 8×10 ⁷ | 2.7×10 ⁷ | 2.7×10 ⁷ | 2.7×10 ⁷ | 2.7×10 ⁷ |
| | G ₁₃ (kN/m ²) | 8×10 ⁷ | 8×10 ⁷ | 8×10 ⁷ | 8×10 ⁷ | 2.7×10 ⁷ | 2.7×10 ⁷ | 2.7×10 ⁷ | 2.7×10 ⁷ |
| | G ₂₃ (kN/m ²) | 8×10 ⁷ | 8×10 ⁷ | 8×10 ⁷ | 8×10 ⁷ | 2.7×10 ⁷ | 2.7×10 ⁷ | 2.7×10 ⁷ | 2.7×10 ⁷ |

Table 5.2 Strut properties (steel and aluminum) of trench box shield protection used for FE modelling in PLAXIS-3D

| Parameter/Property | PLAXIS Nomenclature | Steel Strut | | | Aluminum Strut | | |
|----------------------|--|-----------------------|-----------------------|-----------------------|-----------------------|-----------------------|-----------------------|
| | | 200 mm (8 in.) Ø | 100 mm (4 in.) Ø | 50 mm (2 in.) Ø | 200 mm (8 in.) Ø | 100 mm (4 in.) Ø | 50 mm (2 in.) Ø |
| Material type | Type | Elastic | Elastic | Elastic | Elastic | Elastic | Elastic |
| Young's modulus | E1 or E2 (kN/m ²) | 2×10 ⁸ | 2×10 ⁸ | 2×10 ⁸ | 7×10 ⁷ | 7×10 ⁷ | 7×10 ⁷ |
| Unit weight | γ (kN/m ³) | 78.50 | 78.50 | 78.50 | 26.99 | 26.99 | 26.99 |
| Cross-sectional area | A (m ²) | 0.01 | 0.0028 | 0.0010 | 0.01 | 0.0028 | 0.001 |
| Moment of inertia | I _{2 xx} (m ⁴) | 4.41×10 ⁻⁵ | 3.99×10 ⁻⁶ | 3.67×10 ⁻⁷ | 4.41×10 ⁻⁵ | 3.99×10 ⁻⁶ | 3.67×10 ⁻⁷ |
| | I _{3 yy} (m ⁴) | 4.41×10 ⁻⁵ | 3.99×10 ⁻⁶ | 3.67×10 ⁻⁷ | 4.41×10 ⁻⁵ | 3.99×10 ⁻⁶ | 3.67×10 ⁻⁷ |
| Poisson's ratio | ν ₁₂ | 0.3 | 0.3 | 0.3 | 0.3 | 0.3 | 0.3 |
| 200 mm strut (SCH80) | Outer diameter strut, do(mm) | 215 | 112 | 60 | 215 | 112 | 60 |
| | Inner diameter strut, di(mm) | 190 | 95 | 48 | 190 | 95 | 48 |
| | Area of strut (m ²) | 8.24×10 ⁻³ | 2.83×10 ⁻³ | 9.64×10 ⁻⁴ | 8.24×10 ⁻³ | 2.83×10 ⁻³ | 9.64×10 ⁻⁴ |
| | I _{yy} or I _{xx} for strut (m ⁴) | 4.41×10 ⁻⁵ | 3.99×10 ⁻⁶ | 3.67×10 ⁻⁷ | 4.41×10 ⁻⁵ | 3.99×10 ⁻⁶ | 3.67×10 ⁻⁷ |

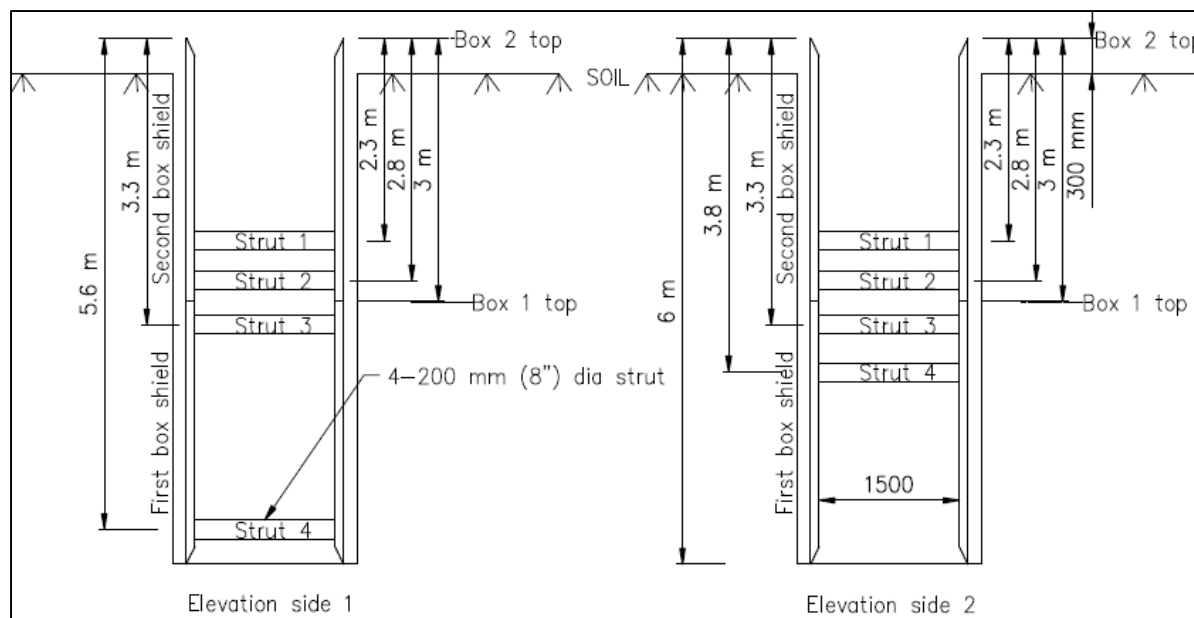


Figure 5.2 Elevation views and strut locations in the two assembled box shields (stacked upon each other) along the trench

In the PLAXIS-3D simulation, the box shield steel built-in plate walls (sandwich plate as per PLAXIS-3D) were modelled as ‘plate elements’ and the struts as ‘beam elements’. Four-cornered ‘hinge joints’ were used between the two box shields (stacked upon each other) to represent the experimental setup shown in Figure 5.3. Similarly, the joints between struts and plates were simulated as ‘hinge joints’ and were representative of the experimental setup illustrated in Figure 5.3. In the in situ experiment, when the 1st box is inserted into the soil and the upper box (2nd box) is pushed on top of the lower box (1st box) using an excavator, the soil provide the relevant lateral support for the bottom end of the lower trench box (1st box). In the FE model, this phenomenon was simulated by using ‘fixed-end anchored element’, as illustrated in Figure 5.3. The pressure measuring locations from the top of the trench box are shown in Figure 5.4. To analyze the non-linear stress-strain behaviour of the soil model in the trench and the soil surrounding the excavation, a Mohr-Coulomb (MC) constitutive material model was chosen in this study.

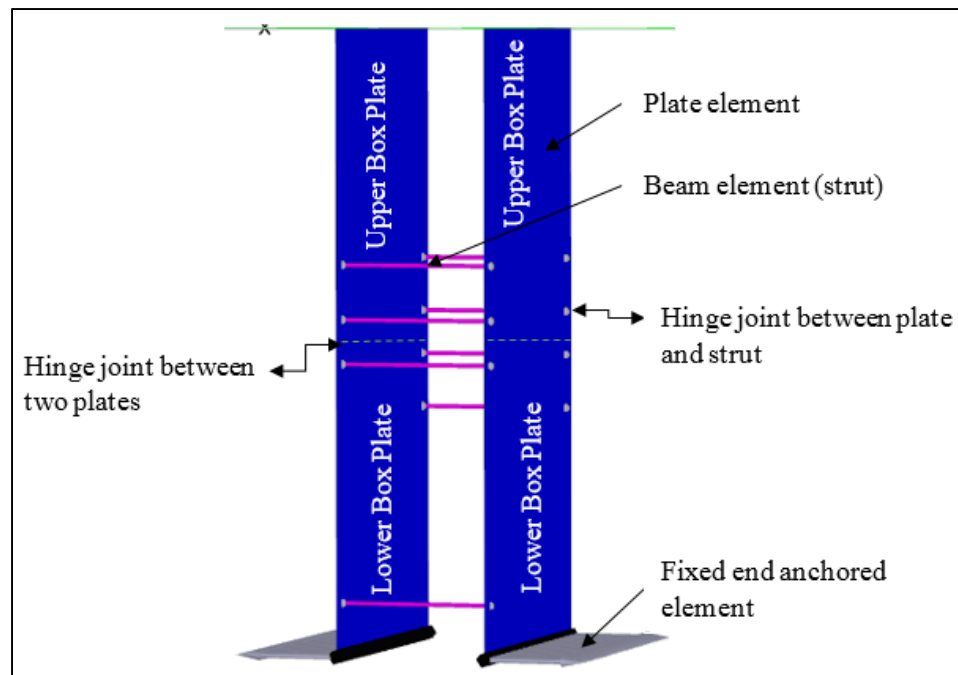


Figure 5.3 Structural simulation view of the two assembled box shields (stacked upon each other) with protection in PLAXIS-3D (number of structural elements: 1050; MC soil model)

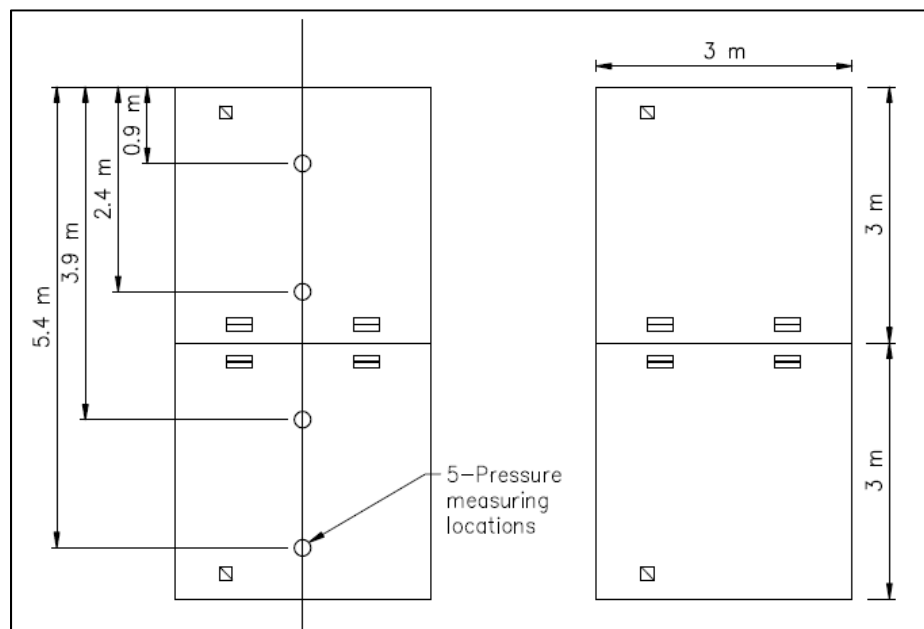


Figure 5.4 Trench box supporting wall side views and pressure measuring locations from the top

5.4 Generating the Mohr-Coulomb (MC) model

The Mohr-Coulomb (MC) model is a simple and widely used linear elastic perfectly plastic model. The linear elastic part of the MC model is based on Hooke's law of isotropic elasticity, and the perfectly plastic part is based on the MC failure criterion (Bentley, 2017). Table 5.3 shows soil properties for the sensitive blue clay, till, dry, wet, and loose sand model parameters used for FE modelling in PLAXIS-3D. The soil stiffness moduli (E) at different depths for sensitive blue clay (Louiseville clay) were calculated from the shear strength (C_u) using the equation proposed by Peck (1975):

$$E = 600 * C_u \quad (5.1)$$

Using Eq. (5.1), E was calculated for each layer, and the average values of E (E_{avg}) were taken as PLAXIS-3D input for the 1 m soil layers (further details are provided in Alam *et al.*, 2021). The total stress soil properties for sensitive blue clay (Louiseville clay) are presented in Table 5.3. For till, dry sand, wet sand, which have different unit weights (γ) of sand and angles of friction (ϕ), these soil parameters for the MC model were used for parametric FE modelling, as shown in Table 5.3. For the different sandy soil stiffness moduli, the maximum shear modulus, G_{max} , was calculated for each meter of depth using Eq. (5.2), developed by Seed and Idriss (1970):

$$G_{max} = 1000K_{2max}(\sigma'_m)^{0.5} \quad (5.2)$$

where σ'_m = effective mean stress = $(\sigma'_v + 2\sigma'_h)/3$, σ'_v = vertical effective stress, σ'_h = horizontal effective stress, $\sigma'_h = K_0 \times \sigma'_v$, K_0 = coefficient of earth pressure at rest. K_{2max} is an empirical factor that varies according to void ratio. Then these calculated maximum shear modulus values (G_{max}) for till, dry sand and wet sand were used separately for each type of soil for drainage analysis in PLAXIS-3D simulation models.

Soil stiffness parameters vary with the depth. Therefore, anisotropy is considered for the soil models, which are subdivided in 1 m deep layers below the first 2 meters, and the parameters E and G_{max} are computed for each layer using Eq. 5.1 and Eq. 5.2 respectively.

Unloading/reloading stiffness parameter is given by G_{\max} and considered elastic, as in Karlsrud and Andresen (2005) study. Further details related to the Louiseville clay soil model can be found in Alam *et al.* (2021).

Table 5.3 Soil properties for sensitive blue clay, till, dry and wet sand model parameters used for FE modelling in PLAXIS-3D

| Parameter /Property | PLAXIS Nomenclature | Sensitive blue clay | Till | Dry sand, medium density | Wet sand, medium density |
|-------------------------------------|--|--------------------------------------|--------------------------------------|--------------------------------------|--------------------------------------|
| Depth of layer | m | 0.0–15 | 0.0–15 | 0.0–15 | 0.0–15 |
| Material model | model | MC | MC | MC | MC |
| Drainage type | type | Undrained | Drained | Drained | Drained |
| Unit wt. above phreatic level | γ_{unsat} (kN/m ³) | 16 | 21.5 | 19.5 | 19.5 |
| Unit wt. below phreatic level | γ_{sat} (kN/m ³) | 17 | - | - | 19.5 |
| Maximum elastic/shear modulus | $E_{\text{avg}}/G_{\text{max}}$ (kN/m ²) | (E_{avg} as per Eq. (5.1)) | (G_{max} as per Eq. (5.2)) | (G_{max} as per Eq. (5.2)) | (G_{max} as per Eq. (5.2)) |
| $K_{2\text{max}}$ | - | - | 70 | 52 | 52 |
| Cohesion | C'_{ref} (kN/m ²) | See Table 5.4 | 5 | 5 | 5 |
| Frictional angle | ϕ [°(degree)] | See Table 5.4 | 42 | 35 | 35 |
| Dilatancy angle | Ψ [°(degree)] | 0 | 0 | 0 | 0 |
| Poisson's ratio | ν'_{ur} | 0.3 | 0.3 | 0.3 | 0.3 |
| Interface strength reduction factor | R_{inter} | 0.5 | 0.65 | 0.65 | 0.65 |
| Initial K_0 determination | K_0 | 0.53 | 1.0 | 0.43 | 0.43 |
| Soil type | | Very fine | | | |
| <2 μm | % | 74 | 10 | 10 | 10 |
| 2 μm –50 μm | % | 11 | 13 | 13 | 13 |

Table 5.4 Parameters for different layers of sensitive blue clay (Louiseville clay)
Taken from Laval University

| Soil Layer | Parameters in total stresses | Drained condition |
|----------------------------------|--|-------------------|
| Fissured brown clay (0 to 0.6 m) | $c' = 5 \text{ kPa}$ and $\phi' = 28^\circ$ | Drained |
| Plastic brown clay (0.6 to 2 m) | $c = c_u$ (Figure 5.1(a)) and $\phi = 0^\circ$ | Undrained |
| Sensitive blue clay (2 to 15 m) | $c = c_u$ (Figure 5.1(a)) and $\phi = 0^\circ$ | Undrained |

5.4.1 Interface model

Trench box steel plate forms a smooth wall, but in construction practice, it is impossible to find a smooth wall that has no roughness (Matsuzawa and Hazarika, 1996). Hence, interfaces were added as a joint element to the plates for proper modelling of soil-structure interaction. They represent a thin zone of intensely shearing material at the contact between a plate and the surrounding soil. Positive and negative interfaces were added (local z-direction) on either side of a plate surface (Figure 5.5 (c)). The interaction between the steel plate wall and the soil was expressed by a suitable strength reduction factor (R_{inter}). This factor relates the interface strength (wall friction and adhesion) to the soil strength (friction angle and cohesion). Recommended values for R_{inter} are as follows: $2/3$ for fissured brown clay and $< 2/3$ for plastic brown and sensitive blue soft clay (Bentley, 2017) (Table 5.3). The interface was assigned a virtual thickness that varied with mesh type and in this case was $103 \times 10^{-3} \text{ m}$. The interface element consisted of pairs of nodes that were compatible with a six-node triangular side of a soil element or a plate element (Bentley, 2017).

For Till, and dry sand analysis, water was not considered (water level below the bottom of the excavation). For the wet sand, water table was considered 2.5 m from top of soil. Inside the trench, water was considered pumped out (to allow work inside the trench). Therefore, water was present in the surrounding soil of excavation, thus creating a total horizontal earth pressure on the wall of trench box shield outside the trench.

Table 5.5 Construction sequence of FE modelling for sensitive blue clay in PLAXIS-3D

| Phase | In the model | Drainage |
|---------|--|--|
| Phase 0 | Only soil elements (no structure) | K_0 - procedure |
| Phase 1 | Excavation (1 st layer, depth: 0.6 m) fissured brown clay | Drained |
| Phase 2 | Excavation (2 nd layer: 0.6 to 2 m) brown clay | Plastic: undrained B ¹ (soil model) |
| Phase 3 | Adding structural element | Plastic: undrained B ¹ (soil model) |
| Phase 4 | Excavation (3 rd layer: 2 m to 6 m) sensitive blue clay | Plastic: undrained B ¹ (soil model) |

Note:

¹ In the undrained (B) drainage type, modelling of undrained behaviour using effective parameters for stiffness and undrained shear strength parameters are allowed.

5.4.2 Mesh generation

Medium coarse 10-noded elements were used for each of the simulation and connectivity plots shown in Figure 5.5 (a and b). This mesh generation process considers the soil, all the structural components, loads, and boundary conditions. As a result of meshing, a total number of elements of 24271, i.e., 23221 soil elements and 1050 structural elements, was reached.

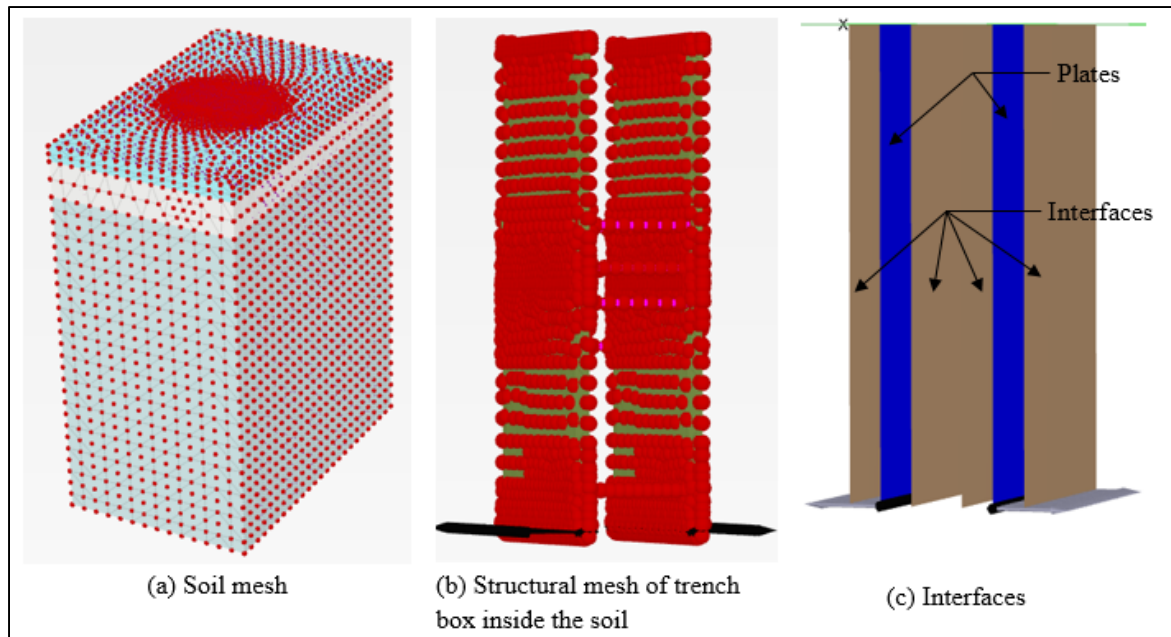


Figure 5.5 Soil and structural mesh elements and interfaces in PLAXIS-3D simulation

5.5 Construction steps and phases in PLAXIS-3D simulation for sensitive blue clay

Poulos *et al.* (2002) showed that the construction details and sequence, as well as the soil-structure interaction, have a significant impact on the movements and lateral loads acting on a flexible retaining structure. Therefore, the construction steps play a major and critical part in this FE simulation. The model includes an assigned step-by-step excavation process, including the structural elements inserted into the excavation. All the phases of the construction sequence are summarized in Table 5.5. Construction and excavation steps are shown in Figure 5.6 for sensitive blue clay.

5.6 Calculations with different K_0

In practice, K_0 for a drained soil is often assumed to be related to the friction angle by Jaky's (1944) empirical expression. In an over-consolidated soil, K_0 would be expected to be larger than the value given by this expression. However, for the Mohr-Coulomb model, the default K_0 value is based on Jaky's formula. Hamouche *et al.* (1995) evaluated the *in-situ* coefficient

of earth pressure at rest for sensitive blue clay. Three values of K_0 (0.55, 1, and 1.5) were chosen to evaluate the effect on the soil pressure on the trench box as follows: (i) $K_0 = 0.55$ which is a common K_0 for normally consolidated eastern Canada clays (with $\phi' = 27^\circ$); (ii) $K_0 = 1$ represents the case of clay in undrained conditions (when $\phi = 0$); and (iii) $K_0 = 1.5$ determined experimentally at 6 m depth by Hamouche *et al.* (1995) for Louiseville clay. Figure 5.7 shows the value of soil pressure with different K_0 values after analysis using the MC model.

5.7 Construction steps and phases in PLAXIS-3D simulation for till, dry sand and wet sand

To simulate till and dry sand, the water table was maintained below excavation level, and 2.5 m below ground for wet sand, which was the lowest level recorded in experimental testing (Alam *et al.* 2021). Then the PLAXIS-3D simulation model was run to perform the analysis. However, when the cohesion value $C=0$ kPa was used, the PLAXIS-3D simulation showed that the excavation steps failed because the soil bodies failed. Hence, trial methods were used with increasing cohesion values in the range of 4–5 kPa. Thereafter, the excavation steps proceeded with the cohesion value of 5 kPa, and the model was run for analysis. However, the numerical analysis results showed that the soil pressure on the box shield was notably low, and at a certain depth, the soil ceased to be in an elastic state.

When only the initial phase was used (meaning no excavation steps, installing the structure inside the soil straight away and then removing the soil inside the trench box), the soil stresses were more reliable and comparable with the Terzaghi and Peck (1967) apparent earth pressure curve for granular soil. It was observed that till created more stress on the shield than any other soil type. Dry sand yielded a higher soil pressure than wet sand except at 5.4 m depth, as shown in Figure 5.8. All the results were compared with the Terzaghi and Peck (1967) curves for till, dry and wet sand, and sensitive blue clay (Louiseville clay), as shown in Figure 5.8.

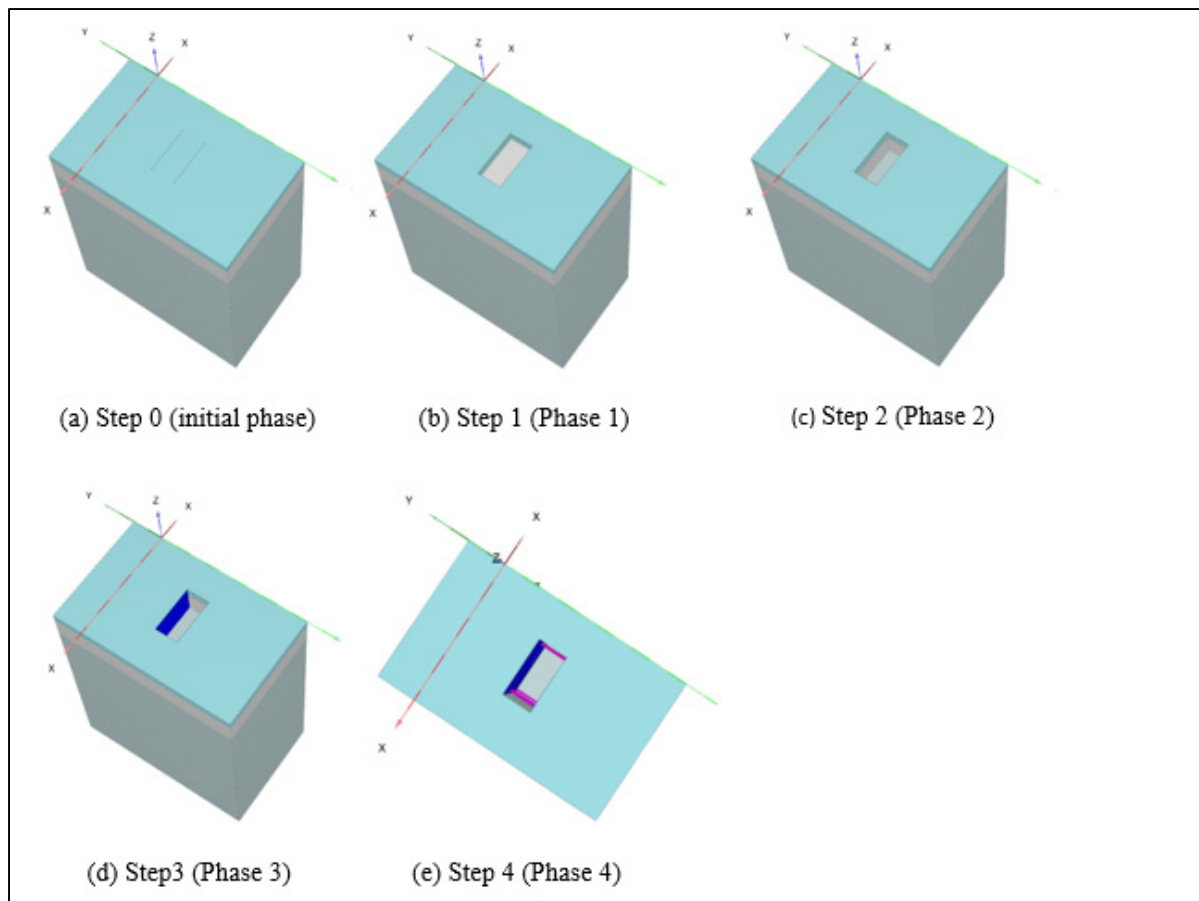


Figure 5.6 PLAXIS-3D simulation of the construction steps

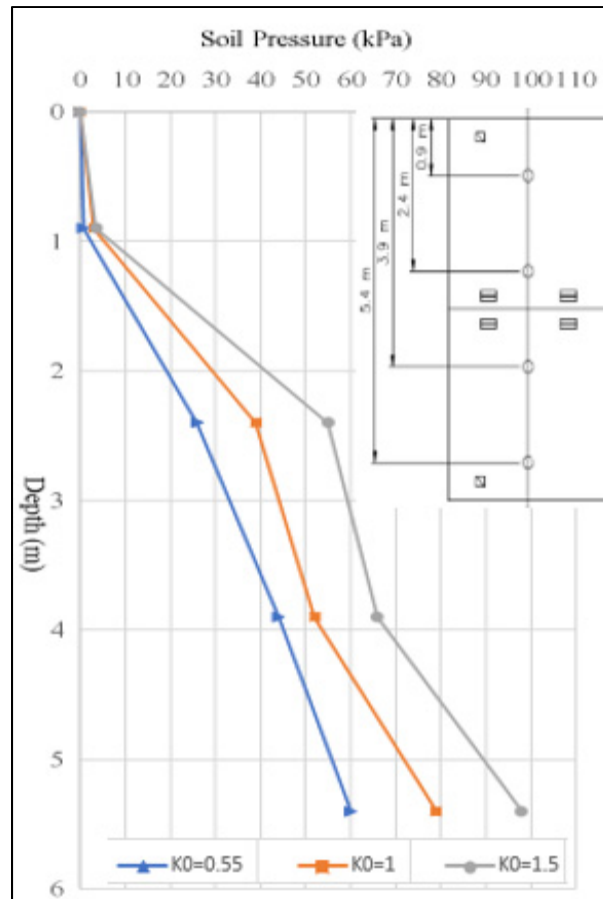


Figure 5.7 Soil pressure at different depths of trench with different K_0 values

5.8 Parametric studies for steel and aluminum trench box for plate and strut geometry

For this type of parametric study, the M-C model for sensitive blue clay (Louiseville clay) was chosen for analysis. The objective was to evaluate the influence of material type and geometry on the earth pressure on the temporary excavation trench box shield. Three scenarios were considered: (i) trench box materials (steel and aluminum), (ii) steel trench box with different plate thicknesses and strut diameters, and (iii) aluminum trench box with different plate thicknesses and strut diameters. A total of 16 trench box configurations were considered (4 thicknesses \times 2 materials \times 2 strut diameters). Table 5.6 shows the simulation matrix, which was used for the PLAXIS-3D simulations.

Table 5.6 Effective soil pressure (drained) for different types of soil with depth of trench and comparison with CFEM analytical formulae

| Wall thickness of the box | Strut diameter | |
|---------------------------|---------------------------------------|---------------------------------------|
| | Steel Box | Aluminum Box |
| 75 mm (3 in.) | 200 mm (8 in.) Ø and 50 mm (2 in.) Ø | 200 mm (8 in.) Ø and 50 mm (2 in.) Ø |
| 100 mm (4 in.) | 200 mm (8 in.) Ø and 100 mm (4 in.) Ø | 200 mm (8 in.) Ø and 100 mm (4 in.) Ø |
| 150 mm (6 in.) | 200 mm (8 in.) Ø and 100 mm (4 in.) Ø | 200 mm (8 in.) Ø and 100 mm (4 in.) Ø |
| 200 mm (8 in.) | 200 mm (8 in.) Ø and 100 mm (4 in.) Ø | 200 mm (8 in.) Ø and 100 mm (4 in.) Ø |

5.9 Overall Results and Comparisons

The FEA results were compared to available theoretical predictions. The Terzaghi and Peck (1967) curves for till, dry and wet sand, and sensitive blue clay (Louiseville clay) were compared with the FEA result. It is evident that when the trench box material type and geometry changed, the earth pressure on the temporary shield also changed for the same soil type. The results are summarized in Figure 5.8 for different types of soil and in Table 5.7 and Figures 5.9 to 5.12 for different materials and geometries. The following comparative observations can be made from the tables and figures:

- 1) Till, dry sand and wet sand versus theoretical predictions: The “Peck” curve was calculated from apparent earth pressure according to the Terzaghi and Peck (1967) method (TPM). From the “Peck” curve, values for till, dry and wet sand were overestimated in the upper part compared to the deeper part of the trench.
- 2) Steel versus aluminum trench box shield: under the same soil condition (Louiseville clay), a significant difference in earth pressures between the steel and aluminum temporary shields was observed. The maximum undrained total stresses decreased by 40.6% when shifting from a steel to an aluminum trench box shield with the same geometry of 100 mm (4 in.) plate thickness and 200 mm (8 in.) strut diameter.

- 3) Steel versus aluminum trench box shield plate thickness: reduction of shield plate thickness influenced soil pressure on both steel and aluminum trench box shields under the same soil condition (Louiseville clay). The FEA results showed that changing the plate thickness from 200 mm (8 in.) to 150 mm (6 in.), 150 mm (6 in.) to 100 mm (4 in.), and 100 mm (4 in.) to 75 mm (3 in.) result in a maximum decrease in soil pressure on the steel trench box of 5.5%, 9.2%, and 17% .This values reached 35.11%, and 33.67% and 13.5% for aluminum trench box shield respectively for the same 200 mm (8 in.) strut diameter.
- 4) Steel versus aluminum trench box shield strut diameter (Louiseville clay): once again, a reduction in shield strut diameter influenced soil pressure on both steel and aluminum shields under the same soil condition. Furthermore, FEA results showed that changing the strut diameter from 200 mm (8 in.) to 100 mm (4 in.) gave a maximum of 1.12%, 1.9%, and 8.4% decrease in soil pressure on the steel trench box and 2.7%, 4.0%, and 9.5% on the aluminum trench box shield respectively for 200 mm (8 in.), 150 mm (6 in.), and 100 mm (4 in.) plate thickness for the same soil condition.

From the above discussions, it is apparent that soil pressure on the trench box shield depends not only on soil type, but also on soil-structure stiffness. For the same material type and geometry, a trench box experiences different scales of pressure for different soil types. On the other hand, a given type of soil trench box experiences different scales of pressure for different types of material and geometry. Hence, the higher the wall rigidity, the greater was the apparent earth pressure. Therefore, it is evident that soil pressure depends not only on soil stiffness, but also on the stiffness of the trench box. Classical theories overestimate soil pressure in the upper part of the trench and may not be safe for the deeper part. When designing a trench box shield, the classical apparent earth pressure envelope may not be the only source of information. Adding *in situ* measurements and numerical data would be a better idea.

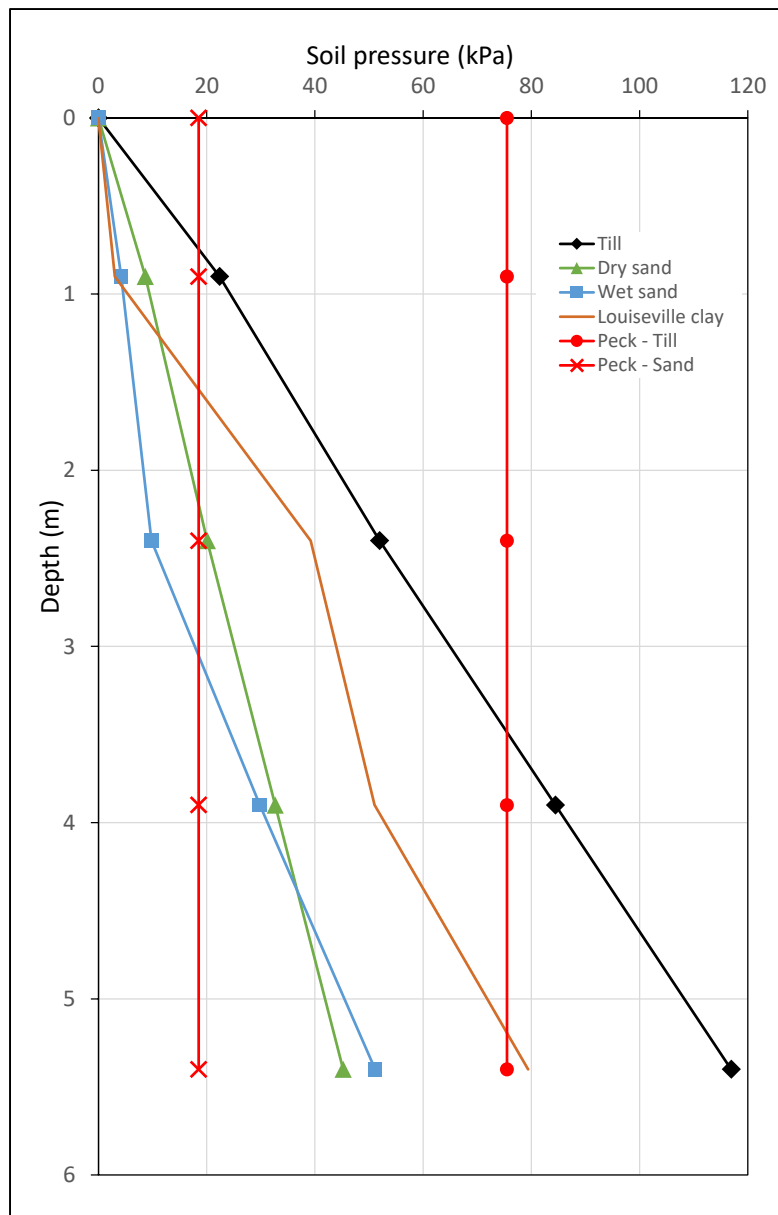


Figure 5.4 Comparisons of soil pressure for different types of soil by numerical analysis with theoretical values in the trench

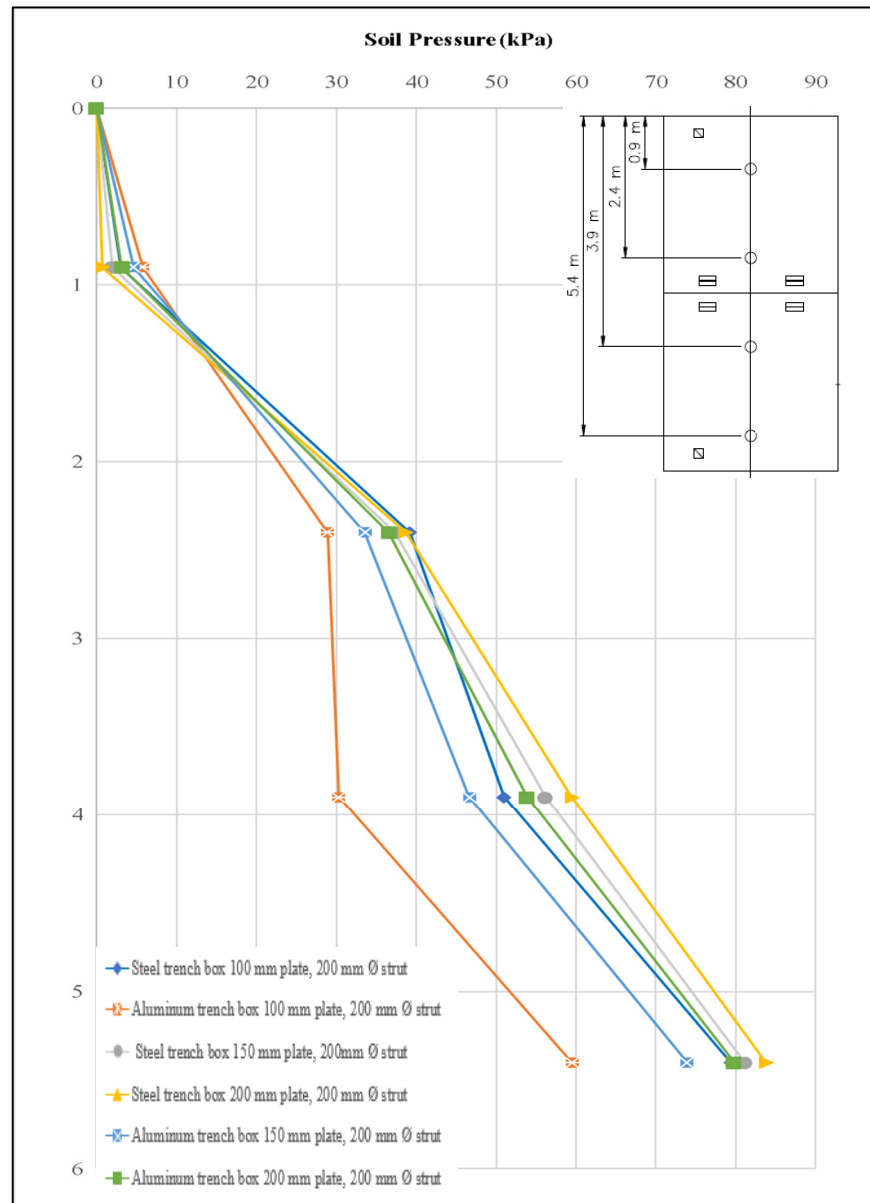


Figure 5.5 Soil pressure (Louiseville clay) on steel versus aluminum trench box shields with the same geometry

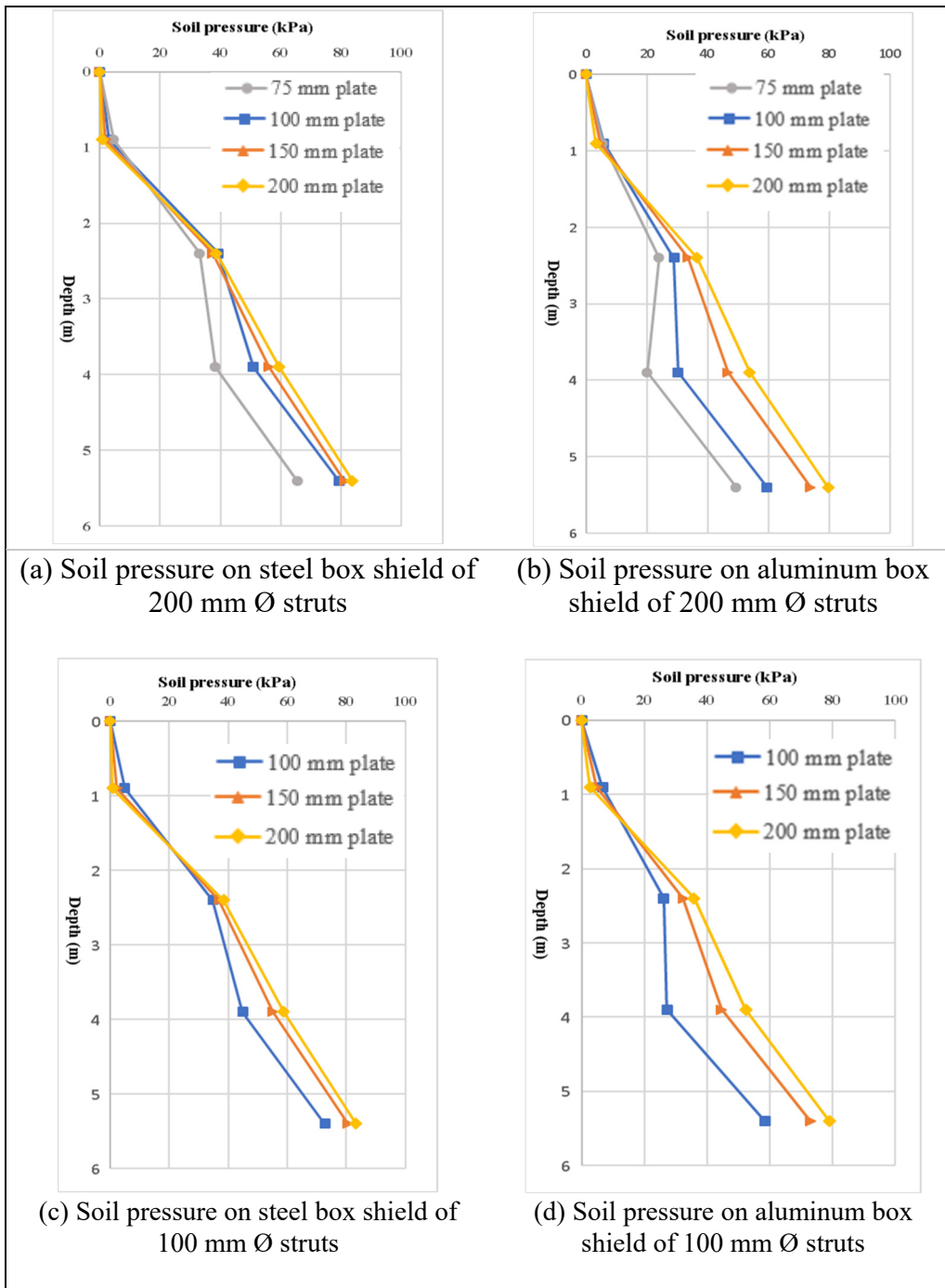


Figure 5.6 Soil pressure (Louiseville clay) on steel and aluminum trench box shields with different plate thicknesses

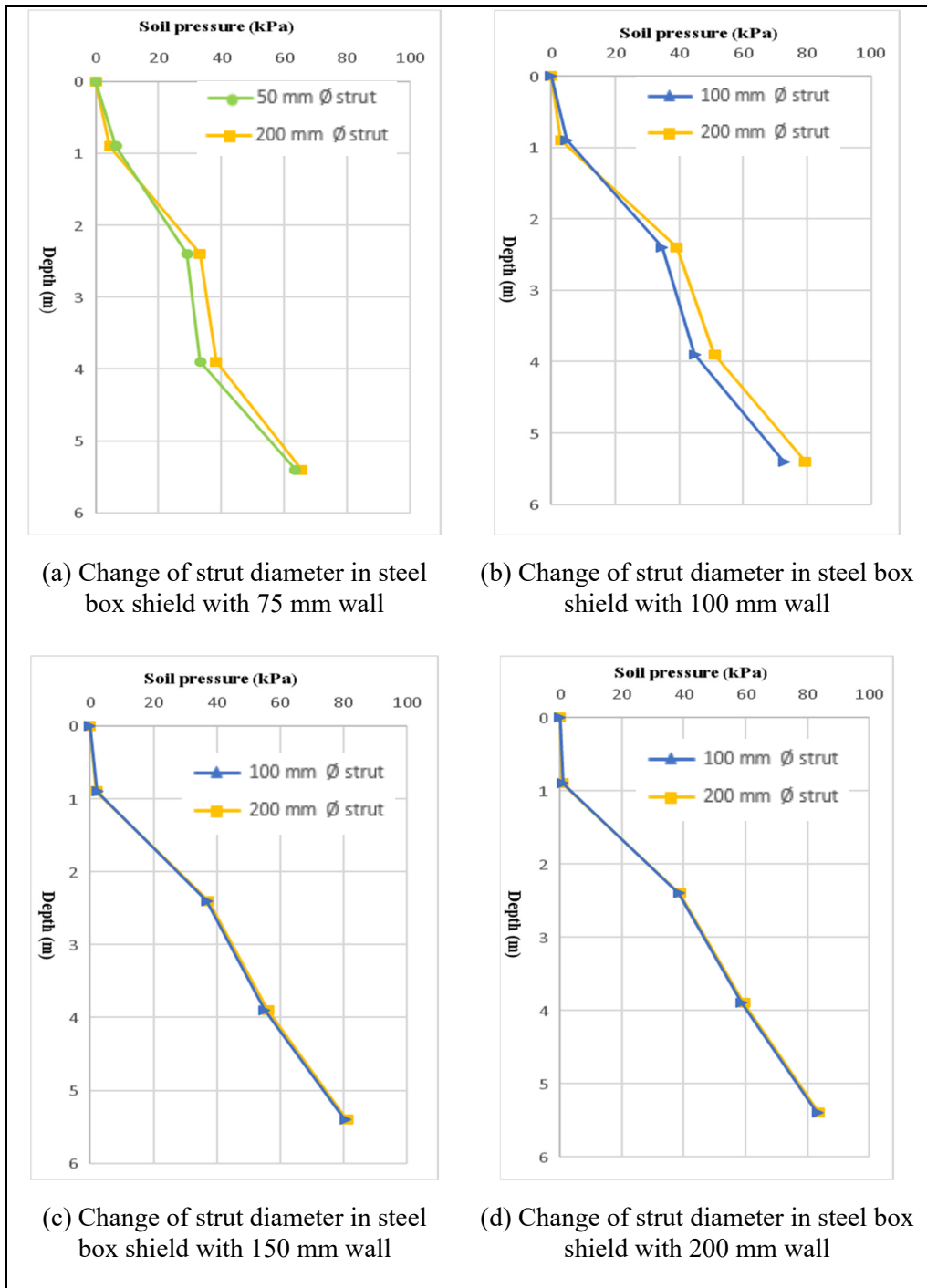


Figure 5.7 Soil pressure (Louisville clay) on steel trench box shields with different plate thicknesses and strut diameters

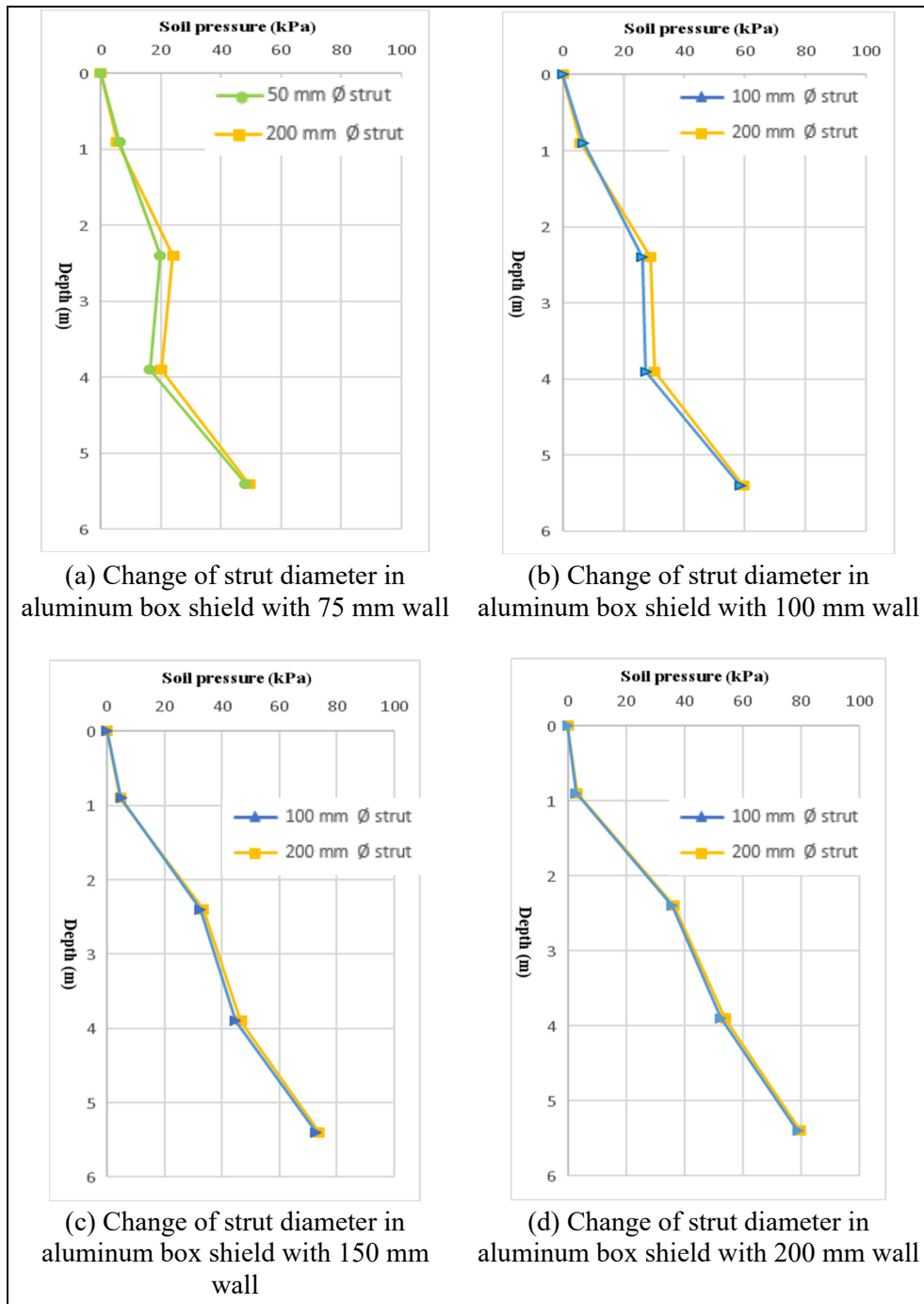


Figure 5.8 Soil pressure (Louiseville clay) on aluminum trench box shields with different plate thicknesses and strut diameters

Table 5.6 Soil pressure on steel and aluminum protection shield boxes with different strut diameters and plate thicknesses

| Steel trench box (kPa) | | | | | | | | | Aluminum trench box (kPa) | | | | | | | |
|------------------------|----------------------------|---------------------------|----------------------------|--------------------------|----------------------------|----------------------------|----------------------------|----------------------------|----------------------------|---------------------------|----------------------------|--------------------------|----------------------------|----------------------------|----------------------------|----------------------------|
| Depth from top (m) | 100mm plate, 200mm Ø strut | 75mm plate, 200mm Ø strut | 100mm plate, 200mm Ø strut | 75mm plate, 50mm Ø strut | 150mm plate, 200mm Ø strut | 150mm plate, 100mm Ø strut | 200mm plate, 200mm Ø strut | 200mm plate, 100mm Ø strut | 100mm plate, 200mm Ø strut | 75mm plate, 200mm Ø strut | 100mm plate, 100mm Ø strut | 75mm plate, 50mm Ø strut | 150mm plate, 200mm Ø strut | 150mm plate, 100mm Ø strut | 200mm plate, 200mm Ø strut | 200mm plate, 100mm Ø strut |
| 0.0 | 0.0 | 0.0 | 0.0 | 0.0 | 0.0 | 0.0 | 0.0 | 0.0 | 0.0 | 0.0 | 0.0 | 0.0 | 0.0 | 0.0 | 0.0 | 0.0 |
| 0.9 | 3.0 | 4.5 | 4.9 | 6.5 | 2.0 | 2.3 | 0.8 | 0.9 | 5.80 | 5.39 | 6.78 | 6.24 | 4.6 | 4.9 | 3.2 | 2.8 |
| 2.4 | 39.2 | 33.2 | 34.8 | 29.2 | 37.4 | 36.9 | 38.7 | 38.4 | 28.90 | 24.04 | 26.26 | 19.81 | 33.6 | 32.5 | 36.6 | 35.9 |
| 3.9 | 51.0 | 38.3 | 44.9 | 33.4 | 56.2 | 55.1 | 59.5 | 58.8 | 30.29 | 20.09 | 27.35 | 16.34 | 46.7 | 44.8 | 53.9 | 52.5 |
| 5.4 | 79.4 | 65.5 | 72.7 | 63.6 | 81.2 | 80.6 | 83.8 | 83.4 | 59.53 | 49.37 | 58.46 | 48.22 | 73.9 | 72.9 | 79.8 | 79.0 |

5.10 Conclusions

The parametric FE studies presented in this paper involve simulation of two trench box shields stacked upon each other, using ‘hinge connections’ to cover the total depth of the 6 m (20 ft) trench in sensitive clay and sandy soils, with the PLAXIS 3D computer code. The goal of these studies is to gain an insightful picture of the effect of (i) soil parameters on the steel trench box shield for till, dry sand, wet sand and sensitive clay soil; and (ii) the trench box material type (steel or aluminum) and geometry on the earth pressure. The FEM analysis results are also compared to published empirical apparent earth pressure diagrams.

Based on the FEA results, the following observations can be made:

- Earth pressure on a steel trench box for till, dry sand and wet sand seems to be underestimated by Terzaghi and Peck (1967) earth pressure diagrams for the lower part of the trench box (beyond 4 m depth in the case of till, and beyond 3 m depth in the case of dry and wet sand).
- A significant difference in earth pressure was found between the steel and aluminum temporary shields. The maximum undrained total stresses decreased by 40.6% when shifting from a steel to an aluminum shield having the same geometry.
- FEA results showed that changing plate thickness from 100 mm (4 in.) to 75 mm (3 in.) resulted in a maximum 17% decrease in soil pressure on steel and a 33.67% decrease on aluminum trench box shields for the same type of soil.
- Changing the strut diameter from 200 mm (8 in.) to 100 mm (4 in.) resulted in a maximum 8.4% decrease in soil pressure on steel and a maximum 9.5% decrease on aluminum trench box shields for the same type of soil.

CHAPTER 6

FIELD TEST PERFORMANCE OF HYDRAULIC SHORING WITH PLYWOOD SHEETING IN A SOFT AND SENSITIVE CLAY

Miah Alam ^a, Omar Chaallal ^b, Bertrand Galy ^c

^{a, b} Department of Construction Engineering, École de Technologie Supérieure,
1100 Notre-Dame West, Montreal, Quebec, Canada H3C 1K3.

^c Department of Research, Québec Occupational Health and Safety Research Institute
(IRSST), 505 de Maisonneuve Blvd. West, Montreal, H3A 3C2, Canada

Paper published in *Global Journal of Advanced Engineering Technologies and Sciences*,
February, 2021.

6.1 Abstract

This paper presents the results of a field experimental case study carried out to investigate the soil pressure on a trench by vertical aluminum hydraulic shoring with plywood sheeting in soft and sensitive clay trench. The installation, instrumentation, and field test procedures are presented for this type of vertical aluminum hydraulic shoring with plywood sheeting (Speed shore) in conformity with United States OSHA guidelines and placed inside the trench to cover the total 2.4 m (8 ft) depth of excavation. The field test results are presented in terms of soil pressure distribution along the depth of excavation with and without a 30 kPa surface surcharge next to the edge of one side of the trench. The results reveal the potential use this type of shoring in an excavation or trench in this type of soil.

6.2 Introduction

During earth excavation work, cave-ins are very frequent and present the most serious risk. This phenomenon is very often underestimated by the construction industry (Lan & Daigle, 2009). Occupational accidents statistics regarding soil cave-ins in trenches or excavations demonstrate the vulnerability of workers inside a trench or excavation within the construction industry. The main causes of accidents were the lack of proper shoring and safe working

practices. This emphasizes the importance for any governmental or local authority to ensure that occupational health and safety regulations are implemented at the work site to protect workers (Alam, *et al.*, 2020).

Vertical aluminum hydraulic shoring with plywood sheeting (Speed shores) is very popular now as a shallow trench protection system. A prefabricated strut and/or wale system manufactured of aluminum or steel gives construction industries a better choice. Hydraulic shoring allows a critical safety advantage over timber shoring because workers do not have to enter the trench to install or remove hydraulic shoring. These are light enough to be installed by one or two workers, gauge-regulated to ensure even distribution of pressure along the trench line, have their trench faces "preloaded" to use the soil's natural cohesion to prevent movement and can be adapted easily to various trench depths and widths (OSHA, 2015). These are designed to shore vertical trenches as well as less uniform excavations and offer optimum adaptability when restrictions are imposed by parallel or crossing utilities (Macnab, 2002).

Generally, no satisfactory consensual theoretical solutions are available to estimate soil pressure for this type of supporting structure with partitions facing land pressures in sensitive clay (NBCC, 2015). Many researchers have suggested theoretical solutions to estimate earth pressure on a flexible temporary support. Consequently, for an excavation shield, the Canadian Foundation Engineering Manual (CFEM) recommends the use of pressure envelopes from empirical data. Terzaghi and Peck (1967) methods (TPM) for estimating apparent earth pressure are very popular among practitioners because they are clearly understood and easy to implement. Equation 1 proposed by Terzaghi and Peck (1967) of apparent earth pressure on a flexible retaining structure in soft to medium clay.

$$p_A = K_A \gamma H, \quad (6.1)$$

where, Coefficient of earth-pressure, $K_A = 1 - \frac{m^4 S_u}{\gamma H}$, γ = unite weight of soil, H = depth of excavation, S_u = the average undrained shear strength value over the height of the wall, H ; and m is an empirical factor accounting for potential base instability effects in deep excavations in

soft clays. When the excavation is underlain by deep soft clay and the dimensionless number ($N = \gamma H/S_u$) exceeds 4, then m is set to 0.4; otherwise, m is set to 1.0 (Flaate, 1966). These formulas are clearly understood and easy to estimate; however, the method does not account for the development of soil failure below the bottom of the excavation. The total active thrust over the excavation depth on a smooth wall, as suggested by Rankine (1856), is given by:

$$P_{\text{Rankine}} = 0.5(\gamma H^2 - 4s_u H). \quad (6.2)$$

Where, γ , H and S_u as defined above.

On the other hand, to determine the apparent earth pressure for soft to medium clay, Henkel (1971) considered the basal stability phenomena as follows:

$$p_A = \left(1 - \frac{4s_u}{\gamma H} + \Delta K\right) \gamma H, \quad (6.3)$$

where the factor ΔK is related to bottom heave stability as follows:

$$\Delta K = \frac{2B}{H \left(1 - \frac{5.14S_{ub}}{\gamma H}\right)}. \quad (6.4)$$

where B is the width of the excavation and S_{ub} is the average undrained shear strength value below the excavation depth H . The distributed horizontal earth pressure (lb/ft^2) according to Yokel *et al.* (1980) can be computed using the following equation:

$$p = We (H + 2) \quad (6.5)$$

where We = lateral weight effect (lb/ft^3) and H = height of the supported bank (ft.) (2 ft. are added to allow for overloading) (Note: $1 \text{ lb/ft}^2 = 48 \text{ Pa}$). The above discussion reveals that calculating earth pressure on a flexible retaining structure is not straightforward and that

various soil parameters must be evaluated and considered when designing or validating a shoring system in a soft clay excavation or trench (Yokel *et al.*, 1980).

This study presents a full-scale field test investigation at a test site comprised of soft and sensitive clay soil of Louiseville, Quebec, Canada, to evaluate the earth pressure on a trench excavation protected with temporary flexible hydraulic shoring with plywood sheeting. The trench was 2.4 m deep and the shoring consist of plywood shield. The field test results are presented in terms of soil pressure with depth of soil. This paper provides a detailed explanation of the installation phase, including instrumentation, and the test phase. The experimental results are presented and compared with available Rankine (1857), Terzaghi and Peck (1967), and Yokel *et al.* (1980) theoretical apparent earth pressure values.

6.3 Full-scale field experimental program

To satisfy the objectives related to the evaluation of earth pressure and the performance validation of a temporary shoring system, an experimental trench was excavated and an excavation protection system (Hydraulic shoring with plywood sheeting) was set up at a site located in Louiseville, Quebec, Canada.

6.3.1 Soil Characteristics of the Field Experimental Site

The field experimental site is located about 100 km north-east of Montreal, on the north shore of the St. Lawrence River. It is along Highway 138, 8 km west of Louiseville village. The elevation of the site is 9.5 m above sea level. The site is known for its so-called sensitive clay soil, and therefore it was selected for the present study. The soil is made up of a 60 m - thick, Champlain Sea high-plasticity clay deposit (Leblond, 1981). According to Leroueil *et al.* (2003), this clay is very homogeneous, with 80% clay fraction, 45% average plasticity index, and an average sensitivity (S_t) of 22 (as determined with the Swedish fall cone). Experimental shear tests were performed at a Laval University (Quebec City) laboratory using a scissometer (Roctest model M-1000). Table 6.1 shows the shear strength data for undrained soil at the

Louiseville experimental site and the soil layers. The shear strength profile with depth is very similar to the shear strength profile obtained by Leroueil *et al.* (2003) for Louiseville sensitive clay.

Table 6.1 Experimental versus Leroueil et al. (2003) undrained soil shear strength values at Louiseville experimental site
(Adapted from Dourlet, 2020)

| Soil type and depth | Experimental Shear strength (kPa) | Shear strength from Leroueil <i>et al.</i> (2003) (kPa) |
|------------------------------------|-----------------------------------|---|
| Fissured brown clay (0.0-0.6m) | 51 | 30 |
| Plastic brown clay (0.6 m - 2.0 m) | | |
| At 1.5 m | 26 | 19 |
| At 2 m | 18 | 22 |
| Sensitive blue clay (2.0 m +) | | |
| At 2.5 m | 23 | 26 |
| At 3 m | 27 | 30 |
| At 3.5 m | 28 | 32 |
| At 4 m | 27.5 | 30 |

Triaxial testing and DSS testing were conducted on soil samples corresponding to 3.05 to 3.65 m depth. Soil samples were obtained with the large diameter Laval tube sampler (200 mm diameter), which has been specifically developed for sensitive clays (Rochelle *et al.*, 1981). The details and results of these three tests are summarized in Table 6.2. Two of them were undertaken in the over consolidated domain and one in the normally consolidated domain. In the over consolidated domain, DSSstat-01 showed a contraction behaviour, whereas DSSstat-02 showed a slight dilation behaviour. In the normally consolidated domain, DSSstat-03 showed a contraction behaviour. Effective stress parameters obtained from DSS tests are presented in Table 6.3. These parameters can be useful to model the long-term behaviour of the trench. They are comparable to data published by Lefebvre (1981) for Champlain Sea clays,

which are a common type of sensitive clay in the Province of Quebec. Extensive characterization and testing of the Louiseville clay (same test site) are presented in Leroueil *et al.* (2003).

Table 6.2 Undrained shear strength from the soil based on DSS testing

| Test | Consolidation | | Initial rupture | | Large deformations | |
|------------------------|-------------------------|-------|-----------------|--------------|---------------------|--------------|
| | σ'_{vc} (kPa) | e_c | S_u (kPa) | g_h (%) | S_{u-gd} (kPa) | g_h (%) |
| DSS _{STAT-01} | 57 | 2.287 | 28 | 2.3 | 23 | 15 |
| DSS _{STAT-02} | 25 | 2.290 | 20 | 2 | 22 | 15 |
| DSS _{STAT-03} | 143 | 1.804 | 40 | 5 | 36 | 15 |

Table 6.3 Effective stress parameters from DSS testing

| Domain | DSS tests |
|-------------------------------|-----------------------------------|
| Over consolidated, domain | $c' = 9$ kPa $f' = 28^\circ$ |
| Normally, consolidated domain | $c' = 0$ kPa $f' = 26.5^\circ$ |

6.3.2 Excavation and Shoring Geometry

The excavated area between the outside of the trench box and the face of the trench should be as small as possible (OSHA, 2015). Considering this recommendation, the contour of the excavation considered in this experiment was 3.8 m (12.5 ft) long and 1 m (3.28 ft) wide, accommodating the hydraulic shoring with plywood protection that was 3.6 m (11.8 ft) long, 1 m (3.28 ft) wide, and 2.4 m (7.87 ft) deep (see Figure 4(a)).

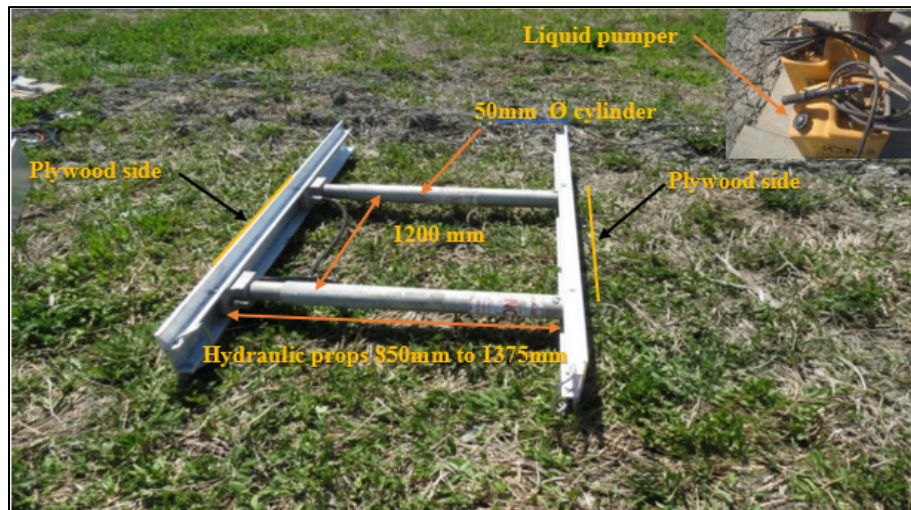


Figure 6.1 Hydraulic shoring protection system

Hydraulic shoring system shown in Figure 6.1 has to apply with the plywood. This system needs manual hydraulic pressure, more labour and more attention for not to slip down workers in to the excavation specially when the soil is soft and sensitive. This system can be used with or without different retaining material such as spot bracing, stacked, waler system (typical) and with plywood (OSHA, 2015). In this experimental purpose, Plywood is chosen as a retaining flexible protection shield with hydraulic props. Two hydraulic props 850 mm (34 in.) to 1375 mm (55 in.) length and 1.2 m (4 ft) apart in a frame with 19 mm ($\frac{3}{4}$ in.) thick Plywood sheets (Speed shore) was used for the trench. Detail geometric properties are shown in Table 6.4.

Table 6.4 Geometric properties of the shield

| Properties (one-shield geometry) | Hydraulic shoring with plywood |
|--|--------------------------------|
| Plywood Length, m (ft.) | 0.9 (3) |
| Height, m (ft.) | 2.4 (8) |
| Thickness of the Plywood, mm (in.) | 19 (3/4) |
| Hydraulic props outer diameter, mm (in.) | 50 (2) |
| Hydraulic props length, mm (in.) | 800-1375 (32-55) |

6.3.3 Instrumentation

Table 6.5 shows the identification and capacities of the pressure cells installed on the plywood side of hydraulic shoring. Four vibrating-wire pressure cells (model TPC) were used to capture the soil pressure at the following soil depths from the top of the plywood shield: 0.9 m (3 ft), 1.8 m (6 ft). At the depth of 0.9 and 1.8m, each pair of cells was used to observe to what extent/ scale the pressure varies in center and beyond the centerline of the hydraulic props. The locations of the pressure cells attached to the plywood sheet for the purpose of the test are shown in Figures 6.3 and 6.4(b), and the locations of the hydraulic props are shown in Figure 6.4(b). Hydraulic shoring system has four sides, only two sides has experiencing soil pressure in the trench. In this experiment, pressure cells are attached in one side only shown in Figure 6.4 (a). Other two sides are open to the soil along the trench shown in the Figure 6.4(b). Note that the vertical and horizontal distance between props are 1.2 m (4 ft), 0.9 m (3 ft) respectively.

Table 6.5 Pressure cell identification and capacities

| Pressure cell identification | Capacity (kPa) |
|-------------------------------------|-----------------------|
| C-P1 | 200 |
| C-P2 | 70 |
| C-P3 | 200 |
| C-P4 | 70 |

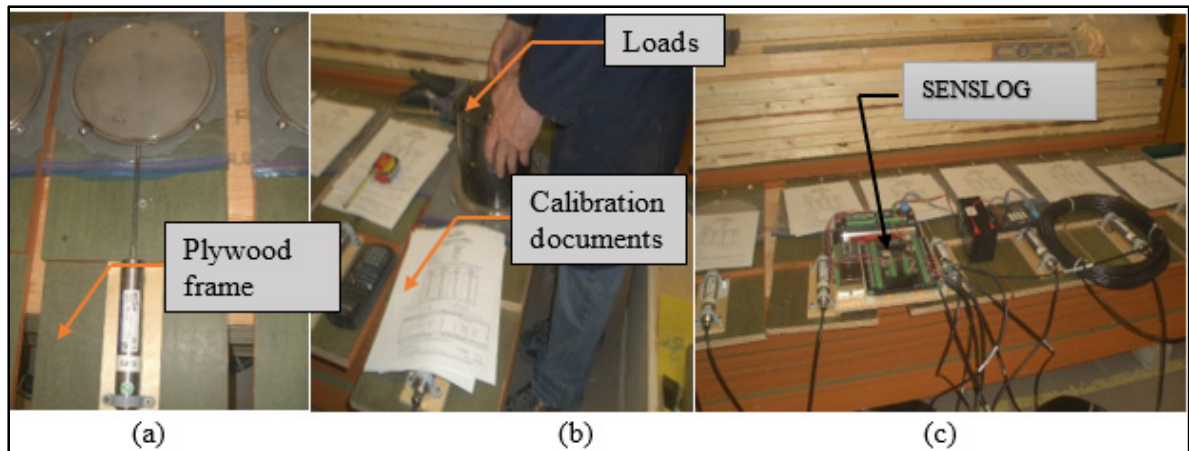


Figure 6.2 (a) Pressure cells are attached to the plywood frame; (b) Pressure are placed on the cell; (c) cells are tested by the SENSLOG in the ETS lab before site installations

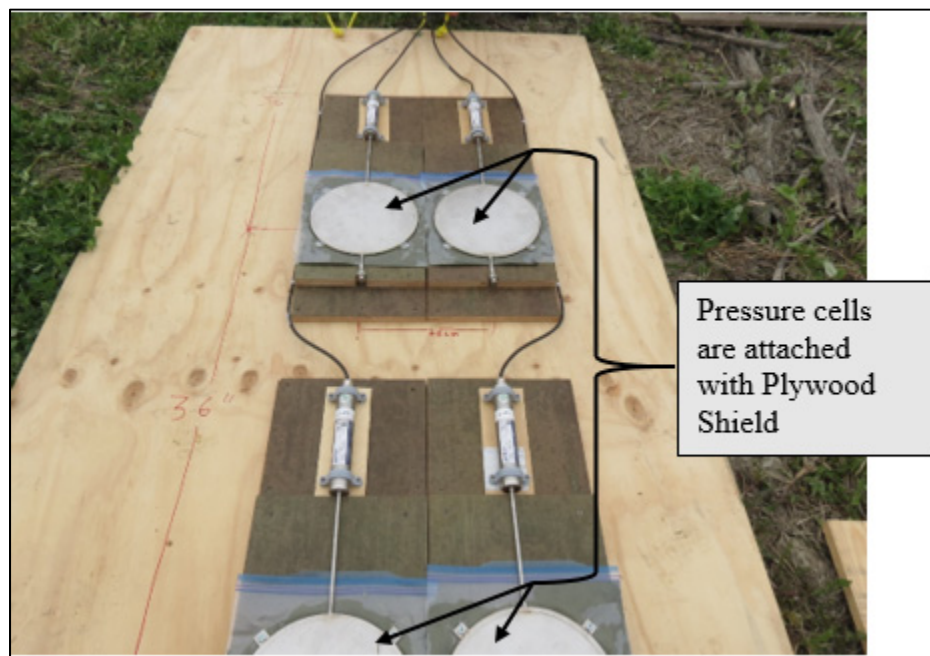


Figure 6.3 Pressures cells installation on the Plywood shield at the site before installations in the trench

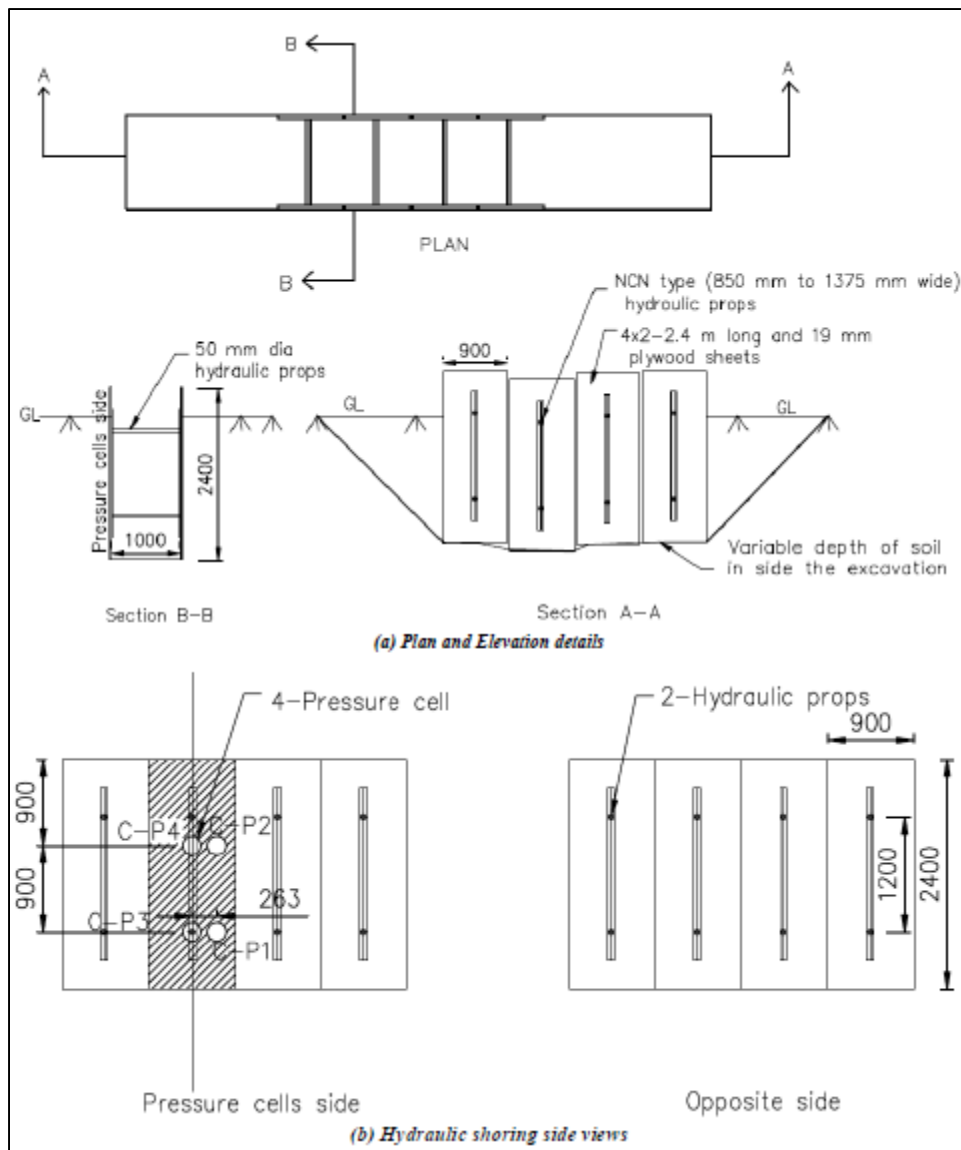


Figure 6.4 Test setup details for Hydraulic shoring (with plywood sheeting) in trench excavation

6.3.4 Laboratory Verification and Field Installation of Test Equipment

The pressure cells were first individually attached to plywood frames 19 mm (3/4 in.) thick with epoxy at the ETS laboratory, as illustrated in Figure 6.2(a). Two main reasons justify this initiative: (i) to be sure that the surface receiving the cells is plane and (ii) to optimize the time required to attach the pressure cells to the box shield protection system at the experimental site

(an open field). After all the pressure cells were bonded to the plywood surface, they were carefully tested in the laboratory to check their functionality under pressure before they were transported to the experimental site (Figure 6.2(b)). To do this, the pressure cells were connected individually with the 'Roctest SENSLOG 1000X' datalogger (a turnkey system used for remote monitoring of virtually any type of instrument), and loads were applied gradually in the structural test laboratory at ETS (Figure 6.2(c)). Note that calibration of the pressure cells was undertaken by the equipment provider and that a calibration document was supplied with the equipment. For pressure cells C-P1(at 1.8 m) and C-P3(at 1.8 m), 0 - 200 kPa range pressure used for the calibration. For C-P2 (at 0.9 m) and C-P4 (at 0.9 m), 0 - 70 kPa range used. As deeper part of the trench experiencing more pressure than the upper part, two 200 kPa capacity are used in the deeper part and two 70 kPa capacity are used in the upper portion. Figure 6.4 and Table 6.5 shown detail of pressure cells. Once all the pressure cells were verified as functional in the laboratory, they were transported to the experimental site. Vibrating wire pressure cells (model TPC) are reliable, faster than all other types, and almost immune to external noise because they rely on the frequency output (Roctest, 2005). A previous experimental study by Lan *et al.* (1999) successfully used this type of pressure cell to measure the apparent earth pressure.

To install the pressure cells on the plywood, wall of the hydraulic shoring (speed shoring), the following steps were undertaken: (i) the plywood wall surface was identified and prepared, and then finally, pressure cells for the speed shoring were simply screwed between plywood holding the pressure cells and plywood which will be used for retaining wall in the speed shoring system shown in the Figure 6.3.

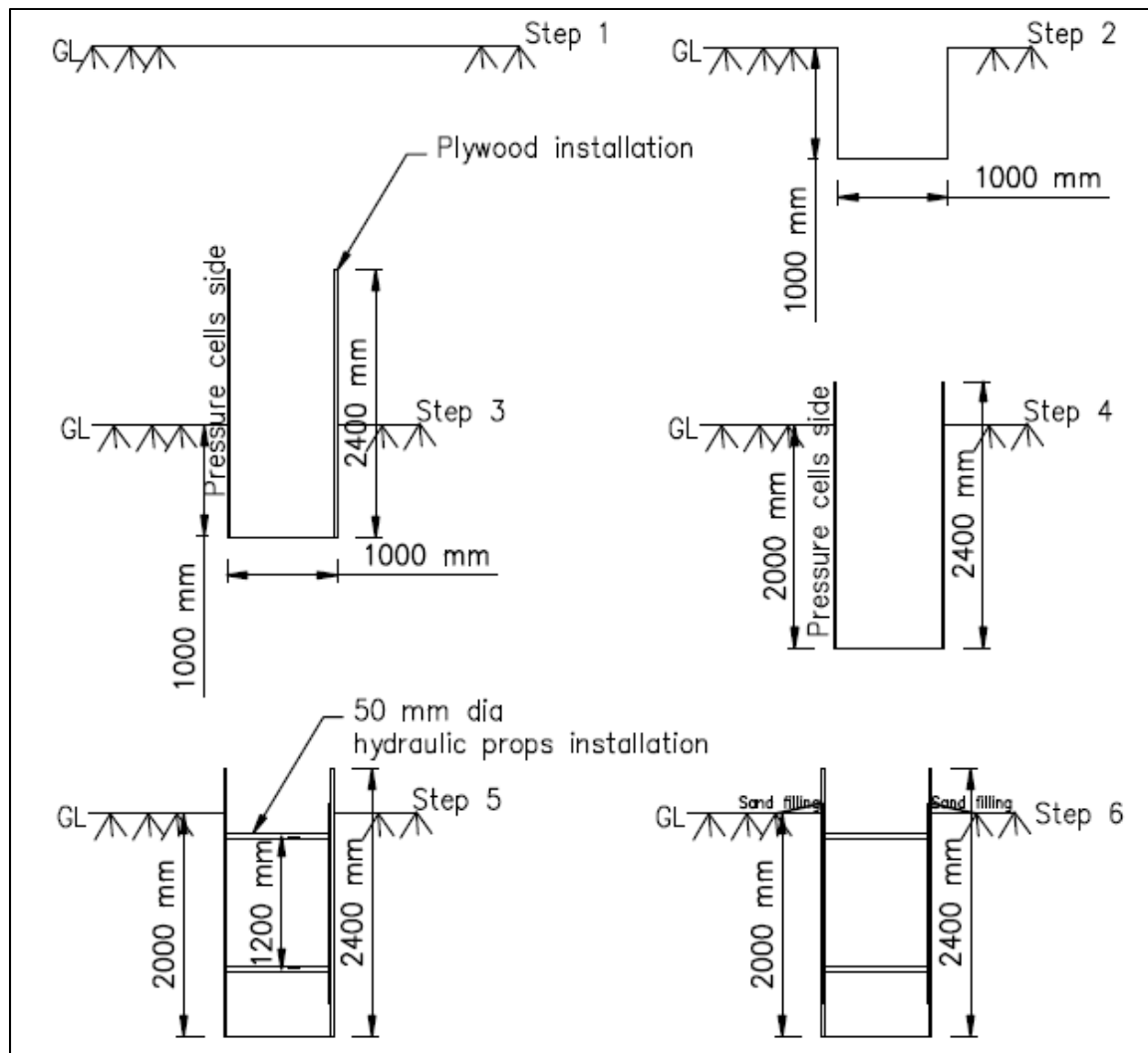


Figure 6.5 Excavation / Construction sequences for Hydraulic shoring with Ply wood sheeting in a trench

6.3.5 Excavation and installation of protection systems

The field tests were performed in 2018 from May 15 to August 8 without surcharge loading and from August 8 to August 10 with a 30 kPa surcharge load consisting of concrete blocks. After all the pressure cells had been bonded to the plywood wall shoring of hydraulic shoring system, after 1m (3.28ft) of soil excavation 19 mm ($\frac{3}{4}$ in.) thick and 2.4 m (8 in.) height plywood sheets has used as quick as possible as a protection shield with the hydraulic props. Hydraulic liquid was pumping through pipes to the props. Excavation was continued until 2 m

depth and pumping has done until the required pressure to hold the plywood sheet in a balanced position against the soil pressure on the plywood. Incremental soil pressure on the pressure cells as well as ply wood were recorded with time (from 15th May-10th August) by the data recorded unit. Detail excavation/construction steps are shown in Figures 6.5 and 6.6 for hydraulic shoring.

A space between plywood shield exterior wall and the surrounding soil was created due to the installation process. The spaces are in a range between 50 mm to 200 mm. OSHA (2015) states that, the space between the plywood shield and the excavation side are backfilled to prevent lateral movement of the shoring system. Therefore, after successfully installing the hydraulic shoring with plywood, the empty space between the retaining (shoring) exterior wall and the surrounding soil was backfilled with sand, as shown in Figure 6.6(c). In addition, the height between the plywood top and the soil surface was kept to 300-350 mm on both sides (Figure 6.6) in compliance with the SCCI (2020) recommendation that “the shoring shall extend 300 mm above the excavation”. Finally, the two other open ends of the trench were closed by inserting 10 mm thick sheet piles, thereby preventing loose soil from falling inside the excavation.



Figure 6.6 Detail installation process of Hydraulic shoring with Plywood in a shallow trench of soft and sensitive clay

6.3.6 Concrete Block (Surcharge load) Installation

Surcharge load of 30 kPa was applied on one side of the trench using $2.44 \text{ m} \times 0.6 \text{ m} \times 0.6 \text{ m}$ concrete blocks during the period from August 8 to 10, 2018, as illustrated in Figure 6.7. The aim of this loading on the surface of the protection system was to examine the movement of the soil as well as the pressure increase due to the overload. The SCCI standard specifies 1.2 m (4 ft.) distance from the excavation (SCCI, 2020). However, OSHA (2015) states that

temporary spoil must be placed no closer than 0.61 m (2 ft.) from the surface edge of the excavation and that permanent spoil should be placed at some distance from the excavation. Considering all these statements, the overload was placed close to the wall to simulate the most unfavorable case.

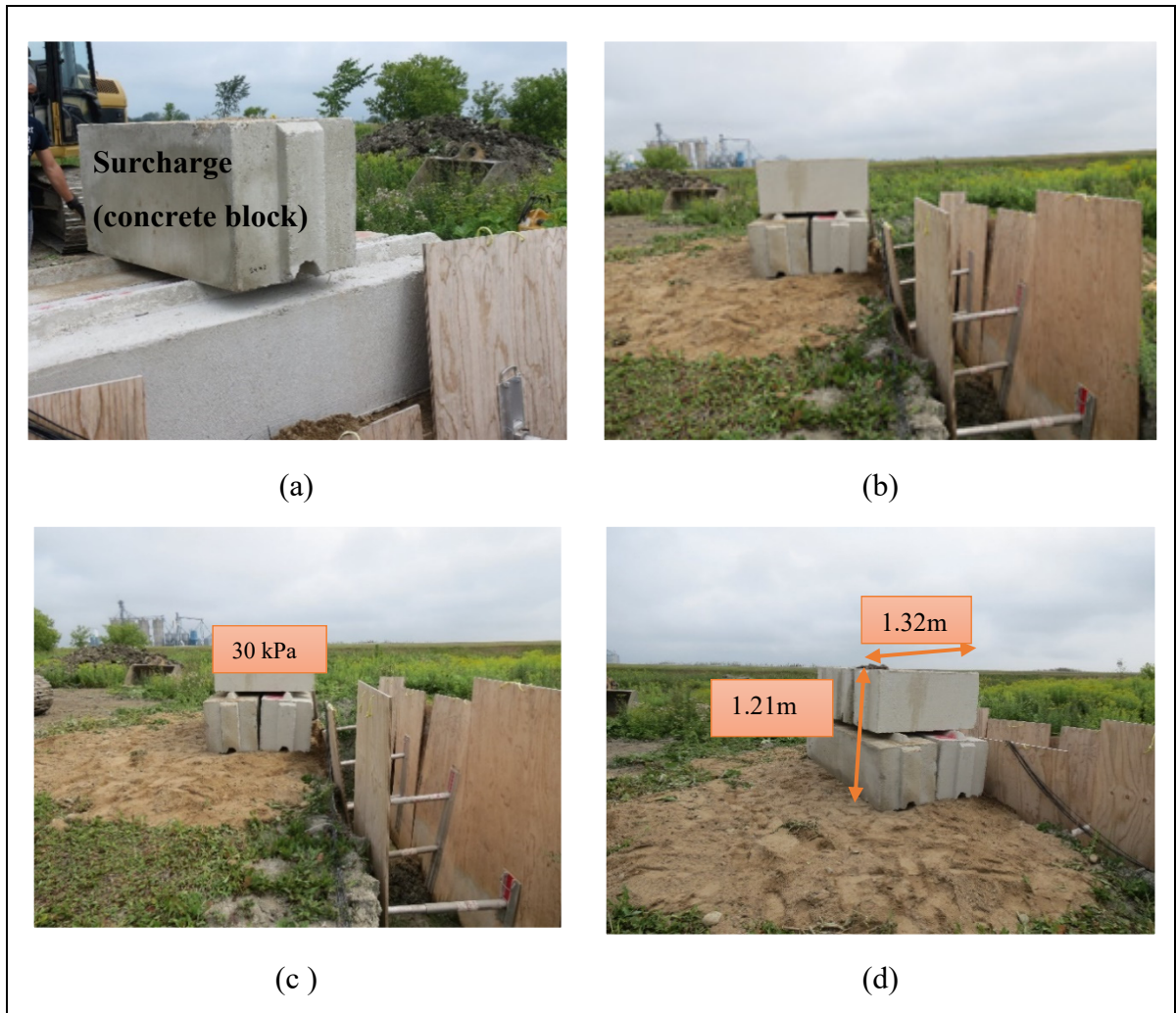


Figure 6.7 Concrete blocks (surcharge load) placing in a trench of soft and sensitive clay

6.3.7 Data Recording Unit and Data Collection

All the sensor cables attached to the pressure cells were brought into the small data acquisition trailer and connected to the appropriate box to record the field test data. Figure 6.8 shows the

small truck trailer chamber that was used at the experimental site to record the test data in real time during the whole course of the field experiment. All the pressure cells were connected to the central sensor box by the sensor cables. Real-time data were collected using Wi-Fi technology from ETS through a dedicated Web site of the equipment provider.

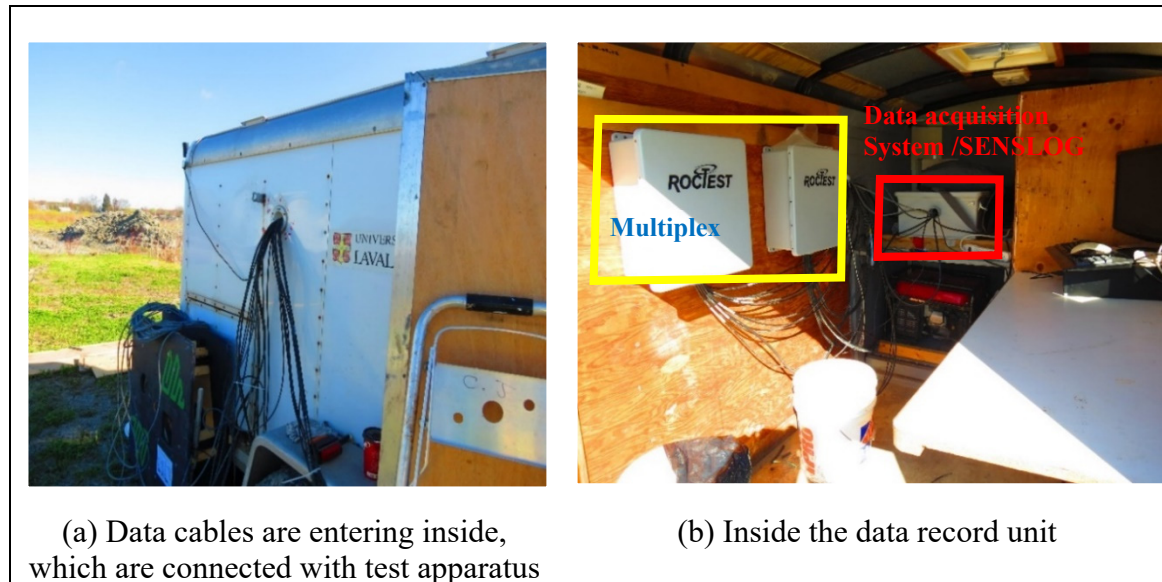


Figure 6.8 Data recording unit in the experimental site

6.3.8 Data Preparation

Data were collected using Wi-Fi technology installed at the field site by the equipment rental company. ETS has access through the file transfer protocol (FTP) to the Web site at any time (24/7) to check and collect data. To reduce their volume, data were recorded at intervals of 30 minutes, 24/7. These data were recorded in the form of raw data such as linear units and Hertz, not directly in kilopascals (kPa) for the pressure cells. Therefore, it was necessary to transform the raw data into an appropriate engineering format using the linear equation recommended by the Roctest (2005) instruction manual related to vibrating-wire total pressure cells. This equation was used as follows for each of the pressure cells separately:

$$P = C_f (L - L_0) \quad (6.6)$$

where P = pressure in kilopascals (kPa); C_f = calibration factor (provided on calibration sheets for each pressure cell separately); L = current reading in linear units (LU); and L_0 = initial reading in linear units (LU). Roctest (2005) also provides a more complex polynomial method. However, the linear method is simpler and easier to use, and the maximum error rate was only 0.23% in the present case. Next, a correction was applied to take temperature changes into account using the following equation recommended by Roctest (2005):

$$P_c = P - C_T(T - T_0) - (S - S_0) \quad (6.7)$$

where P_c = corrected pressure in kPa; P = pressure previously calculated in kPa; C_T = calibration factor for temperature (given in the calibration sheet), in kPa/°C; T = current temperature reading in degrees Celsius; T_0 = initial temperature reading in degrees Celsius; S = current barometric pressure reading in kPa; and S_0 = initial barometric pressure reading in kPa. The correction factor for barometric reading expressed in the above equation by the term $(S - S_0)$ was neglected given its very small value compared with the pressure measured at depth. All the above equations were used to calculate the earth pressure in the trench using Excel worksheets.

6.4 Field test results and discussion

Hydraulic shoring with plywood installation was little bit complicated due to the nature of the soil and nature of the system installation process. This system required more manpower and more attention during the time of installation. Sands were used to fill the gap between plywood exterior wall and the surrounding soils. According to the recorded data, after few days of installation this Hydraulic shoring with plywood system does not work properly. Probable reasons may be the gaps were created between the plywood retaining wall and the surrounding soil. The plywood is unable to hold the soil pressure or the rigidity (stiffness) of the plywood was not sufficient.

6.4.1 Temperature effect

Figure 6.9 shows, for the first week, the daily temperature at different trench depths as captured by the pressure cells. The figure reveals that the day-versus-night fluctuations of soil temperature were more significant in the upper pressure cells (C-P2 and C-P4) than in the deeper pressure cells (C-P1, C-P3) in the trench. The uppermost cells experienced minimum and maximum temperatures of 9°C and 15°C in the first week of the experiment, but the deeper pressure cells (C-P4, B-P3) experienced minimum and maximum temperatures of 6°C and 9°C. Again, Figure 6.10 was developed as per hourly temperature (15th May-10th August) at different depths of trench. It shows the uppermost cells (C-P2, B-P4) experienced minimum and maximum temperatures of 9°C and 30°C in the total period of the experiment, but the deeper pressure cells (C-P1, B-P3) experienced minimum and maximum temperatures of 6°C and 21°C.

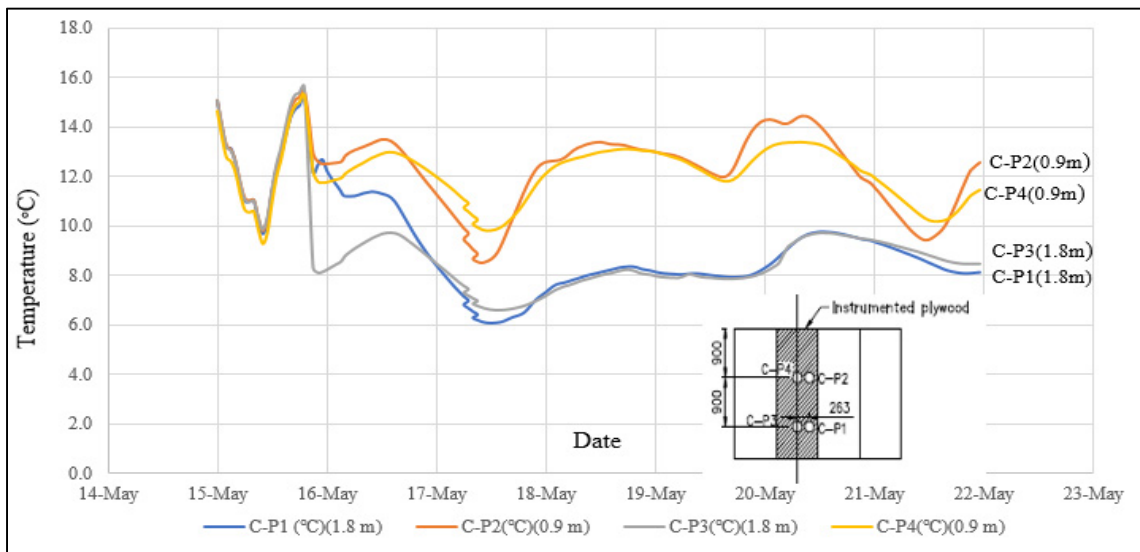


Figure 6.9 First week hourly temperature at different depths of trench

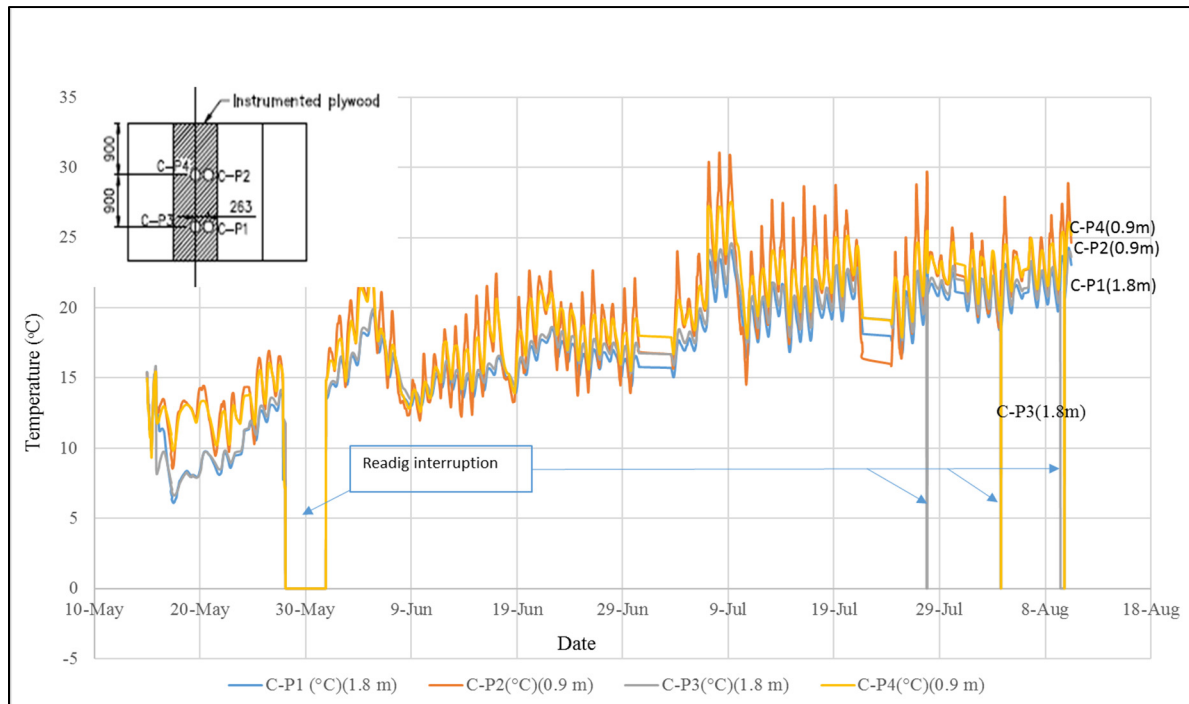


Figure 6.10 Hourly temperature (15th May-10th August) at different depths of trench

6.4.2 Soil pressure over the time period (May 15–August 10, 2018)

From Figure 6.11 and 6.12 the following observations can be made:

- In Figure 6.11 is analyzed on the basis of recorded hourly pressure after temperature corrections for the first week reading. It shows how the pressure varies in different depth of trench during this period. The deeper pressure cells give the less values of kPa then the upper pressure cells. It is evident that the pressure cell (C-P4 at 0.9 m depth) give more values of kPa then the 1.8 m depth pressure cell (C-P1 and C-P3), which is not logical for this type of speed shoring protection system. The probable causes maybe at the 1.8 m depth of trench, hydraulic props unable to create pressure over the plywood sheeting due to the holes, loose soil, soil dried up behind plywood sheets.
- Figure 6.12 is prepared according to the available data for soil pressure on the speed shoring wall during the period of 15th May to 10th August 2018. It shows that some pressure cells (C-P1, C-P2, C-P3, C-P4) were not responding properly, may be the probable causes in long term: (i) hydraulic props unable to create pressure over the

Plywood sheeting due to the holes, loose soil, soil dried up behind Plywood sheet. (ii) hydraulic liquid has less stress or leaking hoses and/or cylinders (iii) heavy rainfall (Figure 6.15) and waste away the surrounding soil behind the plywood sheets; (iv) spot cave-in of soil bottom part of the trench the gaps were created between the plywood retaining wall and the surrounding soil shown in Figures 6.16(c) and (d); and (iv) the plywood sheeting is unable to hold the soil pressure or the stiffness of the plywood was not sufficient for this type of soil. Only pressure cell C-P4 at 0.9 m depth responds better than the other for few days. The maximum pressure on the hydraulic shoring with plywood system recoded 27 kPa in the first week.

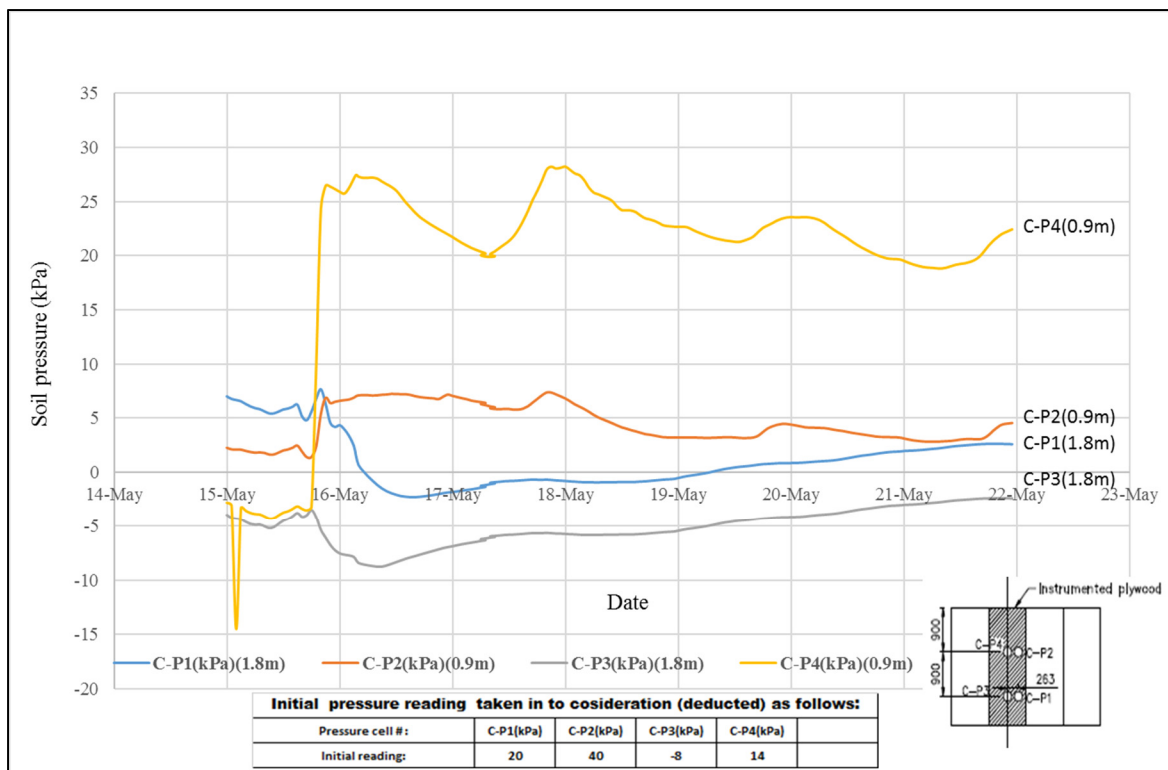


Figure 6.11 First week hourly pressure after temperature correction for trench

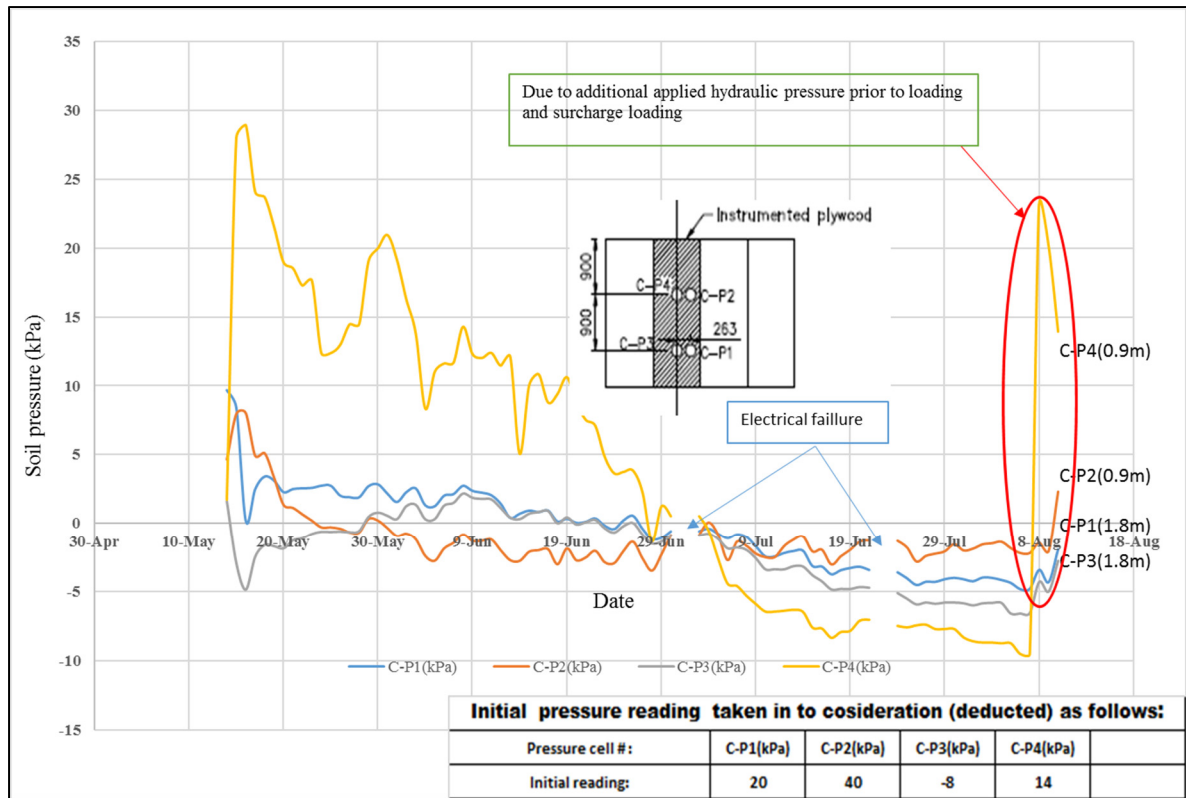


Figure 6.12 Maximum daily soil pressure after temperature correction for trench (15th May – 10th August, 2018)

6.4.3 Surcharge load effect on soil pressure

From Figure 6.13, the following observations can be made:

- Figure 6.13 shows the blow up of last week soil pressure to see the effects of surcharge (concrete blocks) loading at trench. Before the surcharge loading, it was trying to push the more hydraulic pressure to the shoring system to check its functionality. And 30 kPa surcharge (concrete blocks) loading was placed. In the curve, it shows that during the period (6th August, 2018 to 10th August 2018) soil pressure on the speed shoring are high enough.
- Figure 6.13 presents a blown-up view of the last week of soil pressure versus depth to evaluate the effects of the surcharge (concrete blocks) applied near the trench. As

expected, soil pressure at depth 0.9 m (C-P4) increased rapidly. This contrasts with the minor surcharge load effect observed at depths 1.8 m (C-P3, C-P1). Note that the pressure cell at depth 1.8 m (C-P3, C-P1) and 0.9 m (C-P2) recorded almost a constant pressure throughout the last week except some small increase due to additional applied hydraulic pressure prior to surcharge loading. This can be attributed to the fact that the surrounding soil was washed away due to heavy rainfall [Figure 6.16(c)]. It can be concluded that generally the effect of surcharge load was more noticeable on the upper part of the protection shield than on the deeper part of the trench.

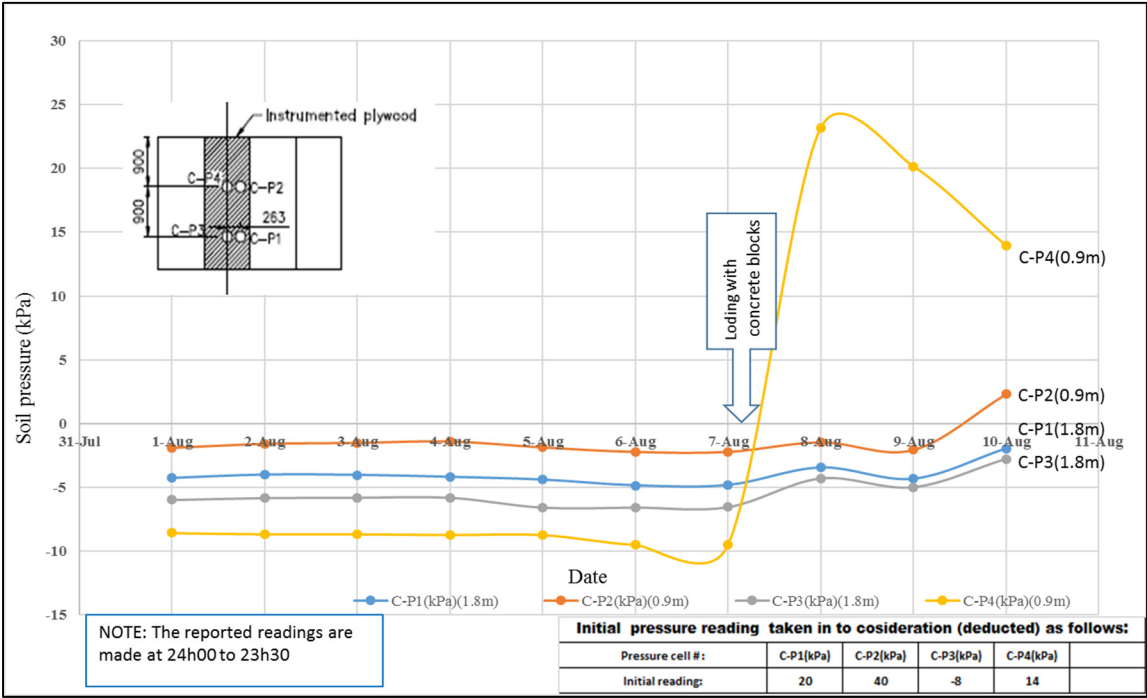


Figure 6.13 Blow up of last week soil pressure to see the effects of surcharge (concrete block) loading at trench

- Figure 6.13 presents a blown-up view of the last week of soil pressure versus depth to evaluate the effects of the surcharge (concrete blocks) applied near the trench. As expected, soil pressure at depth 0.9 m (C-P4) increased rapidly. This contrasts with the minor surcharge load effect observed at depths 1.8 m (C-P3, C-P1). Note that the pressure cell at depth 1.8 m (C-P3, C-P1) and 0.9 m (C-P2) recorded almost a constant

pressure throughout the last week except some small increase due to additional applied hydraulic pressure prior to surcharge loading. This can be attributed to the fact that the surrounding soil was washed away due to heavy rainfall [Figure 6.16(c)]. It can be concluded that generally the effect of surcharge load was more noticeable on the upper part of the protection shield than on the deeper part of the trench.

6.4.4 Total pressure curve

Figure 6.14 presents the absolute maximum soil pressure versus soil depth at the trench excavation without overloading. Experimental values were developed on the basis of experimental field test results (from May 15 to May 22, 2018). The soil pressure at depths 0.9 m (C-P4) of trench was observed to increase rapidly. Up to 0.9 m of depth the curve shows the similarities of TPM (1967) apparent pressure curve. But the lower part has not given correct reading due to soil irregularities such as holes, loose soil, soil dried up behind the pressure cells C-P1, C-P2 and C-P3 or probable causes mentioned above.

6.4.5 Theoretical calculations

The calculations presented in this section are meant to compare theoretical soil pressure with field test results. According to TPM equation (1) and Figure 6.14, the apparent earth pressure for soft clay in Louiseville soil case is $p_A = 15.55$ kPa, with $K_A = 1 - m(4S_u/\gamma H) = 0.5$. Active earth pressure formulae developed by Rankine (1857) and Yokel *et al.* (1980) were also used to calculate theoretical soil pressure; the results are summarized in Table 6.6. Calculated theoretical soil pressures for soft clay soil are compared at different depths of the trench in the present study in Figure 6.14.

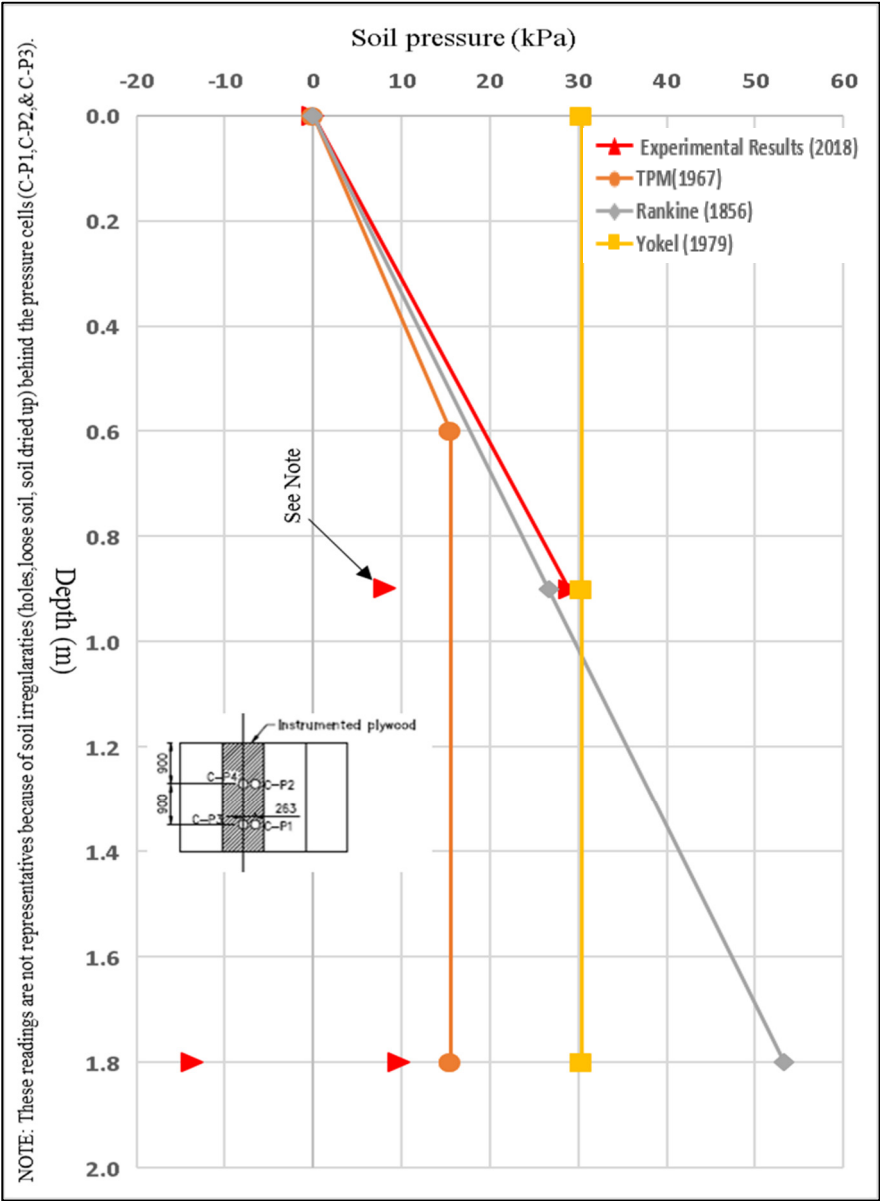


Figure 6.14 Experimental vs. theoretical soil pressure curves with respect to trench depth

Table 6.6 Experimental vs. theoretical and field performance soil pressures at different trench depths in soft clay soil

| Pressure cell identification | Depth from top of the soil (m) | Maximum experimental stress (kPa) | Calculated stress from Terzaghi and Peck (1967): $p_A = 1.0 K_A \cdot \gamma \cdot H$ (kPa) | Calculated stress from Yokel (1980): $p = W_e (H+2)$ (kPa) | Calculated stress from Yokel <i>et al.</i> (1980): $p = W_e (H+2)$ (kPa) |
|------------------------------|--------------------------------|-----------------------------------|--|---|---|
| | 0 | 0 | 0.00 | 0.00 | 30.35 |
| C-P4 | 0.9 | 29 | 15.55 | 26.64 | 30.35 |
| C-P2 | 0.9 | 8 | 15.55 | 26.64 | 30.35 |
| C-P3 | 1.8 | -14 | 15.55 | 53.28 | 30.35 |
| C-P1 | 1.8 | 10 | 15.55 | 53.28 | 30.35 |

Note: H= 1.8 m for above calculated stresses.

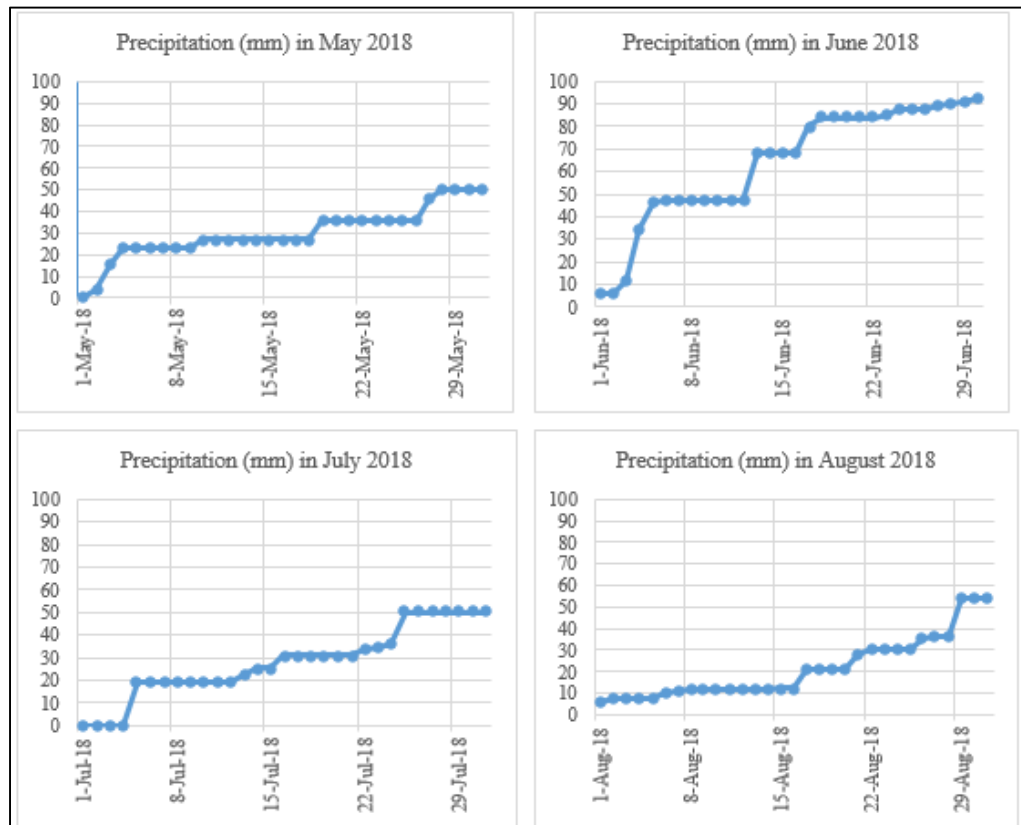


Figure 6.15 Recorded accumulated precipitation quantities (in mm) for each month from May to August 2018 at the Louiseville field test site



(a) Many people are required to installed this shoring system in this soft and sensitive clay



(b) It takes time and manpower to arrange the shoring in this type of soil



(c) Spotted soil cave-in to the trench after the installation of shoring system



(d) Rain water washed away the soil between the plywood and shoring soil

Figure 6.16 Some of irregularities found during and after the installation process of Hydraulic shoring (with Plywood sheeting) in this type of soft and sensitive clay

6.5 Conclusion

The main objective of the field experimental work was to evaluate the soil pressure on the Hydraulic shoring with plywood shield protection at shallow depth in a sensitive clay trench. The study covers the total depth of the 2.4 m (8 ft) trench in sensitive clay soil. Concrete blocks (representing a 30 kPa surcharge load) were installed very close to the trench to produce an extreme load case on the flexible wall of the shield. Soil pressures were captured by total

pressure cells (TPC) using vibrating-wire transducer technology. Based on the results of this study, the following observations can be made:

- Soil temperature variations were more pronounced in the upper part of the trench than in the deeper part.
- The deeper pressure cells in the trench should experienced higher pressures (kPa) than the upper pressure cells. But in that case, it shows that some pressure cells are not responding properly. Probable reasons may be: (i) the gaps were created between the plywood retaining wall and the surrounding soil; (ii) heavy rainfall; (iii) spot cave-in of soil bottom part of the trench; and (iv) the plywood is unable to hold the soil pressure or the rigidity of the plywood was not sufficient. Only pressure cell C-P4 at 0.9 m depth responds better than the other for first few days. The maximum pressure recoded 27 kPa in the first week at 0.9 m depth of trench.
- The effect of an overload applied close to the trench was more pronounced on the upper part of the protection shield than on the deeper part. It follows that the pressure cells at 0.9 m depths were more influenced by the 30 kPa overload in a short period of time. This reveals the need to maintain the minimum distance of 1.2 m (4 ft.) from the excavation when stacking up any materials, in compliance with OSHA and SCCI guidelines.
- Theoretical calculations by Rankine (1857), Terzaghi and Peck (1967), and Yokel *et al.* (1980) for this type of sensitive clay were compared with the pressures obtained from the field test results. Compared to Terzaghi and Peck, analytical values predicted by Rankine and Yokel formulae were closer to experimental values at 0.9m depth of the trench.

Comparing with other trench shoring systems such as Timber, Pneumatic; this vertical aluminum hydraulic shoring with plywood sheeting is relatively new system with some limitations for this kind of soft and sensitive soil. In this experimental purpose, 19 mm thick

plywood was used as a retaining flexible shield (sheeting) with hydraulic shoring was chosen to observe the effectiveness of the overall performance in a soft and sensitive clay. May be the stiffness of the plywood needs more attention and improvement for implementing other material as a protection shield for this kind of soft and sensitive soil. This system needs manual hydraulic pressure, more labour and more attention for not to slip workers in to the excavation when soil is soft and sensitive. This system can be used with different retaining material such as Aluminum or Steel plate with experimental test result in this type of soft and sensitive clay.

CONCLUSIONS AND RECOMMENDATIONS

Conclusions

This PhD research program was carried out to investigate the soil pressure on a temporary flexible trench box shoring in sensitive clay taking into account soil-structure interactions (SSI). It is based on experimental, numerical, and parametric studies. Flexible and semi-flexible supporting structures are used as temporary supports for the vertical sides of excavations. The earth pressure distribution depends on the type of soil, the shoring, and the method of implementation. Generally, no satisfactory consensual theoretical solutions are available to estimate soil pressure for this type of supporting structure with partitions facing land pressures in sensitive clay. Many researchers have suggested theoretical solutions to estimate the earth pressure on a flexible temporary support. A research gap has been observed for trench box shoring at shallow depths of less than 6 m and for SSI. Clearly, there is a lack of studies on trench box shoring taking into account the interaction between the soil mass and the support, flexibility in the development of lateral loads, and the movement of structural elements. This has been the main impetus to carry out this PhD research program focussing on investigating experimentally, numerically, parametrically and analytically as follows:

- 1) A field experimental study carried out to investigate the soil pressure on a temporary flexible trench shoring in sensitive clay. The installation, instrumentation, and field test procedures are presented for two trench boxes ‘stacked upon each other’ in conformity with United-States OSHA regulations and placed inside the trench to cover the total 6 m (20 ft) deep excavation. The field test results are presented in terms of soil pressure distribution along the depth of excavation with and without a 45 kPa surface surcharge applied next to the edge of one side of the trench. The results of this study are published in ISSMGE International Journal of Geoengineering; and can be summarized as follows:
(i) soil temperature variations were more pronounced in the upper part of the trench than in the deeper part; (ii) the deeper pressure cells in the trench experienced higher pressures

(kPa) than the upper pressure cells; (iii) the effect of an overload applied close to the trench was more pronounced on the upper part of the trench box than on the deeper part. It followed that the pressure cells at 0.9 m and 2.4 m depths were more influenced by the 45 kPa overload in a short period of time, revealing thereby the need to maintain a minimum distance of 1.2 m (4 ft) from the excavation when stacking up any materials, in compliance with OSHA and SCCI guidelines; and (iv) Terzaghi and Peck, analytical values predicted by the Rankine and Yokel formulae were closer to experimental values. In terms of soil pressure along the depth of trench, in general, the analytical formulae underestimated the experimental values for the type of sensitive clay considered in this study;

- 2) A 3D finite-element (FE) numerical study using PLAXIS-3D software was carried out to reproduce and validate a full-scale experimental in-situ test and to investigate the earth pressure on a flexible temporary trench box shield in soft and sensitive clay soil. The excavation trench model was 6 m (20ft.) deep and was considered as nonlinear and anisotropic clay. A 45 kPa (0.94 ksf) surface overload on top of the soil near the trench box was also simulated to produce a maximum load case on the flexible wall of the shield. Both Mohr-Coulomb (MC) and hardening soil (HS) constitutive soil models were considered for FE analysis. Different values of the modulus reduction factor (MRF) and the coefficient of earth pressure at rest (K_0) were considered to validate the model. The significant results of this research study are published as a journal paper in *Journal of Modelling and Simulation in Engineering*. They can be summarized as follows: (i) both HS and MC models revealed that the deeper part of the trench experienced higher pressures (kPa) than the upper part. The maximum pressure reached 143 kPa (3.0 ksf) and 87 kPa (1.81 ksf) at 5.4 m from the top of the trench for option [A] and option [C3] models, respectively; (ii) option [A] of the HS model at 3.9 m trench depth yielded a pressure closer to the in-situ experimental test value compared to options [B], [C1], [C2], and [C3] of the MC model. This is attributed to the fact that the elastic modulus ($E_{50} = 2000$ kPa) assumed in the HS model at that depth was extremely close to that on site; (iii) options [C1], [C2], and [C3] of the MC model with MRF results were comparable to those of option [B] of the MC

model without MRF, showing thereby the key role played by the precise shear strength parameters; and (iv) comparisons of theoretical predictions by Rankine (1857), Terzaghi and Peck (1967), and Yokel (1980) for this type of soft and sensitive clay with FEA results revealed that the pressures obtained using Rankine and Yokel analytical formulae were closer to the simulated and experimental values than those of Terzaghi and Peck. Along the depth of trench, the analytical formulae underestimated soil pressure at around 4 m depth for this type of sensitive clay;

- 3) Two parametric finite-element studies were carried out using the PLAXIS-3D computer code. The following objectives and corresponding parameters were considered : (i) to evaluate the effective soil pressure on the steel trench box shield; the parameters studied were related to soil type and material, and the study considered till, dry, wet, and loose sand and sensitive clay soil; (ii) to assess the effect of trench box material and geometry on earth pressure; the parameters studied were related to trench box material (steel versus aluminum) as well as geometry (plate thickness and strut diameter). These studies included simulation of two steel (or aluminum) trench box shields stacked upon each other, using 'hinge connections' to cover the total 6 m (20 ft) deep trench. A Mohr-Coulomb (MC) constitutive material model was chosen for FE analysis. The coefficient of earth pressure at rest (K_0) was considered as a variable in the model. The results of this research study are published in Journal of Modelling and Simulation in Engineering; and can be summarized as follows: (i) Till sand creates more stress on the steel shield than dry, wet, or loose sand and clay soil. The maximum effective soil pressures were 88 kPa (1.84 ksf), 32.75 kPa (0.68 ksf), 22.1 kPa (0.46 ksf), 31.59 kPa (0.66 ksf), and 33.52 kPa (0.7 ksf), respectively for till, dry, wet, and loose sand and sensitive clay at 5.4 m from the top of the trench; (ii) earth pressure for till, dry, wet, and loose sand and sensitive clay on a steel temporary shield was compared with published empirical apparent earth pressure diagrams from CFEM.; (iii) a significant difference in earth pressure was found between the steel and aluminum temporary shields. The maximum undrained total stresses decreased by 40.6% when shifting from a steel to an aluminum shield with the same geometry; (iv) FEA results showed that changing plate thickness from 100 mm to 75 mm resulted in a maximum of

17% decrease in soil pressure on steel and a 33.67% decrease on aluminum trench box shields for the same type of soil; and (v) changing the strut diameter from 200 mm to 100 mm result in a maximum of 8.4% decrease in soil pressure on steel and a maximum of 9.5% decrease on aluminum trench box shields for the same type of soil;

- 4) Again, another field experimental case study was carried out to investigate the performance of vertical aluminum hydraulic shoring with plywood sheeting in a soft and sensitive clay trench. Installation, instrumentation, and field test procedures are presented for this type of vertical aluminum hydraulic shoring with plywood sheeting (speed shoring) in conformity with United-States OSHA guidelines and placed inside the trench to cover the total 2.4 m (8 ft.) depth of excavation. The field test results are presented in terms of soil pressure distribution along the depth of excavation with and without a 30-kPa surface surcharge load applied next to the edge of one side of the trench. The significant results of this research study are published as a journal paper in Global Journal of Advanced Engineering Technologies and Sciences and can be summarized as follows: (i) compared with other trench shoring systems such as timber and pneumatic systems, vertical aluminum hydraulic shoring with plywood sheeting features some limitations for this kind of soft and sensitive soil.; (ii) in this experimental study, 19-mm thick plywood as a retaining flexible shield (sheeting) with hydraulic shoring was chosen to evaluate its overall performance and effectiveness in a soft and sensitive clay. The stiffness of the plywood may require more attention, and investigations should be carried out into implementing other materials as a protection shield for this kind of soft and sensitive soil; and (iii) compared to other systems in use, this system needs manual hydraulic pressure, more labor, and more attention to prevent workers from slipping into the excavation when the soil is soft and sensitive.

Recommendations

This research study mainly focused on steel trench box in soft and sensitive clay soil and with static induced surcharge load. The results achieved on the earth pressure on trench box in soft and sensitive clay are not conclusive. Additional efforts are needed for other types of box material, induced surcharge loading type, and soil type. Therefore, comprehensive analytical and experimental investigations are required to thoroughly understand the behaviour of earth pressure on a flexible trench shield. The following areas of future work are recommended based on the research conducted in this research study:

- 1) Additional experimental field tests should be conducted to evaluate the soil pressure on other type of shoring materials such as Aluminium in soft and sensitive clay.
- 2) Additional experimental field tests can be conducted to examine the effect of other soils such as sand and stiff and hard fissured clay.
- 3) Further field experiments should be conducted to investigate the earth pressure due to dynamic induced loads.
- 4) Additional laboratory analysis should be conducted to investigate the HS model parameters.
- 5) Additional numerical analysis should be conducted to investigate the effect of dynamic loads.
- 6) Additional research should be conducted on the effect of displacement of the trench box, and the development of the 'arching effect' that were beyond our scope of study.

APPENDIX I

DECISION SUPPORT SYSTEM

The following figures are a graphic summary (chart) of the requirements contained in Article 6 for excavations 20 feet or less in depth. Protective systems for use in excavations more than 20 feet in depth must be designed by a registered professional engineer in accordance with 1541.1(b) and (c) of (OSHA).

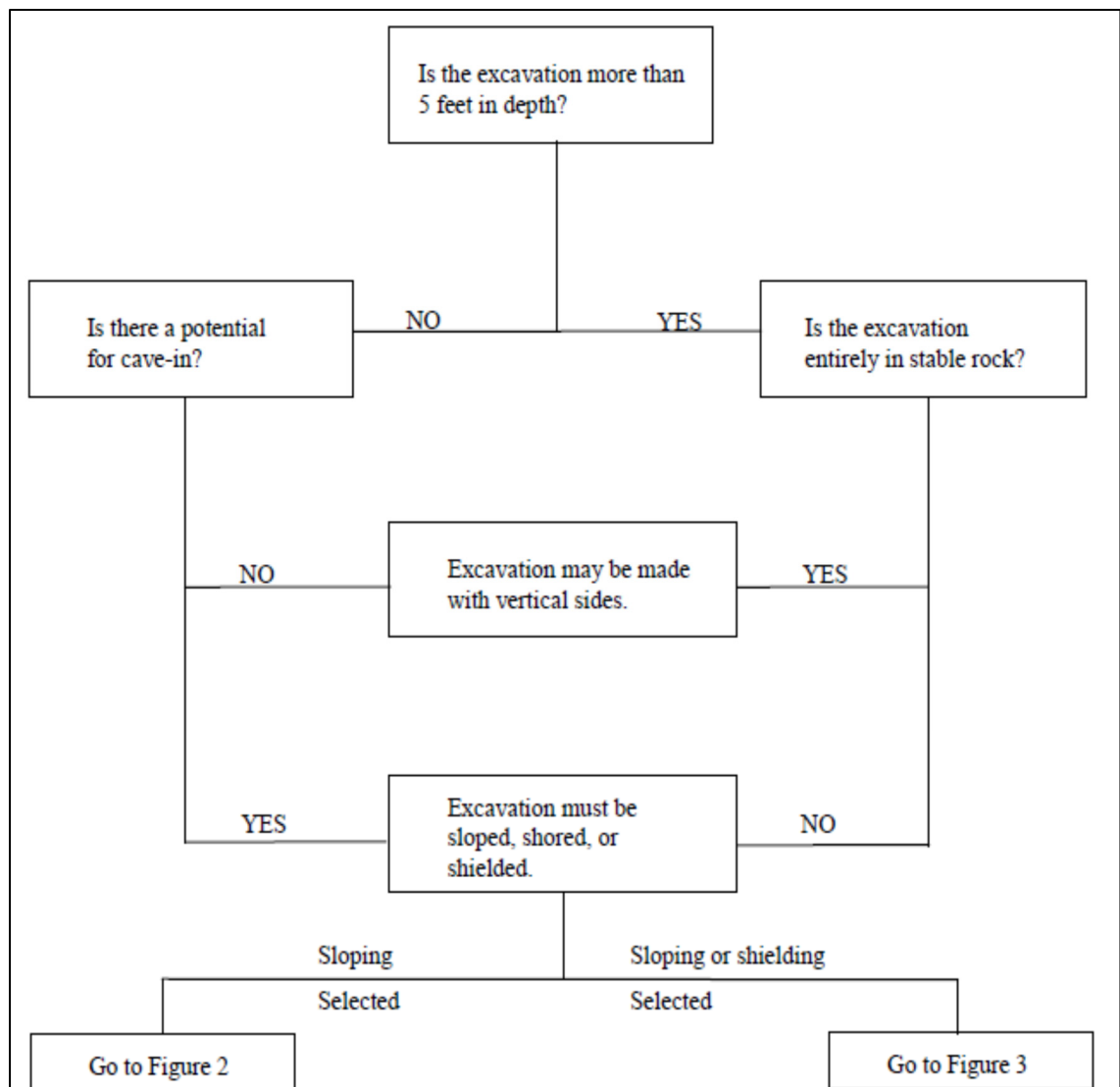


Figure-A I-1 Preliminary decisions
Taken from OSHA (2015)

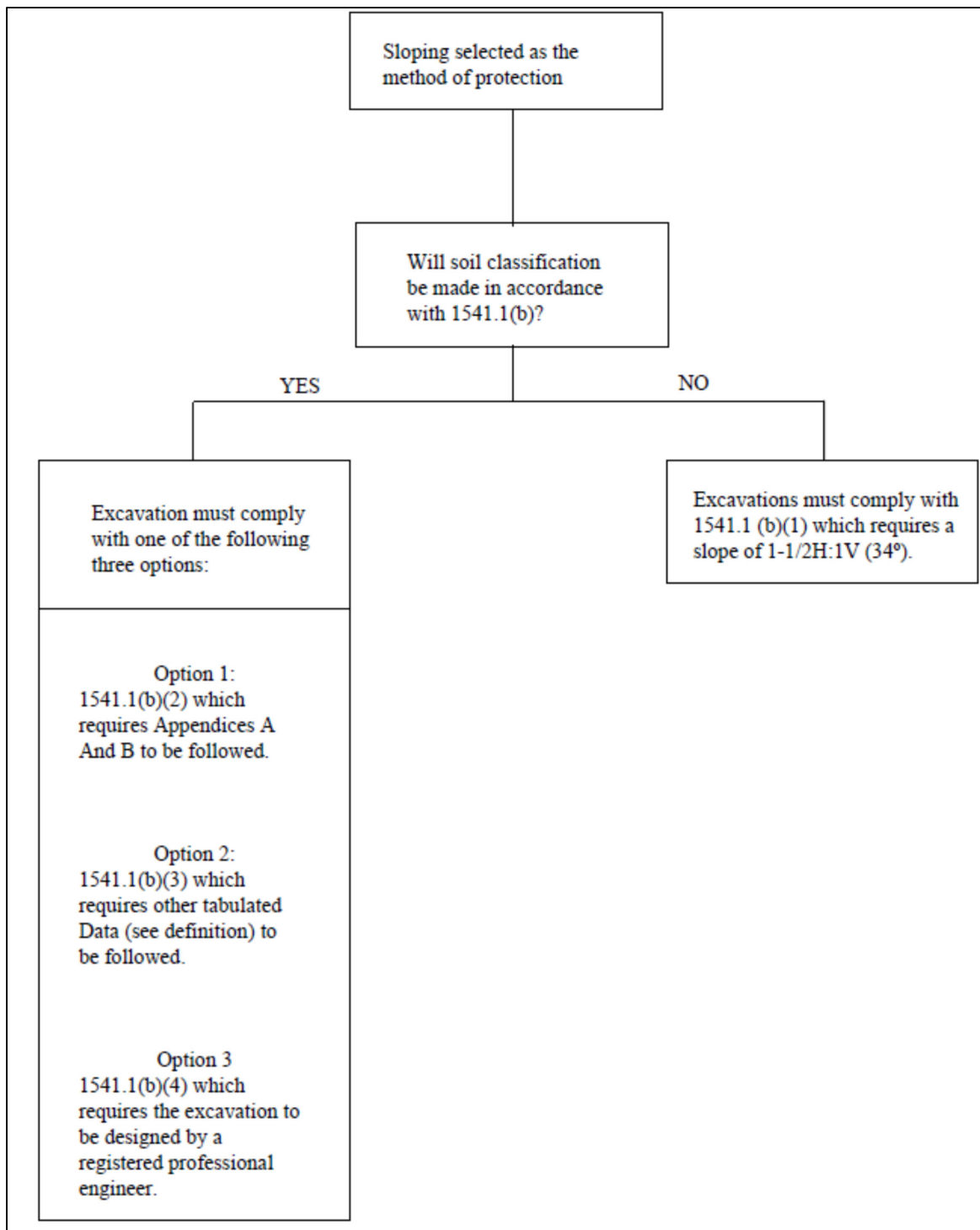


Figure-A I-2 Sloping options
Taken from OSHA (2015)

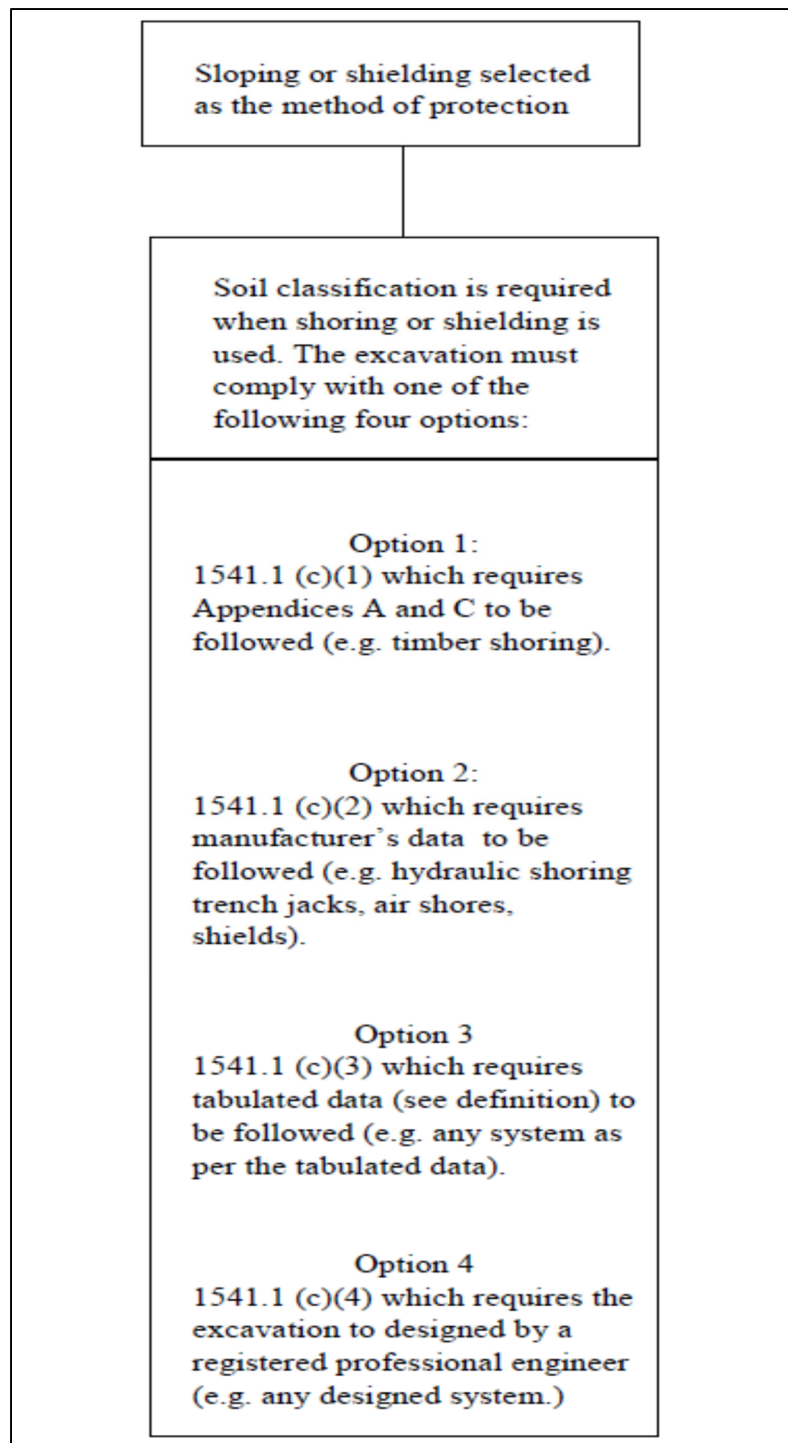


Figure-A I-3 Shoring and shielding options
Taken from OSHA (2015)

APPENDIX II

METHODOLOGY

Table-A II-1 Detailed methodology as related to the phases of the research program

| Phase I | Key Issue and Methodology | Work accomplished |
|--|---|--|
| A-Literature review i) Method of estimating soil pressure on flexible retaining wall of excavation ii) Excavation without support: UL iii) Excavation with support iv) Recent Research on the excavations with retaining structure and excavation related issues | Key Issue: Excavation/Trenching on Quebec soils, estimation of apparent earth pressure on flexible support, slope of the unsupported excavation, type of excavation protections, base stability in excavation, movements of in-situ walls, stiffness of the in-situ walls, effect of surcharge load adjacent to the excavation Methodology: Researchers, worldwide, have shown a vast and growing interest in the field of excavation support/protections. As a result, numerous paper and different codes, standards, and guidelines have been published in the subject. The following three tables are developed to synthesize the state of knowledge related to the subject of interest as follows: (i) Case studies on excavations with shorings, (ii) Theoretical, analytical and numerical studies on excavations with shorings, and (iii) Codes/Standards/ Guidelines related to excavations with shorings or slopings. | Accomplished for excavation with support and shown in Chapter 1 and 2. |
| B- Development of a soil classification system for trench work a) Classify Quebec urban soils based on their geotechnical characteristics following the rock and 3 or 4 types in order of stability. b) Propose apparent earth pressure envelopes based on soil classification c) Develop a simple method to determine in-situ soil type at work site to perform excavation and shoring according to which a risk prevention strategy can be implemented in order to eliminate at the source, the risks of landslides. | Key issue: Soil characterization, evaluation of Mohr-Coulomb parameters, apparent earth pressure evaluation, risk prevention strategy Methodology: This phase was carried out by the researchers of the University of Laval according to IRSST project proposal. This phase helped ETS researchers to better evaluate the types of earth pressures envelope acting on the flexible support during the time of test setup according to the Quebec urban soil class. After success of this phase of work, pressure on the flexible support can be predicted for phase-II. | Accomplished by UL, IRSST and ETS |

Table-A II-1 Detailed methodology as related to the phases of the research program
(continue)

| Phase I | Key Issue and Methodology | Work accomplished |
|--|--|--|
| Validation of shoring systems in clayey soils - Field Testing <p>a) Vertical Excavation (no shoring); accomplished by UL</p> <p>b) Excavation with shielding or trench box; is shown in the chapter 3 which was accomplished by ETS.</p> <p>c) Excavation with trench shoring; an example is shown in the chapter 6 which was also accomplished by ETS.</p> | <p>Key issue: Performance of vertical excavation without shoring, with shoring and with shielding (trench box) experimentally with in-situ soil pressure as per the Quebec soil class.</p> <p>Methodology: Three test trenches are planned as follows: 1) an unsupported trench, 2) an armored trench by a box, and 3) a shored trench. These three trenches will have a depth of up to 6 m, 2.25 width and a length of 10 m. For this type of soil, a 100-day follow up period is recommended to allow time to develop its ground thrust on the shoring system. Both geotechnical and structural instrumentation will be implemented for monitoring/observation as follows: <u>For excavation without shoring</u> - Pore water pressures and horizontal and vertical movements (walls and trench bottom) - Fracture behavior of the open cut soil <u>For excavation with shielding or trench box shoring and screen type shoring</u> - Static test by digging and monitoring of pore water pressures and horizontal and vertical movements in the ground and study the behavior at the maximum depth (6 m) - Static overload test of 45 kPa beside the excavation wall using concrete blocks.</p> | <p>Accomplished in summer 2018. [May 2018 to August 2018.]</p> |
| Phases III | Key Issue and Methodology | Work accomplished |
| Modeling and Simulation of armored and sloped excavations <p>Modeling and 2D and 3D simulations of geotechnical, structural and soil-structure interaction. The objectives of the numerical simulations are as follows:</p> | <p>Key Issue: Numerical 2D/ 3D FE modeling to predict the generalize behaviour of shored or slope excavation and minimize excavation related issues considering the Soil-Structure Interaction (SSI) process and better understand the deflections of the structural system as per the NBCC or other codes. And finally, we have seen how close the numerical simulations results can support the experimental results from phase 2.</p> <p>Methodology: PLAXIS 3D and FLAC software were used to FE model the behavior of the excavation trenches and ground-shield interaction. Specifically, for the different series, this translates into:</p> | <p>Accomplished in Fall 2018 – April 2020</p> |

Table-A II-1 Detailed methodology as related to the phases of the research program
(continue)

| Phases III | Key Issue and Methodology | Work accomplished |
|--|--|---|
| <p>i. To validate the classification of soils</p> <p>ii. To determine safe slope angles for the unsupported excavations</p> <p>iii. To confirm the main elements of a simplified method and practice of structural design shields</p> | <p>Series C.1: The results obtained on site in an unsupported open trench will be used to verify and validate the geotechnical model and trenches calculations (accomplished by UL).</p> <p>Series C.2: Simulations in the series C.2 will provide safe angles of slopes for soils identified in the Quebec soil classification (accomplished by UL).</p> <p>Series C.3: Verified data from different load cases ($q = 0$, $q = 45$ kPa) on shield trench sections and shoring support will be used in a back calculation by FE method. Then the results will be validating the soil-structure interaction (ISS) model, which includes the soil, the interfaces, and the structural elements (accomplished by UL and ETS).</p> <p>C.4 Series: Simulations in this series will use the ISS model has carried out to validate the lateral pressure curves that will be used in the structural design of shields and shorings (accomplished by ETS).</p> <p>Series C.5: The structural analyses in this series was used the pressure envelope curves determined in C.4 to validate the design of shielding (box) when embedded in different types of classified Quebec soils (accomplished by ETS).</p> <p>Series C.6: The structural analyses in this series was used for the pressure envelope curves determined in C.4 to validate the design of shielding (box) embedded in different types of classified Quebec soils. The analysis results from structural and ISS modeling (series C.4, C.5, and C.6) was be used to verify the simplified method for structural design of shields and shorings. These methods of structural analysis will also be adjusted to take into account the recommendations and requirements of the National Building Code of Canada (NBCC), especially at the limit states design (accomplished by ETS).</p> | |
| Phases IV | Key Issue and Methodology | Work accomplished |
| <p>Development of a decision support system Develop a decision support system (flowchart) which will help to select a shoring system based on soil characteristics and structural properties considerations of shorings.</p> | <p>Key Issue: selection of appropriate protection/shoring systems for excavation protection given the Quebec soil class.</p> <p>Methodology: The decision support system was be developed based on Cal/OSHA guideline.</p> | <p>Accomplished in September 2020 by IRSST and UL</p> |

BIBLIOGRAPHY

- Albert, A., Pandit, B., & Patil, Y. (2020). Focus on the fatal-four: Implications for construction hazard recognition. *Safety Science*, vol.128.
- Alam, M., Chaallal, O. & Galy, B. (2021). Flexible Temporary Shield in Soft and Sensitive Clay: 3D FE Modeling of Experimental Field Test. *Modelling and Simulation in Engineering*, vol. 2021, p. 1-15. doi: 10.1155/2021/6626750
- Alam, M., Chaallal, O., & Galy, B. (2020). Protection practices for trench and excavation in Quebec sensitive clay soils: Review of codes, guidelines, and research needs. *Safety science*, vol. 131, p. 1-8. doi: 10.1016/j.ssci.2020.104918
- Association Paritaire pour la santé et la sécurité au travail dans le secteur de la construction (ASP). (2018). *Les tranchées et les excavations: prévenir les dangers d'effondrement, 3 volets—Fiches de prévention*. Montréal: Association Paritaire pour la santé et la sécurité au travail dans le secteur de la construction.
- Arai, Y., Kusakabe, O., Murata, O. & Konishi, S. (2008). A numerical study on ground displacement and stress during and after the installation of deep circular diaphragm walls and soil excavation. *Comput. Geotech*, vol 35(5), p. 791-807.
- Benmebarek, . N., Labdi, H. & Benmebarek, S.(2016). A Numerical Study of the Active Earth Pressure on a Rigid Retaining Wall for Various Modes of Movements. *Soil Mech. Found. Eng.*, vol. (53),p. 39–45.
- British Columbia Occupational Safety and Health Administration (BCOSHA). (2009). *Occupational Health and Safety Regulation*. British Columbia: WorkSafe BC. Available at: <https://www.worksafebc.com/en>.
- Bentley System (2017). *Plaxis Material Models Manual*. Exton, PA: Bentley Systems. Available at: <https://www.bentley.com/en>.
- Bjerrum, L., Clausen, C. J. F., & Duncan, J. M. (1972). *Earth pressures on flexible structures; state-of-the-art report*. p. 1-28. Norwegian Geotechnical Institute.
- Bose, S.K., & Som, N. N. (1998). Parametric study of a braced cut by finite element method. *Computers and Geotechnics*, vol 22(2), p. 91-107.
- Boussinesq, J. V. (1885). *Applications des Potentiels à l'Étude de l'Équilibre et Mouvement des Solides Élastiques*. Gauthier–Villars : Imprimeur-Libraire, Paris.
- Bowles, J. (1996). *Foundation analysis and design* (5e éd.). Peoria, Illinois: McGraw-hill.

- Bryson, . L. S. & Zapata-Medina, D. G. (2012). Method for Estimating System Stiffness for Excavation Support Walls. *Journal of Geotechnical and Geoenvironmental Engineering*, vol 138 (9), p. 1104-1115.
- British Standards Institution (BSI). (2009). *Code of practice for earthworks, BS 6031*. London: British Standards Institution.
- Casagrande, L. (1973). Comments on conventional design of retaining structures. *Journal of the Soil Mechanics and Foundations Division*, vol 99 (2), p. 181-198.
- Canadian Foundation Engineering Manual (CFEM). (2006). *Canadian Foundation Engineering Manual*. Vancouver: Canadian Geotechnical Society.
- Construction Safety Association of Ontario (CSAO). (2009). *Construction Health and Safety Manual*. Etobicoke, Ontario: Construction Safety Association of Ontario.
- Clough, G., & O'Rourke, T. (1990). Construction induced movements of insitu walls. *Proceeding of Design and performance of earth retaining structures*. NY: ASCE.
- Dourlet, S. (2020). *Étude expérimentale de deux excavations à Louiseville*. (Master of Engineering Thesis, Université Laval, Québec, Canada)
- Finno, R.J., & Blackburn, J. T. (2006). Three-Dimensional Modeling of Excavation Sequences. Communication present in *International Conference on GeoCongress 2006*, Atlanta, GA, United States.
- Finno, R. J., Blackburn, J. T. & Roboski, J. F. (2007). Three-dimensional effects for supported excavations in clay. *Journal of Geotechnical and Geoenvironmental Engineering*, vol 133(1), p. 30–36.
- Flaate, K. S. (1966). *Stresses and movements in connection with braced cuts in sand and clay*. (Thesis report for Doctor of Philosophy, University of Illinois, Urbana-Champaign).
- Goldberg, D., Jaworski, W. & Gordon, W. (1976). *Lateral Support Systems and Underpinning, Volume I. Design and Construction*, Washington D.C.: Federal Highway Administration (FHWA).
- Hamouche , K., Leroueil, S., Roy, M. & Lutenegeger, A. (1995). In situ evaluation of K_0 in eastern Canada clays. *Canadian Geotechnical Journal*, vol 32(4), p. 677-688.
- Hashash, Y. M. & Whittle, A. J. (1996). Ground movement prediction for deep excavations in soft clay. *Journal of Geotechnical Engineering, ASCE*, vol 122(6), p. 474-486.
- Hashash, Y. M. A. & Whittle, A. J. (2002). Mechanisms of load transfer and arching for braced excavations in clay. *J. Geotech. Geoenviron. Eng.*, vol 128, p. 187–197.

- Henkel, D. J. (1971). The calculation of earth pressures in open cuts in soft clays. *The Arup Journal*, vol 6(4), p. 14-15.
- Hou, Y., Wang, J. & Zhang, L. (2009). Finite-element modeling of a complex deep excavation in Shanghai. *Acta Geotech.*, vol 4(1), p. 7-16.
- Hsieh, P. & Ou, C. (1998). Shape of ground surface settlement profiles caused by excavation. *Canadian Geotechnical Journal*, vol 35(6), p.1004-1017.
- Irvine, D.J., & Smith, R.J.H. (1983). Trenching practice. *Proceedings of the Institution of Civil Engineers*, vol 76(3), p. 839-842. London: Construction Industry Research and Information Association (CIRIA).
- Jaky, J. (1944). A nyugalmi nyomás tényezője [The coefficient of earth pressure at rest]. *Journal of the Society of Hungarian Architects and Engineers*, vol 78(22), p. 355-358.
- Karlsrud, K. & Andresen, L. (2005). Loads on Braced Excavations in Soft Clay. *International Journal of Geomechanics, ASCE*, vol 5(2), p.107-113.
- Konstantakos, D.C. (2015). Apparent Lateral Earth Pressures Below the Lowest Support Level. *International Foundations Congress and Equipment Expo 2015*. p. 1389-1401. American Society of Civil Engineers. San Antonio, Texas.
- Kramer, S. L. (1996). *Geotechnical earthquake engineering* (1e éd.). India: Pearson Education.
- Kung, Gordon T.C. Hsiaob, Evan C.L. Schusterb, Matt. & Juang, Hsein C. (2007) A neural network approach to estimating deflection of diaphragm walls caused by excavation in clays. *Computers and Geotechnics*, vol.34 (5), p. 385-396. doi:10.1016/j.compgeo.2007.05.007
- LaBaw, S. M. (2009). *Earth Pressure Determination in Trench Rescue Shoring Systems*. (Doctoral thesis, University of Maryland, College Park).
- Lafleur, J., Chiasson, P., Asselin, R. & Ducharme, A. (1987). Évaluation des risques pour les travailleurs dans les excavations (*Research Report GEO-87-001, 141 p. and annexes*). Montreal: Civil Engineering Department, École Polytechnique de Montréal.
- Lam, S. S. Y. (2010). *Ground Movements due to Excavation in Clay: Physical and Analytical Models*. (Doctoral thesis, University of Cambridge, Churchill College).
- Lan, A. (2013). *Analyse des rapports d'accidents graves et mortels de la CSST de 1974 à 2013 (Rapport interne non publié)*. Montréal: Institut de recherche Robert-Sauvé en santé et en sécurité du travail (IRSST).

- Lan, A., Arteau, J., Tremblay, M., Gamelin, S., LeBoeuf, D., Chaallal, O., & Dugré, J-M. (1999). *Conception d'un étançonnement adapté aux excavations en milieu urbain: Phase 2*. Montréal: Institut de recherche Robert-Sauvé en santé et en sécurité du travail (IRSST).
- Lan, A., Daigle, R. (2009). Review of Regulations and Guides for Excavation and Trenches—Comparison with the Québec Safety Code for the Construction Industry. *Practice Periodical on Structural Design and Construction, ASCE*, vol 14 (4), 201-209.
- Lan, A., Daigle, R., LeBoeuf, D., Chaallal, O. (2008). *Recensement des systèmes d'étançonnement et de blindage pour les excavations et les tranchées*. Montréal: Institut de Recherche Robert-Sauvé en Santé et en Sécurité du Travail (IRSST).
- Leblond, P. (1981). *Mesure et caractéristiques de la perméabilité des argiles Champlain*. (Master of Engineering Thesis, Université Laval, Québec, Canada).
- Leroueil, S. (2003). Geotechnical characterization and properties of a sensitive clay from Quebec. In T. Tan, K. Phoon, D. Hight & S. Leroueil. *Characterization and engineering properties of natural soils*. (pp. 363-394). London: CRC Press, Taylor & Francis.
- L'Organisme Professionnel de Prévention du Bâtiment et des Travaux Publics (OPPBTP). (1989). *Guide pratique de travaux de fouilles en tranchées*, OPPBTP, Boulogne-Billancourt, France.
- Malekitabar, H., Ardeshir, A., Sebt, M.H., & Stouffs, R. (2016). Construction safety risk drivers: A BIM approach. *Safety Science*, vol 82, p. 445–455. doi: 10.1016/j.ssci.2015.11.002.
- Macnab, A. (2002). *Earth retention systems handbook*. (1e éd.). New York: McGraw-Hill Education.
- Marr, W. A., & Martin, H. (2010). Displacement-based design for deep excavations. In *Earth Retention Conference 3*. 82-100, American Society of Civil Engineers, Bellevue, Washington.
- Matsuzawa, H. & Hazarika, H. (1996). Analyses of Active Earth Pressure Against Rigid Retaining Wall Subjected to Different Modes of Movement. *Soil and Foundations*, vol 36(3), p. 51-65.
- Mortensen, N., & Lars, A. (2003). Analysis of undrained excavation in anisotropic clay. In *Proc., Int. Workshop on Geotechnics of Soft Soils Theory and Practise, SCMEP*. 245-250.

- Mayne, P. (2006). In-Situ Test Calibrations for Evaluating Soil Parameters. In T. Tan, K. Phoon, D. Hight, & S. Leroueil (Eds.), *Characterization and engineering properties of natural soils*, vol 3, pp. 1601-1652. London: CRC Press, Taylor & Francis.
- Ministère de l'Environnement et de la Lutte contre les Changements Climatiques (MLLCC). (2020). *Ministère de l'Environnement et de la Lutte contre les changements climatiques*. Available at: <https://www.environnement.gouv.qc.ca>.
- National Building Code of Canada (NBCC). (2015). *National Building Code of Canada, Commentary K*. Ottawa, Ontario: National Research Council Canada.
- Occupational Safety and Health Administration (OSHA). (1989). *Safety and Health Regulations for Construction, Part 1926: Excavations*. Washington, DC: U.S. Department of Labor. Available at: <https://www.osha.gov/lawsregs/regulations/standardnumber/1926/1926SubpartP>.
- Occupational Safety and Health Administration (OSHA). (2015). *OSHA Technical Manual (OTM)*, Directive Number: TED-01-00-015, Section V, Chapter 2: Excavations: Hazard Recognition in Trenching and Shoring. Washington, DC: U.S. Department of Labor. Available at: https://www.osha.gov/dts/osta/otm/otm_v/otm_v_2.html.
- Ou, C. Y., Shiau, . B. Y. & Wang, . I. W. (2000). Three-dimensional deformation behavior of the Taipei National Enterprise Center (TNEC) excavation case history. *Canadian Geotechnical Journal*, vol 37(2), 438–448.
- Peck, R. B. (1975). *The selection of soil parameters for the design of foundations* (Nabor Carrillo lecture; 2d). Mexican Society for Soil Mechanics.
- Peloquin, E. (1995). *Étude d'un système de blindage géotextile pour les tranchées de faibles profondeurs*. (Master of Engineering Thesis, École Polytechnique, Université de Montréal, Québec, Canada).
- Potts, D. & Fourie, A. (1986). A Numerical Study of the Effects of wall Deformation on Earth Pressures. *International Journal for Numerical and Analytical Methods in Geomechanics*, vol 10, p.383-405.
- Poulos, H., Carter, J. & Small, J. (2002). Foundations and Earth Retaining Structures-Research and Practice. In *International Conference on Soil Mechanics and Geotechnical Engineering*. vol 4, p. 2527-2606. Netherlands: AA Balkema.
- Rankine, W. (1857). On The Mathematical Theory of The Stability of Earth-work and Masonry. In *Proceedings of the Royal Society of London*, vol 8, 60-61.
- Rice, A. (1992). Shoring and trenching-implementing a training program for safe trenching procedure. *Occup. Health Safety*, vol 8 (2), p. 60-74.

Roctest Limitée (2005). *Instruction manual*. QC, Canada: ROCTEST Limited, pp. 19-21.
Available at: <https://roctest.com/en>.

Rochelle, P. L., Sarrailh, J., Tavenas, F., Roy M., and Leroueil, S. (1981). Causes of sampling disturbance and design of a new sampler for sensitive soils. *Canadian Geotechnical Journal*, vol 18 (1), 52-66.

Safe Work Australia (2015). *Excavation Work Code of Practice*. Canberra: Safe Work Australia. Available at: <https://www.safeworkaustralia.gov.au/doc/model-code-practice-excavation-work>.

Sanni-Anibire, M., Mahmoud, A., Hassanain, M., & Salami, B. (2020). A risk assessment approach for enhancing construction safety performance. *Safety Science*, vol 121, p.15–29. doi:10.1016/j.ssci.2019.08.044.

Safety Code for the Construction Industry (SCCI). (2020). *Safety Code for the construction industry*. Quebec: Government of Quebec. Available at: <http://legisquebec.gouv.qc.ca/en/showdoc/cr/S-2.1,%20r.%204>.

Schanz, T, Vermeer, P. A., & Bonnier, P.G. (1999). The hardening soil model: formulation and verification in Ronald B. J. Brinkgreve (Éd.), *Beyond 2000 in computational geotechnics*, (pp. 281-296). doi: 10.1201/9781315138206

Seed, H. B. & Idriss, I. M. (1970). Soil moduli and damping factors for dynamic response analysis. (*Report EERC 70-10*). University of California, Berkeley: Earthquake Engineering Research Center.

Skempton, A. W. (1951). The bearing capacity of clays. Paper presented at *Building Research Congress*, pp. 180–189. London.

Terzaghi, K., & Ralph, B. P. (1967). *Soil mechanics in engineering practice*, (2e ed.). New York: Wiley.

Vucetic, M., & Ricardo, D. (1991). Effect of soil plasticity on cyclic response. *Journal of geotechnical engineering*, vol 117(1), p. 89-107.

Wang, J. B. (2001). Strut Loads Prediction – Empirical Approach vs Geotechnical Program Solution. In C. F. Lee, & Y. Lee (Éds), *Soft Soil Engineering: Proceedings of the Third International Conference on Soft Soil Engineering*. Kong Polytechnic University, December 6-8, 2001. Taylor & Francis.

- Yokel, F.Y., Tucker, L. R., & Reese, L.C. (1980). *Soil classification for construction practice in shallow trenching*, Washington, DC: National Bureau of Standards.
- Zhang, J. M., Shamoto, Y. & Tokimatsu, K. (1998). Evaluation of Earth Pressure Under any Lateral Deformation. *Soils and Foundations*, vol 38(1), p.15-33.